Université de Montréal

Role of the CBL Family of E3-Ubiquitin Ligases in the Humoral Immune Response

par

Xin Li

Département de Microbiologie, infectiologie et Immunologie

Faculté de Médecine

Thèse présentée à la faculté des études supérieures

en vue de l'obtention du grade de

Philosophiae Doctor (Ph.D.)

en Microbiologie et Immunologie

April-22nd-2018

Abstract

Production of high affinity antibodies is a hallmark of the humoral immune response and occurs in the germinal center (GC). It depends on a stage-wise developmental process that includes B cell activation, antigen processing and presentation to T follicular helper (T_{fh}) cells, proliferation and somatic hypermutation in GC, selection and eventual differentiation into antibody-secreting plasma cells (PC) or memory B cells. Previous studies have shown that B cell development and activation in GC are controlled by different molecular mechanisms, such as protein phosphorylation, transcription, microRNA, and epigenetic modification. My thesis tries to extend these studies by exploring the potential role of protein ubiquitination in the GC reaction.

We have found that both CBL and CBLB are highly upregulated in GC B cells as compared to naïve B cells and, within the GC B cells, light zone (LZ) GC B cells expressed higher level of CBLs compare to dark zone (DZ) cells. To understand the function of CBLs in the GC reaction, we have examined GC B cell development and differentiation in the mutant mice in which CBLs are either conditionally ablated before GC initiation (in $CBL^{dKO\text{-}Mb1}$ mice) or during GC progression (in $CBL^{dKO\text{-}Cg}$ mice). Our findings reveal that CBLs play critical roles in both GC entry and exit checkpoints. At the entry checkpoint of the GC reaction, CBLs are required for naïve B cell antigen uptake, processing, and presentation to T_{fh} cells. They regulate this process by promoting B cell antigen receptor (BCR) internalization and sorting to lysosome for degradation via ubiquitination Igα, a component of the BCR complex. However, after entering the GC stage, CBLs control selection for high affinity antibodies but not the production of total antibodies, because in the absence of CBLs GC B cells can still develop relatively normally but fail to selectively expand high affinity BCR producing clones as compared to control B cells. Our further analyses reveal that CBLs control this step of GC B cell development by promoting

ubiquitination of IRF4, a transcription factor that is upregulated in the later stage GC B cells with high affinity BCR. Together, our studies provide clear evidence that CBL-mediated ubiquitination is an important and novel regulatory mode in B cells that controls different stages of GC reaction and antibody responses. Modulation of the CBL pathway can be a potentially useful approach not only to interfere humoral immunity for the treatment and prevention of human diseases, but also enhance vaccination in the future.

Résumé

La production d'anticorps de haute affinité est une des caractéristiques de la réponse immunitaire humorale; elle a lieu dans le centre germinatif. Elle dépend d'un processus de développement séquentiel qui comprend: l'activation des lymphocytes B par l'antigène, le traitement et la présentation de l'antigène aux lymphocytes T auxiliaires, la prolifération et l'hypermutation somatique dans le CG, la sélection des lymphocytes B produisant des anticorps de haute affinité et finalement la différenciation en plasmocytes sécréteurs ou en lymphocytes B mémoire. Des études antérieures ont montré que le développement et l'activation des lymphocytes B dans le CG sont contrôlés par des mécanismes moléculaires, tels que la phosphorylation des protéines, la transcription, les microARNs et la modification épigénétique. Ma thèse vise à poursuivre ces études en explorant le rôle potentiel de l'ubiquitination des protéines dans le développement du CG.

Nous avons établi que l'expression de CBL et CBLB (protéines CBL) est considérablement augmentée dans les lymphocytes B du CG comparée à celle des lymphocytes B naïves. De plus dans le CG, les protéines CBL sont exprimées préférentiellement dans les lymphocytes B de la zone claire, plutôt que dans ceux de la zone foncée. Nous avons examiné le rôle des protéines CBL dans le développement et la différenciation des lymphocytes B du CG en utilisant des souris mutantes dans lesquelles l'expression des protéines CBL est, soit réduite conditionnellement avant l'initiation du GC (souris $CBL^{dKO\text{-}Mb}$) ou pendant la réaction de formation du CG (souris $CBL^{dKO\text{-}Cg}$). Nos résultats révèlent que les protéines CBL jouent des rôles critiques dans le contrôle de la formation du CG. En effet les protéines CBL sont requises pour l'absorption, le traitement et la présentation de l'antigène aux cellules T auxiliaires par les lymphocytes B naïves. Ces molécules contrôlent ce processus en favorisant l'internalisation du récepteur de l'antigène des cellules B et la sélection vers les lysosomes pour la dégradation par ubiquitination de l'Igα, un

composant du complexe BCR. Cependant après le début de la réaction dans le CG, les protéines CBL contrôlent la sélection d'anticorps de haute affinité, sans toute fois affecter la production totale d'anticorps. En effet en absence des protéines CBL, les lymphocytes B du CG peuvent encore se développer plus ou moins normalement, mais ne peuvent pas produire des clones ayant des BCRs de haute affinité, comparé aux lymphocytes B de type sauvage. Nos analyses ont aussi révélées que les protéines CBL contrôlent cette étape du développement des cellules B du CG en favorisant l'ubiquitination de IRF4, un facteur de transcription exprimé tardivement dans les lymphocytes B du CG ayant vraisemblablement acquis un BCR de haute affinité. L'ensemble nos études montrent que l'ubiquitination induite par les protéines CBL est un mécanisme de régulation important des lymphocytes B. Ces ubiquitines ligases contrôlent les différentes étapes de la réaction CG et d'une façon plus large la génération d'anticorps. Le contrôle des protéines CBL pourrait permettre non seulement de modifier la réponse immunitaire humorale pour le traitement et la prévention des maladies humaines, mais aussi d'améliorer l'immunisation par vaccination.

Keywords

T-dependent immune response, Germinal centre, B cell, T_{fh} cell, Antigen presentation, E3 ubiquitin ligase, CBL, CBLB, Igα, Antibody affinity maturation, IRF4.

Acknowledgements

First, I would like to thank my supervisor **Dr. Hua Gu** for all his supports and guidance during my entire Ph.D. study. He led me into the immunology field, explained the necessary knowledge, trained me to think scientifically, and taught me to perform experiments accurately.

I would like to thank my colleagues: **Haijun Tong, Liying Gong, Weili Sun, Qicheng Lao, Yue Li, Sarah Lecky and Adeline Gadzinski,** for their supports, helps, advice, and friendship in the past five years. I would also like to thank **Dominique Davidson** and **Jin Qian** for their helps on thesis writing.

I would like to express my deep gratitude to my committee members, **Dr. Javier Marcelo Di Noia** and **Dr. André Veillette** for their critiques and suggestions on my projects. I would like to thank **Dr. George Szatmari** for his advice and assistance.

I would like to thank **Daniela Baggio** for her administrative assistance. I am also grateful to **Manon Laprise**, **Caroline Dubé** and **Marie-Claude Lavallee** for their generous helps on my animal experiments. I would like to thank IRCM's core facilities, including **Eric Massicotte**, **Julie Lord**, **Dominic Filion**, **Richard Cimon** and **Simone Terouz**.

Finally, I would like to thank my family for their constant supports and understanding during my study.

TABLE OF CONTENTS

LIST OF FIGURES

Chapter 1

Chapter 2

LIST OF TABLES

LIST OF ABBREVIATIONS

ABP1	Actin-binding proteins
AID	Activation-induced cytidine deaminase
APC	Antigen presenting cell
APC/C	Anaphase-promoting complex/cyclosome
ASC	Antibody secreting cell
B1P	B1 cell progenitor
BACH2	BTB domain and CNC homolog 2
BAFF	B-cell activating factor
BCR	B cell receptor
BCL6	B-cell lymphoma 6
BLNK	B cell linker
BLIMP1	B-lymphocyte-induced maturation protein 1
BMSC	Bone marrow stem cell
BTK	Bruton tyrosine kinase
CB2	Cannobinoid receptor 2
CBL	Casitas B-lineage lymphoma
CCR7	CC chemokine receptor 7
ChIP-seq	Chromatin immunoprecipitation followed by sequencing
CLP	Common lymphoid progenitor

CMAH	CMP N-acetyl hydroxylase
CR1	Complement receptor 1
CR2	Complement receptor 2
CR3	Complement receptor 3
CRLS	Cullin-RING ligases
CTLA-4	Cytotoxic T-lymphocyte-associated protein 4
CXCR4	CXC chemokine receptor 4
CXCR5	CXC-chemokine receptor 5
CSR	Class switch recombination
CVID	Common variable immunodeficiency
DC	Dendritic cell
DL1	Delta ligand 1
DP	Double positive
DZ	Dark zone
E2A	Transcription factor E2-Alpha
EBI2	Epstein-Barr virus-induced G protein-coupled receptor 2
EGFR	Epidermal growth factor receptor
ERM	Ezrin, radixin and moesin
ERK1/2	Extracellular signal-regulated kinases 1 and 2
EZH2	Enhancer of zeste homolog 2

FDC	Follicular dendritic cell
FO	Follicular
FOXO1	Forkhead box protein O1
GC	Germinal center
HEV	High endothelial venule
HECT	Homologous with E6-associated protein C-terminus
HFD	High fat diet
HSC	Hematopoietic stem cell
HIGMs	Hyper-IgM syndromes
IBR	In-between-RING
ICAM1	Intercellular adhesion molecule 1
ICOS	Inducible co-stimulator
ICOSL	Inducible co-stimulator ligand
ID2	Inhibitor of DNA binding 2
ID3	Inhibitor of DNA binding 3
IF	Inter follicle
iLCs	Innate lymphoid cells
IRF4	Interferon regulatory factor 4
IRF8	Interferon regulatory factor 8
ITAM	Immuno-receptor tyrosine-based activation motif

INKT	Invariant natural killer T
JAK3	Janus kinase 3
JNK	c-Jun NH_2-terminal protein kinase
LEDA	GC B cell selection, division and exit
LZ	Leucine zipper
MAPK	Mitogen-activated protein kinase
MAML1	Mastermind-like 1
MHCII	Major histocompatibility complex II
MINT	Msx2-interacting nuclear target protein
MIB1	Mindbomb 1
MOZ	Monocytic leukemia zinc finger protein
MZ	Marginal zone
NK	Natural killer
PAX5	Paired box 5
PCs	Plasma cells
PD-1	Programed cell death 1
PD-L1	Programed cell death 1 ligand
PDGFR	Platelet-derived growth factor receptor
pMHC	Peptide-major histocompatibility complex
PLCγ2	Phospholipase Cγ2

Pre-BCR Pre- B cell receptor

PI3K Phosphatidylinositol 3’ OH kinase

PRDM1 PR domain zinc finger protein 1

PTEN Phosphatase and tensin homolog

PTK2 Protein tyrosine kinase 2

RA Rheumatoid arthritis

RAG Recombination activating gene

RAP Ras-related protein

RBP-Jκ Recombining binding proteins suppressor of hairless

RBR RING-between-RING

RF RING finger

RFs Rheumatoid factors

S1P Sphingosine-1-phosphate

S1PR1 Sphingosine-1-phosphate receptor 1

SAP SLAM-associated protein

SCID Severe combined immunodeficiency

SLAM Signaling lymphocytic activation molecule

SLAMF6 Signaling lymphocyte activation molecule

SH2 Src homology 2

SH3 Src homology 3

SHM	Somatic hypermutation
SHP-1	SH2 domain-containing phosphatase
SHIP-1	SH2 domain-containing inositol 5 phosphatase
SP	Single positive
SRBC	Sheep red blood cell
STAT5	Signal transducer and activator of transcription 5
SIAE	Sialate O-acetyl esterase
T1	Transitional 1
T2	Transitional 2
T_{eff}	T effector
T_{fh}	Follicular T helper
T_{fr}	Follicular T regulatory
T_h	T helper
TBM	Tangible body macrophage
TKB	Tyrosine kinase binding
TLR	Toll-like receptor
TSLP	Thymic stromal lymhopoietin
TNF-R	Tumor necrosis factor receptor
TRAF2	TNF receptor associated factor 2
Ub	Ubiquitin protein

UBCs Ubiquitin-conjugating enzymes

UPR Unfolded protein response

USP12 Ubiquitin-specific protease 12

VCAM-1 Vascular cell adhesion protein 1

XLA X-linked agammaglobulinaemia

ZAP70 Zeta-chain-associated protein kinase

1 Chapter 1: General introduction

Overview of immunity, the T-dependent immune response and B cells

Currently, people are living in the world with various types of pathogens, such as viruses, bacteria, worms and fungi. Our immune system can efficiently distinguish invading pathogens from self-antigens and mount effective immune responses to clear pathogen infections. In mammalian immune system, there are two branches, each with unique features and functions: the innate immune system and the adaptive immune system. To mount an efficient innate immune response, several types of innate immune cells are involved, such as natural killer cells (NKs), dendritic cells (DCs), innate lymphoid cells (iLCs) and macrophages. The innate immune system is considered the first defence line against pathogen invasion since these innate immune cells can be directly activated by pathogens or the complement system and can rapidly produce large amounts of cytotoxic cytokines to eliminate pathogens. For example, macrophages can engulf invade pathogens through 'phagocytosis', and the internalized pathogens was destroyed in lysosome under low pH environment. DCs also have the capacity to eliminate the pathogens through phagocytosis, but the purpose of the capture pathogens is to trigger adaptive immune responses through presenting antigen to T cells. In contrast, NKs possess capacity to eliminate pathogens infected cells and transformed cells through cytotoxic ways, such as releasing perforin and granzymes or binding to FAS ligand[1]. Recently, one novel innate lineage immune cells, called innate lymphoid cells (iLCs), are identified, which differ from T cell, B cell and NK cells[2, 3]. iLCs are further classified into three groups, including iLC1, iLC2 and iLC3, based on their unique functions and

cytokine production. Multiple studies have been shown their important role in protective immunity and modulating immune response[4, 5].

Once the pathogens escape from the innate immune system, the adaptive immune system is activated. The adaptive immune cells, including T and B cell, can generate an antigen-specific immune response to target pathogen-infected cells. T cells can differentiate into T helper (Th) cells and cytotoxic T cells, whereas B cell can give rise to antigen-specific antibody secreting plasma cells (PCs). The adaptive immune system can generate not only a more efficient and antigen specific response but also long-lived memory cells that are responsible for recalling the immune response. The T-dependent immune response can generate antigen-specific antibodies to neutralize foreign pathogens such as bacteria and viruses. $CD4^+$ T cells, B cells and DCs are required for mounting an efficient T-dependent humoral immune response. Antigen-experienced DCs can activate B cells and $CD4^+$ T cells; then, the $CD4^+$ T cells can provide critical 'help' for B cell functional maturation, in which receptor- and ligand-involved cell-cell interactions are required. To ensure that antibodies can neutralize various types of pathogens, the germline B cell receptor (BCR) repertoire is dramatically diversified due to isotype switching and somatic hypermutations (SHM) within germinal center (GC) reactions. The PCs derived from GCs can produce high affinity antigen-specific antibodies. Given that GC B cells are a critical component of the T-dependent antibody response, it is necessary to understand how to increase the affinity of an antigen specific antibody through GC-dependent mechanism. Basic research may promote the enhancement of vaccination efficiency through developing new vaccination strategies and generating novel

immunization antigens. However, the GC reaction is a double-edged sword since the GC reaction in rare cases can lead to B cell lymphoma due to the off-targeting of activation-induced cytidine deaminase [6] mediated DNA modification. Therefore, it is pivotally important to understand the mechanism of GC-related B cell tumourigenesis since it can provide novel, potential therapeutic targets with respect to human B cell lymphoma.

1.1 Development of B Lymphocytes

B cells are one of the key lineages of adaptive immune cells. They are distributed in multiple secondary lymphoid organs in a highly organized way, together with other lineages of haematopoietic cells, including T cells, DCs, and macrophages/monocytes and lymphoid tissue stromal cells such as follicular dendritic cells (FDCs). The main function of mature B cells is to generate the humoral antibody responses, including T-dependent and T-independent antibody response. Splenic B cells can be further divided into two sub-lineages: marginal zone [7] and follicular (FO) B cells, which may execute distinct functions. MZ B cells can rapidly differentiate into short-lived extra-follicular PCs and are the source of evolutionally selected multivalent, cross-reactive, low affinity antibodies that may provide the first line of defence against blood-borne pathogens[8]. In contrast, the FO B cells mainly respond to T-dependent antigens through the GC reaction and further develop into long-lived high-affinity antibody secreting PCs of different Ig isotypes and memory B cells. Both mature MZ and FO B cells are derived from bone marrow haematopoietic stem cells. In the following sections, I will provide a general review covering the development of B cells.

1.1.1 Early B cell development in the bone marrow

Early B cell development occurs in the bone marrow and starts from haematopoietic stem cells (HSC). According to the current model, the HSCs first generate common lymphoid progenitor (CLP) cells, which retain the multi-potential to differentiate into T, B and NK lineages of cell [9]. CLPs are characterized by cell surface c-Kit^{+} and IL-7Ra^{+} but lack the surface expression of multiple lineage markers, including B220, CD4, CD8, CD11b, GR1 and Ter119. Based on the surface marker expression, Richard Hardy and colleagues further demonstrated that early B cell development can be fractionated into several developmental stages sequentially from fraction A to D (Fr. A-D), also termed Richard Hardy Fractions[10]. In this scheme, Fr. A cells are characterized by cell surface markers B220^{+}, CD19^{-}, HSA^{low}, CD43^{+} and AA4.1^{+}. These cells start to express recombination-activating gene 1 (*Rag1*) and recombination-activating gene 2 (*Rag2*), and rearrange their D and J gene segments of the immunoglobulin genes. The transition from Fr.A to Fr. B cells is dependent on IL-7 mediated signalling. At the Fr. B stage, which is characterized by cell surface markers B220^{+}, CD24^{+} and BP-1^{-}, the successfully rearranged heavy chain can pair with a surrogate light chain, λ5VpreB, and Ig accessory proteins Igα and Igβ to form the pre-B cell receptor (pre-BCR) [11]. The pre-BCR can drive the development and expansion of Fr. B cells, a process called pre-B selection. The signalling of the pre-BCR is tonic and independent of antigen triggering, and the importance of the pre-BCR in this stage of early B cell development has been demonstrated in severe combined immunodeficiency (SCID) mice[12], *Rag*-, *Igα*–, and *Igβ*–deficient mice because these mutant mice showed impaired development of early B

cells at the same Fr. B to Fr.C transition stage [13]. At the Fr. C stage, antigen-independent pre-BCR signalling supports the robust proliferation of Fr.C' cells, while the expressions of RAG and TdT are downregulated through allelic exclusion. The pre-BCR signalling promotes the transition from Fr.C' to Fr.D, during which the re-expressed RAG specifically targets the light chain of the immunoglobulin genes (Figure 1.1). Once the light chain of immunoglobulin genes is successfully rearranged, the surface IgM, composed of light chains and heavy chains, is successfully expressed at the small pre-B stage. These small pre-B cells may undergo BCR-based positive selection, migrate out of the bone marrow, and continue further maturation in the secondary lymphoid organs[14]. In contrast, if the cells express an inappropriately paired BCR or an auto-reactive BCR, they will undergo apoptosis either by neglect or by negative selection.

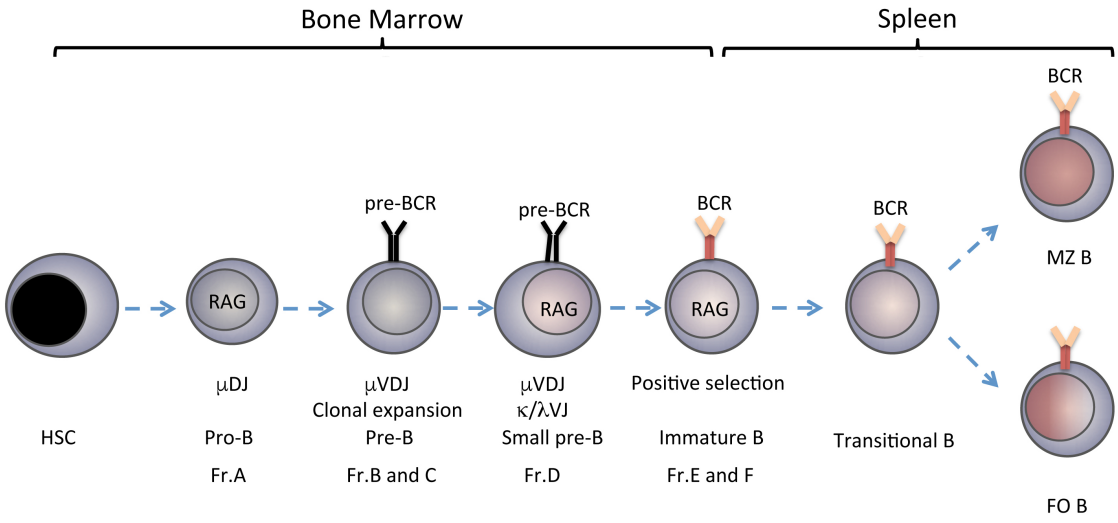

Figure 1.1 B cell development

B cell lineage is derived from HSCs in bone marrow. The early B cell development, from Pro-B to Immature B, occurs in bone marrow, during which the immature B cells generate mature BCR complex dependent on RAG. Once they pass the positive and negative selection, they migrate to secondary lymphoid organs to further differentiate into either MZ B or FO B.

1.1.2 Migration and maturation of newly generated B cells in secondary lymphoid organs

Once immature B cells complete positive selection with mature BCR surface expression, immature B cells enter the blood stream and the lymph, homing to secondary lymphoid organs. The migration of immature B cells is dependent on adhesion molecules and chemokine receptors. The sphingosine-1-phosphate (S1P) receptor has been shown to be responsible for the egress of immature B cells from the bone marrow[15], as the migration of immature B cells from the bone marrow to secondary lymphoid organs is blocked upon the deletion of *S1p* receptor 1 in mice[16]. In addition to S1P, Cannabinoid receptor 2 (CB2) has been shown to play a role in the retention of immature B cells in the bone marrow for sufficient repertoire generation[17]. *Cb2*-deficient mice show a reduced frequency of $Ig\lambda^+$ B cells in secondary lymphoid organs and blood. In contrast, although CXCR4 (C-X-C chemokine receptor type 4) is required for the retention of HSC and B cell precursors in the bone marrow, it does not seem to be required for the migration of immature B cells[18].

1.1.3 Transitional 1 (T1) and Transitional 2 (T2) B cells

In the secondary lymphoid organs, newly immature B cells undergo further stage-wise maturation before becoming mature B cells. The most recently generated immature B cells in the bone marrow and spleen are defined as T1 B cells, which express $B220^+AA4.1^+HSA^+CD23^-CD21/CD35^-$. In the follicles, T1 B cells mature into T2 B cells, as defined by the expression of $B220^+AA4.1^+ HSA^+CD23^+CD21/CD35^+$. Previous

study has shown that T1 and T2 B cells also undergo negative selection, indicating that this is another critical stage of B cell development for immune tolerance induction[19].

1.1.4 B-1 vs B-2 B cells

Mature B cells in peripheral tissues and secondary lymphoid organs can be divided into B1 and B2 cells with distinct functions and locations. The function and development of B2 B cells will be introduced in the next section. B1 cells, located at peritoneal and pleural cavities, are long lasting and self-renew since the majority of them are generated at the foetal liver stage. Based on surface marker CD5, B1 B cells can be further characterized as B-1a ($CD5^+$) and B-1b ($CD5^-$). They express relatively low levels of B220 and IgD, high levels of IgM, intermediate levels of Mac-1. In addition to these typical B cell surface markers, they also express a high level of migration-related integrin, such as α4, α6, β1 and β7[20, 21]. Upon commensal bacterial stimulation, B1 cells can rapidly differentiate into IgM or IgA antibody producing PCs[22]. B1 cell-derived PCs produce antibodies with low affinity and poly-specificity[23].

The generation of B1 cells is derived from B1 specified progenitor cells (B1P), characterized as $Lin^-CD45R^{lo/neg}CD19^+$ cells[24]. The development of B1P cells is dependent on cytokines IL-7 and thymic stromal lymphopoietin (TSLP)[25, 26]. Previous studies have showed that BCR-mediated signalling is critical for the maturation of B1 cells because deficiency of BCR signalling key components, such as CD19, B cell linker (BLNK), CD21, VAV and bruton tyrosine kinase (BTK), leads to a greater reduction in number of CD5+ B1 cells than B2 cells[27-29]. Consistently, an enlarged population of

CD5+ B cells was detected in a BCR signal hyper-activation mouse model by the deletion of *Shp-1* or *Lyn*[30].

However, the maintenance of peritoneal B1 cells is still not clear. There are two possible sources: (i) new generation from bone marrow B1 progenitors as there is little input from the bone marrow in adulthood, and (ii) antigen-stimulated expansion. Upon bacteria stimulation, B1 cells migrate to the omentum and mesenterum, which contain multiple types of lymphocytes[31]. In lymphocyte-enriched regions, type 2 innate lymphocytes (iLC2) can promote the proliferation of B1 cells through an IL-5 dependent mechanism[32].

1.1.5 Marginal zone vs follicular B cells

In the secondary lymphoid organs, T1 and T2 B cells further mature into multiple mature B cell lineages, including B1, MZ B, and FO B cells. In contrast to FO ($B220^{+}HSA^{+}$ $AA4.1CD21^{hi}CD23^{hi}IgM^{lo}$ IgD^{hi}) B cells, which reside in B cell follicles, MZ B cells are characterized as $B220^{+}HSA^{+}AA4.1CD21/CD35^{hi}CD23^{lo}IgM^{hi}$ IgD^{lo} and are distributed in the MZ, an anatomically distinct location at the interface between the red pulp and white pulp. This region contains not only MZ B cells but also specialized macrophages and reticular stromal cells. Due to their unique location, MZ B cells can rapidly respond to blood-borne pathogens. At present, the mechanism for the fate choice between MZ and FO B cells is not yet clear; however, it is generally believed that this cell fate choice is determined when mature T2 B cells migrate to the spleen and requires different signals to be imposed on them.

1.1.5.1 NOTCH signalling pathway in MZ B cell commitment

It has been shown that NOTCH2-mediated signalling is critical for both precursor and mature MZ B cells commitment since *Notch2*-deficient mice exhibit defective MZ B cell development [33]. Consistently, the downstream targets of the NOTCH signalling pathway, such as recombining binding-protein suppressor of hairless (RBP-Jκ) and Mastermind-like 1 (MAML1), are also required for MZ B cell development [34-36]. Both *Rbp-jκ*– and *Maml1*-deficient mice show MZ B cell deficiency and consequently an impaired T-independent antibody response. Furthermore, the deletion of *Notch* signalling suppressor MSX2-interacting nuclear target protein leads to an enlarged MZ B cell population in the spleen [37, 38]. The physiologically relevant ligand for NOTCH signalling, delta ligand 1 (DL1), is highly expressed in both red pulp and the marginal zone [39]. Knockout mice lacking *Dl1* also show defects in MZ B cell development. The endocytosis of DL1 has been shown to be regulated by E3 ubiquitin ligase Mindbomb1 (MIB1), which is required for both T cell and MZ B cell development [40]. NOTCH signalling can indirectly target three different transcription factors, including E2A, ID2 and ID3, to execute its function in MZ B cell development. The expression of helix-loop-helix transcription factor E2A is regulated by NOTCH signalling mediated-ubiquitination [41]. *E2a*-deficient mice show an increased MZ B cell population, which suggests that E2A-mediated gene transcription has a suppressive role in MZ B cell development. Other members of E protein family proteins, inhibitor of DNA binding 2 (ID2) and inhibitor of DNA binding 3 (ID3), are negative regulators of E2A. Compared to the enlarged MZ B population in *E2a*-deficient mice, *Id3* knockout mice exhibit decreased MZ B cell

development, which suggests an indirect regulatory role of NOTCH signalling in MZ B cell development via regulating the expression of *Id2* and *Id3* [42].

1.1.5.2 BCR signal strength in FO and MZ B cell development

In the past decade, experiments have revealed a critical role of BCR signal strength during the fate decision between FO B and MZ B. It has been shown that weak BCR signalling is required for the commitment of MZ B cells, whereas a strong BCR signal favours the survival of FO B cells. For example, it has also been found that impairment of the BCR-BTK pathway by genetically deleting *Btk* or phospholipase Cγ2 (*Plcγ2*) leads to the loss of FO B cells and the relative preservation of MZ B cells [43]. Consistently, in the absence of the positive regulator of BCR signalling CD21/CR2, MZ B cells are significantly expanded compared to WT mice [44]. It has been shown that genetic modification of the tyrosine residues on immunoreceptor tyrosine activation motif (ITAM) of Igα leads to the loss of only MZ B cells, due to the enhanced BCR signalling [45]. In contrast, mice lacking sialate O-acetyl esterase (SIAE) or CMP N-acetyl hydroxylase (CMAH), the ligand of the CD22-mediating BCR inhibitory signalling pathway, display a dramatic reduction of MZ B cells [6]. A question that remains unresolved is whether there is a crosstalk between BCR and Notch-signalling that collectively determines MZ vs FO B cell fate determination.

1.1.5.3 Other regulators in MZ and FO B cell development

B-cell activating factor (BAFF), a trimeric member of TNF family protein, is highly expressed in lymphoid follicles and is critical for the survival of T2 B cells and mature FO B cells. In addition to supporting B cell survival, BAFF is also required for MZ B cell

development through activating both non-canonical and canonical NF-κB pathway through different substrates [46]. Deletion of *p50* and *p65* of the canonical NF-κB pathway leads to defective MZ B cell development [47]. In addition to BAFF, chemokine receptors and integrin may play a role in the migration and retention of MZ B cells. For example, lymphocyte function-associated antigen 1 (LFA-1) and α4β1 have shown to contribute to the retention of MZ B cells in the marginal zone [48]. The abnormal integrin signalling through mutating protein tyrosine kinase 2(*Ptk2*) leads to the blockade of MZ B cell development, suggesting that migration- and retention-related factors are critical for MZ B development [49]. Interestingly, Martin Turner's group recently showed that RNA-binding proteins of the ZFP36 family regulate MZ B cell development through post-transcriptional mechanism [50]. It will be interesting to determine whether ZFP36 proteins regulate MZ B cell development through the aforementioned molecules.

1.1.6 Follicular B cells

Most mature B cells migrate to secondary lymphoid organs and become follicular B cells, which can be simply identified as $IgM^{lo/hi}IgD^{hi}$ B cells. B cell follicles are always close to the T cell zone, which provides a convenient way for activated B cells to interact with activated T helper cells at the interface of the T cell and B cell zones during T-dependent immune responses. Unlike MZ and B1 B cells, FO B cells have a broad BCR repertoire that allows them to recognize almost unlimited epitopes expressed by various types of pathogens.

1.2 The Germinal Centre Reaction

The GC is a temporary micro-lymphoid structure in secondary lymphoid organs such as the spleen and lymph nodes, which emerges upon pathogen infection or vaccination [51]. In 1884, Walther Flemming first described the GC as a distinct micro-anatomical structure in secondary lymphoid organs that contains dividing cells. After this first report, a series of studies from multiple different groups proposed that the GC is a possible source of lymphocytes throughout the body. In 1936, Hellmann contested this conclusion based on his studies in which the germ-free guinea pigs completely lacked a GC but had a normal lymphocyte distribution. Subsequently, several immunization experiments demonstrated that the great majority of germinal centre cells are highly proliferating B cells during immune responses. Visible GCs appear at approximately 6 days, and those foci increase rapidly in size and reached their peak at approximately 14 days in the B cell follicles of the lymph nodes and spleen. Once the GC reaction has passed its peak, the latitude of the GCs starts to decline due to limited antigens and enhanced differentiation of PCs [52]. Although the GC sizes start to shrink after the peak, they can be detected up to at least 95 days. This observation thus provides an explanation for why vaccination can induce a prolonged production of high affinity antibodies in the protective immune response. In the following section, I will review what we know about the regulation of the structure, function and outcomes of the GC reaction.

1.2.1 Cell types in the GC

1.2.1.1 GC B cells

The predominant cell types in the GC are activated B cells, which are quite different from naïve B cells in terms of size, phenotypic marker expression and function. For example, GC B cells are larger than naïve B cells and display a highly polarized morphology [53, 54]. GC B cells are highly proliferating, with extensive protein synthesis and DNA replication, whereas naïve B cells are at a steady state. Based on surface phenotypic markers, GC B cells are characterized as expressing high levels of apoptotic receptor FAS and GL7, as binding to peanut agglutinin (PNA), and as having lost of naïve B cell markers such as IgD and CD38[55-57]. Two critical intracellular/nuclear proteins for GC B cell phenotype and function are the transcription factor B-cell lymphoma 6 (BCL6) and AID [58-60]. BCL6 is highly upregulated in GC B cells. *Bcl6*-deficient mice cannot form GCs or generate high affinity antibody secreting PCs [61]. The transcriptional repressor BCL6 selectively silences PC-related gene expression such as PR domain zinc finger protein 1 (Prdm1) and interferon regulatory factor 4 (*Irf4)*, which demonstrates that BCL6 is critical for the maintenance of GC B cell identity [62]. Another important feature of GC B cells is a proneness to apoptosis since BCL6 suppresses anti-apoptotic protein BCL2 expression [63]. Since GC B cells undergo massive DNA replication and mutation, BCL6 is required for the tolerance to DNA damage through BCL6-mediated silencing of p53 and ATR [64, 65]. The DNA deaminase AID is mainly expressed in GC B cells. Both BCR isotype switching and affinity maturation are dependent on AID activity in GC B cells through targeting the cytidine residues in the VDJ and switch regions of the Ig

gene [60]. On the basis of different surface markers and cell statuses, GC B cells can be divided into two sub-populations: centroblasts and centrocytes, which will be reviewed in the next section.

1.2.1.2 The follicular dendritic cells

FDCs are strictly located in the LZ of the GC, where they are considered the maker for LZ in histology and fluorescence microscopy [66, 67]. In GCs, FDCs are the primary source of antigens that can stimulate the maturation and selection of GC B cells. FDCs can capture antigens through complement receptors 1 (CR1) and 2 (CR2), which can help them retain immune-complex-coated bodies on the cell surface [68]. Antigen-specific GC B cells selectively acquire antigen complexes from FDCs based on the affinity of the BCR, leading to further proliferation, mutation, and maturation. In addition to their role as APCs in GCs, FDCs also secrete chemokines and cytokines that can support the formation of GCs. For instance, the ablation of intercellular adhesion molecule 1(ICAM-1) and vascular cell adhesion protein 1 (VCAM-1) on FDCs leads to reduced GC size and impaired affinity maturation [7]. The cytokines IL-6 and BAFF secreted from FDCs play critical roles in GC maturation [69-71]. The organization of LZ is also dependent on the chemo-attractant signals provided by FDCs since they produce the ligand for CXC-chemokine receptor 5 (CXCR5).

1.2.1.3 Follicular T helper cells and follicular regulatory T cells

T_{fh} cells are one subset of $CD4^+$ T helper cells that are mainly present in GCs. They express the chemokine receptor CXCR5, which is critical for the migration from T cell zones to B cell follicles. T_{fh} cells also display a high level of co-stimulatory molecules

such as inducible co-stimulator (ICOS) and PD-1, as well as signalling lymphocyte activation molecule 6 (SLAMF6) and SLAM-associated protein [72, 73]. The development of early T_{fh} cells is dependent on the cytokine IL-6 produced by antigen-experienced DCs [74, 75]. T_{fh} cells provide a pivotal survival signal to GC B cells through those receptors that involve a cognate interaction. Based on their cytokine production, T_{fh} cells are further divided into two subpopulations: IL-21$^+$ T_{fh} and IL-4$^+$ T_{fh}. The *Il-21r*-deficient mice display impaired affinity maturation and generation of long-lived PCs, suggesting that IL-21 is a key component for optimal GC reaction [76, 77]. The isotype switch of GC B cells is dependent on IL-4 [78-80]. Those two distinct populations display a unique function in GC B cell maturation: IL-4$^+$ T_{fh} promoting class switch recombination (CSR) and differentiation of PCs, and IL-21$^+$ T_{fh} supporting clonal selection, and expansion [81].

Recently, a new sub-population of follicular T cells is identified as follicular regulatory T cells (T_{fr}), characterized as CD4$^+$CXCR5$^+$PD-1$^+$BCL6$^+$FOXP3$^+$ [82, 83]. T_{fr} cells display suppressive function on GC B cell and T_{fh} cell growth. Similar to T_{fh} cells, T_{fr} cell development depends on GC B cells, SAP and BCL6. This suppressive population is derived from natural Treg cells, not naïve T or T_{fh} cells. However, their antigen specificity is still unknown.

1.2.1.4 Other populations

In addition to T_{fh} and GC B cells, GCs also contain tangible-body macrophages (TBMs) and a small population of DCs. TBMs can eliminate apoptotic B cells that are outcompeted through clonal selection. Defects in TBM function lead to systemic lupus

erythematosus [84], suggesting they may control immune tolerance in the GC [85]. Although DCs are observed in GCs, their role in GCs is still unclear [86].

A unique subset of T cells, called invariant natural killer T cells (iNKT cells), is also found in the GC region. The TCR repertoire of iNKT cells is restricted, composed of the α-chain variable region 14-α-chain joining region 18 paired with the V_β8.2, V_β7 or V_β2 TCR β-chain [87]. After the cognate interaction with antigen-specific B cells, iNKT cells produce cytokine IL-21, which can promote GC formation, affinity maturation and the IgG antigen response [88]. Interestingly, iNKT cells can further differentiate into NKT_{fh} through a CD28-BCL6-dependent mechanism [89]. However, the NKT_{fh} cell-induced GC displays limited affinity maturation.

1.2.2 The Structure of the GC

Matured GCs are characterized as having two functional regions: DZ and LZ [90]. The original definition of DZ and LZ came from early conventional histology techniques. The DZ was visualized as a darkly stained region because of highly proliferating centroblasts; the LZ contained smaller, non-proliferating B cells known as centrocytes, as well as antigen-coated FDCs and antigen-specific T_{fh} cells. The current model indicates that these two segregated regions of the GC may have different functions. In the DZ, GC B cells proliferate and undergo SHM of the Ig variable region. In contrast, the LZ area is where GC B cells expressing a mutated BCR undergo antigen-receptor-based selection and differentiation into PCs and memory B cells (Figure 1.2).

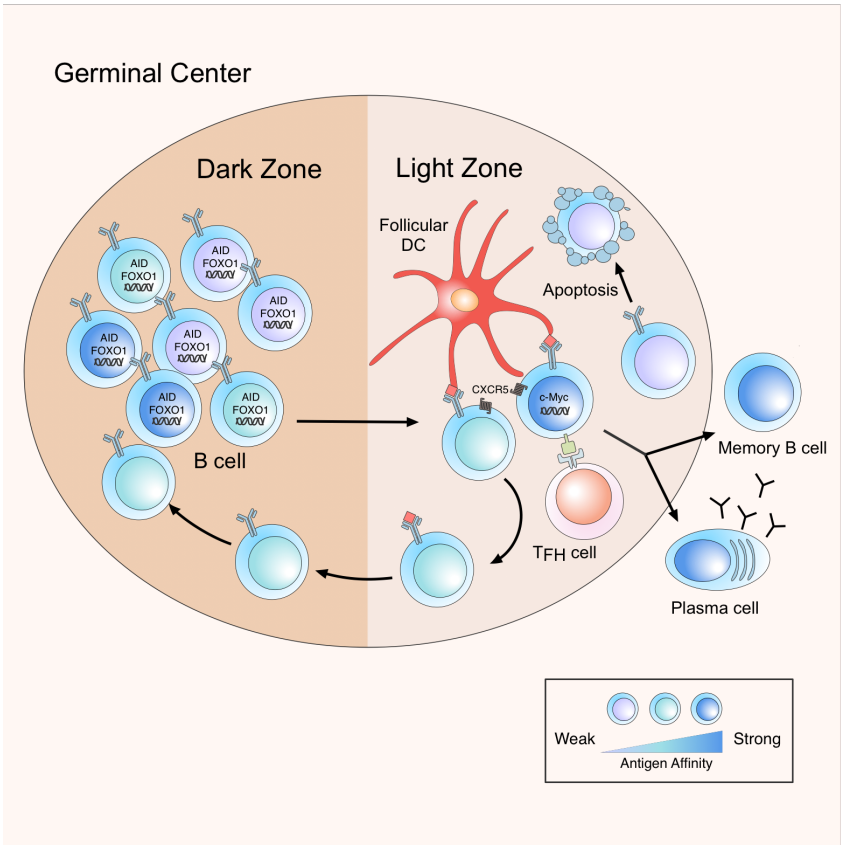

Figure 1.2 Germinal center.

The GC is composed of DZ and LZ. The different regions contain different cell types and carry out distinct functions. The LZ contains centrocytes, T_{fh} and FDC. T_{fh} and FDC both provide unique survival and differentiation signals to centrocytes. For example, antigen loaded-FDC provides antigens to centrocytes through BCR affinity based competition, while the T_{fh} provide survival signals to them through cognate interaction. Once centrocytes acquire survival signals, they migrate to DZ through upregulation of CXCR4 and c-Myc. In the DZ, the centroblasts turn on the expression of FOXO1 and AID, which can promote the clonal expansion and SHM. After 2-3 round of proliferation, centroblasts migrate back to LZ through the upregulation of CXCR5. Due to the limited amount of 'help' provided by FDC and Tfh, B cells with low affinity BCR undergo apoptosis. The high-affinity B cells have three potential fates: re-entry into DZ for further expansion and mutation; exit from GC into PCs or memory B cell.

1.2.2.1 Dark zone of the GC

To generate a broad BCR repertoire against pathogens, AID is highly upregulated in DZ GC B cells [6], which creates mutations in DNA by deaminating cytosine into uracil. The

U:G mismatch caused by AID can lead to the conversion of C:G to T:A during cell replication. Since the frequency of SHM in Ig V genes is significantly enhanced (10^6-fold) compared to the natural somatic mutation rate in the genome, it allows GC B cells to acquire many point mutations in IgV genes within the cell cycle, leading to improvements in both the affinity and the specificity of the BCR [91]. The CSR from the IgM isotype to other isotypes of Ig is also dependent on the activity of AID through targeting the switch regions of the BCR heavy chain gene. When AID targets single strand DNA during transcription, the AID may target some regions other than the Ig locus, called off-target regions. This process may cause a very low frequency of mutations in oncogenes, such as *Myc* and *p53*, consequently leading to the initiation of chromosome translocations that eventually contribute to the development of GC B-cell-derived lymphomas [92].

1.2.2.2 Light zone of the GC

The LZ of the GC is heterogeneous in terms of its cell composition, which includes FDCs, T_{fh} cells, centrocytes, and TBMs. The main function of the LZ is to provide an environment for FDC- and T_{fh}-dependent affinity-based selection and differentiation of centrocytes [93] . The FDC is considered an antigen-presenting cells within GCs and has been shown to be necessary for the maturation and maintenance of GCs [51, 94]. Due to the limited availability of antigens captured by FDCs, the centrocytes must compete for antigens based on the affinity of the BCR, so that only the B cells with high affinity BCRs can acquire antigens to support their further T-B cognate interaction, maturation

and clonal expansion. In contrast, due to insufficient FDC and T cell help, B cells expressing low affinity BCRs undergo apoptosis and are then rapidly cleaned by TBMs.

The cognate interaction between antigen-specific GC B cells and T_{fh} cells is critical for T_{fh} expansion and re-entry of centrocytes into the DZ. This interaction involves multiple receptors and ligands on both T and B cells. For example, ICOS-mediated signalling is critical for T_{fh} cell expansion since the expression of BCL6 and IL-21 is induced by ICOS signalling [95, 96]. The interaction of CD40 with CD40 ligand (CD40L) is required for GC B cell proliferation and differentiation. The signalling lymphocytic activation molecule (SLAM)-SLAM has been shown to be necessary for both B and T_{fh} cell survival [97]. Those interactions execute their biological functions through their corresponding downstream signal pathways to promote the establishment of the GC reaction. In addition to promoting GC B cell proliferation, FDC and T_{fh} are also required for the differentiation of PCs and long-lived memory B cells. I will review the detailed mechanism of post-GC fate decision in section 1.2.6.

1.2.3 The Initiation of the germinal centre reaction

The spleen can be structurally divided into red pulp and white pulp. The majority of T and B lymphocytes are located in the white pulp, which can be further characterized into B cell follicles containing IgM^+IgD^+ naïve B cells and a T cell zone comprising $CD4^+$ and $CD8^+$ T cells. In this subsection, how activated B cells interact with antigen specific $CD4^+$ T cells at the initiation stage of the GC reaction will be introduced.

1.2.3.1 T-B cognate interaction

In the spleen, naïve B cells are activated by exogenous T-dependent antigen-loaded FDCs within the follicle. The activated B cells migrate to the border of the T cell and B cell zone where they cognately interact with antigen-specific T cells. Afterwards, a small fraction of activated B cells directly differentiates into short-lived plasmablasts through an extra-follicular reaction. In addition to extra-follicular PCs, Marc Jenkins' group reported that some of the GC B cell precursors ($CD38^+GL7^+$) directly differentiated into IgM^+ or isotype-switched Ig^+ memory B cells in a GC-independent fashion[98], while a small fraction of activated B cells differentiated into GC B cells. Michel Nussenzweig and colleagues proposed that entry into GCs is determined by the amount of peptide-major histocompatibility complex (pMHC) presented to cognate T cells within clusters at the T-B border, which means that T-cell-mediated signals control the clonality and antigen specificity of GC B cells [99]. This T-B cognate interaction ensures that only antigen specific T and B cells can enter GC cycle. Although B cells are dispensable for the priming of $CD4^+$ T cells and initial T_{fh} programme, they are critical for the functional maturation of T_{fh} cells during the early stage of GC reaction [100-102].

1.2.3.2 Antigen presentation by B cells

The cognate interaction of B and T cells is initiated by the interaction between antigen-peptide-loaded major histocompatibility complex II (MHCII) and antigen-specific T cell receptor (TCR), followed by the ligation of multiple co-stimulatory molecules and ligands. At this stage, B cells act as classic APCs, which can acquire both soluble and large antigens through different mechanisms. For instance, Kathryn Pape and Drew

Catron used fluorescence-coupled small soluble antigens to track how B cells capture antigens for subsequent T cell-dependent activation. Their system clearly showed that small antigens can be rapidly supplied to the lymph node through the afferent lymph vessels and then diffuse to the B follicle without the help of DC or B cell migration [103].

Complex antigens, such as viral particles, immune complexes or antigen-coated microspheres, cannot directly diffuse to the B cell zone; thus the capture of antigens by B cells is dependent on the specialized APCs. In the draining lymph node, a population of $CD11b^{+}CD169^{+}MHCII^{+}$ macrophages in the subcapsular sinus is specializes in preserving intact antigens. It has been shown that subcapsular sinus macrophages can capture antigens through two different mechanisms: complement receptor 3 (CR3) or the FcγRIIB-mediated complement-IgG-opsonized immune complex, or SIGLEC-1 and the mannose receptor [104]. The neighbouring follicular B cells can rapidly capture antigens through receptor CD21 from antigen-coated macrophages and antigens transported into the FDCs located in the B cell follicle [103]. Interestingly, this type of antigen transportation is independent on the BCR. For example, influenza A virus is captured and presented to B cells by subcapsular sinus macrophages [105]. However, several studies have shown that antigen-specific B cells are directly bound to their cognate antigens on subcapsular sinus macrophages through ICAM-1- and VCAM-1-mediated cell adhesion [106, 107]. After acquiring cognate antigens, activated B cells migrate back to the T/B border for T-B cognate interaction.

Given that B cells enter lymph nodes through high endothelial venules (HEVs), they can immediately interact with antigen-loaded APCs in the paracortex. Three independent

studies identified a population of DCs located in the paracortex that can present intact antigens to B cells [108, 109]. Additionally, a recent study showed that lymph node resident DCs are loosely distributed in the T cell zone and T/B border where they continuously interact with T and B cells[86, 110]. The lymph node resident DCs can capture influenza A viral particles through receptor SIGN-R1. Depletion of this population suppresses the antiviral immune response [105]. Furthermore, Ronald Germain's group by using two-photon intravital microscopy showed that B cells located in the extra-follicular region survey locally antigen-coated DCs, which leads to migration arrest, activation and antigen acquisition [111]. Once the B cells acquire antigens, they upregulate migration-related proteins, such as CC chemokine receptor7 (CCR7) and Epstein-Barr virus-induced G protein-coupled receptor 2 (EBI2), to guide those activated cells to the T cell border for full activation through T-B cognate interaction [112, 113].

The recognition of the antigens on the membrane of APCs through BCR engagement leads to the formation of a stable immunological synapse. The BCR has two main functions: first, BCR engagement triggers intracellular signalling cascades, leading to B cell activation, proliferation and differentiation; second, the BCR can capture, internalize and process the antigen-BCR complex into peptides to be presented to T cells via MHCII [114]. These two functions are interdependent since the BCR-associated signalling is required for BCR internalization and promoting the transport of antigen-BCR complexes to lysosomes for degradation [115]. To maintain the stable immunological synapse, the LFA-1/ICAM-1 interaction increases the adhesion of B cells under the circumstance of limited antigen availability, which can lower the threshold for B cell activation [116].

The stabilization of this synapse is also dependent on the BCR-induced rapid actin-involved membrane-spreading response. After the formation of stabilized synapses, the antigens are transported into BCR micro-clusters and sorted to central clusters through ERM (ezrin, radixin and moesin) and the microtubule-based motor protein dynein-dependent rearrangement of cortical actin cytoskeleton [117, 118]. The GTPase Ras-related protein (RAP) can activate the actin-severing protein cofilin to support this process. Moreover, RAP also controls the polymerization of the actin cytoskeleton through F-actin [119].

The BCR is a multimeric protein complex including antigen-binding arms consisting of Ig heavy chains and Ig light chains that are non-covalently associated with two signal-transducing heterodimers of Igα and Igβ. The BCR signals are initiated by SRC-kinase-mediated tyrosine phosphorylation of ITAM on Igα and Igβ, followed by the ubiquitination of the BCR complex through a SYK-dependent pathway [120]. Two different E3 ubiquitin ligases, ITCH and CBL, have been shown to be responsible for this process. Both ubiquitin ligases can directly target the phosphorylated Igα and Igβ complex, leading to the internalization of the BCR complex [121, 122]. The spatial organization in the membrane micro-domain is also critical for the internalization of the BCR complex since the tyrosine-phosphorylated clathrin is associated with rafts upon BCR stimulation [123]. The internalized BCR is trafficked through early endosomes to the late endosomes and LAMP-1^+ multi-vascular compartments, during which mitogen-activated protein kinase (MAPK), extracellular signal-regulated kinase 1/2 (ERK1/2), p38 and c-Jun NH_2-terminal protein kinase (JNK) are involved [124]. In addition, some

actin cytoskeleton related proteins, such as actin-binding proteins (ABP1) and BTK, are also involved in the sorting of the BCR complex[125]. To maintain prolonged production of the antigenic peptide-MHCII complex, the excessive MHCII molecules are co-localized in degradation lysosomes. The transport of the MHCII and BCR-Ag complex is highly regulated through actin-associated motor myosin II. Taken together, BCR-induced downstream signals activate multiple genes and re-organize the actin cytoskeleton, both of which are highly coordinated and required for intracellular vehicle transport and B cell antigen processing/presentation.

1.2.4 Early GC formation and progression

1.2.4.1 Initiation of early GC and Tfh

Due to the broad usage of intravital microscopy, three independent groups have shed new light on the early dynamics of GC formation in lymph nodes. Cortty and collaborators found that DC-primed antigen-specific $CD4^+$ T cells to exhibited an early Tfh phenotype that was characterized as $CXCR5^+$, programmed cell death 1^+ (PD-1) and $GL7^+$ at day 2 of LCMV infection. ICOS signalling can induce the expression of CXCR5 on Tfh cells through a BCL6-dependent mechanism, which supports the migration of Tfh cells to the GC region [100]. In addition, Takaharu Okada and colleagues, by using the *Bcl-6* reporter mice, found that BCL6 expression in B cells was continuously upregulated after day 3 of immunization. Strikingly, some fractions of T_{fh} cells gradually lost the Bcl6 expression after day 3 of immunization, which might lead to memory T_{fh} cell phenotypes such as terminated proliferation and upregulation of the IL-7 receptor [102, 126]. Although the induction of T_{fh} cells is initiated by antigen experienced DCs, the maintenance of T_{fh} is

dependent on antigen-specific B cells since the T_{fh} population in B cell deficient mice was dramatically reduced at day 4 of immunization. In terms of T_{fh} function, these T_{fh} cells were functionally immature, as evidenced by the reduced IL-4 and IL-21 production, suggesting a critical role of cognate T-B cell interaction in the maintenance or functional maturation of T_{fh} cells in the GC. Collectively, the commitment of early T_{fh} and pre-GC B cells occurs at the IF (inter-follicular) zone, and T_{fh} cell differentiation and migration precedes pre-GC B cells by 1 day. It would be interesting to dissect which signals are responsible for the initiation of pre-GC B cells.

1.2.4.2 Transcriptional regulation of Tfh and GC B cells

Since BCL6 is critical for GC initiation, extensive studies have been carried out on the BCL6 transcription and its regulatory modes. Several transcription factors, including *Irf4*, interferon regulatory factor 8 (*Irf8*), basic leucine zipper transcription factor 2 (*Bach2*), paired box 5 (*Pax5*), and *Prdm1*, have been shown to be dynamically regulated by BCL6. For example, BCL6 and BLIMP1 mutually suppress each other's function since these two transcription factors bind to each other's promoters and repress each other's expression, which consequently antagonizes the functions of two opposite groups of genes manifested by GC B cells and PCs [127]. It was shown that BACH2, IRF8 and PAX5 stabilizes the expression of BCL6, which in turn suppresses PCs differentiation [127]. However, IRF4 is an unusual component in this gene regulatory network, since IRF4 has diverse, dose-dependent and context-dependent functions in Tfh and GC B cell development. Michael Lohoff's group showed that the *Irf4*-deficient mice failed to generate proper Tfh cells and GCs after *L. major* infections, which could be rescued by

the administration of WT $CD4^+$ T cells. This result suggested that IRF4 is required for T_{fh} development [128]. Moreover, the strength of the TCR signal determines the concentration of IRF4 that is required for both BCL6-expressing T_{fh} and BLIMP-1-expressing T effector cells [129]. Mechanically, abundant IRF4 expression leads to low-affinity binding sites within Prdm1 including Teff cis- regulatory components [130]. Not surprisingly, IRF4 is also critical for the GC B cells since the *Irf4*-deficient B cells driven by CD19-Cre failed to differentiate into GC B cells. Based on chromatin immunoprecipitation followed by sequencing (ChIP-seq) analysis of *in vitro* antigen-activated B cells, IRF4 could directly induce the *Bcl6* and *Pou2af1* expression by binding to the region 24k bp upstream of the *bcl6* gene [131]. In contrast, Cγ1-Cre-driven *Irf4* deletion did not affect the proper formation of GCs since the Cγ1-Cre-mediated deletion occurred at approximately day 2 after immunization. Although these mutant mice were able to mount a proper GC, PCs were undetectable in both the spleen and bone marrow after hapten NP-carrier antigen immunization [132]. Thus, IRF4 is not only required for the initial pre-GC B development for a limited time window but also necessary for promoting post-GC PCs differentiation. Interestingly, IRF4 and IRF8, a transcription factor structurally related to IRF4, can directly bind to DNA motifs *Pu.1*, *Spi-b* and *Batf* [133]. However, the expression of these two transcription factors leads to distinct consequences in terms of lymphocyte lineage commitment and cell activation. The loss of IRF8 protein in B cells leads to a reduced GC reaction and enhanced PCs differentiation [134]. Thus, IRF4 and IRF8 are likely mutually suppressive through a

double-negative feedback loop mechanism that determines the fate choice of extra-follicular plasmablast or GC reaction in the early stage of the GC reaction.

1.2.4.3 The survival of GC B cells

Once B cells differentiate into GC B cells, several surface receptors and ligands are upregulated to support their survival and maturation. Among these molecules, the death receptor FAS (also called CD95) is highly expressed. FAS is a member of the tumour necrosis factor receptor (TNF-R) family [135]. Activation of FAS by its physiological ligand FASL has been proven to trigger apoptosis. The upregulation of FAS in GC B cells suggests that FAS is the negative regulator of autoimmune disorders relate to GC reaction. Consistent with this hypothesis, *Fas*-deficient B cells showed hyper-activation and enhanced proliferation. Other apoptotic proteins, such as BCL2L1 (BCL-XL), BCL2 and BIM, are also involved in the caspase-mediated cell apoptosis [136-138]. Although multiple apoptotic factors are involved in this negative selection, so far, only one pro-survival molecule, MCL1, has been shown to regulate GC B cell survival, as identified by David Tarlinton's group. The *Mcl1*-deficient mice driven by *Aicda*-cre could not form proper GC reactions and memory B cells, suggesting that MCL1 is continuously required throughout the entire GC reaction [139]. More importantly, the requirement to obtain an effective GC reaction is dependent on the level of MCL1 expression. Cellular extrinsic factors, such as T cell and FDC 'help', also provide critical survival signals for GC B cell survival. In LZ, Tfh cells express high levels of CD40L, for which it was shown that the CD40-CD40L interaction could rescue FAS-induced apoptosis of centrocytes through the NF-κB-dependent upregulation of BCL-XL and c-FLIP [140, 141]. The surface receptor

CD9 on human GC B cells, which is a member of the transmembrane 4 superfamily, also supports the survival of GC B cells. In human tonsillar tissues, $CD9^+$ GC B cells were highly enriched in the LZ area of GCs compared to $CD9^-$ GC B cells, which suggested that the CD9-meditated interaction could promote GC B cell survival through interacting with FDC. Consistently, *in vitro* $CD9^+$ GC B cells survive better than $CD9^-$ GC B cells in the presence of FDC line HK cells [142].

1.2.5 Interzonal movement and maturation of GC B cells

The early GC emerges at approximately day 4 post-immunization and is derived from the extensive expansion of activated antigen specific B cells. The mature GC featuring two different cell zones appears until day 7 post immunization. After the establishment of DZ and LZ, the antigen-specific B cells undergo interzonal migration for clonal expansion, affinity maturation and selection. In this subsection, I will review the recent findings about this interzonal migration and maturation theory.

1.2.5.1 GC B interzonal migration

The DZ and LZ functionally segregate GC B cells into two subpopulations: centroblasts (characterized as $CXCR4^{hi}CD83^{low}CD86^{low}$) and centrocytes (characterized as $CXCR4^{low}CD83^{hi}CD86^{hi}$). The *Cxcr4*-deficient GC B cells are mainly located in the LZ of the WT GC structure, which demonstrates that CXCR4 is required for the migration of centroblasts towards the CXCR4 ligand SDF-1 (CXCL12) expressed in the DZ. The chemokine receptor CXCR5 guides the migration of centrocytes to the CXCL13-enriched LZ since the ablation of CXCL13 leads to a deficiency of LZ organization in these mutant mice. In 2007, two independent studies demonstrated that albeit motile, all

antigen-specific B cells are physically restricted to the GC but migrate bi-directionally between the DZ and LZ [143, 144]. More recent works have focused on the molecular mechanism that controls the migration between DZ and LZ. Two groups found that transcription factor *c-Myc* is repressed by BCL-6 in the DZ but induced among antigen-driven selected LZ GC B cells for the re-entry into the DZ. This finding suggests that *c-Myc* is required for the DZ-LZ circulation of GC B cells [84, 145]. Interestingly, the induction of AP4 is dependent on c-MYC during T-B cognate interaction, while the IL-21 can maintain the AP4 expression in GC B cells. Although the ablation of *Ap4* did not affect DZ-LZ organization, the *Ap4*-deficient GC B cells displayed a decreased GC B cell population and a reduced SHM and humoral antibody response against LCMV infection, coupled with a reduced proliferation rate of DZ GC B cells [146]. These findings suggest that AP4 is required for the clonal expansion of DZ GC B cells and the subsequent antibody response. The expression of transcription factor forkhead box protein O1 (FOXO1) is restricted to DZ GC B cells, whereas the LZ GC B cells display a high level of PI3K activity. The PI3K signalling and FOXO1 play opposite roles in the organization of DZ and LZ GC B cells. The ablation of *Foxo1* or the hyperactivation of PI3K activity results in impaired LZ organization with blocked CSR and impaired affinity maturation, despite normal AID expression, which may be due to the downregulation of chemokine receptor CXCR4 [147, 148]. Surprisingly, although CXCR4 is required for the formation of DZ, the *Cxcr4*-deficient mice display normal antibody responses against hapten antigens and slightly reduced responses against influenza [149, 150]. Further study showed that BATF is also involved in the FOXO1 mediated DZ-LZ organization [151].

Collectively, it is still unclear why the GCs segregate the affinity-based selection from proliferation and SHM.

1.2.5.2 Clonal selection and expansion

Current models propose that the maturation and selection of GC B cells are driven by BCR affinity. Micheal Nussenzweig's group revealed that 50% of DZ GC B cells rapidly and continuously migrate to the LZ by 4 hrs of photon-activation, while less than 15% of LZ GC B cells can translocate to the DZ within 6 hrs post photon-activation. This study further demonstrated that the ability of interzonal migration is determined by the availability of antigen-specific T_{fh} help. The number of the GC B cell divisions per DZ-LZ cycle, varies from 1 to 6, is determined by the number of antigens acquired from FDCs. Since the GC B cells capture antigens from FDCs through the BCR, the GC B cells with high-affinity BCRs acquire more antigens in the LZ, leading to the clonal expansion of these high-affinity GC B cells and outcompeting the lower-affinity GC B cells. Consequently, the greater number of proliferation cycles in GC B cells is associated with a higher mutation frequency of the BCR repertoire and enrich for the high-affinity mutations due to the BCR-based affinity selection [91]. Later, the "Brainbow" transgenic mouse was applied to study the relationship between clonal diversity and expansion [152]. This transgenic mouse relied on stochastic Cre-mediated recombination to turn on one of four possible fluorescent proteins, which can generate ten different colour combinations. The early GCs (8 days post-immunization) were composed of equal proportions of CFP^+, YFP^+ and RFP^+ cells and a lower proportion of GFP^+ and doubly recombined cells, which suggested that early GCs are highly diversified and composed of

multiple different clones [153]. In the late GCs (20 days post-immunization), selective clonal expansion may have led to the single-colour dominance of each late GC, while a small proportion of GCs were still highly diversified in terms of colour dominance. However, affinity maturation occurred in both single-colour dominant GC and colour diversified GC. This phenomenon suggests that GC selection does not inevitably lead to high clonal dominance. Similarly, another independent study showed that GC B cells from complex-antigen-immunized mice exhibited enrichment of high-affinity clones. However, this *in vitro* single cell analysis also demonstrated that GC reactions to complex antigens generate a broad range of specificity and affinities, which could result in advantages for broad protection [154]. These studies provide new insights that GC selection is not as strict as we expected.

1.2.6 Post-GC cell fate decision

PCs secreting high-affinity antibodies and long-lived memory B cells are derived from the optimal GC reaction. The high-affinity antibody-secreting PCs mainly home to the bone marrow, while the long-lived memory B cells circulate in the lymph and blood system. However, the differentiation of these cell lineages is generated at different time points and determined by distinct mechanisms. The fate decision of GC B cells is determined by multiple factors, which will be reviewed in this section.

1.2.6.1 Memory B cell formation

Based on the surface Ig isotype expression, three types of memory B cell are derived from the GC reaction, including $IgG1^+$, IgM^+ and IgA^+. The underlying molecular mechanism for the differentiation of memory B cells from GCs remains unclear. Taking

advantage of different transgenic mouse models, several studies have provided new insights about memory B cell differentiation. The GC B-cell-specific inducible *in vivo* tracking mouse model clearly showed that GC-dependent $IgG1^+$ memory B cells are derived from $IgG1^+$ LZ GC B cells with a relatively low affinity at the early stage of the GC reaction, through a CD40-BACH2 dependent mechanism [155]. Recently, Shlomchik and colleagues showed that maturation of the GC reaction promotes the sequential formation of memory B cell subsets and long-lived PCs[156]. Consistent with a previous study, the differentiation of $IgG1^+$ memory B cells occurs in the early phase of the GC reaction and reaches its peak at day 8 post-immunization, while the generation of long-lived PCs starts from day 14 until more than 5 weeks post-immunization. Due to the longevity of memory B cells, the anti-apoptotic proteins are also required for memory B cell formation. For example, forced over-expression of BCL2 and BIM leads to the expansion of IgG^+ antigen-specific memory B cells [138]. Cytokine IL-21, which is critical for T_{fh} expansion, serves as a negative regulator of GC-dependent memory B cell formation since IL-21R-deficient mice show biased expansion of antigen-specific memory B cells with germline Ig sequences [76]. Although SHM and CSR are both required for the affinity maturation and diversity of Ig class antibodies, their specific functions in the post-GC decision are difficult to distinguish since both functions are initiated by AID. A recent study separating the function of CSR and SHM, using *Aicda* engineered CSR reporter mice with impaired SHM, demonstrated that $IgG1^+$ BCR promotes the formation of bone marrow PCs and attenuates memory B cell fate without affecting clonal expansion in GCs [157]. Additionally, memory B cells with polyreactive

BCRs show a reduced lifespan, suggesting that AID-mediated SHM can negatively affect the longevity of memory B cells. Consistently, Marc K. Jenkins also showed that IgM^+ memory B cells possess a longer lifespan compared to isotype-switched subsets. However, the IgG1+ memory B cells have dominant roles in the secondary response since these cells can be rapidly activated and differentiated into PCs [158]. The less-mutated IgM^+ memory B cells may be the backup reservoir for memory responses when the isotype-switched memory B cells disappear [159].

1.2.6.2 PCs differentiation

The molecular mechanism behind PCs differentiation has been well studied during the past decade. The generation of PCs requires transcriptional re-programming towards a PC transcriptome in GC B cells, such as upregulation of PC master transcription factors *Irf4*, *Blimp1* and *Xbp-1*. As discussed above, IRF4 is a unique protein in both the GC B and the PC transcription regulatory networks. In GC B cells, IRF4 binds to *Pu.1* and *Batf* to form a stable complex to promote the GC fate and CSR in a dose-dependent manner [160, 161]. Once reaching a certain threshold, high levels of IRF4 can repress *Bcl6* and activate *Prdm1*-related transcription factor zinc finger and BTB domain-containing protein 20 (*Zbtb20*), which activates the downstream targets that can initiate the PC transcriptome [162].

BLIMP1 is a transcriptional repressor of B cell-linage genes (*Pax5*, *Bach2* and *Bcl-6*) and is exclusively expressed in plasmablasts and PCs. However, plasmablasts and PCs possess different levels of BLIMP1, and its function in initiating PC differentiation and maturation is still unclear. Stephen Nutt and colleagues reported that *Prdm1*-deficient B

cells were able to differentiate into PCs with a low amount of immunoglobulin production, suggesting that BLIMP1 is required for the full PC differentiation and function, but not the initiation [163]. These *Prdm1*-deficient PCs also had a smaller size than control PCs had, with severe disruption of the distinctive, dense endoplasmic reticulum and impaired lysosomal trafficking, which could explain the insufficient immunoglobulin secretion in *Prdm1*-deficient PCs [164]. Notably, the function of BLIMP1 in the unfolded protein response (UPR) is not only restricted to the activation of key transcription factors such as *Atf6*, *Xbp1* and *Ern1* but also directly bound to 38% of UPR genes expressed in PCs. Thus, the transcription repressor BLIMP1 is critical for the functional maturation of PCs through a UPR-dependent mechanism.

Several other factors are also involved in this post-GC fate decision. For instance, the epigenetic modifier histone methyltransferase enhancer of zeste homologue 2 (EZH2) can protect GC B cells from AID-induced genotoxic damage [165, 166]. Moreover, Stefano Casola and colleagues found that EZH2 could directly modify histone H3K27me3 to repress PC programming through modifying the expression of *Irf4* and *Prdm1*. Another histone acetyltransferase, epigenetic modifier monocytic leukaemia zinc finger protein (MOZ), is also involved in the regulation of the post-GC decision [167]. Although the *Moz*-deficient mice show a decreased GC reaction and reduced affinity maturation, the antigen-specific memory B-cell formation was enhanced, which suggested that the MOZ could influence the lineage commitment between PCs and memory B cells. Interestingly, the NF-κB subunit RELA, not c-REL, is specifically required for PC differentiation from GC B cells by inducing BLIMP1 expression through an IRF4-independent pathway[168].

Although the signal that triggers memory B cell differentiation is still unknown, the driven stimulus for high-affinity GC B cell differentiation into PCs has been well studied. The $IRF4^{+}$ plasmablast precursor is initiated in the LZ and then migrates to the DZ to complete the process of PC differentiation [169, 170]. Based on current data for affinity-based selection, migration pattern, cell-cell interaction and asymmetric cell division, a mathematical model LEDA (GC B cell selection, division and exit) has been developed. It shows that high-affinity GC B cells that acquire help from T_{fh} cells and antigens from FDCs migrate to the DZ for asymmetric division into two distinct daughter cells. The cells without antigens differentiate into PCs and leave the GC [171]. Consistent with the LEDA model, Robert Brink and colleagues have shown that a majority of early PC precursors (characterized as $IgG1^{hi}$ and $BLIMP1^{lo}$ GC B cells) are located in the LZ, while late PC precursors (characterized as $IgG1^{lo}$ and $BLIMP1^{hi}$ GC B cells) are located in the DZ [172]. The CD40 signal from T_{fh} cells and the BCR signal from FDCs are both required; the CD40 signal is responsible for the initiation of PC programming and BCR signalling is required for the completion of the programme. Mechanically, Riccardo Dalla-Favera's group found that CD40 signalling can directly promote BCL6 degradation and IRF4 upregulation, which lead to the loss of GC B cell identity and direct cell differentiation into plasmablasts [173].

1.3 Protein Ubiquitination

Protein ubiquitination is a post-translational modification process. The researchers Avram Hershko, Aaron Ciechanover and Irwin Rose were rewarded the 2004 Nobel Prize in Chemistry for their pioneer work on the ubiquitin system during 1978-1980[174]. Their

initial studies showed that the degradation of reticulocytes is dependent on the availability of ATP and requires one small heat-stable protein. Moreover, they found that the substrates become larger in terms of molecular weight [175]. Later, they identified that the heat-stable protein was ubiquitin protein (Ub). Then, this novel proteolytic pathway was termed UPS, the ubiquitin-proteasome system, including proteasomal-mediated degradation and non-proteasomal fates of ubiquitination.

Ubiquitination is a broad and diverse intracellular event, as recent proteomic studies have revealed a large number of ubiquitinated proteins that have yet to be described. The translocation of membrane, cytosolic and nuclear proteins is initiated through ubiquitination. Histone and transcription factors can also be ubiquitinated, which leads to the regulation of gene expression. Ubiquitination is also involved in several branches of signalling pathways by the modification of key regulators or adaptor proteins. It has also been shown that cell metabolic pathways are regulated through a ubiquitin-dependent mechanism. Proteins can be ubiquitinated on a single or multiple lysine residues, leading to two different types of protein ubiquitination: monoubiquitination and multiubiquitination. Proteins can also be subjected to polyubiquitination through several rounds of adding Ub to proteins to form polyubiquitination chains. The detailed process of ubiquitination will be introduced in the following section.

1.3.1 The process of ubiquitination

This step-wised intracellular event requires three enzymes: E1 (ubiquitin-activating enzyme), E2 (ubiquitin-conjugating enzyme) and E3 (ubiquitin ligase). Twenty-one E1

enzymes, 37 E2 enzymes and more than 600 E3 ligases have been identified [176, 177]. The first enzyme, E1, activates ubiquitin through an ATP-dependent manner. The ubiquitin carboxyl group located at the C-terminal is adenylated and transferred to a cysteine residue on E1. Then, the activated ubiquitin is transferred from E1 to E2. The E2 enzyme further associates with the complex containing E3 and the substrate. There are two types of E3 ligase: RING/U-box and homologous with E6-associated protein C-terminus (HECT). E2-ubiquitin can directly transfer ubiquitin to RING/U-box-associated substrates. In the case of HECT-type E3, E2-ubiquitin must first transfer the ubiquitin to an E3 cysteine sulfhydryl before transfer to the substrate. The ubiquitination can repetitively occur on the same substrate through either additional sites or the same site. Different types of ubiquitination can result in diversified downstream outcomes. For example, polyubiquitinated proteins can be recognized by ubiquitin-binding proteins and sorted to the proteasome complex [178]. In the proteasome, the substrates are de-ubiquitinated, unfolded and degraded into peptides.

Ubiquitin is a 76-amino acid polypeptide with a molecular weight of approximately 8500 Da, containing seven lysine residues: K^{6}, K^{11}, K^{27}, K^{29}, K^{33}, K^{48} and K^{63}. All these lysine residues can be potentially ubiquitinated and form isopeptide-linked ubiquitin chains [72, 179, 180]. Among those chains, more than 50% of the linkage in cells is the K^{48}-linked chain, which is characterized as the label for proteasome-mediated degradation [181]. The K^{63} linkage chain is considered a non-degradative signal that is involved in inflammatory signalling and NF-κB activation [182]. The remaining 'atypical' ubiquitin modifications are still under extensive study. One study showed that K^{6}- and K^{33}-linked

chains are highly upregulated upon UV genotoxic stress, indicating their important role in the DNA damage response [183]. Combined with Met1-linked chains, K^{11}-linked chains are involved in cell cycle regulation[184]. The K^{29}-linked chain is assembled by the HECT E3 ligase and involved in proteasome degradation since the K^{29}-linked chain is highly enriched in proteasome-inhibitor-treated human cell lines [185]. K^{33}-linked chains are assembled by HECT E3 ligase AREL1, which is responsible for post-Golgi membrane protein trafficking [186]. Therefore, the formation of the ubiquitin chain type is dependent on the availability of E3 ubiquitin ligases.

1.3.2 E3 ubiquitin ligases

E3 ubiquitin ligases are a large and diverse group of proteins, which can be divided into three types based on their functional domains and the method of transferring ubiquitin to substrate proteins. RING E3s are the most abundant type of ubiquitin ligase, characterized by the presence of a unique zinc-binding (RING finger domain) domain or a U-box domain [175]. Due to the RING finger domain and U-box domain, the RING E3s can act as a scaffold protein to promote E2-ubiquitin-complex direct transfer of ubiquitin to substrate proteins. The RING E3s can function as monomers, homodimers or heterodimers. For instance, cullin-RING ligases (CRLs) form the E3 ubiquitin ligase complex, composed of a cullin scaffold, RING-BOX domain and adaptor protein, as well as a substrate receptor. In the RING E3 family, the anaphase-promoting complex/cyclosome (APC/C) is another important multi-subunit member. CBL proteins belong to the RING E3 family, which will be introduced in the following section.

Another two types of E3 ligase are HECT E3 and RBR (RING-between-RING). The C-terminus of HECT contains the functional domain, with a bi-lobar architecture, the N-terminal lobe, for interacting with ubiquitin-E2 [187]. The C-terminal determines the catalytic activity and substrate specificity. In humans, there are three subfamilies of HECT, including the NEDD4 family, the HERC family and others. Similar to HECT E3s, the RBR E3s also require a two-step reaction to transfer the ubiquitin from E2 to the substrate. There are two predicted RING domains on the RBR, which are separated by an IBR (in-between-RING) domain.

1.4 Structure and Function of the CBL Family of Proteins

The CBL (Casitas B-lineage Lymphoma) family proteins in mammalian cells are composed of three evolutionary conserved members, including CBL, CBLB and CBLC. In 1989, Herbert Morse III and colleagues first identified the short version of CBL protein (called v-CBL) from a murine retrovirus, which can induce pre-B and pro-B cell lymphomas [188]. Sequencing results revealed that this 100 kDa protein carried by this retrovirus showed no homology with any known oncogenes. v-CBL does not have any kinase activity but is expressed in a range of haematopoietic lineage. Later, W. Langdon's group further discovered the 120 kDa full-length CBL protein localizing in the cytoplasm, with a cytosolic and cytoskeletal distribution [189]. Although v-CBL is oncogenic due to its nuclear distribution, the full-length CBL proteins cannot induce acute transformation. Another two mammalian members plus their invertebrate orthologues in *Drosophila melanogaster* (D-CBL) and *C. elegans* (SLI-1) have been identified and are highly conserved in structure. Further studies have demonstrated that

CBL family proteins are E3 ubiquitination ligases, which can recruit ubiquitin-conjugating enzymes (UBCs), as well as tyrosine kinase Sky and Zeta-chain-associated protein kinase (ZAP70), to form complexes. To date, extensive studies have been carried out to demonstrate their important role in different signalling pathways, which will be introduced in the following sections.

1.4.1 The Structure of CBL proteins

The domain structures of CBL proteins are depicted in Figure 1.3. The N-terminal region of all three CBL proteins include a tyrosine kinase binding (TKB) domain, a RING finger domain, and a linker region and is highly conserved between the three members of CBL family proteins. CBL and CBLB are ubiquitously expressed in all haematopoietic lineages, while CBLC is mainly expressed in the gastrointestinal tract, liver, kidney, pancreas and prostate [190, 191]. CBLC is shorter compared to the other two members due to the lack of the key C-terminal domains and carboxy-terminal leucine zipper (LZ) motif. The TKB domain consists of a four-helix bundle, a calcium-binding EF hand domain and a variant Src homology-2 (SH2) domain, which directly binds to specific pY-containing peptide, such as epidermal growth factor receptor (EGFR), SYK, ZAP70 and the platelet-derived growth factor receptor (PDGFR) [192-195]. This protein-binding capacity allows CBL proteins to act as adaptor proteins for signal transduction. Apart from the adaptor function, CBL proteins can also serve as E3 ubiquitin ligases, as the RING finger domain was shown to be required for recruiting E2 ubiquitin-conjugating enzymes. Further studies have shown that the point mutation of a cysteine to an alanine substitution at amino acid 373 located at the RING finger domain of CBL-B (CBL-

BC373A) can completely block the ubiquitination of downstream substrates. The C-terminal proline-rich domain of CBL and CBL-B provide a platform to interact with SH3

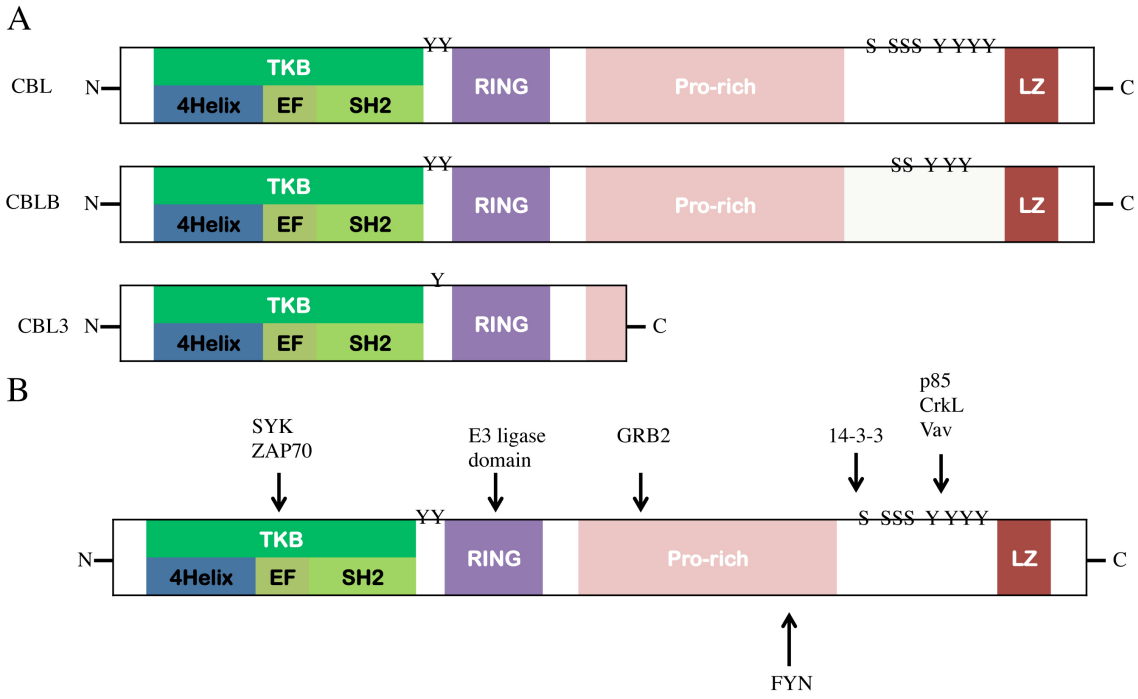

Figure 1.3. The structure of CBL family proteins and corresponding functions

(A) The individual domain of the three members of the mammalian CBL family proteins is highlighted. All of those three members have TKB domain and RING finger domain. TKB domain includes 4H, EF and SH2 domain, the function of which is recruiting phosphorylated tyrosine kinases. The following domain is RING finger domain, which is critical for the E3 ubiquitin ligase function. Proline-rich domain and UBA domain locate at C-terminal, which are deleted in CBL-3. (B) The functional domains of CBL family proteins. The TKB domain can bind to phosphorylated tyrosine on tyrosine kinases, such as SYK, ZAP70 and SRC-family kinases. The RING finger domain is required for the recruitment of ubiquitin (Ub)-conjugate enzymes (E2s). Then the E2s are transferred to TKB domain leading to the proteasomal degradation of the binding substrates. The Proline-rich domain can associate with many SRC-homology 3 (SH3)-binding proteins, such as GRB2, NCK and FYN. There are several tyrosine and Serine residue at the C-terminal region, which can be phosphorylated and interact with the proteins containing SH2 domain such as VAC, p85 and 14-3-3 family proteins.

domain-containing proteins such as Src-family kinases, GRB2, CIN-85, etc. There is an LZ motif domain located near the C-terminus of CBL and CBL-B, which may help to form homo- or heterodimers of CBL. There are three tyrosine residues in this region, which can be phosphorylated upon cellular activation and are associated with different downstream signalling proteins, such as VAV2, p85 and CRKL [196-198]. Finally, the UBA domain of CBL and CBL-B is able to mediate ubiquitin-dependent dimerization and target polyubiquitinated proteins to 26S proteasome for degradation [199].

1.4.2 Roles of CBLs in the function of T Cells

The function of CBL family proteins in T cell development and activation has been well studied during the past decade. The CBL family proteins regulate thymocyte development through two distinctive mechanisms, thymic selection and MHC-dependent signals. Thymic development consists of positive selection and negative selection based on the strength and duration of TCR signals. The optimal TCR signalling strength is required for the proper thymocyte development. Either too strong or too weak signalling can lead to negative selection or cell death [200, 201]. The deletion of CBL in 5C.C7 H-Y TCR transgenic mice results in the expansion of $CD4^+$ T cells in the thymus, which suggests that CBL, not CBLB, is a negative regulator of $CD4^+$ T cell lineage commitment [202], which may be due to the ZAP-70 dependent hyper-activation of TCR signals in *Cbl*-deficient thymocytes [203]. In CD4 and CD8 double-positive (DP) thymocytes, CBL not only negatively regulates ZAP-70 activation but also suppresses TCR-induced activity of MAPKs and ERK1/2. As mentioned above, the MHC-dependent signals are also critical for the maturation and selection of DP thymocytes to $CD4^+$ or $CD8^+$ single-

positive thymocytes. The ablation of both CBL and CBLB can drive the differentiation of DP thymocytes into $CD4^+$ and $CD8^+$ single-positive thymocytes in the absence of TCR-MHC engagement, which suggests that CBL proteins provide another layer of regulation of thymocyte development through an MHC-independent mechanism. The impaired ubiquitination of CD3ζ and pre-TCR down-modulation in *Cbl* and *Cblb* double-deficient DP thymocytes lead to constitutive activation of pre-TCR signals, which can bypass the positive selection signal.

Two signals are required to achieve full T cell activation. The first signal is delivered by the cognate interaction between the TCR complex and the peptide-loaded MHC accompanied by the second co-stimulatory signal from antigen presenting cells. Among the co-stimulatory molecules expressed on T cells, CD28, the receptor of CD80 and CD86, is the most prominent one, which activates NF-κB, NFAT and AP-1 [204]. Two independent studies have shown that *Cblb*-deficient T cells produce a large amount of IL-2 upon anti-CD3 stimulation alone without anti-CD28 co-stimulation, suggesting that CBLB is a negative regulator in CD28-induced signalling [90, 205]. In detail, CBLB regulates CD28 signalling through the VAV pathway since anti-TCR can solely induce a high level of VAV activation in CBLB-deficient T cells. In contrast, the induction of VAV activation requires both anti-CD3 and anti-CD28 stimulation in wild-type counterparts. Another downstream target of CD28 signalling is PI3K. In the Jurkat cell line, CBLB promotes the ubiquitination of p85 PI3-K and prevents the association of p85 with CD28 after TCR stimulation [206]. However, a recent study showed that CBLB may indirectly inhibit PI3K by suppressing phosphatase and tensin homolog (PTEN)

inactivation[207]. CBLB is critical for this regulation, as it can recruit another E3 ubiquitin ligase (NEDD4) to promote ubiquitination of PTEN.

During the past decade, many studies have demonstrated that CBL proteins also play a significant role in immunosuppression and anti-tumour immunology. TGF-β, secreted by tumour cells and tumour-infiltrating Tregs, can suppress T cell activity and promote the immune evasion of tumour cells. TGF-β–induced suppressive signal is regulated through CBL proteins. *Cblb*-deficient mice can efficiently reject or reduce the growth of three different tumour cell lines *in vivo* through CD28-independent mechanism [208, 209]. *Cblb*-deficient $CD8^+$ T cells are resistant to TGF-β suppression since SMAD7, a negative regulator of TGF-β signalling, cannot be ubiquitinated [210]. Consistently, the ablation of SMAD7 in *Cblb*-deficient mice restores the TGF-β suppression signal and leads to tumour growth and similar survival rates as those in wild-type controls. Moreover, CBL proteins are also involved in negative regulation of PD-1 signalling in $CD8^+$ T cells [211]. The blocking of programmed cell death ligand 1 (PD-L1) on DCs suppresses the up-regulation of CBLB in $CD8^+$ T cells after OVA antigen stimulation, leading to enhanced cytotoxicity and an anti-tumour immune response in the EG.7 tumour mouse model. Another potential anti-tumour target, cytotoxic T-lymphocyte-associated protein 4 (CTLA-4), is also regulated by CBLB. Stimulation of CTLA-4 on $CD8^+$ T cells leads to up-regulation of CBLB expression through transcriptional regulation [212]. Taken together, due to the negative role of CBL proteins in T cell activation, CBLs will be a promising target for tumour immunotherapy in the future.

1.4.3 Roles of CBLs in B cell activation

The CBL-B protein becomes phosphorylated upon BCR stimulation, and the protein level reaches the peak at 2 min and then decreases to approach undetectable levels by 30 mins, which suggests that CBL-B protein plays a direct role in BCR signalling. The CBLB proteins have been clearly shown to associate with the protein tyrosine kinase SYK and promote ubiquitination of SYK after BCR stimulation. A few key target proteins of BCR signalling, such as BLNK, BTK and PLC-γ2, are constitutively phosphorylated in CBLB-deficient B cells, which leads to hyper-responsiveness of Ca^{2+} signalling. However, CBL-B deficiency does not appear to affect the direct downstream targets of PI3-K path way Akt, but ERK1/2 and JNK showed prolonged phosphorylation upon BCR cross-linking. Because of the hyper-activation of BCR-induced signalling, these mutant B cells form a prolonged BCR cap after BCR stimulation. Interestingly, although CBL and CBL-B share similar structure domains and play several redundant functions in T cell activation, these two proteins show opposite functions in BCR-mediated signalling. In a *Cbl*-deficient DT40 B cell line, CBL negatively regulated the phosphorylation of PLC-γ2 though its adaptor function [213]. Mechanically, the SH2 domain of CBL competes with the PLC-γ2 SH2 domain for the association with BLNK, leading to the inhibition of PLC-γ2 activation. Consistently, CBL in mouse B cells also serve as a positive regulator for BCR-mediated signalling [214]. Cbl-deficient B cells showed reduced phosphorylation of tyrosine kinases SYK and BTK, while CD19-mediated PI3-Kinase activity is enhanced. The TNF-R family member CD40 plays a critical role in B cell function and homeostasis. *Cblb*-deficient B cell displays reduced proliferation of upon CD40 stimulation and an

enhanced T-dependent antibody response through a cell intrinsic mechanism. CBL-B selectively suppresses the CD40-induced activation of NF-κB and JNK through inhibiting the association of TNF receptor-associated factor 2 (TRAF2) with CD40 for the activation of downstream signals.

To study the function of CBL and CBL-B in B cell activation and to exclude the functional redundancy between the two proteins, B cell-specific deletion of both *Cbl* and *Cblb* transgenic mice were generated in our laboratory [215]. More than half of the mutant mice produced IgG-isotype anti-dsDNA and anti-nuclear antigens. Further pathological studies showed that these mice developed a spontaneous systemic lupus-like autoimmune disease characterized by massive infiltration of leukocytes in multiple organs and heavy IgG antibody deposits in the kidney glomeruli. Although mutant B cells displayed enhanced BCR signalling, the mutant mice were not hyper-responsive to *in vivo* or *in vitro* antigen stimulation, suggesting that the SLE autoimmune disease was not due to enhanced BCR signalling. By crossing CBL double-deficient mice to soluble HEL (sHEL) and HEL BCR (Ig^{HEL}) transgenic mice, the mutant mice clearly showed impaired B-cell anergy to self-antigens, which demonstrated that CBL proteins controlled the B-cell tolerance through regulation of B-cell anergy.

1.4.4 Role of CBLs in other immune cells

CBL proteins are not only critical for T and B cell activation and functions but also involved in the regulation of innate lymphocyte lineages, such as DCs, myeloid cells and NK cells. NK cells are specialized in cytotoxic effector functions and modulate the local

immune response, and NK cells are critically required for the immunosurveillance of

increased proliferation and perforin levels, as well as increased cytotoxicity, resulting in

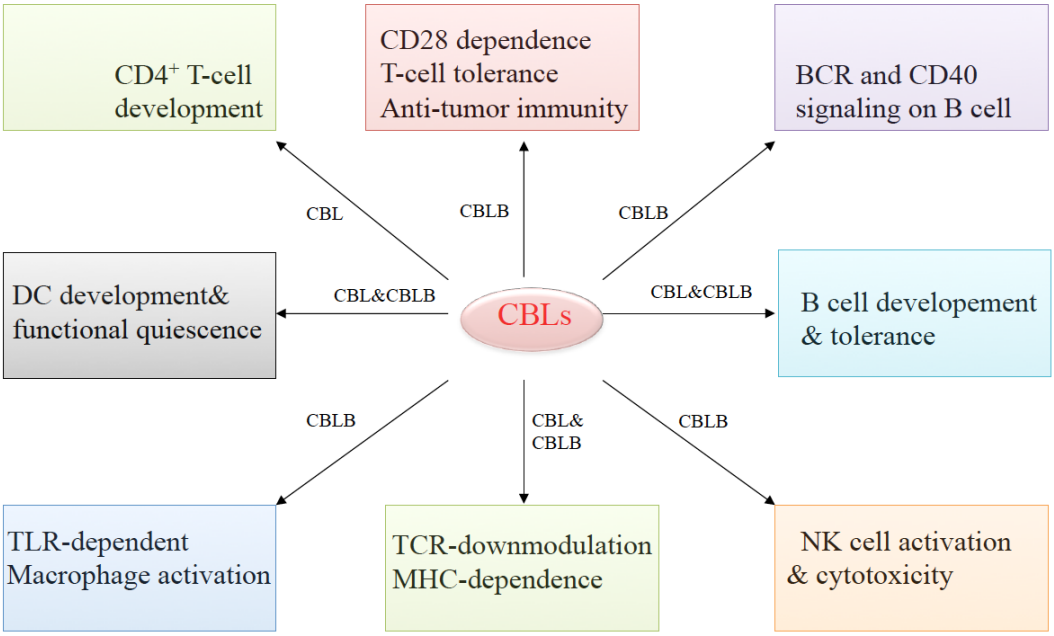

Figure 1.4. Function of CBL family proteins in immune cells activation

The function of CBL family proteins in adaptive and innate immune cells is highlighted. CBL regulates the $CD4^+$ T cell development. Two different studies demonstrated that CBLB regulate T cell activation through CD28-dependent machinery and anti-tumor immunity. The CBL and CBLB proteins are negative regulator of TCR signalling and MHC-dependent thymocytes selection. These two proteins also negatively regulate B cell tolerance and signalling through BCR and CD40. In innate immune cells, CBL proteins also act as a negative regulator in terms of cell activation and function.

increased proliferation and perforin levels, as well as increased cytotoxicity, resulting in prolonged survival and reduced metastasis in B16F10 melanomas model [216].

Interestingly, NK cells with point mutations in the CBLB ring finger domain showed a similar phenotype as *Cblb*-deficient NK cells, which suggests that the E3 ligase activity is necessary for this effect. The TAM family of cell-surface tyrosine kinase receptors on NK cells were identified as the top ubiquitination target of CBLB *in vivo* and *in vitro* through the downregulation of these receptors. Small molecule inhibitors of TAM receptor kinases increase NK cell cytotoxicity, as seen in *Cblb* knockout mice. CBL plays a critical role in NKG2D- and CD244-mediated synergistic activation signals [217], which is mediated by the phosphorylation of a combination of tyrosine residues on the adaptor protein SLP-76[218]. Taken together, CBL proteins played a negative role in the modulation of NK cell activation and cytotoxic function.

Recently, David Spencer's group reported that CBL modulates the activation status of DC through Toll-like receptor (TLR) [219]. Upon the TLR stimulation, many pro-inflammatory cytokines and chemokines, such as IL-1a, IL-1b, IL6, IL-12p70 and CXCL1/KC, were upregulated in *Cbl*-deficient DCs, correlating with a greater potency of DC-based vaccines against established tumour. In detail, *Cbl* deficiency reduced both p50 and p105 levels, which led to increased NF-κB activity. By using the ectopic expression of different forms of CBL mutants, this pro-inflammatory phenotype of *Cbl*-deficient DC was caused by the lack of E3 ubiquitin ligase activity. Not surprisingly, CBLB is also highly expressed in DCs and acts as a negative regulator for TLR-mediated DC activation [220]. Bone-marrow-derived DCs with CBL-B deficiency exhibit higher levels of pro-inflammatory cytokines and slightly enhanced antigen presentation ability.

In comparison with other cell types, the role of CBL proteins in the myeloid lineage has been less studied. CBLB proteins also act as a negative regulator of TLR-triggered signalling in macrophages. The tyrosine kinase SYK is activated by integrin CD11b, leading to degradation of the TLR adaptor proteins MYD88 and TRIF through CBLB-mediated ubiquitination [221]. In the context of high-fat diet (HFD)-induced obesity, *Cblb*-deficient mice show exaggerated HFD-induced insulin resistance through saturated fatty-acid mediated macrophage activation, which is restored by blockade of TLR4 signalling[222]. *Cbl*-deficient mice showed massive macrophage infiltration and activation, leading to peripheral insulin resistance[223].

1.5 Rationale

GC reaction is a step-wised process each of which is controlled by different mechanisms and involved different subsets of cells. At the initiation stage of the GC reaction antigen activated B and T cells must meet each other to form cognate interaction so that only antigen specific B and T cells are allow to continue development into GC cells. In this interaction, GC B cells are the major player because they may capture antigen, process antigen into antigen peptide-MHC-II complexes, and present these antigenic complexes to T cells. However, while we already knew that antigen capturing requires BCR and antigen interaction, the molecular mechanisms that control B cell antigen processing remains not fully understand. Previous studies in our laboratory have shown that CBL proteins play a redundant, however, critical role in promoting antigen-induced TCR and BCR downmodulation. These findings thus suggest that CBLs could act as a central

regulator to control B cell antigen processing, hence the cognate interaction of T and B cells responsible for the initiation of the GC reaction.

Once B cells enter the GC, SHM of the Ig genes, selection and expansion for the mutated high affinity B cells occur through the GC DZ and LZ cycle. At this stage, SHM B cells must decide whether to stay in the DZ and LZ cycle to continue this selection or opt to differentiate into PCs or memory B cells. While it has been shown that BCR and CD40 signals are involved in this regulation, they seem to promote both GC B cell fate and PC differentiation. In this regard, it is reasonable to assume that some B cell intrinsic regulators are need to interpret the strength of incoming BCR and CD40 signals so that B cells with moderately improved affinity stay in the DZ and LZ cycle and only those B cells with sufficiently high affinity are allowed to differentiate into PCs. Our previous studies demonstrate that CBL proteins may modulate the strength of TCR signalling through ubiquitinating multiple TCR downstream signalling molecules. These results thus suggest that CBLs can be good candidates in this regulation and play a important role in resolving the strength of BCR and CD40 signalling in GC B cells, consequently determine the cell fate of GC B cells during GC B cell affinity selection.

1.6 Hypothesis

My central hypothesis is that CBL proteins may control the GC reaction at two critical checkpoints, the initiation stage of GC reaction and selection and expansion stage of high affinity GC B cells, through different cellular mechanisms. For the first stage, they control the initiation of GC B cell development through dictating T-B cognate interaction. They may do so by regulating B cell antigen presentation, specifically

through ubiquitinating the components of BCR complex, Igα and Igβ, consequently controlling BCR-antigen complex internalization and sorting to the lysosomal compartment for antigen degradation and processing. For the second stage, CBL family proteins may regulate antibody affinity maturation by retaining GC B cells in the DZ and LZ GC cycle and preventing GC B cell from differentiation into PCs until high affinity BCRs are generated. This regulation is achieved through post-transcriptionally controlling the ubiquitination dependent clearance of IRF4, a transcription factor that is constantly induced in GC B cells by BCR and CD40 signals and may determine and drive B cell differentiation to PCs during GC reaction. By spatial and temporal control of IRF in GC B cells, CBLs determines that only high affinity B cells that may degrade CBLs are allowed to terminate GC fate and differentiate into PCs

1.7 Aims and Objectives

Aim 1: To understand the role and mechanisms of CBL-mediated ubiquitination in establishment of the cognate T-B cell interaction and initiation of the GC reaction.

Objective:

1. To establish an animal model that specifically ablated CBL and CBLB in naïve B cells (termed here as $CBL^{dKO\text{-}Mb1}$ mice) and analyzed the general impact of such a mutation in B cell early development.
2. To study the function CBL proteins in B cell function. This included comparing *in vitro* B cell activation and differentiation and *in vivo* T-dependent and T-independent antibody responses between WT and $CBL^{dKO\text{-}Mb1}$ mice.

3. To investigate the impact of the $CBL^{dKO\text{-}Mb1}$ mutation in GC reaction upon immunization with T-dependent antigens.
4. To elucidate the cellular mechanism by which CBL used to control cell extrinsic factors, T_{fh} development, and FDCs network.
5. To understand the molecular mechanism by which CBLs controlled T-B cognate interaction and T_{fh} cell development.
6. To identify the direct targets of CBL proteins in the regulation of B cell antigen presentation by biochemical studies. To evaluate the relevance of ubiquitin modification of these targets to their function during GC reaction.
7. To determine whether CBLs exert their GC regulatory function through E3 ubiquitin ligase activity.

Aim 2: To investigate the role of CBL proteins in the progression of the GC reaction and antibody affinity maturation.

Objective:

1. To understand the dynamics of CBL and CBLB expression during GC B cell development and differentiation by immunofluorescence and biochemical studies.
2. To study CBLs function in already established GC B cells, I generated a mutant mouse model carrying the CBL and CBLB double null mutation in GC B cells using the Cγ1-CRE transgenic allele ($CBL^{fl/fl}$ $CBLB^{-/-}$ Cg-Cre tg; termed as $CBL^{dKO\text{-}Cg}$ mice). I used this animal model to study antibody affinity maturation and GC B cell development after T-dependent antigen NP-KLH immunization.

3. To investigate the impact of CBLs on antibody affinity maturation by analyzing the SHM of Ig genes and clonal selection of GC B cells in immunized WT and $CBL^{dKO\text{-}Cg}$ mice.
4. To study whether CBLs influence antibody affinity maturation through controlling the B cell proliferation or differentiation of PCs by both *in vivo* and *in vitro* methods.
5. To identify the direct target(s) of CBLs in the regulation of GC B cell affinity selection by transcriptome and biochemistry studies.
6. To determine whether CBLs control GC affinity selection through their ubiquitin ligase function. To examine whether the putative target(s) identified in my study is relevant to the GC phenotypes observed in $CBL^{dKO\text{-}Cg}$ mice.

2 Chapter 2: CBL-mediated ubiquitination controls the initiation of GC reaction

Xin Li[1,2], Daisuke Kitamura[4], Wallace Y. Langdon[5]& Hua Gu[1,2,3,6]

[1]Montreal Clinical Research Institute, Montreal, QC H2W 1R7, Canada

[2]Department of Microbiology and Immunology, University of Montreal, Montreal, QC H3T 1J4, Canada

[3]Division of Experimental Medicine, McGill University, Montreal, QC H3A 0G4, Canada

[4]Research Institute for Biomedical Sciences, Tokyo University of Sciences, Noda, Chiba 162-8601, Japan

[5] School of Biomedical Sciences, University of Western Australia, Crawley, Western Australia 6009, Australia

[6]Lead Contact

2.1 Summary

Germinal center (GC) is a microlympoid organ located in peripheral lymphoid tissues and its function is to generate high affinity antibody secreting PCs and memory B cells. While development of the GC requires the cognate interaction between antigen specific follicular (FO) B cells and $CD4^+$ T cells, it remains unclear about the mechanisms as to how B cell intrinsic molecules control the cognate interaction. In my studies, I have found that E3 ubiquitin ligases CBL and CBLB (CBLs) controlled both T-independent antibody response and GC dependent antibody production. In the former case, CBLs are required for the development of marginal zone B cells, so that in the absence of CBLs the type-I T-independent antibody response is deficient. In contrast, in the latter case, although ablation of CBLs does not affect FO B cell development, it impairs the development of T follicular helper (T_{fh}) cells, thus the germinal center reaction. My further studies reveal that CBLs control BCR-mediated antigen internalization and sorting to lysosomes for degradation, impairment of which leads to defective B cell antigen presentation to T cells, consequently disrupting the cognate interaction between antigen specific B and T cells. Using biochemical and genetic approaches, I have found that CBLs control BCR internalization by promoting the ubiquitination of BCR-associated molecules Igα and Igβ. Disruption of Igα ubiquitination is sufficient to recapitulate the GC phenotypes observed in CBL-ablated mice. My findings for the first time identify a novel ubiquitination-dependent regulatory pathway in BCR-mediated antigen presentation, rather than BCR signalling, in the initiation of the GC program.

2.2 Introduction

GC reaction emerges in secondary lymphoid organs upon vaccination or infection, which can generate high affinity secretion PCs and long-lived memory B cells [51, 94]. The GC B cells are mainly derived from FO B cells. The initiation of GC B cells requires different cell-cell interaction such as B-DC and T-B, in which multiple receptors and ligands ligation are involved. Within GC reaction, the maturation and termination the fate of GC B cells are also dependent cell-cell interaction[52]. BCR mediated signals plays a critical role throughout the whole process.

B cell development, survival and differentiation are all dependent on BCR mediated signals. The ligation between antigens and BCR lead to two distinct branches of activation. First, the adaptor proteins of BCR, Igα and Igβ, are phosphorylated by tyrosine kinase SYK, then lead to phosphorylation of BLNK [224], which lead to the activation of multiple different signalling pathways such as PI3K, Erk1/2, NF-κB and $Ca2^{+}$ influx [225, 226]. Second, the BCR complex can capture, degrade and deliver the antigen peptides to the MHC class II antigen-presenting compartment through endocytic pathway. The trafficking of membrane proteins to lysosomes for degradation is dependent on proper cell signalling and membrane metabolism. Ubiquitination promotes this process by marking which proteins should be transported to lysosome through multivesicular endosome pathway [227]. Upon BCR stimulation, Igα and Igβ are ubiquitinated by multiple different E3 ubiquitin ligases such as ITCH, CBL and CBLB [120, 228, 229]. Although both Igα and Igβ are required for receptor internalization upon BCR stimulation [230, 231], it has been shown that blockade of Igα not Igβ meditated

signalling through the mutagenesis of ITAM motif suppress the optimal T-dependent immune response. However, previous experiments are mainly focus on function of Igα and Igβ transduced signals not antigen presentation ability in T-dependent antibody response. The function of Igα and Igβ mediated antigen presentation in GC formation is still unknown.

CBL and CBLB (CBLs) are E3 ubiquitin ligase proteins, which play an important role in protein post-transcriptional regulation[232]. Several studies have been shown that CBLs negatively regulate BCR signalling through various molecular mechanisms. However, their function in T-dependent and T-independent immune response is still unclear. Here our findings clearly showed that CBL family proteins played an important role in bone marrow and splenic B cell development. Because Fr.C and Fr.D bone marrow immature B cells were extensively expanded in *Cbls*-deficient mice. The development of MZ B cells was blocked in mutant mice, which lead to the impaired antibody responses against Type-I and Type-II T-independent antigens. In addition, we showed that $CBL^{dKO\text{-}Mb1}$ mice displayed severely impaired GC formation after two different types of T-dependent antigen immunization, which is due to impaired T-B cognate interaction. Our results clearly demonstrate CBL proteins regulate T-B cognate interaction through B-cell intrinsic mechanism. The E3 ubiquitin ligase function of CBL proteins regulates B cell antigen presentation through targeting BCR adaptor Igα and Igβ proteins. Furthermore, the ubiquitination of Igα is critical for the formation of GC B cells since this process initiates the B cell antigen presentation.

2.3 Results

2.3.1 CBL $^{dKO-Mb1}$ mutation controls the development of MZ B cells

2.3.1.1 Generation of CBL $^{dKO-Mb1}$ mice

To study the function of CBL family proteins in B cell development and activation, we generated B-cell specific *Cbl* and *Cblb* knockout mice by crossing Mb1-cre transgenic mice with $CBL^{F/F}$ $CBLB^{-/-}$ mice, termed as $CBL^{dKO-Mb1}$. The resulting mutant mice carried a germline *Cblb* mutation and a conditional Mb1-cre-meidated *Cbl* deletion, resulted with specifically deletion of both *Cbl* and *Cblb* in B cell-linage. To examine whether CBL protein was specifically deleted in B cell linage, we crossed $CBL^{dKO-Mb1}$ mice to $Tomato^{Rosa26}$ reporter mice, in which Tomato was turned on by the *Mb1* gene promoter driven Cre-mediated recombination[233]. Our results clearly showed the Cre recombinase constantly expressed in B-lineage cells starting from B cell progenitors to multiple different subsets of mature B cells (Figure 2.1 A). By contrast, DCs and T cells displayed minimal expression of Cre recombinase (Figure 2.1 A). We further validated the deletion of CBL in splenic mature B cells by western blot (Figure 2.1 B). This result showed that $CBL^{dKO-Mb1}$ mice indeed carried specific *Cbl* and *Cblb* mutations in majority of naïve B cells.

2.3.1.2 CBL mutations affect MZ and B1 B cell development

To determine whether the CBLs double mutation affected early B cell development, we examined immature B cell subsets in the bone marrow and mature B cell subsets in spleen from $CBL^{dKO-Mb1}$ mice. The flow cytometry analysis revealed that the mutant mice

had significant expansion of Fr. C and Fr. D B cells in the bone marrow as compared to WT mice (Figure 2.2 A), while Fr.A and Fr.B B cells were slightly reduced (Figure 2.2 A). B cell development in spleen appeared to be altered in $CBL^{dKO\text{-}Mb1}$ mice, with the mutant mice possessed comparable number of FO ($B220^{+}CD24^{low}AA4.1^{low}CD21^{+}CD23^{+}$) B cells, however, four times less MZ ($B220^{+}CD24^{low}AA4.1^{low}CD21^{low}CD23^{high}$) B cells and two times more B1 ($B220+\ CD24^{low}\ AA4.1^{low}\ CD21^{low}\ CD23^{low}$) (Figure 2.2 B). Immunofluorescence analysis confirmed the impaired architecture of the marginal zone but normal B cell follicle region in the spleen based on CD1d and SIGN-R1 staining in $CBL^{dKO\text{-}Mb1}$ mice (Figure 2.2 C). The above results clearly showed that CBL family proteins negatively regulated the expansion of Fr.C, Fr.D immature B cells and B1-B cell. CBLs are required for the development of MZ B cells while they are dispensable for FO B cell development.

2.3.2 CBL proteins regulate humoral immune response

2.3.2.1 Impaired T-independent and T-depdent antibody responses in $CBL^{dKO\text{-}Mb1}$ mice

To examine whether the $CBL^{dKO\text{-}Mb1}$ mutation affected B cell function, we compared T-dependent and T-independent antibody responses between the mutant and WT mice. The main responder of T-independent antigens was MZ B cell since MZ B cell can rapidly differentiate into antigen-specific antibody secreting PCs upon T-independent antigen stimulation. As expected, we found that $CBL^{dKO\text{-}Mb1}$ mice produced significantly less amount of anti-NP IgM and IgG3 isotype antibodies upon type-I (NP-LPS) and type-II (NP-Ficoll) T-independent antigens challenging compare to WT mice (Figure 2.3 A and

B). This deficiency in mutant mice could be attributed to the reduced number of MZ B cells in the mutant mice. Upon immunization with T-dependent antigen NP_{36}-KLH, the mutant mice produced lower level of antigen-specific IgG1 isotype antibody; furthermore, at day 14 post-immunization they produced 5 folds less both low and high-affinity antibodies of IgG1 isotypes, and this trend continued up to day 31 after immunization (Figure 2.3 C and D). The above results thus indicated that the CBL proteins were required for the both T-independent and T-dependent immune response. The defective of high affinity anti-NP IgG1 antibody production in T-dependent antigen immunized mutant mice further suggested the $CBL^{dKO\text{-}Mb1}$ mutation impaired GC reaction.

2.3.2.2 Crippled GC reaction in CBL $^{dKO\text{-}Mb1}$ mice

High affinity antigen-specific IgG1 antibody secreting PCs were derived from GC B cells. Since high affinity antibody production was impaired in $CBL^{dKO\text{-}Mb1}$ mice, we examined whether the deletion of CBL proteins on B cells affected the development of GC B cell in SRBC immunized mutant mice. Flow cytometry analysis revealed that the development of GC B cells was severely attenuated in terms of both the cell number and percentage compare to WT control mice (Figure 2.4 A). Consistent with the flow cytometry result, immunofluorescence staining results revealed few GCs in the spleen of CBL $^{dKO\text{-}Mb1}$ mice based on PNA staining (Figure 2.4 B), which further demonstrated that the CBL $^{dKO\text{-}Mb1}$ mutation affected GC reaction. The impairment of GC reaction was also found in the mutant mice immunized with another type of T-dependent antigen NP_{36}-KLH (Figure 2.4 C), indicating that this GC deficiency was applied to both soluble and

particular antigens. Although CBL and CBLB are two different proteins, they share similar structure and play redundant functions in the regulation of TCR and BCR induced signalling pathways. To investigate whether CBL and CBLB played redundant function in the regulation of GC formation, we examined the development of GC B cells in $CBL^{KO\text{-}Mb1}CBLB^{+/-}$ and CBL-$B^{-/-}$ single knockout mice post 10 days of SRBC immunization. Interestingly, the $CBL^{KO\text{-}Mb1}CBLB^{+/-}$ and $CBLB^{-/-}$ mice showed similar GC B cells numbers as compared to WT controls (Figure 2.4 D). Thus these results indicated that CBL family proteins were critical for GC reaction, and this function was redundant between CBL and CBL-B.

2.3.3 $CBL^{dKO\text{-}Mb1}$ B cells are defective in supporting T_{fh} development

The development of GC B cells is dependent on both cell intrinsic and extrinsic factors. Amongst extrinsic factors the FDC network and T_{fh} cells have been shown to be critical for GC formation[67]. Ablation of FDCs in B cell follicle leads to the disappearance of GCs. Previous study showed that the formation of FDC is regulated by GRB2 mediated lymphotoxin B secreted by B cells [234]. Since GRB2 can associate with CBL, we first examined whether the network of FDC was affected by CBLs mutation. Previous studies have been shown that FDCs within primary B cell follicles expressed extremely high level of CD35, and the anti-CD35 antibody was used as marker for FDC network [67, 235]. The immunofluorescence analysis revealed that the WT and mutant mice displayed comparable FDC networks based on CD35 staining in B cell follicles (Figure 2.5 A). This result indicates that the GC B deficiency in our mutant mice is unlikely caused by lack of FDC. To determine whether the GC B cell deficiency in $CBL^{dKO\text{-}Mb1}$ mice was related with

T_{fh} development, we examined the T_{fh} development in the mutant mice. We found that the number of T_{fh} cells in the mutant mice was 4 folds lower than that in WT controls at day 10 post-immunization of SRBC (Figure2.5 B). Since development of T_{fh} cells and GC B cells are mutually dependent, we hypothesised whether the presence of normal T_{fh} rescued $CBL^{dKO\text{-}Mb1}$ GC B cell development. We generated BM chimeras between WT ($CD45.1^+$) and $CBL^{dKO\text{-}Mb1}$ ($CD45.2^+$) mice, and then immunized these mice with SRBC. We found that in the immunized BM chimeras the development of T_{fh} cells derived from both WT and the mutant donors appeared to be normal, demonstrating that presence of WT ($CD45.1^+$) B cells is sufficient to restore T_{fh} development in $CBL^{dKO\text{-}Mb1}$ ($CD45.2^+$) donor cells. However, even in the presence of T_{fh} cell, only WT ($CD45.2^+$) donor cells but not $CBL^{dKO\text{-}Mb1}$ donors ($CD45.2^+$) can give rise to GC B cell population (Figure 2.5 C). This finding indicated that B cell intrinsic CBL proteins were essential for the development of T_{fh} cells. In addition, it also suggested that the cognate interaction between antigen specific B and T_{fh} cells, rather than bystand T_{fh} cell or soluble factors produced by T_{fh} cells, was necessary for GC B cell development.

2.3.4 CBL proteins regulate B cell antigen presentation

2.3.4.1 $CBL^{dKO\text{-}Mb1}$ B cells are defective in antigen presentation to cognate T cells

Cognate interaction between T_{fh} and GC B cells requires TCR recognition of MHCII-peptide antigen complexes expressed by GC B cells. In addition, interaction between co-stimulatory molecules such as ICOS-ICOSL, CD40L-CD40, Dock8 and SLAM-SLAM expressed by T_{fh} and B cells, respectively, are also pivotal for the formation of stable T-B conjugates[37, 95, 236-238]. Since the expression of most of the aforementioned

accessary molecules, except PD-L1, was not significantly altered in $CBL^{dKO\text{-}Mb1}$ B cells (Figure 2.6 A), we decided to examine whether the $CBL^{dKO\text{-}Mb1}$ mutation affected antigen presentation by the mutant B cells to T cells. To mimic as closely as possible the antigen uptake, processing, and presentation by naive B cells to T cells, we generated mini antigens (Anti-IgM $F(ab)_2$ conjugated with OVA protein) that can target OVA antigen to the BCR, which can be used to test the antigen capture, internalization, processing and presentation on B cells (Figure 2.6B). Naive B cells were pre-treated with mini antigens or processed $OVA_{323\text{-}339}$ peptides, then co-cultured with Celltrace-labeled OT-II $CD4^+$ T cells for 3 days and proliferation of T cells were evaluated by flow cytometry based on Celltrace dilution. We found that 22% of proliferating $CD4^+$ T cells was detected in WT B cell co-cultured group while T cells co-cultured with mutant B cells cannot proliferate (Figure 2.6 C). This result indicated that CBLs deficient B cells failed to form cognate interaction and present antigens to OT-II $CD4^+$ T cells. Since the mutant B cells loaded with $OVA_{323\text{-}339}$ peptide supported $CD4^+$ T cell proliferation as efficiently as did by the WT T cells (Fig.2.6 C), we concluded that that antigen presentation post intracellular antigen processing remained normal in the mutant cells.

2.3.4.2 Processed peptide antigen partially rescues *in vivo* GC B development in $CBL^{dKO\text{-}Mb1}$ mice

Since the $OVA_{323\text{-}339}$ peptide can directly loaded to MHC and bypass the defective antigen processing on $CBL^{dKO\text{-}Mb1}$ B cells, we investigated whether administration of the processed $OVA_{323\text{-}339}$ peptide could restore the deficiency of *in vivo* cognate T-B interaction cells and promote the differentiation of GC B cells. To this end, we

immunized the mutant mice that have received adaptively transferred OT-II $CD4^+$ T cells at day 0 with NP_{16}-OVA antigen, followed by two doses of the processed $OVA_{323-339}$ peptide on day 2 and day 5, and then analyzed GC B cell development on day 7 (Figure 2.7A). We found that the mutant mice received processed antigenic peptide possessed four to five folds more GC B cells and T_{fh} cells than the mutant mice without administration (Figure 2.7 B and C). However, the development of both GC B cells and Tfh cells was not fully restored as the mutant mice still had slightly lower numbers of GC B and Tfh cells than WT control mice, suggesting that impaired antigen processing in $CBL^{dKO\text{-}Mb1}$ B cells can only partly explain the defective GC phenotypes. The reason for this will be described in Chaptor4 in my thesis.

2.3.5 The $CBL^{dKO\text{-}Mb1}$ mutation attenuates BCR downmodulation and degradation in naïve B cells

BCR-mediated antigen processing included internalization of BCR-antigen complexes and subsequent sorting of the internalized complexes to lysosomes for degradation. To further pinpoint at which checkpoints the CBL family proteins affected the antigen processing, we examined BCR-mediated antigen downmodulation and translocation to lysosomal vehicles. To track BCR complex internalization and lysosome sorting, we first labelled surface IgM BCR with anti-IgM $[236]_2$-biotin on ice, and then calculated internalization rate of BCR complex for various periods. We found that $CBL^{dKO\text{-}Mb1}$ B cells displayed decreased BCR internalization rate compare to WT B cells, as the rates of cell surface BCR downmodulation was attenuated at various time points (Figure 2.8. A). The transportation of internalized BCR complex to lysosomal degradation was evaluated

by the co-localization between BCR and LAMP-1^+ lysosomes. While most of the internalized antigen complexes co-localized with LAMP-1^+ lysosomes in WT Naïve B cells within 30 min, mutant B cells cannot transport the BCR complex to lysosome for degradation. (Figure 2.8 B). To further validate whether CBL family proteins regulate BCR complex degradation, we used an antigen degradation sensor to track the sorting of the internalized antigen to acidic lysosomes as previously described [239]. In brief, the antigen degradation sensor was composed by three parts: Alexa633-DNA-Quench sequence, Streptavidin and FITC labelled Anti-IgM $F(ab)_2$. At steady state, this sensor was FITC emission positive and Alexa633 negative because the emission of Alexa633 was absorbed by the Quench sequence. Once the antigen degradation sensor entered naïve B cells after incubation at 37°C, the Quench sequence was disassociated with Alexa633, leading to FITC and Alexa633 double positive (Figure 2.9 A).

In this experimental setting, the antigen sorted to the lysosomes could be quantitatively determined by FACS and visualized through confocal microscopy. We found that the CBLs deficient naïve B cells showed severely decreased degradation rate of the antigen sensors based on the percentage of FTIC and Alexa633 double positive population compare to WT naïve B cells at early time points examined by FACS (Figure 2.9 B). Similarly, after 30mins of 37°C incubation, the red and green double positive dots can be visualized from confocal microscopy in WT naïve B cells while there is very low level of red dots in mutant B cells (Figure 2.9 C). Taken together, the above results strongly demonstrate that CBLs regulated B cell antigen presentation through dictating the BCR complex internalization and transportation to lysosome for degradation.

2.3.6 CBL family proteins promote Igα and Igβ ubiquitination

Transportation of the internalized endosomes associated membrane proteins to lysosome compartment is guided by protein ubiquitination. Due to the unique transmembrane domain and short cytoplasmic tail of IgM, IgM complex need to associate with Igα and Igβ proteins, which is necessary to stabilize IgM expression on the cell surface and transduce BCR signals. Since CBL proteins are E3 ubiquitin ligases that may initiate the BCR complex internalization through ubiquitination of gα and Igβ proteins, we examined whether Igα and Igβ expressed by the naïve B cells was ubiquitinated upon anti-IgM $[236]_2$ crosslinking. After 5 minutes of BCR stimulation, ladder-like poly-ubiquitinated Igα and Igβ proteins were detected in WT B cells (Figure 2.10 A and B), which suggested that Igα and Igβ proteins were poly-ubiquitinated by CBLs upon BCR stimulation. By contrast, the ladder-like poly-ubiquitinated Igα and Igβ proteins cannot be detected in stimulated mutant B cells (Figure 2.10 A and B). Together these findings suggested that the impaired BCR complex internalization and degradation in $CBL^{dKO\text{-}Mb1}$ naïve B cells was due to block of Igα and Igβ ubiquitination.

2.3.7 Ubiquitin ligase activity of CBL proteins is required for the initiation of GC reaction

As mentioned in first chapter, the CBL family proteins serve as both adaptor proteins and E3 ubiquitin ligases. To distinguish which function was involved in the initiation of GC reaction, we crossed $CBL^{KO\text{-}Mb1}CBLB^{-/-}$mice with $CBLB^{C373A/C373A}$ mutant mice to obtain $CBL^{KO\text{-}Mb1}$ $CBLB^{C373A/-}$ mice, in which B cells only expressed one allele of the mutant

form of $CBLB^{C373A}$ with another non-functional allele. The CBL-B^{C373A} carried a cysteine (373) to alanine mutation at the RING finger domain of CBL-B, which inactivated the E3 ubiquitin ligase but not the adaptor function of CBL-B. After immunization with NP_{36}-KLH, the $CBL^{KO\text{-}Mb1}$ $CBLB^{C373A/-}$ mice displayed a severely reduction in GC B cells compared to WT control mice (Figure 2.11 A). Consistently, the mutant mice could not support normal T_{fh} population (Figure 2.11 B). Furthermore, mutant B cells could not undergo GC-dependent antibody affinity maturation, CSR, and differentiate into high-affinity IgG1 secreting plasma cells since mutant mice lack of both total and high affinity antigen-specific IgG1 secreting PCs based on the ELISPOT results (Figure 2.11 C). Since $CBL^{KO\text{-}Mb1}$ $CBLBC^{373A/-}$ mice completely recapitulated the phenotype of the $CBL^{dKO\text{-}Mb1}$ mice, we concluded that the GC phenotype we found in $CBL^{dKO\text{-}Mb1}$ mice could be attributed to CBL proteins mediated E3 ubiquitin ligase function. This finding of course will not pre-exclude the possible role of CBL's scaffolding function in the GC reaction.

2.3.8 E3 ubiquitin ligase activity of CBL proteins regulates B cell antigen presentation

Since the $CBL^{KO\text{-}Mb1}CBLB^{C373A/-}$ mice completely recapitulated the phenotype of the $CBL^{dKO\text{-}Mb1}$ mice, we decided to determine whether CBL ubiquitin ligase activity is required for naïve B cell antigen presentation. To investigate the antigen presentation of $CBL^{KO\text{-}Mb1}CBLB^{C373A/-}$ naïve B cells, mini antigen or $OVA_{323\text{-}339}$ peptide treated naïve B cells were co-cultured with Celltrace labeled OT-II $CD4^+$ T cells for 72 hrs. Proliferation of OT-II T cells was measured based on the dilution of Celltrace. Mini antigen treated

WT naïve B cells can stimulate around 20% of $CD4^+$ OT-II T cells to proliferate. Similar to $CBL^{dKO\text{-}Mb1}$ B cells, we observed that mini antigen treated $CBL^{KO\text{-}Mb1}CBLB^{C373A/-}$ B cells could not efficiently (1% of $CD4^+$ OT-II T cells) promote OT-II $CD4^+$ T proliferation, despite that both $CBL^{KO\text{-}Mb1}$ $CBLB^{C373A/-}$ and WT control B cells promoted OTII T cells proliferation efficiently (90% of $CD4^+$ OT-II T cells) in the presence of the processed $OVA_{323\text{-}339}$ peptide (Figure 2.12 A). This result thus demonstrate that CBL mediated E3 ubiquitin ligase activity is required for B cell antigen presentation. To further investigate how CBLs mediated E3 ubiquitin ligase activity regulates the B cell antigen presentation, we examined which step of antigen presentation process was affected by the lacking of CBLs mediated E3 ubiquitin ligase activity. $CBL^{KO\text{-}Mb1}$ $CBLB^{C373A/-}$ and WT control naïve B cells were treated with anti-IgM $[236]_2$-biotin on ice, then incubated at 37°C for various time. We found that BCR internalization rate of $CBL^{KO\text{-}Mb1}$ $CBLB^{C373A/-}$ B cells was up to 40%. Compared to 70% in WT B cells, $CBL^{KO\text{-}Mb1}$ $CBLB^{C373A/-}$ B cells showed significantly reduced antigen internalization rate (Figure 2.12 B). Similar to $CBL^{dKO\text{-}Mb1}$ B cells, $CBL^{KO\text{-}Mb1}$ $CBLB^{C373A/-}$ B cells also failed to efficiently sort the internalized BCR complex to lysosomes, as 70% of the internalized antigen complexes co-localized with LAMP-1^+ lysosomes in WT within 30 min. (Figure 2.12 C). Similar result was obtained by using DNA sensor to quantify the rate of antigen degradation. Those $CBL^{KO\text{-}Mb1}$ $CBLB^{C373A/-}$ B cells show significantly delayed and decreased rate (25% of degradation after 30mins treatment) based on the turn of Alexa633-DNA-sensor while around 55% of WT naïve B cells can degrade the quench sequence and turn on Alexa633 within 30mins (Figure 2.12D). Based on these findings,

we concluded that the E3 ubiquitin ligase function of CBL proteins was critical for the initiation of GC reaction, and this function was mainly executed via promoting BCR-antigen complex internalization and sorting to lysosome for B cell antigen processing and presentation.

2.3.9 Blockade of Igα ubiquitination is sufficient to block GC formation

Previous results revealed that CBL family proteins regulated GC reaction through ubiquitination of two potential targets Igα and Igβ. However, it is not clear whether the ubiquitination of Igα and Igβ is sufficient for CBL-mediated regulation in the GC reaction. To examine whether Igα ubiquitination was critical for the formation of GC, three potential ubiquitination lysine residues (K161, K167 and K219) at cytoplasmic tail were mutated to arginine residues (K161R, K167R and K219R, here termed as: 3M-Igα) (Figure 2.13 A). The 3M-Igα and WT-Igα was respectively introduced into *Igα*-deficient bone marrow hematopoietic stem cells through a GFP-based retrovirus-mediated gene transfer, so GFP^+ B cells from bone marrow chimeric mice carried the retroviral vector introduced transgene (Figure 2.13 B). We found that B cell development as well as the BCR signalling between WT Igα and 3M-Igα retrovirus-infected chimeras was comparable, except the slightly reduced Ca^{2+} signalling (Figure 2.13 C-F). While B cell expression WT-Igα protein could efficiently differentiate into GC B cells, the GC B cells were undetectable in those 3M-Igα chimera mice upon NP_{36}-KLH immunization (Figure 2.13 G). This result indicated that the ubiquintiation of Igα protein was an essential step for the formation of GC B cells.

2.3.10 The ubiquitination of Igα is required for B cell antigen presentation

To investigate how the blockade of Igα ubiquitination affected the formation of GC B cells, we examined B cell antigen presentation ability of 3M-Igα B cells. Mini antigen treated WT-Igα and 3M-Igα B cells were co-cultured with Celltrace labelled OT-II $CD4^+$ T cells. Strikingly, the 3M-Igα B cells could not support the proliferation of the cognate OTII $CD4^+$ T cells based on the Celltrace dilution assay while WT-Igα control B cells can promote 10% of OTII $CD4^+$ T cells proliferation (Figure 2.14 A), indicating that the antigen presentation of B cells depends on the ubiquitination of Igα protein. As mentioned above, the BCR-mediated antigen presentation involves three steps: BCR internalization, BCR degradation in lysosomes, and peptide loading to MHCII. To distinguish which steps were affected by the mutation, we first examined BCR internalization. The BCR downmodulation rate of WT-Igα naïve B cells went up to around 60% upon anti-IgM $F(ab)_2$ stimulation. By contrast, the 3M-Igα B cells showed dramatically reduced BCR downmodulation rate (30%) (Figure 2.14 B). Next we examined if the BCR degradation was also affected by 3M-Igα mutation. The DNA-sensor treated 3M-Igα B cells were unable to turn on the expression of Alexa633, while 30% of WT-Igα B cells can efficiently degrade the DNA-sensor(Figure2.14 C). Thus, the above results demonstrated that the ubiquitination of Igα protein played a critical role in BCR-mediated antigen uptake and sorting to the lysosome degradation.

2.3.11 K161 and K167 lysine were responsible for the BCR-mediated antigen presentation

To further identify which lysine in the Ig-α tail is responsible for the antigen presentation mediated GC formation, we individually mutated three lysine residues (termed as: K161R, K167R and K219R) (Figure 2.15 A). These different mutants were transferred into *Igα*-deficient bone marrow stem cells and generated bone marrow chimeric mice, respectively (Figure 2.15 B). The development of GC B cells in these mice was analyzed after NP_{36}-KLH immunization. We found that B cells reconstituted with K219R Igα mutant were able to differentiate into GC B cells (around 8% among $B220^{+}IgD^{lo}$ population). By contrast, the K161R or K167R B cells failed to differentiate into GC B cells (Figure 2.15 C). The above results demonstrated that K161 and K167, not K219R, were two critical potential ubiquitination sites on Ig-α, which were required for the initiation of GC reaction through antigen presentation dependent mechanism. Interestingly, there is an activated B cell population ($B220^{+}GL7^{+}Fas^{-}$) detected in both K167R and 3M-Igα mutant mice, which could be the precursor of GC B cells. We will discuss this phenomenon in Chaptor 4.

2.4 Discussion

The MZ and FO B cells are respectively responsible for T-independent and T-dependent antibody response. Here I showed that the expansion of early bone marrow Fr.C and Fr.D B cell was negatively regulated by CBLs, whereas the development of splenic MZ B cells was positively controlled by CBLs. Ablation of *Cbls* in naïve B cells lead to severely reduced T-dependent antibody response and impaired GC B cells formation. I provided

evidence that CBLs regulated B cell antigen presentation through ubiquitination of BCR-associated protein Igα and Igβ. The *Cbls*-deficient naïve B cells displayed significantly reduced BCR internalization and impaired BCR-antigen complex degradation, which lead to insufficient promotion of cognate $CD4^+$ T proliferation. The specifically inactivation of E3 ubiquitin ligase function was sufficient to recapitulate this GC phenotype, which demonstrated the important role of CBLs as E3 ubiquitin ligase in GC B cells formation. In addition, blocking the ubiquitination of CBLs downstream target Igα was sufficient to suppress GC B cells formation and block antigen presentation of B cells. Taken together, those results demonstrated that CBLs controlled the entry checkpoint of GC B cells through post-transcriptional regulatory pathway.

Bone marrow, a central lymphoid organ, gives rise to mature B cells throughout life since the HSCs continuously differentiate into immature B cells under certain cytokine environment[240]. The $CBL^{dKO\text{-}Mb1}$ mice displayed enlarged number of bone marrow Fr.C and Fr.D B cells with relatively comparable number of total splenic B cells, which indicated the accumulation of Fr.C and Fr.D B cells was not due to altered bone marrow B cell development. This result suggests that CBL family proteins selectively suppress the clonal expansion of early pre-B cells. Cytokine IL-7 is essential for mouse B cell development while humans with IL-7 mutation still can generate mature B cells in blood and secondary lymphoid organs[241]. IL-7R is a heterodimer protein composed of the α chain and the γ chain. Previously studies showed that B cell development in *Il-7* or *Il-7r* deficient mice was completely blocked at the early pro-B cell stage. In addition, IL-7R could be degraded in $CD8^+$ T cells through HIV protein HAT induced ubiquitination,

which was mediated through E3 ubiquitin ligase CIS[242]. Interestingly, I found enhanced IL-7R surface expression on $CBL^{dKO\text{-}Mb1}$ deficient early pre-B cells (data not shown), which indicated that CBLs may regulate the internalization and degradation of IL-7R on early pre-B cells. However, I cannot exclude the possibility that CBLs may negatively regulate the IL-7 mediated signalling pathway through targeting the downstream protein such as signal transducer and activator of transcription 5(STAT5) and Janus kinase 3 (JAK3)[243, 244]. Thus, the detail molecular mechanism needs to be explored in the future study.

There are two types of T-independent antigens: type I and type II. I found that ablation of *Cbls* in naïve B cells resulted in the significant reduction of antibody response against both type I and type II T-independent antigens. The impaired T-independent response could attribute to blocked MZ B cell development in $CBL^{dKO\text{-}Mb1}$ mice. This result suggests that CBL family proteins are essential for the formation of MZ B cells. This phenomenon raises a question: How CBL family proteins regulate MZ B cell development. The MZ and FO B cells are derived from T2 B cells. Under insufficient BTK-mediated inhibitory signals, T2 B cells with poor BCR reactivity would differentiate into MZ-precursor cells, which further give rise to MZ B cells through NOTCH2 dependent signalling pathway[245]. The ablation of NOTCH2 signalling component or ligand leads to impaired MZ B cell development. The NOTCH signalling is negative regulated by ubiquitin-specific protease 12(USP12)[246]. Recent study showed that the USP12 associated with CBLB in Jurkat T cells[247]. Thus, I speculate that CBL proteins may serve as a positive regulator of NOTCH signalling pathway

through degradation of USP12. In addition, recent study has been shown that IRF4 controls the positioning of mature B cells in the lymphoid microenvironment. The ablation of *Irf4* in mature B cells lead to enlarged MZ B cell population since IRF4 negatively regulate NOTCH2 signalling [248]. In Chapter 3, I demonstrate that CBL proteins can ubiquitinate IRF4 protein in 293T and GC B cells. Since $CBL^{dKO\text{-}Mb1}$ mice displayed severely reduced MZ B cell population, this result leads us to speculate that CBLs may regulate T2 B cell fate decision through negatively regulation of IRF4 expression. $CBL^{dKO\text{-}Mb1}$ B cells may express relatively enhanced level of IRF4 protein, which can suppress NOTCH2 signalling pathway and block MZ B cell differentiation.

Recent study has been shown that splenic MZ B cells migrate bidirectionally between marginal zone and follicle. This interfollicle movement is dependent on adhesion molecules such as sphingosine-1-phosphate receptor 1 (S1PR1) [249]. Consistently, the expression of S1PR1 and other integrin molecules are enhanced in *Irf4*-deficient marginal B cells, which could attribute to expand splenic MZ B cells population [248]. Previous study showed that CBL could negatively regulate α5 integrin in fibroblast through its E3 ubiquitin ligase function [250, 251]. Thus, we speculate that CBL proteins may control the MZ B cell development through targeting some unknown integrin molecules to suppress their shuttling to marginal zone area.

Thus, it would be interesting to investigate the molecular mechanism of how CBLs regulate MZ B cell development. The findings related to T-dependent antibody response and GC reaction will be discussed in Chapter 4.

2.5 Acknowledgement

We thank J. Di Noia and A. Veillette for comments. Supported by The Canadian Institute of Health Research (CIHR) Operating Grant (MOP142279) and A. Aisenstadt Chair Fund to H.G.; Chinese Scholarship Council Ph.D. training grants to X. L.; National Health and Medical Research Grant (1101318) to W. Y. L.

2.6 Author contribution

X.L. did mouse, biochemical, and flow cytometric analyses; D. K. generated 40LB feeder cells; W. Y. L. generated CBL-B^{C373A} mice.

2.7 Material and Methods

2.7.1 Animals and cell lines

C57BL/6J mice were obtained from Jackson Laboratory (#000664, USA). Germline *Cblb* knockout mice were generated from our own lab at National Institutes of Health (NIH), USA. In brief, the Neo gene was inserted into the third exon of *cbl-b* gene. Then the CBL-B$^{-/-}$ mice had been backcrossed to C57BL/6J mice for over six generations from the mixed 129 and C57BL/6J genetic background, which had been further verified to contain 99.9% C57BL/6J genetic background by Jackson Laboratory [205]. The *Cbl*$^{f/f}$ mice were also generated from our own lab. The floxed *Cbl* allele was generated by introducing two

loxP sites into the targeting plasmid [202]. Then the *Cbl*$^{f/f}$ mice with mixed 129 and C57BL/6J genetic background was backcrossed to C57BL/6J mice to obtain 99.9% C57BL/6J genetic background. The Mb1-Cre mice were obtained from Dr. Michael Reth[252]. To generate B cell-lineage specific deletion of *Cbl* and *Cblb*, I crossed the Mb1-Cre mice to *Cbl*$^{f/f}$*Cblb*$^{-/-}$ mice (termed as CBL$^{dKO\text{-}Mb1}$). To obtain Igα knockout mice, I crossed the Mb1-Cre mice with Mb1-Cre mice to get the homozygous mice. The Tomato^{Rosa26} mice were obtained from Dr. Suh lab. The CBL$^{dKO\text{-}Mb1}$Tomato^{Rosa26} mice were generated by crossing CBL$^{dKO\text{-}Mb1}$ mice to Tomato^{Rosa26} mice. The CBLB Ring finger domain mutant mice CBLB$^{C373A/C373A}$ was obtained from Dr. Wallace Langdon[253]. To investigate the function of CBLB-mediated ubiquitination, I crossed the CBL$^{KO\text{-}Mb1}$CBLB$^{-/-}$ mice with CBLB$^{C373A/C373A}$ to generate CBL$^{KO\text{-}Mb1}$CBLB$^{C373A/-}$ mice. OT-II mice were obtained from Dr. Andre Veillette lab. Rag1$^{-/-}$ and B6/SJL mice were purchased from Jackson Laboratory. The Phoenix virus packaging cell line was obtained from Dr. Andre Veillette lab. The 40LB cell line was obtained from Dr. Daisuke Kitamura.

2.7.2 Genotyping

The genotype of transgenic mice was screened by PCR. In brief, the tails from different transgenic mice were digested in lysis buffer (100mM Tris-HCL, 50mM EDTA, 0.2% SDS, 200mM NACL, 50μg/ml Proteinase K) at 55°C for overnight. Followed by vertex and maximum speed centrifugation, the supernatant was collected and equal volume mixed with 100% ethanol to precipitate the genomic DNA. Then the genomic DNA pellet was obtained after another round of maximum speed centrifugation. Finally, the genomic

DNA pellet was re-suspended in 200ml 10mM Tris-HCL buffer, which was ready to use for PCR.

For the genotyping of Igα$^{-/-}$ mice by FACS, 2-3 drops of blood were collected from mice and quickly mixed with Solution A buffer (20mM EDTA and 0.1% Sodium Azide in PBS). The blood sample from WT mice was used as positive control. Cell pellets were collect by centrifugation at 1800rpm for 4mins, then the erythrocytes were depleted by ACK lysing buffer. The peripheral blood mononuclear cells (PBMC) were stained with anti-CD19 and anti-B220 at the concentration of 0.2ng/μl of each antibody in FACS buffer (1% BSA and 0.05% Sodium Azide in PBS) for 20mins on ice. Samples were washed twice, and re-suspended in FACS buffer followed by analyzing on CYAN or Fortesa.

2.7.3 Plasmid and cloning

To investigate the function of Igα ubiquitination in antigen presentation and GC reaction, multiple mutant forms of Igα were generated. Briefly, to generate 3M-Igα, two fragments with three different point mutations of the *Igα* CDS region were amplified from cDNA, and fused these two PCR fragments together. The fused fragment was sub-cloned into MIGR1-MSCV and verified by DNA sequencing. To generate K161R and K167R, two PCR fragments with each single point mutation was obtained from cDNA. Then those two mutants were respectively sub-cloned into MIGR1-MSCV and verified the DNA sequence. The K219R was generated from one-step PCR and then sub-cloned

into MIGR1-MSCV. The primers for the generation of Igα mutants were listed as Table 2.1.

Table 2.1 The sequences of cloning primers

Gene Name	Primer Name	Sequence
WT–Igα	CD79a WT Forward	AGTCCTCGAGATGCCAGGGGGTCTAGAAG
	CD79a WT Reverse	AGTCGAATTCTCATGGCTTTTCCAGCTGGG
3M–Igα	CD79a WT Forward	AGTCCTCGAGATGCCAGGGGGTCTAGAAG
	CD79a Set1 Reverse	CTCATTTTGCCACCGTCTCCTGAAT
	CD79a Set2 Forward	CGGTGGCAAAATGAGAGATTTGGGG
	CD79a Set2 Reverse	AGTCGAATTC TCATGGTCTTTCCAGCTGGG
K161R	CD79a WT Forward	AGTCCTCGAGATGCCAGGGGGTCTAGAAG
	CD79a Set1 Reverse	CTCATTTTGCCACCGTCTCCTGAAT
	CD79a Set3 Forward	CGGTGGCAAAATGAGAAGTTTGGGG
	CD79a WT Reverse	AGTCGAATTCTCATGGCTTTTCCAGCTGGG
K167R	CD79a WT Forward	AGTCCTCGAGATGCCAGGGGGTCTAGAAG
	CD79a Set3 Reverse	CTCATTTTGCCACCGTTTCCTGAAT
	CD79a Set2 Forward	CGGTGGCAAAATGAGAGATTTGGGG
	CD79a WT Reverse	AGTCGAATTCTCATGGCTTTTCCAGCTGGG
K219R	CD79a WT Forward	AGTCCTCGAGATGCCAGGGGGTCTAGAAG
	CD79a Set2 Reverse	AGTCGAATTC TCATGGTCTTTCCAGCTGGG

2.7.4 Immunization

To test T-independent antibody response in $CBL^{dKO\text{-}Mb1}$ mice, two types of T-independent antigens, NP-LPS or NP-Ficoll, were injected through i.p. injection at the does of 50μg per mice. After 7 days, blood serum antibody was collected, antigen specific antibody response was quantified through ELISA.

To test T-dependent antibody responses and germinal center reaction, mice were immunized with either 10^9 sheep red blood cells (SRBCs) (Innovative Research) in PBS by i.v. inejection or 50μg of NP_{36}-KLH (BioSources) precipitated in alum adjuvant (Imject Alum, ThemoScientific) by i.p. injection.

To monitor the antigen specific antibody affinity maturation, the mice were immunized with 50mg of NP_{36}-KLH through i.p. injection. After that, the blood samples were collection at day7, day14, day24 and day31 post-immunization. The serum from those blood samples was applied for ELISA.

To rescue the deficiency of GC initiation in $CBL^{dKO\text{-}Mb1}$ mice, the following immunization schedule was used: at day-1, 2million of OT-II+ CD4+ T cells were adaptively transferred to the mice through i.v. injection; at day0, the mice were immunized with 50mg of NP_{16}-OVA through i.p injecition; at day2 and day 5, the mice received two doses of $OVA_{323\text{-}339}$ peptide through i.v. injection.

2.7.5 Naïve B cell purification

To obtain large quantity of naïve B cells for *in vitro* antigen presentation assay, BCR downmodulation assay, antigen degradation assay and biochemistry analysis, total

splenic cells were obtained from unimmunized WT, $CBL^{dKO\text{-}Mb1}$ and $CBL^{KO\text{-}Mb1}CBLB^{C373A/-}$ mice. Then naïve B cells were purified from total splenic cells by using B cell enrichment kit (Stem cell). The efficiency of purification was confirmed by FACS (more than 95% of $B220^{+}$ B cell).

2.7.6 Flow cytometry and cell sorting

Single cell suspension was prepared from spleen by using the 70mm nylon cell strainer (#352350, BD Bioscience). The erythrocytes were depleted by ACK lysing buffer. Total splenic cells or splenic B cells were resuspended in FACS buffer (5%BSA in PBS (PH=7.2)) and stained with the corresponding antibodies on ice for 30 min. Cells were washed twice with FACS buffer and then subjected to analysis on a BD Fortessa or Cyan or to cell sorting on a FACS Aria or Moflo. The following antibodies were used for the staining: anti-B220, anti-GL7, anti-CD11c, anti-CD11b, anti-Gr1, anti-F4/80, anti-NK1.1, anti-TCRβ, anti-CD3ε, anti-CD86, and anti-CD38 (eBioscience); anti-Fas, anti-CD138, anti-BCL6, anti-CXCR4, anti-IgG1, anti-CD45.2, anti-IgD (BD Pharmingen).

2.7.7 ELISA and ELISOT

Total splenic cells from NP_{36}-KLH immunized mice were cultured at 37°C in antigen pre-coated 96-well Multiscreen-HA filter plates (Millipore) overnight. Spots of antibody secreting cells were stained with rabbit anti-mouse IgG1 antibodies conjugated to horseradish peroxidase (Invitrogen), and then developed by addition of AEC substrate (BD Pharmingen). Plates were washed extensively and spots were counted on a dissect

microscopy. The antigens used for plate coating were NP_4-BSA or NP_{30}-BSA, respectively.

To measure the NP-specific IgG1 and IgM antibody affinity maturation, the blood serums from sequential bleeding were used for this study. Briefly, capture antigen NP_4-BSA or NP_{30}-BSA was coated on 96-well ELISA plate overnight, and then blocked with 5%BSA in PBS. After that, diluted serum was added to each well to incubate for overnight. Secondary antibody anti-Mouse IgM or IgG1 antibodies conjugated with HRP (Invitrogen) were used to detect the serum antibody level. Finally, the plate was developed with 1-StepTM Ultra TMB-ELISA substrate (#34028, Thermo scientific).

2.7.8 Immunoprecipitation and Immunoblotting

30 million of naïve B cells were pre-treated with lysosomal blocker MG132 (20μM) for 4 hours, and then non-stimulated or stimulated with anti-IgM $F(ab)_2$ for 5mins. To immunoprecipitate Igα and Igβ , samples were lysed in 800μl 1x TNE buffer (1% NP40, 50mM Tris pH8.0, 2mM EDTA) with protease and phosphatase inhibitors. The total cell lysate was first incubated with 10μl Protein A agarose beads (#9863, Cell signaling Technology) to pre-clean the lysate for 1hr at 4°C with rotation. After the pre-clean, the lysate was incubated with 1μg of anti-Igα or anti-Igβ antibody to pull-down the target proteins for overnight at 4°C with rotation. Then 20μl of Protein G agarose beads (Sigma) were added to the lysate for additional 2hrs incubation. The beads were collected by centrifugation and wash 4 times. The beads were re-suspended by 30μl 3xSDS sampling buffer (6% SDS, 10% 2-mercaptoethanol, 30% glycerol, 0.006% bromophenol

blue, 0.185M Tris-HCL, pH6.8) and incubated at 100°C for 6mins. The supernatant was collected for immunoblotting. The samples and Kaleidoscope protein ladder (#1610395, Bio-Rad) were applied on 10% SDS-PAGE gel and 6% stacking gel. Proteins were transferred from the SDS-PAGE gel to a PVDF membrane (#IPVH00010, EMD Millipore). Then the membrane was incubated with blocking buffer (5% milk in TBS/T) for 1hr at room temperature. After blocking, the membrane was blotted with different primary antibodies for overnight at 4°C. Then incubate with HRP-conjugated secondary antibody. The membrane was developed by the ECL™ Primer Western Blotting Detection Reagent (#RPN2232, GE Healthcare).

2.7.9 B cell antigen presentation assay

To evaluate the antigen presentation ability of Naïve B cells, the following in vitro assay was developed. Two types of antigen were used: $OVA_{323-339}$ peptide and OVA-BCR mini antigen. The OVA-BCR mini antigen included three different components: anti-IgM $F(ab)_2$-Biotin, Streptavidin and OVA-Biotin. To generate this mini antigen, those three components were mixed at 4:1:4 mole ratio, and incubated on room temperature for 30mins. The purified Naive B cells were incubated with either peptide antigen or mini antigens for 30mins at 37°C. Then washed twice to deplete the remaining antigens. Meanwhile, OT-II^+ $CD4^+$ T cells were purified and labelled with cell proliferation Celltrace e450 (#34557 Thermo). The antigen incubated Naïve B cells were co-cultured with Celltrace labelled OT-II^+ $CD4^+$ T cells at the ratio 1:5 for 72 hours. After the co-culture, the samples were collected and stained with anti-B220 PE-CY7 (ebioscience) and anti-CD4 APC (ebioscience) for 30mins on ice. The readout of B cell antigen

presentation ability was the rate of OT-II$^+$ CD4 T cell proliferation based on the Celltrace dilution.

2.7.10 BCR down-modulation assay

Naïve B cells were purified from spleen by B cell enrichment kit (Stem cell). Purified naïve B cells were stained with anti-IgM F(ab)$_2$-Biotin on ice for 30min. Then put those anti-IgM F(ab)2-Biotin labelled cells back to 37°C for BCR internalization, and the reaction was stopped at various time points by adding 2%PFA in PBS. Then surface remaining anti-IgM F(ab)2-Biotin was stained with Streptavidin-PE-CY7 (ebioscience). Here was the formula to calculate the internalization rate:

Normalized Internalization Rate= (MFI of PE-CY7 at 0'-MFI of PE-CY7 at desire time point)/ MFI of PE-CY7 at 0'

2.7.11 Measurement of antigen degradation

To quantify the antigen degradation rate, the degradation sensor was used in this study. The degradation sensor was composed by three parts, including the special DNA oligonucleotides, Streptavidin and Anti-mouse IgM and IgG F(ab)2-FITC. To generate the special DNA oligonucleotides, the following two oligonucleotides were purchased from IDT with HPLC purification: Fluorescent strand sequence (5'-Atto647N-TCCGG CTGCCTCGCTGCCGTCGCCA-Biotin) and quencher strand sequence (5'-TGGCG ACGGCAGCGAGGCAGCCGGA-Iowa Black RQ)[239]. Both oligoes were re-suspended to 100μM in duplex buffer (100mM potassium acetate, 30mM HEPES, pH7.5). Mix equal volume amounts and add $MgCl_2$ to a final concentration of 2mM. To

anneal those two oligoes together, the mixture was denatured for 2mins at 94 and them put the tube on the bench to cool down gradually to room temperature (around 30mins). Then mix the antigen senor with Streptavidin and Anti-mouse IgM and IgG F(ab)2-FITC at the molar ratio of 4:1:4, and incubate at room temperature for 30mins.

Purified naïve B cells or 40LB cultured iGC B cells were incubated with the antigen sensor BCR complex on the ice for 30mins, and washed once to deplete the rest of antigen sensor BCR complex. Put those labeled cells back to 37 for different incubation time (0', 10', 30', 60'). To stop the internalization and antigen degradation, the cells were added into 2%PFA PBS solution and incubated for 10mins. To quantify the degradation rate of antigen complex, the samples were analyzed by FACS.

2.7.12 Immunofluorescence

Spleens were embedded in optimum cutting temperature compound (Sakura) and flash-frozen in liquid nitrogen. Tissue sections were cut on Cryotome (Leica), fixed in ice-cold acetone (Sigma), blocked with PBS+5%BSA for 1 hour at 25°C, and stained with PNA – Biotin (VectorLab). The following secondary antibodies were used to detect primary antibodies: Streptavidin Alexa-488 (Invitrogen), Anti-B220-APC (ebioscience). Images were acquired on a Zeiss LSM700 or 710 confocal microscopies.

To visualize the DNA sensor BCR complex degradation, the samples collected from different stimulation time (0min and 30min) were put on positive charged slides through Cytospin, then fixed the samples for 10mins at room temperature followed by extensive

wash and mounting the slides with DAPI. Images were acquired on a Zeiss LSM700 or 710 confocal microscopies.

Another way to quantify the BCR complex degradation was used by checking the co-localization of BCR complex and lysosomes through immunofluorescence. Navie B cells from WT, $CBL^{dKO\text{-}Mb1}$ and $CBL^{KO\text{-}Mb1}CBLB^{C373A/-}$ mice were incubated with Anti-IgM F(ab)2-Biotin on ice for 30mins. The uncoupled BCR complex was depleted by extensive wash. Then put those samples back to 37 to incubate for different time point (0min and 30min). After the incubation time, the samples were put on positive charged slides through Cytospin, followed by 2% PFA fixation and 0.1% Triton X-100 permeablization. The primary antibody anti-LAMP1 was used to stain for the lysosomes in cytoplasma. The secondary antibodies, anti-rabbit Alexa568 and streptavidin Alexa488, were used to label the lysosomes and BCR complex. The slides were analyzed and acquired the image Zeiss LSM700 or 710 confocal microscopies.

2.7.13 Generation of bone marrow chimeric mice

The 50:50 bone marrow chimeric mice were generated from $Rag1^{-/-}$ mice. The recipient $Rag1^{-/-}$ mice were lethally irradiated at the dose of 9.5Gy. Those recipient mice received total 4 million of bone marrow cells in 1:1 ratio from B6.SJL background ($CD45.1^{+}$) mice and either WT or $CBL^{dKO\text{-}Mb1}$ mice with C57BL/6J background ($CD45.2^{+}$). After 6-8 weeks of reconstitution, those chimeric mice were immunized with SRBC through i.v. injection, and analyzed the GC and T_{fh} formation at different time point.

To generate Igα-WT, Igα-3M, K161R, K167R and K219R bone marrow chimeric mice, retroviral stocks were prepared by transfection of Phoenix cells with different forms of Igα expression retroviral vector together with the packaging vector pCL-Eco by the standard calcium transfection. Viral supernatants were collected 48 h and 72 h after the transfection, respectively. To obtain bone marrow stem cells, donor mice were treated with 5-FU (5 mg/mouse, i.p.). Four days later, bone marrow stem cells were collected and cultured under optimal stem cell culture condition. After two-rounds retroviral spin-infections, bone marrow cells were adaptively transferred into lethally irradiated (9.5 Gy) $Rag1^{-/-}$ recipient mice. Five weeks later, mice were subjected to different immunization.

2.7.14 Statistical analysis

Statistical significance was determined by unpaired two-tailed Student's t test using Prism software (GraphPad). A P value<0.05 was considered statistically significant.

2.8 Figures and Figure Legends

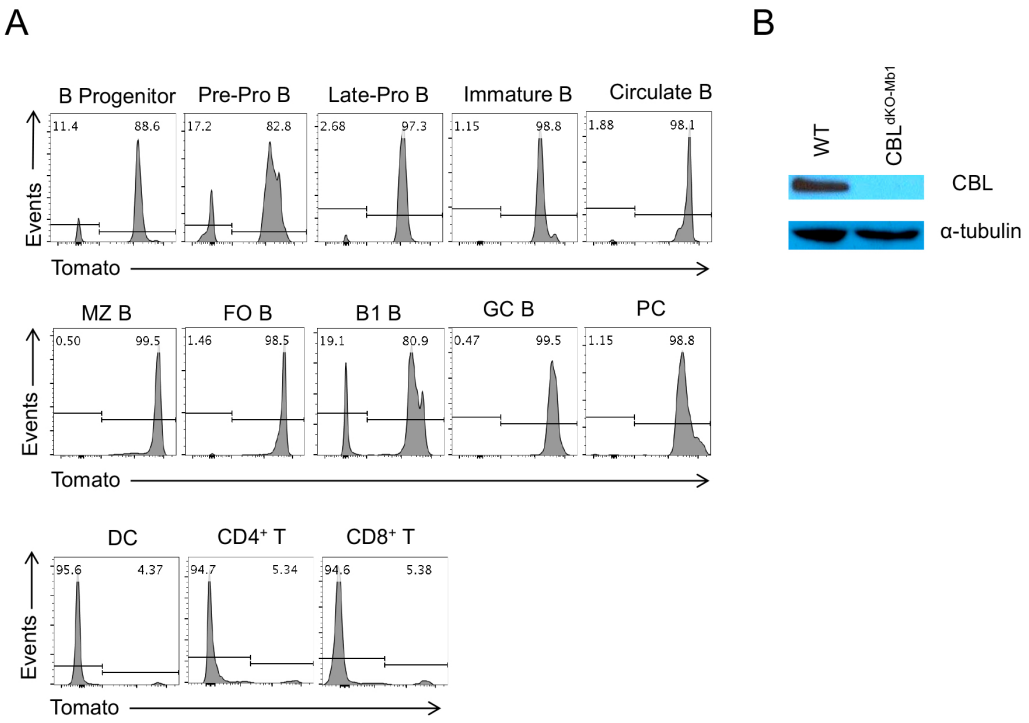

Figure 2.1 Generation of CBL$^{dKO\text{-}Mb1}$ mice

(A)FACS analysis deletion of *Cbl* gene in different cell linages from CBL$^{dKO\text{-}Mb1}$Tomato^{Rosa26} mice based on the Tomato expression. Gating strategy: B cell Progenitor: B220^{+}c-Kit^{+}; Pre-pro B cell: B220^{+}CD43^{+}; Late-Pro B cell: B220^{+}CD43^{-}IgM^{-}; Immature B cell: B220^{+}CD43^{-}IgM^{inter}; Circulate B cell: B220^{hi}CD43^{-}IgM^{hi}; MZ B cell: B220+ CD24^{low} AA4.1^{low} CD21^{low} CD23^{high}; FO B cell: B220+ CD24^{low} AA4.1^{low} CD21^{+} CD23^{+}; B1B cell: B220+ CD24^{low} AA4.1^{low} CD21^{low} CD23^{low}; GC B cell: B220+ Fas^{hi} GL7^{hi}; PCs: B220$^{lo/-}$CD138^{hi} **(B)**Western blot analysis of CBL expression in purified splenic Naïve B cells from WT and CBL$^{dKO\text{-}Mb1}$ mice. α-Tubulin was the loading control.

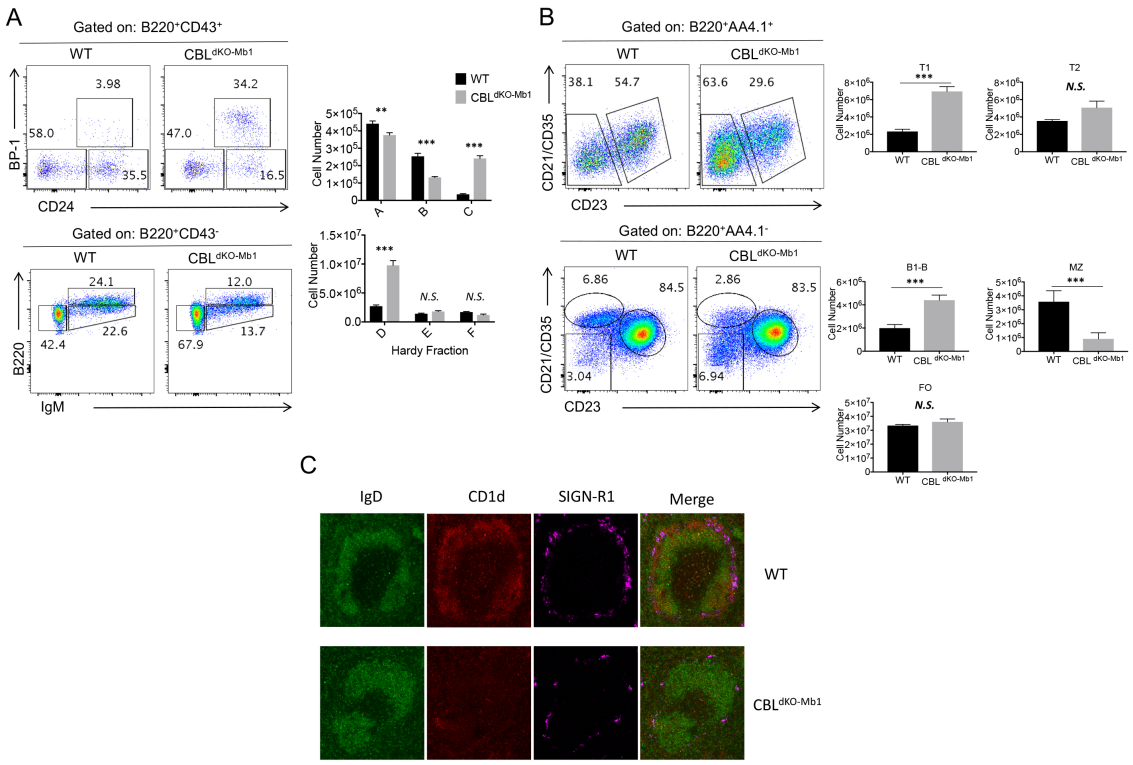

Figure 2.2 Impaired MZ and T1 B cell development in CBL$^{dKO\text{-}Mb1}$ mice

(A) Bone marrow B cell development in CBL$^{dKO\text{-}Mb1}$ mice. The dot plot (left) and statistic analyses of BM B cell development (n=5). Gating strategy: Fr.A (B220^{+}CD43^{+}BP1^{-}CD24^{-}); Fr.B (B220^{+}CD43^{+}BP1^{+}CD24^{+}); Fr.C (B220^{+}CD43^{+} BP1^{+}CD24^{+}); Fr.D (B220^{+}CD43^{-}IgM^{-}); Fr.E (B220^{+}CD43^{-}IgM^{+}); Fr.F (B220^{hi}CD43^{-}IgM^{+}). **(B)** Splenic B cell development in CBL$^{dKO\text{-}Mb1}$ mice. The dot plot (left) and statistics analyses of splenic B cell development (n=5). Gating strategy: T1(B220^{+}AA4.1^{+}CD21^{-}CD23^{-}); T2(B220^{+}AA4.1^{+}CD21^{+}CD23^{+}); B1-B(B220^{+}AA4.1^{-}CD21^{+}CD23^{-}); MZ(B220^{+}AA4.1^{-}CD21^{hi}CD23^{-}); FO(B220^{+}AA4.1^{-}CD21^{+}CD23^{+}). **(C)** Immunfluoresence staining of MZ region in spleen. Greed: IgD; CD1d: Red; SIGN-R1: Pink. *p<0.05, **p<0.001, ***p<0.0001 (un-paired two-tail T test). Data are pooled from two or three independent experiments. Error bars represent SEM.

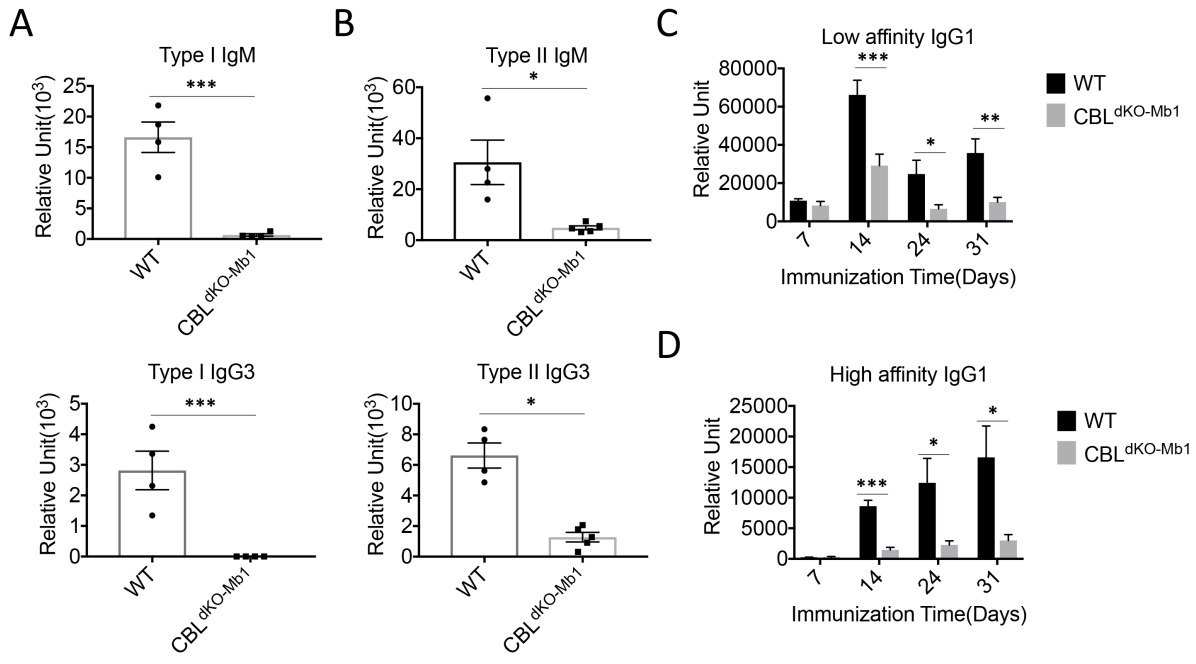

Figure 2.3 CBL family proteins were required for T-independent and T-dependent immune response

(A) Antibody response against Type-I T-independent antigen. The serum antibody titer of NP specific IgM and IgG3 antibody at day 7 post NP-LPS immunization (n=4-5). **(B)** Antibody response against Type-II T-independent antigen. The serum antibody titer of NP specific IgM and IgG3 antibody at day 7 post NP-Ficoll immunization (n=4-5). **(C)** Total IgG1 isotype antibody response against T-dependent antigen. The kinetics of serum total (anti-NP_{30}) antibody of IgG1 isotype from NP_{36}-KLH immunized mice (n=5). **(D)** High affinity IgG1 isotype antibody response against T-dependent antigen. The kinetics of serum high affinity (anti-NP_4) antibody of IgG1 isotype from NP_{36}-KLH immunized mice (n=5). *p<0.05, **p<0.001, ***p<0.0001 (un-paired two-tail T test, A-D). Data are from four to five mice per group. Error bars represent SEM.

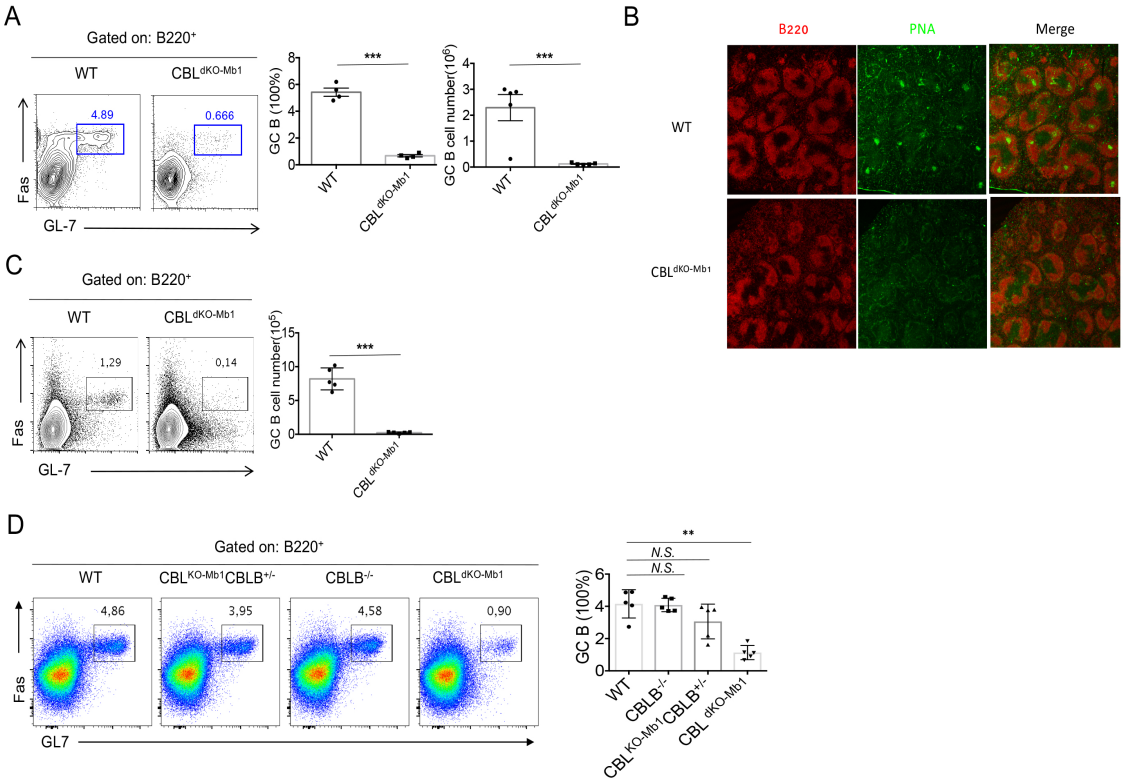

Figure 2.4 Impaired GC B cell development in CBL$^{dKO\text{-}Mb1}$ mice

(A) GC B cell development against T-dependent antigen SRBC in CBL$^{dKO\text{-}Mb1}$ mice. The contour map (left) and statistics analyses of the development of GC B cells (gated as: B220^{+}Fas^{hi}GL7^{hi}) from mice post 10 days of SRBC immunization (n=4). **(B)** The immunofluoresence analysis of GC reaction from post 10 days of SRBC immunization. Red: B220; Green: PNA. **(C)** GC B cell development against T-dependent antigen NP_{36}-KLH in CBL$^{dKO\text{-}Mb1}$ mice.The contour map (left) and statistics analyses of GC B cells (gated as: B220^{+}Fas^{hi}GL7^{hi}) from mice post 10 days of NP_{36}-KLH immunization (n=5). **(D)** Redundant function of CBL and CBLB in GC B cell development. The dot plot (left) and statistic analyses of GC B cells (gated as: B220^{+}Fas^{hi}GL7^{hi}) from different genotype control mice (WT, CBL$^{KO\text{-}Mb1}$CBL$^{+/-}$, CBLB$^{-/-}$ and CBL$^{dKO\text{-}Mb1}$) at day 10 after SRBC immunization (n=5). **p<0.001, ***p<0.0001 (un-paired two-tail T test, A, C, D). Data are from two or three independent experiments. Error bars represent SEM.

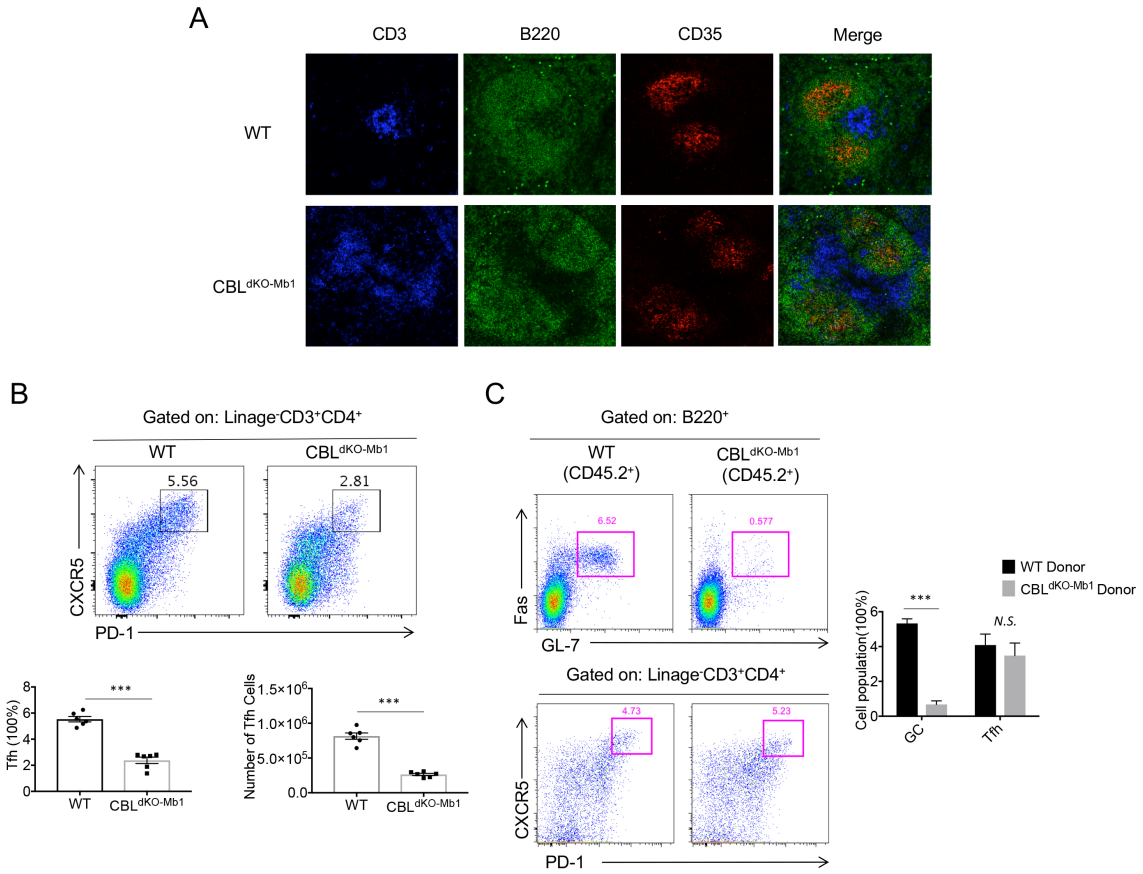

Figure 2.5 CBL family proteins regulate T_{fh} development through B cell intrinsic mechanism

(**A**) Immunofluoresence staining of FDC network in spleen from WT and CBL$^{dKO\text{-}Mb1}$ mice post 10 days of SRBC immunization. Blue: CD3; Green: B220; Red: C35. (**B**) CBL$^{dKO\text{-}Mb1}$ mutation block Tfh formation in mutant mice.The flow cytometric (top panel) and statistics (bottom panel) analyses of T_{fh} cells (gated as: Linage$^-$ CD4$^+$CD3e$^+$CXCR5^{hi} PD-1^{hi}) from mice day 10 post SRBC immunization (n=5). (**C**) B cell intrinsic defect of GC B cell formation in CBL$^{dKO\text{-}Mb1}$ mice. The dot plots (left) and statistics analyses of GC B cells (gated as: CD45.2$^+$B220$^+$Fas$^+$GL7$^+$) and T_{fh} cells (gated as: CD45.2$^+$Linage$^-$CD4$^+$CD3e$^+$CXCR5^{hi} PD-1^{hi}) from bone marrow chimeric mice at day 10 post SRBC immunization (n=6). Mixed bone marrow cells (WT/SJL and CBL$^{dKO\text{-}Mb1}$/SJL) were adaptively transferred to lethal irradiated Rag1$^{-/-}$ recipient mice through I.V. injection. After over one month reconstitution, chimera mice were immunized with SRBC. ***p<0.0001 (un-paired two-tail T test, B C). Data are from two or three independent experiments. Error bars represent SEM.

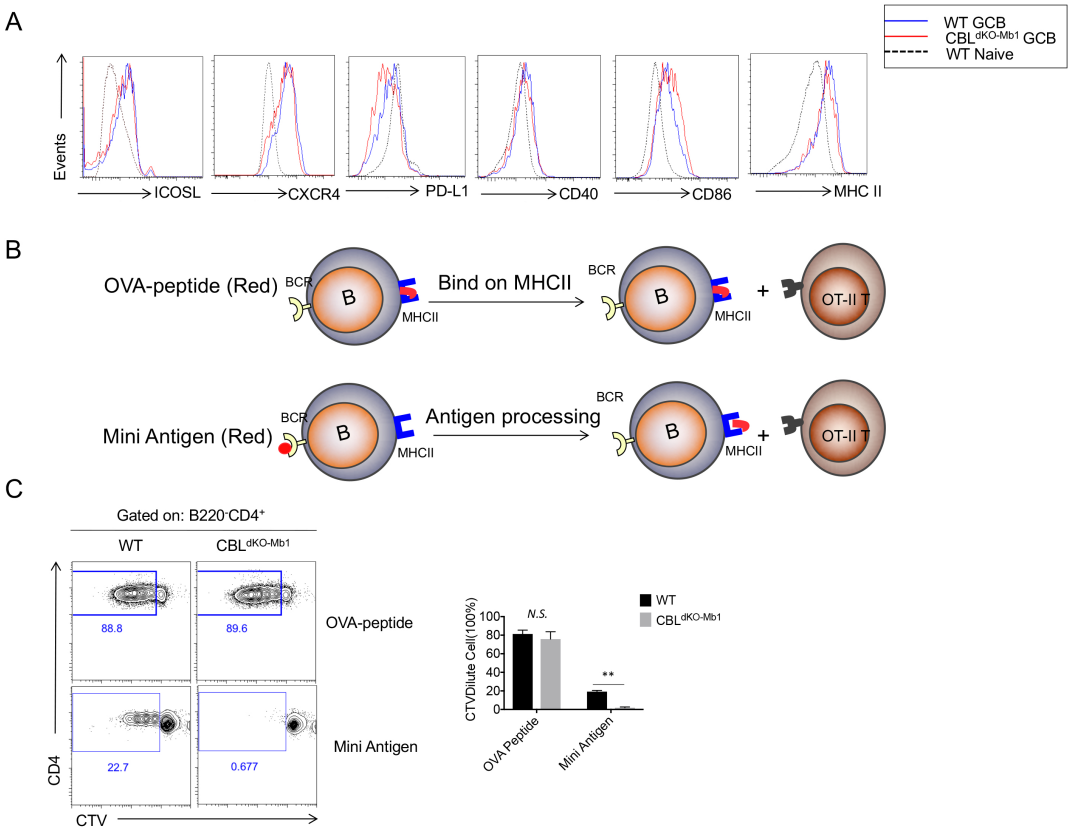

Figure 2.6 Impaired antigen presentation to cognate CD4+ T cells in CBL double deficient B cells

(**A**) Intact co-stimulatory surface receptor expression on CBL$^{dKO\text{-}Mb1}$ GC B cells. FACS analysis of surface receptors, including ICOSL, CXCR4, PDL1, CD40, CD86 and MHCII, expression on WT and *Cbls*-deficient GC B cells (gated as: B220^{+}Fas^{hi}GL7^{hi}) from 10 days post-immunization mice. The WT naïve B cells (gated as: B220^{+}Fas^{-}GL7^{-}) were set as control. (**B**) Strategy of *in vitro* B cell antigen presentation assay. Two types of antigen were used to test *in vitro* B cell antigen presentation to cognate T cells. Top panel: OVA$_{323\text{-}339}$ peptide can directly bind to MHCII on B cells, then present to OT-II CD4^{+} T cell. Bottom panel: mini antigen can be captured through BCR, then internalized, processed and presented on MHCII. Celltrace labelled OT-II CD4^{+} T cells were co-cultured with pre-treated WT and mutant B cells. (**C**) Cognate T-B *in vitro* co-culture. The contour map (left) and statistical analysis of in vitro B cell antigen presentation to OT-II CD4^{+} T cells after 72 hrs of T-B co-culture. **p<0.001 (un-paired two-tail T test, B). Data are from three independent experiments. Error bars represent SEM.

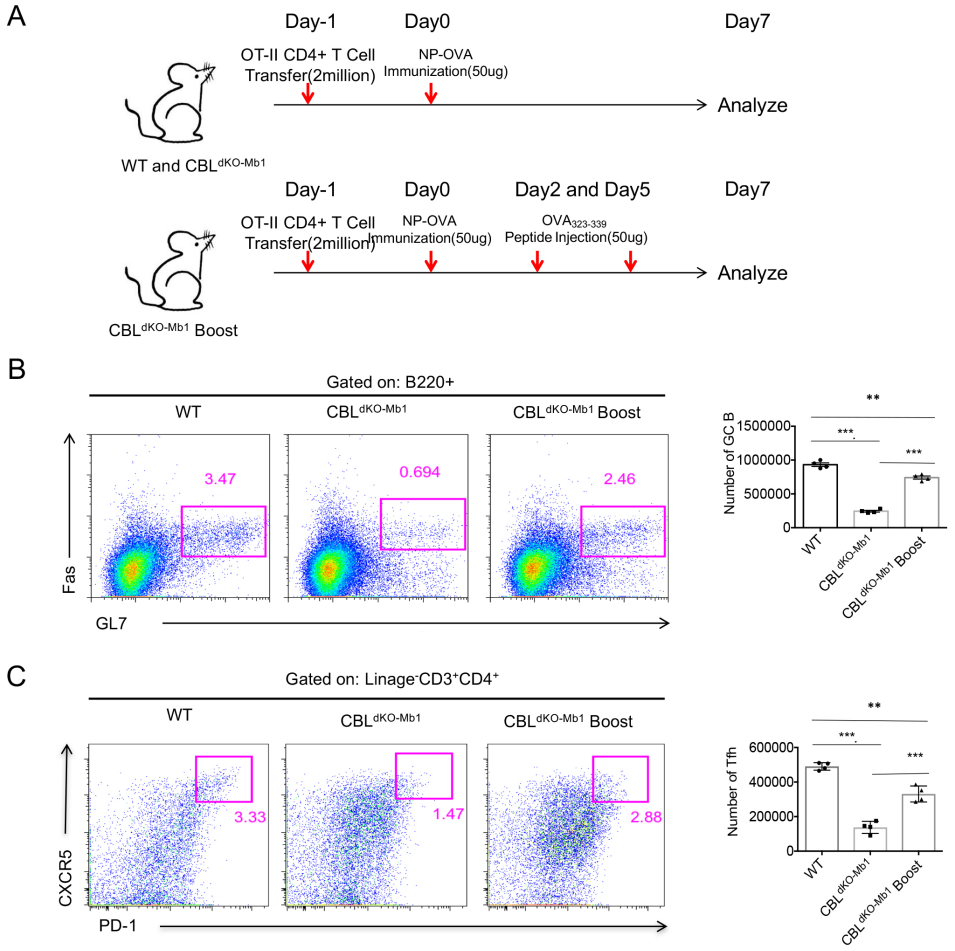

Figure 2.7 Partially rescue of GC B and T_{fh} development in $CBL^{dKO\text{-}Mb1}$ mice through administration of processed peptides

(**A**) Immunization strategy of peptide boost. At day -1, 2 million OT-II $CD4^+$ T cells were adaptively transferred into WT and $CBL^{dKO\text{-}Mb1}$ mice, and immunized with NP_{16}-OVA on day0. The group of $CBL^{dKO\text{-}Mb1}$ boost mice received two doses of $OVA_{323\text{-}339}$ peptide at day2 and day5. Three groups of mice were sacrificed and analyzed on day7. (**B**) Partially rescue T_{fh} development through peptides boosting. Dot plot (left) and statistical analyses of GC B (gated as: $B220^+Fas^{hi}GL7^{hi}$) development from with or without peptide treated NP_{36}-KLH immunized mice (n=4). (**C**) Partially rescue GC B cell development through peptides boosting. Dot plot (left) and statistical analyses of T_{fh} (gated as: $Linage^-CD3^+CD4^+CXCR5^{hi}PD\text{-}1^{hi}$) development from with or without peptide treated NP_{36}-KLH immunized mice (n=4). **p<0.001, ***P<0.0001 (un-paired two-tail T test). Data are from two independent experiments. Error bars represent SEM.

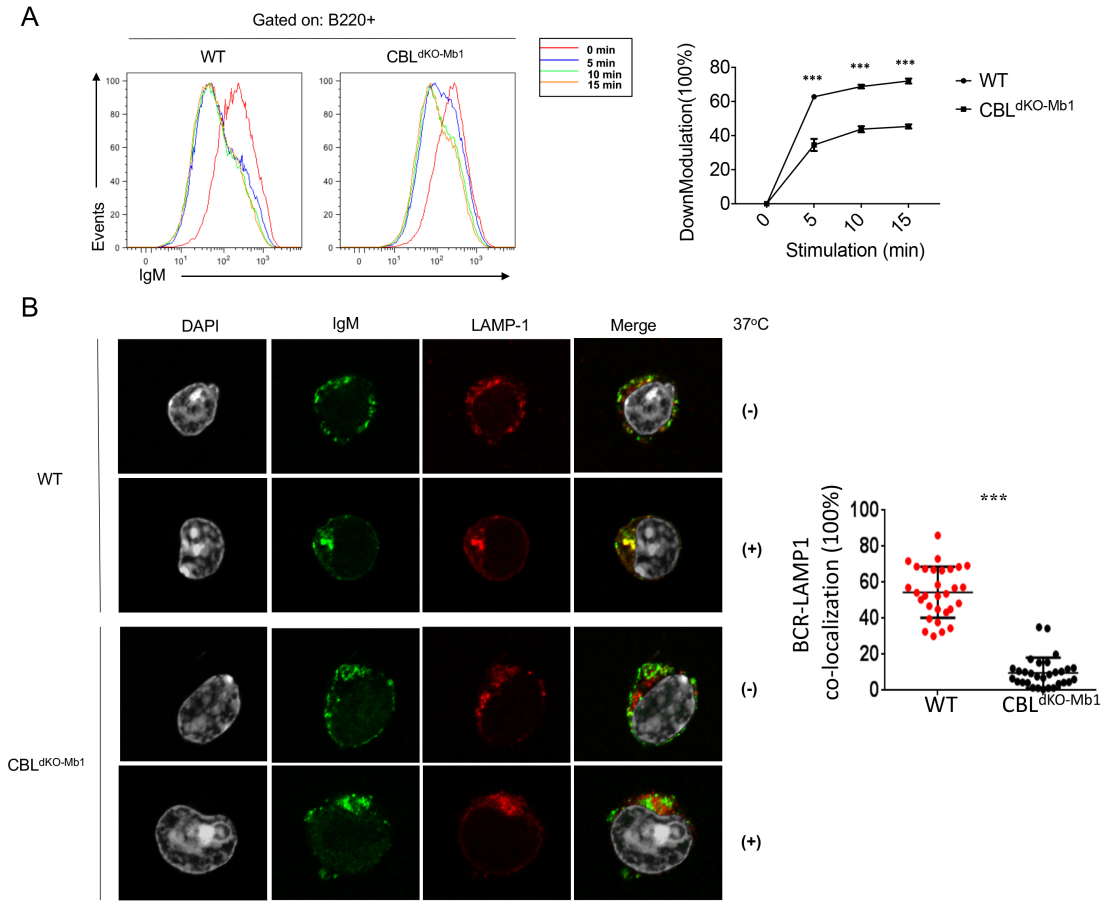

Figure 2.8 CBL proteins regulate Naïve B cell BCR downmodulation and lysosome sorting

(**A**) FACS analysis of BCR downmodulation from purified naïve B cells. The histogram (left) and statistics analyses of BCR downmodulation at various time points (n=3). The downmodulation rate= (MFI of IgM at time 0'-MFI of IgM at desire time)/ MFI of IgM at time 0'. (**B**) Immunofluoresence analysis of BCR degradation in mutant naïve B cells. The co-localization of BCR complex and lysosome based on marker LAMP-1. Samples from two different time points (0' and 30') were examined. Grey: DAPI; Green: IgM; Red: LAMP-1. BCR-lysosome co-localization rate=MFI of BCR complex in LAMP-1 region/ Total MFI of BCR complex. ***P<0.0001 (un-paired two-tail T test, A, B). Data are from two or three independent experiments. Error bars represent SEM.

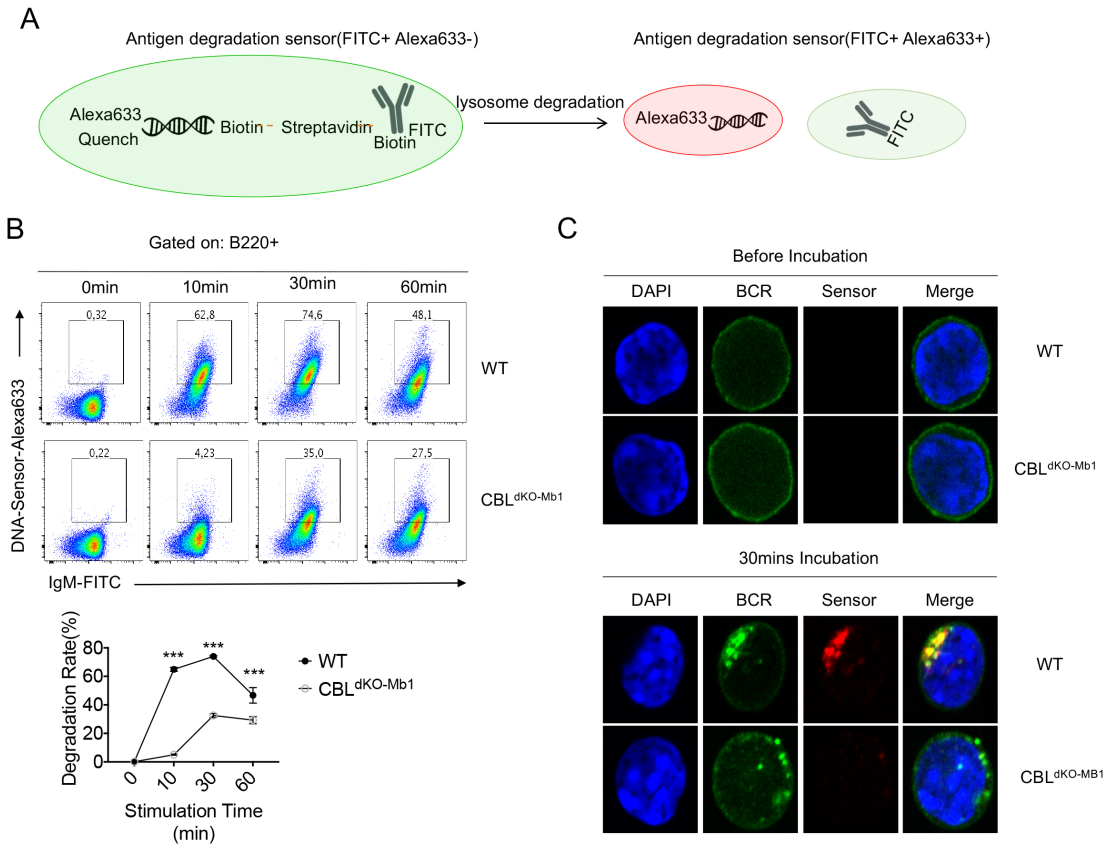

Figure 2.9 Severely impaired antigen degradation in *Cbls*-deficient Naïve B cells

(**A**) The principle of antigen degradation sensor. The sensor included three parts: Alexa633-DNA sequence-Quench sequence, Streptavidin, FITC-anti-IgM F(ab)2. At steady state, the sensor was $FITC^{+}$ $Alexa633^{-}$ since the quench sequence was associated with Alexa633. Once the sensor was internalized by naïve B cells through BCR and sorted to lysosome for degradation, the Alexa633 and Quench sequence were rapidly de-associated, then the cells turned into $FITC^{+}Alexa633^{+}$. (**B**) Monitoring antigen sensor degradation by FACS. The dot plot (left) and statistics analyses of antigen sensor degradation at various time points (n=3). Naïve B cells were pre-treated with antigen sensor for 30mins on ice, then incubated at 37°C for various time points (0', 10', 30', 60'). (**C**) Visualization of the antigen sensor degradation by confocal microscopy. Samples were from two different stimulation time points (0' and 30'). Blue: DAPI; Green: BCR; Red: Alexa633 sensor. ***P<0.0001 (un-paired two-tail T test, B). Data are from three independent experiments. Error bars represent SEM.

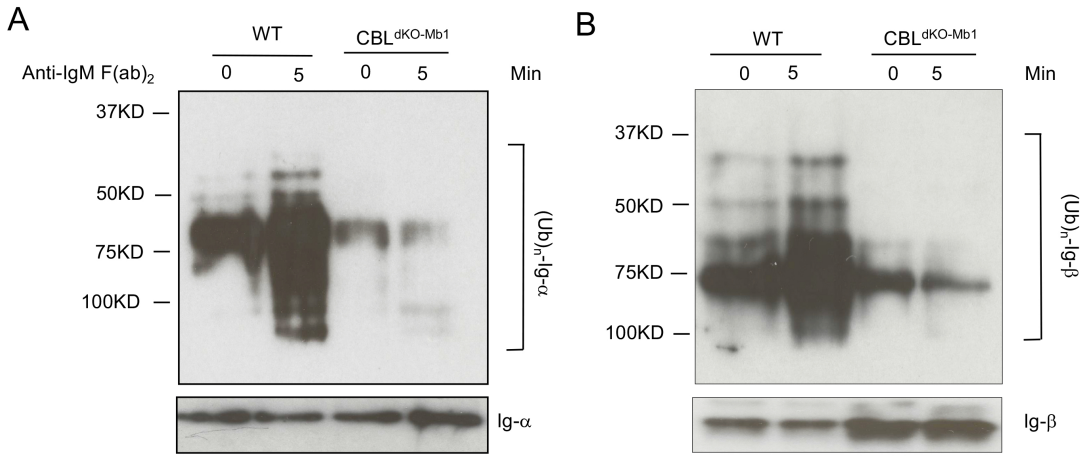

Figure 2.10 Impaired Igα and Igβ ubiquitination upon BCR stimulation

(A) Western blot analysis of Igα ubiquitination. The Naïve B cells were first treated with MG132 for 4hrs, then were non-stimulated (0') or stimulated (5') with Anti-IgM $F(ab)_2$ for 5mins. The Igα protein was pulled down through immunoprecipitation for western blot (n=2). (B) Western blot analysis of Igβ ubiquitination. The Naïve B cells were treated with MG132 for 4hrs, then were non-stimulated (0') or stimulated (5') with Anti-IgM $F(ab)_2$ for 5mins. The Igβ protein was pulled down through immunoprecipitation for the detection of its ubiquitination (n=2).

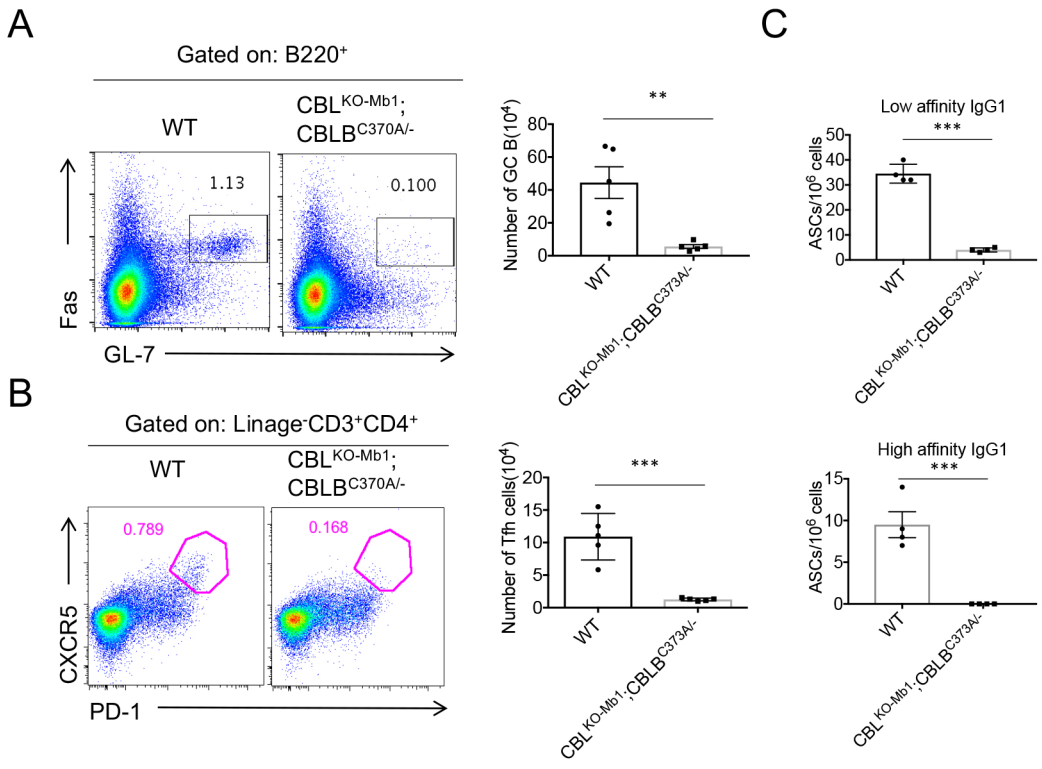

Figure 2.11 E3 ubiquitin ligase function of CBL proteins regulate the initiation of GC reaction

(**A**) GC B cell deficiency in $CBL^{KO\text{-}Mb1}CBLB^{373A/-}$ mice. The dot plot (left) and statistical analysis of GC B cells (gated as $B220^{+}Fas^{hi}GL7^{hi}$) at day 14 after NP_{36}-KLH immunization (n=5). (**B**) Impaired T_{fh} development in $CBL^{KO\text{-}Mb1}CBLB^{373A/-}$. The flow cytometric (left) and statistical analysis of the T_{fh} cells (gated as $Linage^{-}CD4^{+}CD3e^{+}CXCR5^{hi}PD\text{-}1^{hi}$) at day14 post NP_{36}-KLH immunization (n=5). (**C**) The statistical analyses of splenic total (top panel) and high affinity (bottom panel) anti-NP antibody secreting plasma cells from post 14 days NP_{36}-KLH immunized mice (n=4). **p<0.001, ***P<0.0001 (un-paired two-tail T test, A, B, C). Data are from two or three independent experiments. Error bars represent SEM.

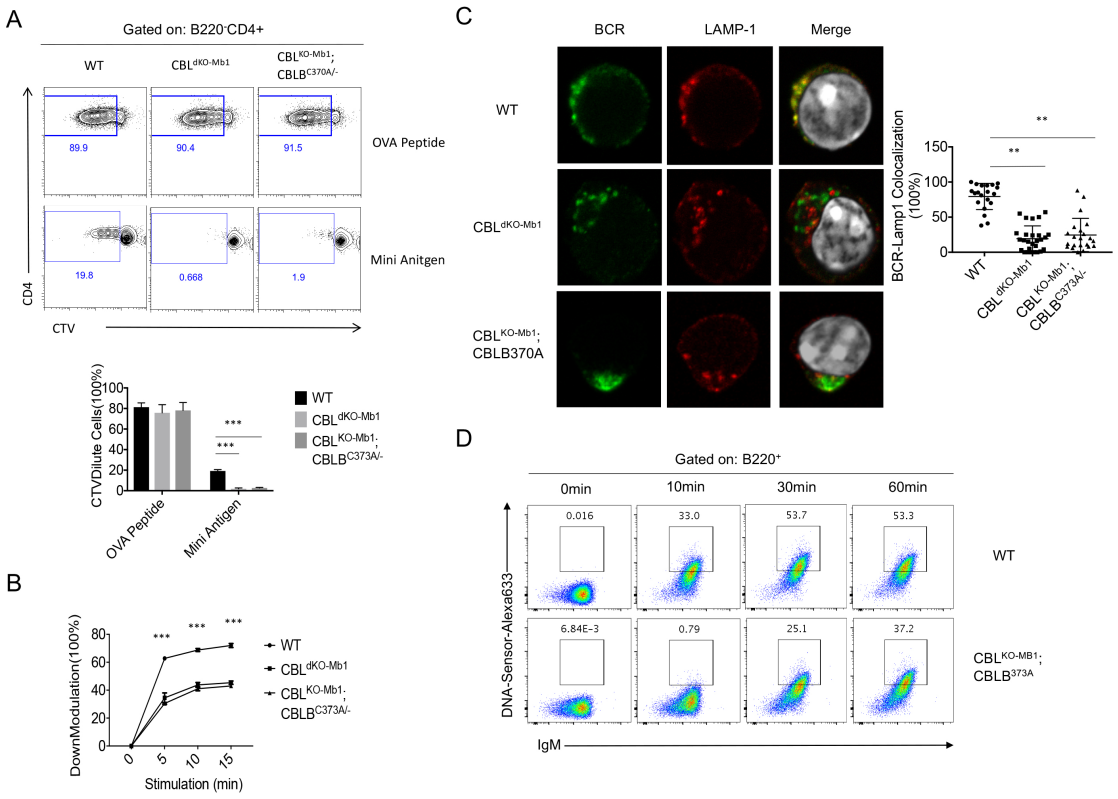

Figure 2.12 E3 ubiquitin ligase function of CBL proteins was required for antigen presentation through BCR related mechanism

(**A**) In vitro B cell antigen presentation assay. The contour map (top panel) and statistics (bottom panel) analysis [254][250]of the Celltrace labeled OT-II $CD4^+$ T cell proliferation after 72 hrs of co-culture with mini antigen or $OVA_{323-339}$ peptide pretreated Naïve B cells (n=6). (**B**) The FACS analysis of BCR stimulation induced BCR downmodulation at various time point (n=3). The downmodulation rate= (MFI of IgM at time 0'-MFI of IgM at desire time)/ MFI of IgM at time 0'. (**C**) The BCR and lysosome co-localization was visualized (left) and quantified (left) by confocal microscopy and volocity. Green: BCR; Red: LAMP-1. The BCR-lysosome colocalization rate=MFI of BCR complex in LAMP-1 region/ Total MFI of BCR complex. (**D**) Monitoring DNA-antigen sensor degradation by FACS. **p<0.001, ***p<0.0001 (un-paired two-tail T test, A, B, C). Data are from two or three independent experiments. Error bars represent SEM.

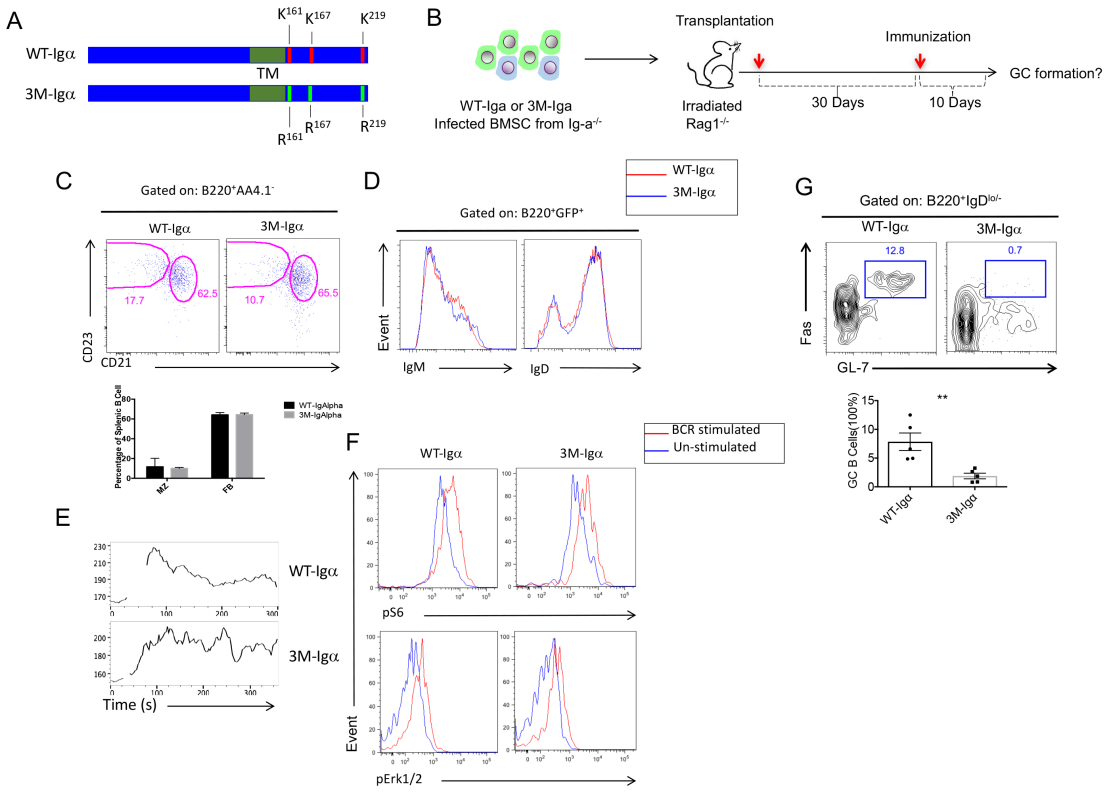

Figure 2.13 The ubiquitination of Igα was required for GC B cell development

(**A**) Schematic of Igα mutant protein. Three potential ubiquitination sites at the cytoplasmic tail of Igα were replaced from Lysine to Arginine (termed as 3M-Igα). (**B**) Generation of WT-Igα and 3M-Igα bone marrow chimeric mice. *WT-Igα* and *3M-Igα* genes were respectively introduced into $Ig\alpha^{-/-}$ bone marrow stem cells (BMSC) through GFP based retroviral vector. Then BMSC were transferred to lethally irradiate $Rag1^{-/-}$ recipient mice. After one month of reconstitution, the chimeric mice were immunized with NP_{36}-KLH. The GC reaction was analyzed at day 10 post-immunization. (**C**) Splenic B cell development in 3M-Igα mutant mice. The dot plot (top panel) and statistic (bottom panel) analyses of mature B cell development (MZ B gated as $B220^{+}AA4.1^{-}CD21^{hi}CD23^{-}$; FO B gated as $B220^{+}AA4.1^{-}CD21^{int}CD23^{+}$) (n=3). (**D**) Intact surface BCR expression on 3M-Igα naïve B cells. The surface expression of IgM and IgD (Gated on: $B220^{+}GFP^{+}$) on splenic B cells was shown in histograms. (**E**) The flow cytometric analysis of the BCR induced $Ca2^{+}$ flux signalling in splenic naïve B cells. (**F**) The histogram of BCR induced mitotic signalling (Gated on: $B220^{+}GFP^{+}$) in splenic naïve B cells. (**G**) GC B cell development in 3M-Igα mutant mice. The contour map (top panel) and statistic (bottom panel) analyses of GC B cells (Gated as $B220^{+}IgD^{-/lo}Fas^{hi}GL7^{hi}$) development from post 10 days of NP_{36}-KLH immunization mice (n=5). **p<0.001, (un-paired two-tail T test, F). Data are from three independent experiments. Error bars represent SEM.

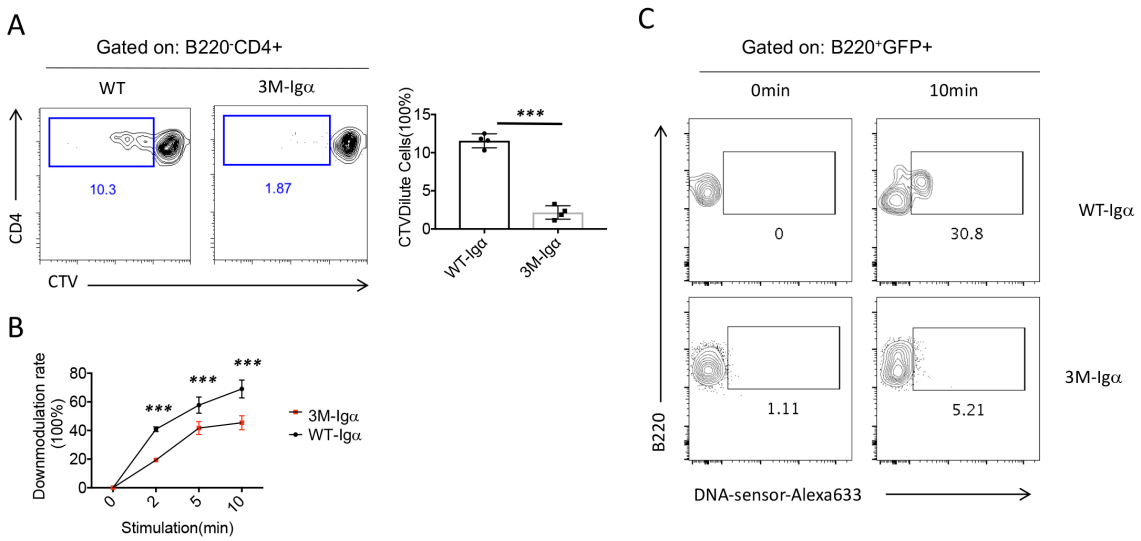

Figure 2.14 Blockade of Igα ubiquitination lead to impaired antigen presentation

(**A**) In vitro B cell antigen presentation assay. The contour map (left) and statistics analysis of the Celltrace labeled OT-II CD4+ T cell proliferation after 72 hrs of co-culture with mini antigen pretreated naïve B cells (n=4). (**B**) The process of Igα ubiquitination is required for BCR internalization. Statistic analysis of anti-IgM $F(ab)_2$ induced BCR downmodulation at various time points (0', 2', 5', 10) (n=4). (**C**) FACS quantification of DNA sensor degradation. ***P<0.0001 (un-paired two-tail T test, A, B). Data are from three independent experiments. Error bars represent SEM.

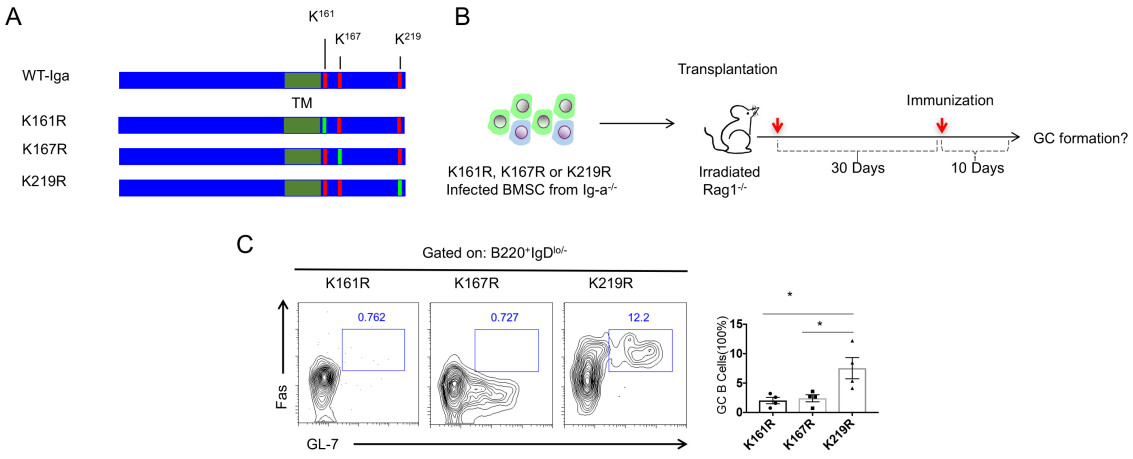

Figure 2.15 K161 and K167 are the ubiquitination site of Igα

(A) Schematic of three Ig-α single mutants (termed as: K161R; K167R; K219R). Three potential ubiquitination sites at the cytoplasmic tail of Igα were individually replaced from Lysine (K) to Arginine (R). (B) Generation of bone marrow chimeric mice. *K161R*, *K167R* and *K219R* genes were respectively introduced into $Ig\alpha^{-/-}$ bone marrow stem cells (BMSC) through GFP based retroviral vector, then BMSC were transferred to lethally irradiate $Rag1^{-/-}$ mice. After one month of reconstitution, the chimeric mice were immunized with NP_{36}-KLH. The GC reaction was analyzed at day 10 post-immunization. (C) The contour map (left) and statistic analysis of GC B cell (Gated on: $B220^{+}IgD^{lo/-}$ $Fas^{hi}GL7^{hi}$) development from mice post 10 days of NP_{36}-KLH immunization (n=4-5). *P<0.05 (un-paired two-tail T test, B). Data are from three independent experiments. Error bars represent SEM.

3 Chapter 3: CBL ubiquitin ligases control the exit checkpoint of the germinal centre reaction

Xin Li[1,2], Adeline Gadzinsky[1], Liying Gong[1,3], Haijun Tong[1,2], Virginie Calderon[1], Yue Li[1,4], Daisuke Kitamura[5], Ulf Klein[6], Wallace Y. Langdon[7], Fajian Hou[8], and Yong-Rui Zou[9] & Hua Gu[1,2,3,10]

[1]Montreal Clinical Research Institute, Montreal, QC H2W 1R7, Canada

[2]Department of Microbiology and Immunology, University of Montreal, Montreal, QC H3T 1J4, Canada

[3]Division of Experimental Medicine, McGill University, Montreal, QC H3A 0G4, Canada

[4]Department of Microbiology and Immunology, McGill University, Montreal, QC H3A 0G4, Canada

[5]Research Institute for Biomedical Sciences, Tokyo University of Sciences, Noda, Chiba 162-8601, Japan

[6] Leeds Institute of Cancer and Pathology, School of Medicine, University of Leeds, Leeds LS97TF, United Kingdom

[7] School of Biomedical Sciences, University of Western Australia, Crawley, Western Australia 6009, Australia

[8]Shanghai Institute of Biochemistry and Cell Biology, Chinese Academy of Sciences, Shanghai 200031, China

[9]The Feinstein Institute for Medical Research, Manhasset, NY 11030, USA

[10]Lead Contact

3.1 Summary

High affinity antibodies are generated by SHM of BCR in the DZ of GC. The resulting high-affinity B cells are then selected in the LZ to become PCs or return to the DZ for further SHM by a less understood regulatory mechanism. We found that ubiquitin ligases CBL and CBL-B (CBLs) in GC B cells controlled high affinity antibody production. Ablation of CBLs, while imposing little effect on SHM or on the DZ-LZ recirculation, impeded the expansion of high-affinity GC B cells and expedited differentiation into PCs. This effect could be attributed to CBL-mediated ubiquitination of the PC-promoting transcription factor IRF4. Thus, our finding reveals a critical GC LZ program that prevents B cells from exiting the DZ-LZ cycle before acquisition of high-affinity BCRs.

3.2 Introduction

Production of high affinity antibodies is central to T cell-dependent humoral immunity against pathogens and occurs in GC through a process termed antibody affinity maturation[255, 256]. Upon encounter with antigen, activated B cells enter GCs to undergo clonal expansion and somatically mutate their BCR genes via activation-induced cytidine deaminase-mediated SHM in the anatomically distinct dark zone [90, 94, 257-260]. B cells with a mutant BCR then migrate to the LZ to compete for the antigen presented by FDC and the help from T_{fh} cells[94, 258, 261-263]. Higher affinity BCRs have advantages to compete for the antigen, allowing B cells to receive more help such as CD40L stimulation from T_{fh} cells[91, 94, 144, 171]. Surviving high affinity GC B cells may terminate the GC B cell fate and differentiate into memory B cells or PCs, or migrate back to the DZ for a further round of SHM and clonal expansion[52, 94, 264-

266]. The spatial and temporal circulation between the GC DZ and LZ enables B cells with higher affinity BCRs being preferentially expanded and selected to enter the memory or PC pool.

Given the critical role of such a GC interzonal circulation in the generation and selection of high affinity BCR-expressing B cells, much effort has been invested to understand the mechanisms by which B cells are instructed to stay in or exit the DZ-LZ cycle to become memory B cells or PCs. At the transcriptional level, maintenance of the GC B cell fate is controlled by GC B cell promoting transcription factors such as BCL6[267]. In contrast, the identity of PCs depends on BLIMP1 and IRF4[132, 160, 268]. These two groups of transcription factors antagonistically regulate each other and dictate the steady-state distinctive characteristics of GC B cells and PCs, respectively[269, 270]. In addition to these transcription factors, MYC, FOXO1, and NFκB have been reported to provide additional layers of regulation during the GC reaction[84, 93, 145, 147, 148, 151, 168]. Inactivation of NFκB, or MYC in GC B cells resulted in the collapse of the GCs, due to the impaired recirculation of LZ B cells to the DZ. Foxo1 was found to be essential for the DZ phenotype, as mice with deletion of *foxo1* in GC B cells have only LZ cells. A question that remains unanswered is what is the molecular mechanism that senses BCR affinity cues in GC B cells and instructs B cells to continue the DZ and LZ circulation or to initiate the differentiation program to PCs.

CBL and CBL-B (CBLs) are two members of the CBL family of E3 ubiquitin ligases expressed in hematopoietic cells[271]. In B cells, they play a crucial role in the induction of immune tolerance, possibly by regulating the negative selection of autoreactive B

cells. It has been shown that inactivation of CBLs using the *Cd19-cre* allele results in a moderate increase in IgM and reduction in IgG isotypes of T-cell dependent antibody responses[215]. However, the function of CBLs in the GC reaction and antibody affinity maturation has not yet been investigated. Here, we show that CBLs are essential for the selection of high affinity GC B cells and antibody affinity maturation. In GC, CBLs are minimally expressed in DZ B cells, markedly upregulated in LZ B cells, and suppress IRF4 expression by promoting IRF4 ubiquitination. Ablation of CBLs in GC B cells upregulates IRF4, leading to impaired clonal expansion of high affinity B cells and expedited GC differentiation, despite normal SHM and DZ-LZ circulation of GC B cells. Consistent with this result, ectopic expression of IRF4 alone or inactivation of the ubiquitin ligase activity of CBLs is sufficient to recapitulate the GC phenotypes found in CBLs mutant mice. Thus, our data indicate that B cell-intrinsic CBLs-IRF4 axis constitutes an ubiquitination dependent regulatory cascade that temporally controls GC B cells to stay in the DZ-LZ circulation until the acquisition of high affinity BCRs.

3.3 Results

3.3.1 Expression patterns of CBLs in B cell subsets and the GC reaction

To evaluate whether CBL proteins regulate T-dependent antibody response, we first examined the expression patterns of CBL and CBLB in naïve and GC B cells. We found decreased amounts of both *Cbl* and *Cblb* mRNA in GC B cells as compared to naïve B cells; however, GC B cells expressed higher amounts of CBL and CBLB proteins as compared to naïve B cells (Figures 3.1 A, 3.1 B and 3.2 A). The marked alteration

seemed to be a GC phenomenon, since activation of B cells with anti-IgM or anti-CD40 induced only a mild increase or a decrease in both CBL and CBLB proteins, respectively (Figure 3.2 B). Within GC B cell populations, the LZ GC B cells possessed significantly more CBL and CBLB proteins but not mRNAs compared to the DZ B cells (Figures 3.1 C, 3.1 D, 3.2 C and 3.2 D). These results indicate that CBL proteins are post-transcriptionally and dynamically modulated during the GC reaction.

3.3.2 Ablation of CBL proteins in GC B cells impairs antibody affinity maturation

We then generated *c-Cbl*$^{fl/fl}$, *Cbl-b*$^{-/-}$, IgCγ-cre Tg mice in which the IgCγ–cre allele drove Cre recombinase expression in GC B cells so that only GC B cells carried the CBL and CBL-B double null (termed here CBL$^{dKO\text{-}Cg}$) mutation, whereas other cells of the mice harbored the germline CBL-B mutation[202, 205, 272]. Ablation of CBL and CBL-B proteins in GC B cells was confirmed by Western blot analysis and immunofluorescent staining (Figure 3.3 A and B). Inspection of CBL$^{dKO\text{-}Cg}$ mice revealed normal development of B cells (Figure 3.3 C and D). Compared to WT mice, the mutant mice produced similar levels of total anti-NP (NP_{30}) antibodies of IgM and IgG1 isotypes initially, after immunization with (4-Hydroxy-3-Nitrophenyl) Acetyl-Keyhole Limpet Hemocyanin (NP-KLH); however, they displayed a significantly lower level of IgG1 at day 28 (Figure 3.4 A). In addition to the antibody titer, the CBL$^{dKO\text{-}Cg}$ mice exhibited impaired antibody affinity maturation, as the level of anti-NP_4 as well as the ratio of high affinity anti-NP (NP_4) vs total anti-NP (NP_{30}) IgG1 was severely impaired in the mutant mice compared to the WT controls (Figure 3.4 B and C). Consistent with the antibody production, the mutant mice possessed slightly more IgM antibody-secreting cells (ASCs) against NP_{30}

antigen. In contrast, they had markedly reduced numbers of total (anti-NP_{30}) as well as high affinity (anti-NP_4) IgG1 ASCs relative to their WT counterparts (Figure 3.4 D).

In T-cell dependent immune responses, ASCs or PCs are mostly derived from GC B cells. To examine whether the $CBL^{dKO\text{-}Cg}$ mutation affected the GC reaction, we analyzed the kinetics of GC B cell development during the course of immunization. At day 8 after immunization, WT and $CBL^{dKO\text{-}Cg}$ mice developed equal percentages of GC B cells; however, while WT mice exhibited a peak GC development at day 12 and declined GC B cell numbers thereafter, the mutant mice maintained GC B cells at a steady level up to day 18 (Figure 3.4 E). The altered kinetics of GC B cell development in the mutant mice could be partly attributed to a combinatory effect of expedited differentiation and reduced apoptosis, because $CBL^{dKO\text{-}Cg}$ GC B cells generated more plasma cells (see below) and expressed a lower number of active Caspase positive cells compared to the WT controls, respectively (Figure 3.4 F). The proliferation of GC B cells was not affected by the $CBL^{dKO\text{-}Cg}$ mutation (Figure 3.3 E). In addition to the altered kinetics of GC B cell expansion, the mutant mice had a markedly lower number of GC B cells expressing a high affinity cell surface IgG1 BCR against NP antigen relative to the WT mice throughout the course of immunization (Figure 3.4 G). The influence on high affinity BCR-expressing GC B cells was not caused by IgCγ-Cre tg and appeared to be redundant between CBL and CBL-B, because IgCγ-Cre tg mice had normal numbers of total and high affinity GC B cells, and ablation of *Cbl* or *Cblb* alone exhibited only a relatively mild effect on the numbers of high affinity NP-binding GC B cells compared to $CBL^{dKO\text{-}Cg}$ mutants (Figure 3.3 F and G). Together, our results indicate that CBL proteins control

antibody affinity maturation rather than total antibody production. In addition, this regulation occurs at the stage of GC B cells.

3.3.3 CBL proteins regulate GC selection for high affinity antibody-producing B cells

Deficiency in generating high affinity antibody producing cells could be a result of impaired SHM or lack of selection for high affinity B cells in the GC. To distinguish these two possibilities, we analyzed SHM in IgH genes in GC B cells. We isolated Igλ1$^+$ GC B cells from NP-KLH immunized mice by FACS sorting at day 12 postimmunization and examined SHM in Ig V_H186.2 by DNA sequencing according to the previous publication (Figure 3.5 A)[145]. We found that while all (20/20) V_H186.2 genes isolated from WT GC B cells carried at least one mutation (range: 1-15 mutations), about ~85% (17/20) of V_H186.2 genes from $CBL^{dKO\text{-}Cg}$ GC B cells were mutated (range: 1-9 mutations) (Figure 3.6 A)[52, 258]. In addition, V_H186.2 genes from WT GC B cells carried five replacement mutations/clone and 65% (13/20) of V_H186.2 genes harbored a tryptophan to leucine mutation at position 33 (W33L), a mutation known to encode a high affinity BCR (Figure 3.6 B and C). In contrast, V_H186.2 genes from $CBL^{dKO\text{-}Cg}$ B cells possessed merely two replacement mutations per clone on average and only 15% (3/20) of clones carried a W33L mutation. Analysis of the replacement vs silent mutations (R/S ratio) in V_H186.2 genes revealed that while the V_H genes from WT GC B cells had undergone strong selection (R/S = 4.4), those from $CBL^{dKO\text{-}Cg}$ B cells exhibited an R/S ratio equivalent to that expected for the random mutation (R/S = 2.2) (Figure 3.6 D). The frequencies of the silent mutations in V_H186.2 genes were comparable between WT and $CBL^{dKO\text{-}Cg}$ B cells

(Figure 3.6 B), indicating that the SHM *per se* is not affected by the $CBL^{dKO\text{-}Cg}$ mutation. To ascertain that the above phenomenon in $V_H186.2$ genes indeed reflected that in NP-specific BCRs, we also compared SHM in $V_H186.2$ genes isolated from NP_{38}-binding GC B cells. Consistent with that observed in $IgG1^+$ GC B cells, the number of $V_H186.2$ genes carrying a W33L mutation was also significantly reduced in the mutant NP-specific GC B cells compared to WT controls (Figure 3.6 B and C).

To directly examine whether CBLs regulated cellular selection of high affinity BCR-expressing cells inside GCs, we compared the kinetics of high affinity NP (NIP_5) and total NP (NP_{38})-binding GC B cell development at different time points upon NP-KLH immunization (Figure 3.6 E). At day 8 after immunization, WT mice had approximately 20% of NIP_5-binding and 31% NP_{38}-binding GC B cells, indicating that approximately 65% of total NP-specific GC B cells express a high affinity BCR as defined by NIP_5-binding capability. By day 14, the ratio of NIP_5 vs NP_{38}-binding GC B cells increased to more than 90%, indicating that the high affinity NP specific B cell population is selectively expanded within total NP specific GC B cells. In contrast to WT mice, $CBL^{dKO\text{-}Cg}$ mice possessed relatively lower numbers of NIP_5 and NP_{38}-binding GC B cells at day 8 (average 5% and 9%, respectively), equivalent to approximately 61% of NIP_5-binding cells among total NP_{38}-binding cells. By day 14, this ratio only increased slightly to less than 70%, indicating that the selection for NIP_5-binding cells is severely impaired in the mutant mice.

Taken together, the above data demonstrate that CBLs are required for the selection of high affinity BCR expressing B cells during GC reaction. However, they appear to be dispensable for the regulation of SHM in GC B cells.

3.3.4 The CBL$^{dKO\text{-}Cg}$ mutation expedites GC B cell differentiation

During affinity maturation, GC B cells undergo multiple cycles of proliferation and SHM in the DZ and selection in the LZ[171, 273]. Disruption of these cycles may impair affinity-driven selection of GC B cells. To understand the mechanisms by which CBL proteins regulate GC affinity selection, we examined whether the CBL$^{dKO\text{-}Cg}$ mutation affected the development of DZ and LZ GC B cells or the differentiation dynamics of GC B cells to PCs. The DZ and LZ architecture in the immunized CBL$^{dKO\text{-}Cg}$ mice appeared to be normal (Figure 3.7 A). In addition, flow cytometric analysis of the DZ and LZ GC B cells could not reveal any difference between the WT and CBL$^{dKO\text{-}Cg}$ mice (Figure 3.7 B). These results indicate that the CBL$^{dKO\text{-}Cg}$ mutation does not significantly influence the development of DZ and LZ GC B cells at the population level. However, B220^{+} GL7^{hi} Fas^{hi} GC B cells in CBL$^{dKO\text{-}Cg}$ mice possessed significantly more plasma cell precursor-like cells that expressed lower Bcl6 and slightly higher CD138 (Figure 3.7 C), suggesting that the CBL$^{dKO\text{-}Cg}$ mutation expedites GC B cells to PC differentiation.

We then performed BrdU labeling experiment to determine whether GC B cell development into PCs was increased in the mutant mice. At day 12 after immunization, in both WT and CBL$^{dKO\text{-}Cg}$ mice approximately 90% of GC B cells incorporated BrdU after twenty-four hours of BrdU labeling (Figure 3.8 A), consistent with previous findings that

GC B cells are vigorously proliferating. In contrast, the mutant mice generated 50% more $BrdU^+$ PCs as compared to WT mice (17% vs 11%) during the same period, which was equivalent to the genesis of 6,000 PCs/hour/spleen in $CBL^{dKO\text{-}Cg}$ mice compared to 4,000/hour/spleen in WT controls (Figures 3.9 A and B). These $BrdU^+$ PCs were mostly newly generated from NP-KLH activated B cells, rather than derived from spontaneous immune responses or existing PCs and proliferating plasma blasts, because twenty-four hours BrdU labeling of un-immunized WT and $CBL^{dKO\text{-}Cg}$ mice produced only 1-2% of $BrdU^+$ PCs (Figure 3.8 B). Given that the mutant mice had less GC B cells than WT controls at day 12 after immunization (Figure 3.4 E), the increased PC genesis in $CBL^{dKO\text{-}Cg}$ mice is consistent with the idea that CBL proteins are responsible for retaining GC B cells in the DZ-LZ cycle and preventing them from differentiation into PCs.

To directly assess the effect of CBLs on the fate choice of B cells in developing GCs in the context of affinity selection, we examined the development of high affinity NP-specific GC B cells and PCs upon inducible ablation of CBLs. We transferred B cells from ER-Cre tg (Control) or $Cbl^{fl/fl}$ Cbl-$b^{-/-}$ ER-Cre tg (termed $CBL^{dKO\text{-}UBC}$) mice into μMT recipient mice and immunized the chimeric mice with NP-KLH so that the donor B cells could enter and initiate GC reaction. We then deleted CBL by tamoxifen at day 7 after immunization, at which stage about 60% of NP specific B cells already acquired a high affinity BCR (Figure 3.6 E), and analyzed NIP_5-binding GC B cells and PCs at day 12 by flow cytometry. Mice ablated *Cbls* showed a marked reduction in the number of NIP_5-binding GC B cells; however, the total number of GC B cells was only reduced to a half of that in controls (Figure 3.9 C). Consistently, *Cbl* ablation led to significant increases in

the numbers of total and NIP_5-binding PCs relative to mice without CBL deletion (Figure 3.8 C and D). Given that high affinity PCs are mostly generated through GC reaction, concomitant reduction in NIP_5-binding GC B cells and increase in NIP_5-binding PCs supports the idea that loss of CBLs facilitates the high affinity GC B cells to choose the PC fate and differentiate into PCs.

To determine whether CBLs control the PC differentiation program via these signaling pathways, we compared CD40 and BCR-induced B cell differentiation to PCs *in vitro*. Stimulation of naïve B cells from $CBL^{dKO\text{-}Mb1}$ mice, with either membrane-bound CD40L expressed on 40LB feeder cells or soluble anti-CD40, generated significantly more $B220^{+}$ $CD138^{+}$ and $B220^{+}$ $CD138^{+}$ cells (Figures 3.9 D and 3.8 E). These cells appeared to be PCs or plasma blast-like cells because they expressed intracellular Ig, upregulated IRF4, and downregulated BCL6 (Figure 3.8 F). Similarly, culture of freshly isolated $CBL^{dKO\text{-}Cg}$ GC B cells on CD40LB feeders also generated more $B220^{+}CD138^{+}$ plasma blast-like cells relative to WT controls (Figure 3.9E). In contrast, anti-IgM stimulation alone produced comparable numbers of $B220^{+}CD138^{+}$ cells from the mutant and WT B cells, suggesting that BCR signaling induced PCs is not enhanced by the CBLs mutation (Figure 3.9 E). Neither CD40 nor BCR-induced proliferation of B cells was affected by the $CBL^{dKO\text{-}Mb1}$ mutation (Figure 3.8 G). Together, these data indicate that ablation of CBL proteins does not affect CD40 or BCR induced mitotic signaling but rather expedites CD40-induced B cell differentiation into PCs.

The frequency of B cell differentiation into PCs increases with each cell division cycle[274]. To study the influence of the CBLs mutation on PC differentiation in each

cell division, we labeled naïve WT and $CBL^{dKO\text{-}Mb1}$ B cells with CellTrace, stimulated them with 40LB feeder cells, and then examined PC differentiation in different divisions of proliferating B cells by monitoring both the IRF4 and CD138 expression. Consistent with the above finding, ablation of CBLs did not affect the rate of B cell division; however, the mutant B cells generated 50% more $IRF4^{hi}$ cells relative to WT controls in the third and fourth cell division (Figure 3.9 F). A similar increase in $CD138^{+}$ cells was also found in the $CBL^{dKO\text{-}Mb1}$ compared to the WT B cell culture (Figure 3.8 H). These findings together indicate that, while still maintaining vigorous cell division, loss of CBLs induces more B cells to exit B cell fate and turn on the PC differentiation program in each cell division.

3.3.5 The $CBL^{dKO\text{-}Cg}$ mutation enhances the expression of IRF4 protein but not mRNA in GC B cells

The identities of GC B cells and PCs are respectively controlled by BCL6 and BLIMP1. IRF4 provides another layer of regulation by repressing BCL6 and promoting BLIMP1 gene transcription[275]. To elucidate how the $CBL^{dKO\text{-}Cg}$ mutation affected the GC B cell differentiation program, we compared the gene expression profiles of GC B cell and PC identity genes in WT and $CBL^{dKO\text{-}Cg}$ GC B cells at day 12 after immunization. RNA-seq analysis revealed ~900 genes that were downregulated and ~50 genes upregulated for at least two-fold in $CBL^{dKO\text{-}Cg}$ GC B cells as compared to WT controls (Figure 3.10 A); however, this analysis revealed a slightly lower expression of several known GC B cell or PC identity genes such as *Bcl6*, *Bach2, Irf4,* and *Aicda* (Figure 3.10 B). qPCR analysis confirmed that while *Bcl6*, *Bach2*, and *Aicda* were slightly downregulated, the PC identity gene *Irf4* was not upregulated in the mutants compared to WT GC B cells

(Figure 3.11 A). Despite this observation, the mutant GC B cells elevated the expression of multiple genes related to RNA processing, protein translation, and secretion involved in PC function (Figure 3.11 B and 3.10 B), suggesting that some mutant B cells already initiate the PC differentiation program.

To determine whether the $CBL^{dKO\text{-}Cg}$ mutation influenced the PC development program at the protein level, we examined CD40 and BCR signaling, as well as the levels of BCL6 and IRF4 proteins in GC B cells. We found that activation of CD40 or BCR signaling pathways, including canonical NF-κB, AKT, S6K, and ERK, was not altered by the $CBL^{dKO\text{-}Cg}$ mutation (Figure 3.10 C-D). In contrast, the expression of IRF4 protein was markedly increased in freshly isolated mutant GC B cells compared to the controls (Figure 3.11 C). To gain insight into the expression of IRF4 and BCL6 during GC B cell differentiation at the single cell level, we examined intracellular BCL6 and IRF4 in developing GC B cells by flow cytometry. In WT mice, a majority of GC ($B220^{+}Fas^{+}GL7^{+}$) B cells expressed a high level of BCL6 ($BCL6^{hi}$), whereas only approximately 10% of GC B cells downregulated BCL6 ($BCL6^{lo}$) and about half of them simultaneously upregulated IRF4 ($BCL6^{lo}IRF4^{hi}$) (Figure 3.11 D). Stimulation of CD40 and BCR for 3 hours significantly increased the $BCL6^{lo}IRF4^{hi}$ subset to ~40% of the total GC B population (Figure 3.11 E). In contrast to WT mice, $CBL^{dKO\text{-}Cg}$ mice already possessed significantly more (15%) $BCL6^{lo}IRF4^{hi}$ GC B cells in the absence of any stimulation, and CD40 and BCR stimulation boosted $BCL6^{lo}IRF4^{hi}$ population to more than ~60% of total GC B cells (Figure 3.11 D and E). Western blot analysis confirmed that IRF4 protein was indeed elevated in $CBL^{dKO\text{-}Cg}$ GC B cells compared to WT cells with or without CD40 and

BCR stimulation (Figure 3.11 F). This result, along with the mRNA expression data, indicates that CBLs do not affect the major signaling pathways downstream of CD40 or the BCR. Instead, they may retain GC B cells fate by suppressing the expression of IRF4 protein rather than *Irf4* transcription.

3.3.6 CBLs promote nuclear IRF4 ubiquitination and degradation

CBL proteins are known cytosolic E3 ubiquitin ligases, whereas IRF4 is a transcription factor that functions mainly in the nucleus. We therefore examined at which subcellular location CBL proteins exert their regulatory function on IRF4. Confocal microscopy analysis showed that IRF4 was barely detectable in freshly isolated WT GC B ($B220^{+}GL7^{+}Fas^{hi}$) cells and significantly accumulated in the nucleus after CD40 and BCR stimulation (Figure 3.12 A and B). In contrast, a significant proportion of $CBL^{dKO\text{-}Cg}$ GC B cells already possessed a high level of nuclear IRF4 in the absence of any stimulation (Figure 3.12 A and B). In agreement with this observation, Western blot analysis confirmed that IRF4 was expressed in both cytosol and nucleus, with the mutant GC B cells expressing several folds more IRF4 than WT cells in the nucleus even in the absence of any stimulation (Figure 3.12 C). As for CBLs, in freshly isolated WT GC B cells both CBL and CBL-B were expressed in the cytosol and nucleus in the absence of CD40 stimulation, with CBL more strongly in cytosol and CBL-B in the nucleus (Figure 3.12 D). CD40 and BCR stimulation for one hour significantly diminished CBL-B and for three hours reduced both CBL-B and CBL in the nucleus. The stimulation concomitantly increased the level of nuclear IRF4 (Figure 3.12 D), suggesting that nuclear CBL proteins eradicate IRF4 in GC B cells.

To determine whether CBL proteins regulated IRF4 expression by promoting IRF4 ubiquitination, we co-expressed IRF4 with either CBL or CBL-B in 293T cells and examined IRF4 association with, and ubiquitination by, CBL or CBL-B by immunoprecipitation and Western blot analysis. IRF4 associated with, and became ubiquitinated by, either CBL or CBL-B in 293T cells (Figures 3.12 E and F). The association of IRF4 with CBL and CBL-B in freshly isolated WT GC B cells, as well as its ubiquitination in WT but not in $CBL^{iKO\text{-}Mb1}$ iGC B cells, was confirmed by co-immunoprecipitation and Western blot hybridization (Figure 3.12 G and H). Thus, the observed dynamic change of IRF4 expression in GC LZ B cells is at least partly regulated by CBL-dependent IRF4 ubiquitination and degradation.

3.3.7 Lack of CBL ubiquitin ligase activity or increased IRF4 expression is sufficient to impair GC affinity selection

Our aforementioned results suggest a hypothesis that the elevated level of CBLs in GC B cells removes IRF4 by promoting IRF4 ubiquitination, consequently allowing continuation of GC cycle until high affinity BCRs are acquired. If this was the case, we expect that inactivation of CBL ubiquitin ligase activity or an increased IRF4 expression in GC B cells impairs antibody affinity maturation. To examine whether CBL ubiquitin ligase activity is required for antibody affinity maturation, we bred $CBL^{fl/fl}CBLB^{-/-}$ mice to IgCγ–Cre tg and $CBL\text{-}B^{C373A/C373A}$ mice[253], the latter expressed a mutant CBL-B whose ubiquitin ligase activity was inactivated by a cysteine to alanine mutation at position 373 of the CBL-B. The resulting $CBL^{fl/fl}$ $CBL\text{-}B^{-/C373A}$ IgCγ-Cre tg (termed $CBL^{KO\text{-}Cg}CBL\text{-}B^{-/C373A}$) mice were immunized with NP-KLH. The development of high affinity GC B cells and

PCs were examined by flow cytometry and ELISPOT, respectively. $CBL^{KO\text{-}Cg}$CBL-$B^{-/C373A}$ mice recapitulated GC B cell phenotypes found in $CBL^{dKO\text{-}Cg}$ mice, as they produced a slightly lower number of GC B cells compared to $CBL^{KO\text{-}Cg}$CBL-$B^{-/+}$ and WT controls at day 12 after immunization (Figures 3.13 A and 3.14 A). In addition, the numbers of high affinity anti-NP (NP_s) GC B cells as well as anti-NP_s IgG1 secreting PCs were all reduced in the mutant mice relative to the controls (Figures 3.13 B, 3.13 C and 3.14 A).

To determine whether increased IRF4 was sufficient to abolish antibody affinity maturation, we ectopically expressed IRF4 in WT hematopoietic stem cells by a retroviral vector and generated BM chimeras (termed IRF4-MSCV BM mice). Expression of the transgenic IRF4 was confirmed by Western blot analysis (Figure 3.14 B). These mice were then immunized with NP-KLH, and selection of high affinity NP-binding GC B cells and PCs was analyzed by flow cytometry. Similar to that found in $CBL^{dKO\text{-}Cg}$ and $CBL^{KO\text{-}Cg}$CBL-$B^{-/C373A}$ mice, in IRF4-MSCV BM chimeras the transgene *Irf4* expressing B cells generated a slightly lower number of GC B cells at day 12 compared to empty retrovirus (MIGR-MSCV) infected B cells (Figure 3.14 D), indicating that Irf4-overexpressing B cells can enter GC reaction. However, the production of high affinity anti-NP_s IgG1 expressing GC B cells was impaired in the mutant (IRF4-MSCV, GFP^+) but not in WT controls (MIGR-MSCV, GFP^+) (Figure 3.14 E). The numbers of PCs generated from IRF4-MSCV infected B cells were consistently increased as compared to empty vector infected cells (Figure 3.14 F).

Together, these results indicate that lack of ubiquitin ligase activity of CBLs or excessive IRF4 expression is sufficient to abolish the development of high affinity GC B cells.

3.4 Discussion

Selective expansion of high affinity BCR-expressing B cells in GCs is a critical step in antibody affinity maturation. Our study showed that CBLs play an indispensable role in this regulation, as ablation of CBL in GC B cells selectively impaired the development of GC B cells expressing high but not low affinity BCRs. We also provided evidence that the $CBL^{dKO\text{-}Cg}$ mutation did not significantly alter the efficiency of SHM, but rather impeded the clonal expansion of high affinity B cells. Since inactivation of CBL ubiquitin ligase activity is sufficient to recapitulate this GC phenotype, our studies thus support the notion that CBLs define a novel ubiquitination-dependent regulatory pathway that enforces affinity-driven clonal selection of high affinity GC B cells by preventing premature termination of GC recirculation.

It is generally envisioned that high affinity BCRs facilitate clonal expansion and selection of GC B cells via two modes of regulation. First, high affinity BCRs may drive more vigorous cell proliferation, because they elicit stronger BCR signaling than low affinity BCRs. However, this proposition has received conflicting evidence, as attenuated rather than enhanced BCR signaling is favorable for GC B cell expansion and high affinity BCRs tend to cease GC B cell fate and initiates PC differentiation[172, 276]. As an alternative to the signaling role of the BCR in GC affinity selection, high affinity BCRs are thought to capture more antigen than BCRs with inferior affinity, thus giving high affinity B cells the advantage of competing for T_{fh} cell help mainly via the upregulated CD40L[91, 237]. Either way, a challenging question is how B cells interpret BCR affinity cues differently since the same signals control both the mitotic and differentiation

pathways of GC B cells. In our studies, we found that ablation of CBLs expedited GC B cell differentiation but not proliferation upon CD40 and/or BCR stimulation. This finding thus puts CBLs at the branch of signaling pathway to prevent the B cell differentiation rather than proliferation. In line with this view, we observed that the $CBL^{4KO\text{-}C\delta}$ mutation did not affect CD40 and BCR induced mitotic signaling such as AKT, S6K, ERKs, and canonical NF-κB. Instead, it resulted in the accumulation of IRF4 protein in GC B cells. We also found that CBLs promote IRF4 ubiquitination. CD40 and BCR stimulation downregulated CBL and conversely upregulated IRF4 in GC B cells. These data together extend our previous understanding about the role of CD40 and BCR in GC affinity selection. By clearing IRF4 protein rather than regulating the mitotic signaling pathways, CBLs allow CD40 and BCR to promote GC B cell stay in the DZ-LZ circulation without activating the differentiation program into PCs. This regulation can be reversed in high affinity GC B cells in which strong CD40 and BCR signaling generated by the high affinity BCRs cue downregulates CBLs, consequently allowing these cells to upregulate IRF4 and be selected into the PC pool.

The fates of GC B cells and PCs are determined by transcription factors BCL6, IRF4, and BLIMP[270, 275]. However, a recent transcriptome study revealed that transcription of *Bcl6* was abruptly downregulated whereas that of *Irf4* and *Pmdr1* was abruptly upregulated in plasmablasts, hence raising the question as to what is the initial "push" that drives the transition of this transcriptional network from the equilibrium state of GC B cells to that of PCs[277]. Our data reveal that in WT mice a small population of GC B cells downregulated BCL6 and upregulated IRF4 ($BCL6^{lo}IRF4^{hi}$). Triggering of CD40 and

BCR for a short period increased this cell subset, suggesting that these cells represent emerging plasmablasts or plasma cell precursors. Development of this subset appeared to be controlled by CBLs, because they were significantly increased in the GCs of $CBL^{dKO\text{-}Cg}$ mice. In GC B cells, we showed that CBLs ubiquitinated IRF4. Strong CD40 and BCR stimulation decreased the expression of CBL proteins and concomitantly increased the expression of IRF4. We therefore propose that relief of IRF4 from CBL-mediated ubiquitination upon strong CD40 and/or BCR triggering is the earliest PC fate commitment event occurring in the LZ GC B cells, preceding the conversion of transcriptomes from the state of GC B cells to that of PCs. This of course will not refute the role of CD40 in promoting *Irf4* gene transcription, which may be compromised in LZ B cells at the IRF4 protein level until CBLs are degraded.

Previous studies have shown that selection of high affinity GC B cells depends on the transcription factors NFκB, MYC, and FOXO1, in a B cell-intrinsic fashion. Both MYC and canonic NFκB were expressed or activated in a small subset of LZ GC B cells[84, 93, 168]. Ablation of *Myc*, *Rel* or *Relb* genes in GC B cells resulted in the collapse of the GC reaction, because these factors are required for the maintenance of the GC reaction by facilitating LZ to DZ recirculation. FOXO1 is required for sustaining the DZ program, as inactivation of *Foxo1* gene disrupts the expansion of DZ B cells possibly by dysregulating the function of the transcription factor BATF[151]. In contrast to the above regulations, CBLs control GC affinity maturation by determining the time when a GC B cell is allowed to enter the PC pool. In this regard, CBLs seem to represent a new regulation that controls the exit checkpoint of the DZ-LZ circulation, consequently

contributing to affinity selection. It will be interesting to determine whether this mechanism also contribute to the recently described temporal switch in the differential output of memory B cells and PCs during the GC reaction.

Selection of high affinity B cells occurs in the GC LZ where BCR affinity cues can be accessed via interaction with antigen presented on follicular dendritic cells[278]. Our findings that CBLs were markedly upregulated in GC LZ B cells at the protein but not at the mRNA level, and that CD40 and BCR downregulated CBLs, raise an interesting question as to how the expression of CBLs is spatially and temporally controlled during the GC DZ-LZ circulation. CD40 is known to activate RING-domain containing TRAFs or cIAPs, both of which regulate their respective downstream signaling molecules by ubiquitination. Along this line, TRAF6 and TRAF2 have been shown to associate with CBL-B[279]. Alternatively, CD40 could downmodulate the translation of CBL proteins through a microRNA dependent mechanism. Consistent with this speculation, it has been found that CD40 stimulation enhances expression of multiple microRNAs among which miR155 may influence CBL-B expression in B cells[254, 280]. Nevertheless, it will be interesting to investigate whether the modulation of the CBL pathway can be used as a strategy to improve the clinical benefit such as the efficiency of vaccination in future.

3.5 Acknowledgements

We thank F. Huang (Fudan University Medical College, Shanghai, China) for MSCV-IκB-GFP reporter, R. Chen (IRCM, Montreal, Canada) for HA-Ubiqutin vector, and J. Di Noia, T. Möröy, W.-K. Suh, and A. Veillette for comments. Supported by The Canadian Institute of Health Research (CIHR) Operating Grant (MOP142279) and A. Aisenstadt

Chair Fund to H.G.; Chinese Scholarship Council Ph.D. training grants to X. L. and H.J.T.; NCI-NIH R21 CA175461 to U. K.; National Health and Medical Research Grant (1101318) to W. Y. L.; and a NSHLIJ Institutional Fund to YR Z.

3.6 Author contributions

X.L. did mouse, biochemical, and flow cytometric analyses; A.G, H.G.T., L.Y.D., and Y.L. contributed to the design and method refinement of biochemistry and flow cytometry analyses and daily discussion; D. K. generated 40LB feeder cells; V. C., contributed to bioinformatics analysis; U.K. contributed to IRF4 analysis and manuscript writing; and W. Y. L. generated CBL-B^{C373A} mice. Y.R.Z. contributed to fluorescent imaging analysis and manuscript writing; All authors had editorial input.

3.7 STAR method

Table 3.1 Key resource

REAGENT or RESOURCE	SOURCE	IDENTIFIER
Antibodies		
anti-CD4 e450	Ebioscience/Thermo	Cat#48-0042-82
anti-CD8 e450	Ebioscience/Thermo	Cat#48-0032-82
anti-Gr1 e450	Ebioscience/Thermo	Cat#48-5931-82
anti-CD11c e450	Ebioscience/Thermo	Cat#48-0114-82
anti-CD11b e450	Ebioscience/Thermo	Cat#48-0112-82
anti-Ter119 e450	Ebioscience/Thermo	Cat#48-5921-82
anti-F4/80 e450	Ebioscience/Thermo	Cat#48-4801-82
anti-B220 e450	Ebioscience/Thermo	Cat#48-0452-82

anti-B220 PE-CY7	Ebioscience/Thermo	Cat#25-0452-82
anti-GL7 e450	Ebioscience/Thermo	Cat#48-5902-82
anti-GL7 FITC	Ebioscience/Thermo	Cat#53-5902-82
anti-IgM PE	Ebioscience/Thermo	Cat#12-5890-81
anti-CD23 PE-CY7	Ebioscience/Thermo	Cat#5-0232-81
anti-CD24 PE	Ebioscience/Thermo	Cat#12-0241-81
anti-CD93 APC	Ebioscience/Thermo	Cat#17-5892-82
anti-CXCR4 PE	Ebioscience/Thermo	Cat#12-9991-82
anti-Irf4 PE	Ebioscience/Thermo	Cat#12-9858-80
anti-B220 FITC	Ebioscience/Thermo	Cat#11-0452-82
Strepavidin PE-CY7	Ebioscience/Thermo	Cat#24-4317-82
anti-CD86	Ebioscience/Thermo	Cat#17-0862-81
anti-phospho-S6(S235/S236)	Ebioscience/Thermo	Cat#12-9007-42
anti-B220 APC	Biolegend	Cat#103212
anti-CD38 APC	Biolegend	Cat#102712
Alexa647 anti-BrdU	Biolegend	Cat#364108
anti-Igλ	Biolegend	Cat#407306
anti-Fas PE	BD	Cat#554258
anti-Fas PE-CY7	BD	Cat#557653
anti-IgG1 FITC	BD	Cat#553443
anti-IgD FITC	BD	Cat#553439
anti-CD21/CD35 FITC	BD	Cat#553818
Alexa647 anti-Bcl6	BD	Cat#561525

anti-CD138 PE	BD	Cat#553714
anti-CD35 Biotin	BD	Cat#553816
anti-CD138 e450	BD	Cat#562610
Alexa647 anti-AKT(p473)	BD	Cat#560343
Alexa647 anti-ERK1/2(pT202/pY204)	BD	Cat#612593
NP_{38}-PE	Bioresearch Technologies	Cat#N-5070-1
NP_{8}-PE	Bioresearch Technologies	Cat#N-5070-1
Purified anti-CD40	ENZO	Cat#ALX-805-046-C100
Purified anti-IgMF$(ab)_2$	Jasckson ImmunoResearch	Cat#115-006-020
anti-mouse Cbl	Santa Cruz	Cat#SC-170
anti-mouse Irf4	Santa Cruz	Cat#SC-6059
anti-LAMINB	Santa Cruz	Cat#SC-374015
anti-HA	Santa Cruz	Cat#SC-805
HRP conjugated anti-β-ACTIN	Abcam	Cat#AB49900
anti-Flag	Sigma	Cat#F1804-50UG
anti-Goat IgG HRP	Santa Cruz	Cat#SC-2020
anti-Rabbit IgG HRP	Cell Signaling	Cat#7074P2
anti-Mouse IgG HRP	Cell Signaling	Cat#7076P2
anti-Mouse Cbl-b	Cell Signaling	Cat#9498S
anti-Mouse IgG1 HRP	Thermo	Cat#A10551
anti-Mouse IgM HRP	Thermo	Cat#M31507

anti-a-Tubulin	Sigma	Cat#T4026-.2ML
PNA Biotin	Vector	Cat#B-1075
PNA FITC	Vector	Cat#FL-1071
Strepavidin Alexa488	Thermo	Cat#S-32354
Strepavidin Alexa568	Thermo	Cat#S-11226
Donkey anti-Goat Alexa594	Thermo	Cat#A-11058
Goat anti-Rabbit Alexa568	Thermo	Cat#A-11036
Bacterial and Virus Strains		
E.coli5 competent cells	Thermo	Cat#18265017
Stbl2™competent cells	Thermo	Cat#10268019
Stbl3™competent cells	Thermo	Cat#C737303
Chemicals, Peptides, and Recombinant Proteins		
5-Fluorouracil	Sigma	Cat#F6627-5G
MG132	Sigma	Cat#C2211
NHS-Biotin	Thermo	Cat#21335
Recombinant mouse IL-4 protein	R&D	Cat#404-ML-050
Recombinant mouse SCF protein	R&D	Cat#455-MC-050
Recombinant mouse IL-6 protein	R&D	Cat#406-ML-025/CF
Recombinant mouse IL-3 protein	R&D	Cat#403-ML-050/CF
Celltrace Proliferation dye	Ebioscience/Thermo	Cat#C34557
SYBR Green qPCR Master Mix	Life Technology	Cat#4309155

NIP_5-BSA-Biotin	Bioresearch Technologies	Cat#N-1027-5
NP_4-BSA	Bioresearch Technologies	Cat#N-5050L-10
NP_{30}-BSA	Bioresearch Technologies	Cat#N-5050L-10
rProtein G Agarose	Thermo	Cat#15920-010
Tamoxifen	Toronto Research Chemicals Inc.	Cat#T006000
Sheep Red Blood Cells	Innovative Research	Cat#IC100-0210
NP_{16}-OVA	Bioresearch Technologies	Cat#N-5051-100
NP_{36}-KLH	Bioresearch Technologies	Cat#N-5060-25
1-Step™Ultra TMB-ELISA Substrate Solution	Thermo	Cat#34029
Critical Commercial Assays		
FITC-BrdU kit	BD	Cat#559619
Nuclear Extract Kit	Active motif	Cat#40010
AEC Substrate Set	BD	Cat#551951
B cell negative selection kit	Stem cell	Cat#19854
CaspaseGlowTM FITC Active Caspase Staining Kit	Biodivision	Cat#A10551
Experimental Models: Cell Lines		
293T cell line	Laboratory of Gu	N/A
Phoenix cell line	Laboratory of Gu	N/A

40LB cell line	Laboratory of D. Kitamura	N/A
Experimental Models: Organisms/Strains		
Cbl flox/flox conditional knockout mice	Laboratory of Gu	N/A
Cbl-b germline knockout mice	Laboratory of Gu	N/A
Mb1-cre mice	Laboratory of Michael Reth	
Cγ-cre mice	Laboratory of K. Rajewsky	N/A
$Cblb^{C373A}$ mutation mice	Laboratory of W. Langdon	N/A
UBC-Cre-ERT2 mice	The Jackson Laboratory	Stock#007001
μMT mice	The Jackson Laboratory	Stock#002288
C57BL/6 mice	The Jackson Laboratory	Stock#000664
B6.SJL mice	The Jackson Laboratory	Stock#002014
Rag1-/- mice	The Jackson Laboratory	Stock#002216
Oligonucleotides		
Cbl-b qPCR primer Forward: 5'-GGGGACGGCAATATCCTACAG-3' Reverse: 5'-TATAGCTCCGCCCATCAGGA-3'	IDT	N/A

Cbl qPCR primer Forward: 5'-CTCCTCCTTTGGCTGGTTGT-3' Reverse: 5'-TTCTCCGAGGGAATGGTTTGG-3'	IDT	N/A
Acida qPCR primer Forward: 5'-AAGGGACGGCATGAGACCTA-3' Reverse: 5'-AGCCAGACTTGTTGCGAAGG-3'	IDT	N/A
Irf4 qPCR primer Forward: 5'-AGGTCTGCTGAAGCCTTGGC-3' Reverse: 5'-CTTCAGGGCTCGTGGTC-3'	IDT	N/A
Actin qPCR primer Forward: 5'-CGATGCCCTGAGGCTCTT-3' Reverse: 5'-TGGATGCCACAGGATTCCA-3'	IDT	N/A
Gapdh qPCR primer Forward: 5'-TCGTCCCGTAGACAAAATGGT-3' Reverse: 5'-CGCCAAATACGGCCAAA-3'	IDT	N/A

Bcl6 qPCR primer Forward: 5'-TTTCTGGTTCACTGGCCTTGA-3' Reverse: 5'-CCTGCAGATGGAGCATGTTG-3'	IDT	N/A
Bach2 qPCR primer Forward: 5'-AGTAAGAACCGCATTGCAGC-3' Reverse: 5'-TTCCTTCTCGCACACCAGTT-3'	IDT	N/A
Recombinant DNA		
Mouse Cbl-b sequence-verified cDNA	Laboratory of Gu	N/A
Mouse Cbl sequence-verified cDNA	Laboratory of Gu	N/A
Mouse Irf4 sequence-verified cDNA	Laboratory of Gu	N/A
HA-UB expression vector	Dr.Chen	N/A
pCDNA vector	Invitrogen	Cat#V790-20
MIGR1-MSCV retro-expression vector	Addgene	Plasmid#27490
p3xFlag-CMV™ 7 vector	Sigma	Cat#E7533
MSCV IκB-GFP fusion vector	Dr.Huang	N/A
Software and Algorithms		
Prism(6.0-7.0)	Graphpad	
FlowJo(v9-10)	Treeview	
Volocity	PerkinElmer	

3.8 Material and methods

3.8.1 Mice

C57BL/6 mice, B6.SJL mice, μMT mice, Rag1$^{-/-}$ and UBC-Cre-ERT2 mice were from the Jackson Laboratory. *Cbl*-floxed and *Cblb*$^{-/-}$ mice were described previously[202, 205]. To generate CBL$^{dKO\text{-}Cg}$ mice, *Cbl* floxed/floxed (*Cbl*$^{fl/fl}$) and *Cblb*$^{-/-}$ mice were crossed to Cγ1-Cre transgenic mice kindly provided by S. Casola and K. Rajewsky[272]. Cblb^{C373A} mice were described previously[253]. Cg1-cre Cblf/f Cblb$^{-/-}$ mice were crossed with Cblb^{C373A} to obtain CBL$^{KO\text{-}Cg}$CBLB$^{C373A/+}$ mice. TO generate inducible CBL$^{dKO\text{-}UBC}$ mice, *Cbl* floxed/floxed (*Cbl*$^{fl/fl}$) and *Cblb*$^{-/-}$ mice were crossed to UBC-Cre-ERT2 transgenic mice. Animal experimentation was done in accordance with the Canadian Council of Animal Care and approved by the Institut de Recherches Cliniques de Montreal (IRCM) Animal Care Committee.

3.8.2 Plasmids, cell lines and culture

cDNA encoding *Irf4* was PCR amplified and cloned into plasmid p3xFlag-CMV™ 7 expression vector. cDNAs encoding *Cbl* and *Cbl-b* were separately cloned into pCDNA vector. For the construction of IRF4 overexpression vector, cDNA encoding *Irf4* was cloned into MSCV-MIGR-GFP retroviral vector. IκB-GFP fusion protein retrovirus expression vector was kindly provided by Dr. F. Huang. Hemagglutinin (HA)-tagged ubiquitin vector was a gift from Dr. R. Chen. To prepare retrovirus, Phoenix cells were transfected with the appropriate amount of retroviral vector and package plasmids (30

μg) by Calcium precipitation, according to previous publication[281]. For 40LB culture, naïve WT and $CBL^{dKO\text{-}Mb1}$ cells were purified from WT (C57BL-6 or C57BL/6 Mb1-Cre tg) and $CBL^{dKO\text{-}Mb1}$) mice by a magnetic column (StemCell Technologies), respectively. GC B cells were purified by FACS sorting. Purified B cells were seeded onto irradiated (900 RAD) 40LB cells described previously. B cells were cultured at 37°C for five days, trypsinized and replated onto a fresh 40LB plate for two more days before being subjected to FACS analysis.

3.8.3 Immunization and GC B cell purification

To test T-dependent antibody responses and germinal center reaction, 6 to 10 week-old mice were immunized with either 10^9 sheep red blood cells (SRBCs) (Innovative Research) in PBS or NP_{36}-KLH (BioSources) precipitated in alum adjuvant (Imject Alum, ThemoScientific) by i.p. injection. Mice were analyzed at different days after immunization. To examine the expression of CBLs in GC B cells, SRBC immunized mice were sacrificed at day 8 and B cells were enriched by a magnetic column, stained with anti-B220, CD138, GL7, Fas, CXCR4 and CD86. GC ($B220^+GL7^{hi}Fas^{hi}$) B cells were then purified by FACS sorting on a FACS Aria or Moflo. To obtain a large quantity of GC B cells for *in vitro* stimulation and culture, mice were sequentially immunized at day 0 ($1x10^8$ SRBCs) and day 5 ($1x10^9$ SRBCs) by i.v. injection. Immunized mice were sacrificed at day 12, B cells were enriched by a magnetic B cell enrichment column (StemCell) and subsequently sorted as $B220^+$ $CD138^-$ $GL7^+$ cells. Purity of the isolated GC B cells was confirmed by FACS analysis and was shown to be more than 95% pure for cell surface markers $B220^+GL7^{hi}Fas^{hi}$ (Figure3.14 C).

3.8.4 Flow cytometric analysis and cell sorting

Total splenic cells or splenic B cells were re-suspended in FACS buffer (5%BSA in PBS (PH=7.2)) and stained with the corresponding antibodies on ice for 30 min. Cells were washed twice with FACS buffer and then subjected to analysis on a BD Fortessa or Cyan or to cell sorting on a FACS Aria or Moflo. The following antibodies were used for the staining: anti-B220, anti-GL7, anti-CD11c, anti-CD11b, anti-Gr1, anti-F4/80, anti-NK1.1, anti-IRF4, anti-Igλ, anti-TCRβ, anti-CD3ε, anti-CD86, and anti-CD38 (eBioscience); anti-Fas, anti-CD138, anti-BCL6, anti-CXCR4, anti-IgG1, anti-IgD (BD Pharmingen); NP_{8}-PE (BioSearch). High affinity and total NP-binding B cells and plasma cells were stained with NP_8-PE, NIP_5APC, and NP_{38}-PE (BioSearch), respectively. Specificity of NIP_5–APC and NP_{38}-PE to NP-specific but not to carrier protein specific BCRs was confirmed using GC B cells from OVA or NP_{16}-OVA immunized mice (Figure 3.14 D). To analyze nuclear proteins BCL6 and IRF4, total splenic cells were first stained for B220, Fas, and GL7, fixed and permeabilized with FOXP3 staining buffer according to the manufacturer's instructions (eBioscience), and then stained with anti-BCL6 and IRF4. For cell cycle analysis, mice were injected intravenously with 1 mg of BrdU (BD Pharmingen) in DPBS. Cells were then surface stained with corresponding antibodies, and BrdU labeled cells were stained using an anti-BrdU kit according to the manufacturer's protocols (BD Pharmingen). To track newly generated PCs *in vivo* by cell surface molecule-labeling and tracking assay, NHS-Biotin (1 mg/mouse) (Sigma) in DPBS was injected intravenously into NP_{36}-KLH immunized mice at day 12 postimmunization. Two and 24 hours later, mice were sacrificed, and biotin-labeled

molecules on the cell surface of naïve B, GC B and plasma cells were visualized by staining with streptavidin-PE-CY7, together with anti-B220, anti-GL7, anti-Fas, and anti-CD138, and analyzed on a FACS, respectively.

3.8.5 qPCR and RNA-Seq analysis

To study the gene expression profiling, naïve B cells and GC ($B220^{+}CD138^{-}GL7^{+}Fas^{+}$) B cells from wildtype and $CBL^{dKO\text{-}Cg}$ mice were purified by FACS sorting. Total RNAs from sorted cells (pooled from three mice) was extracted using an RNEasy Mini Kit (Qiagen), and reversely transcribed into cDNA using a Reverse-Transcription kit (Invitrogen) according to manufacturer's instructions, respectively.

RNA-seq was performed using the Illumina TruSeq Stranded mRNA Kit according to manufacturer's instructions on an Illumina HiSeq 2000 sequencer. Read quality was confirmed using FastQC v0.10.1. Read alignment was performed using TopHat v2.0.10 on the mouse GRCm38/mm10 genome. Differential expression analysis was performed with DESeq2 from the raw alignment counts calculated with featureCounts. Differentially expressed genes were defined as genes with a logFC(counts)|>2 and counts > 500 in both experiments. Shown are log2 (counts) expression values of 982 downregulated and 51 upregulated genes in $CBL^{dKO\text{-}Cg}$ than in WT GC B cells.

A SYBR Green PCR mix (Thermo Scientific) and gene-specific primers were used for quantitative RT-PCR analysis (20-50 ng cDNA per reaction). All reactions were done in triplicates with ViiA7-96 Real Time PCR System (Applied Biosystems). Results were

analyzed by the change-in-threshold ($2^{-\Delta\Delta CT}$) method, with β–Actin or GAPDH as 'housekeeping' reference genes, respectively.

3.8.6 Immunofluorescence

Spleens were embedded in optimum cutting temperature compound (Sakura) and flash-frozen in liquid nitrogen. Tissue sections were cut on Cryotome (Leica), fixed in ice-cold acetone (Sigma), blocked with PBS+5%BSA for 1 hour at 25°C, and stained with anti-CBL (Santa Cruz), anti-CBL-B (Santa Cruz), anti-CD35 (BD Pharmingen), anti-B220 (BD Pharmingen), and/or PNA (VectorLab), in different combination. The following secondary antibodies were used to detect primary antibodies: anti-Rabbit Alexa-568 (Invitrogen), Streptavidin Alexa-488 (Invitrogen), Streptavidin Alex-633 (Invitrogen). Images were acquired on a Zeiss LSM700 or 710 confocal microscope.

For intracellular staining of IRF4, GC B cell or stimulated GC B cells were purified by FACS sorting. Cells were fixed with 4% PFA, permeabilized with 0.1% Triton X-100, blocked with PBS+5% BSA, and stained with anti-IRF4 (Santa Cruz), followed by anti-Goat Alexa 568 secondary antibody. Cell nucleus was counter stained with DAPI. Images were acquired on a Zeiss LSM710 confocal.

3.8.7 Ig V_H186.2 gene isolation and DNA sequencing

GC ($B220^+$, Fas^+, $GL7^+$, $Ig\lambda^+$) B cells were isolated by FACS from three NP_{36}-KLH immunized WT and $CBL^{dKO\text{-}Cg}$ mice, respectively, at day 12 after immunization. Genomic DNA was extracted from the sorted cells using a QuickExtract™ DNA Extraction Solution (Epicentre). For V_H186.2 sequencing, V_H186.2-J_H2 joints were amplified from genomic

DNA by PCR using specific primers for the 5' end of V_H186.2 gene and 3' end of J_H2 gene according to a previous protocol. PCR products were gel extracted and cloned into a TOPO vector (Invitrogen). High quality traces were analyzed using MacVector for base pair mismatches and deletions as compared to the germline V_H186.2 gene sequence. Only mismatches mutations in the productive V_H186.2-J_H2 joints were counted as mutations. Ig V_H sequences were analyzed using the IMGT/V-QUEST system to identify the W33L mutation. Primers used were: V_H 186.2: 5'-AGCTGTATCATGCTCTTCTTGGCA -3'; J_H2: 5'-AGATGGAGGCCAGTG AGGGAC -3'.

3.8.8 Enzyme-linked immunospot (ELISPOT) assay and enzyme-linked immunosorbent assay (ELISA)

Total splenic or bone marrow cells were cultured at 37°C in antigen pre-coated 96-well Multiscreen-HA filter plates (Millipore) overnight. Spots of antibody secreting cells were stained with rabbit anti-mouse IgM or IgG1 antibodies conjugated to horseradish peroxidase (Invitrogen), and then developed by addition of AEC substrate (BD Pharmingen). Plates were washed extensively and spots were counted on a dissect microscopy. The antigens used for plate coating were NP_4-OVA and NP_{30}-OVA, respectively. Anti-NP ELISAs were performed as described previously[234].

3.8.9 Immunoprecipitation and Immunoblot analysis

Cells were lysed in TNE buffer (50mM Trise; 140mM NaCl; 5mM EDTA; 0.5% SDS), and immunoblotting was performed following standard procedures. For immunoprecipitation, proteins were immunoprecipitated by incubation of cell lysate

overnight at 4°C with the appropriate antibodies (1μg), followed by precipitate the protein-antibody complexes by incubating with protein G agarose (Invitrogen) for another 1 hour at 4°C. Immunoprecipitates were washed four times with TNE buffer, boiled in 40 μl loading buffer and immunoblotted to a PVDF membrane for Western blot analysis. The following antibodies were used for biochemical study: anti-IgM $F(ab)_2$ (BioSource); anti-CD40 [89]; anti-CBL (SantaCruz); anti-IRF4 (SantaCruz); anti-Lamin B (SantaCruz); anti-BLIMP1 (SantaCruz); anti-HA (SantaCruz); anti-CBL-B (Cell signaling); anti-β Actin (abcam); anti-Flag (Sigma). Horseradish-peroxidase-conjugated goat anti-rabbit, goat anti-mouse or donkey anti-goat antibody was used as a secondary antibody, respectively. Membranes were developed with an enhanced chemiluminescence detection system (GE Healthcare).

A Nuclear extraction kit was used to fractionate nuclear and cytoplasmic proteins according to manufacturer's instructions (Active motif).

3.8.10 Generation of bone marrow chimeric mice

To generated IRF4 over-expression or IκB-GFP expressing bone marrow chimeric mice, retroviral stocks were prepared by transfection of Phoenix cells with MSCV-MIGR1 (empty vector), MSCV-IRF4 or MSCV-IκB-GFP retroviral vector together with the packaging vector pCL-Eco by the standard calcium transfection. Viral supernatants were collected 48 h and 72 h after the transfection, respectively. To obtain bone marrow stem cells, donor mice were treated with 5-FU (5 mg/mouse, i.p.). Four days later, bone marrow stem cells were collected and cultured under optimal stem cell culture condition.

After two-rounds retroviral spin-infections, bone marrow cells were adaptively transferred into lethally irradiated (10 Gy) $Rag1^{-/-}$ recipient mice. Six weeks later, mice were subjected to different immunization regimens.

To generate $CBL^{dKO\text{-}UBC}$ chimeric mice, $1.5x10^7$ splenic B cells from either ER-Cre tg (control) or $CBL^{fl/fl}$ CBL-$B^{-/-}$ ER-Cre tg ($CBL^{dKO\text{-}UBC}$) mice were transferred into μMT mice by i. v. injection. Chimeric mice were immunized i.p. with NP-KLH in Alumjet adjuvant the next day (day 0), and given daily tamoxifen (200μg/g body weight) from day 7-10 by oral administration. Mice were sacrificed at day 12, and splenic cells were subjected for FACS analysis. High affinity NP (NIP_5-binding) GC B cells and PCs were identified by cell surface and intracellularly staining, respectively, using NIP_5-APC in combination with surface markers for GC B cells ($B220^+$ $GL7^{hi}$ Fas^{hi}) or PCs ($B220^{-/lo}$ $CD138^+Lin^-$).

3.8.11 Cell division and differentiation assay

Purified B cells were labeled with CellTrace fluorescent according to manufacturer's instructions. Cells were cultured on 40LB feeder for five days and then labeled with CellTrace fluorescent according to manufacturer's instructions. Labeled cells were plated on a fresh 40LB plate and cultured for two more days. Cultured B cells were harvested and cell proliferation was analyzed on a FACS. To examine culture B cell differentiation to PCs, cells were stained with B220, CD138, and IRF4. IRF4 and CD138 positive cells in each cell division were analyzed on a FACS.

3.8.12 Statistics Analysis

Statistical analyses were performed with a two-tailed, unpaired Student's t-test or Mann-Whitney test with the assumption of equal sample variance, with GraphPad Prism V7 software. A *P* value <0.05 was considered statistically significant.

3.9 Figures and Figure Legends

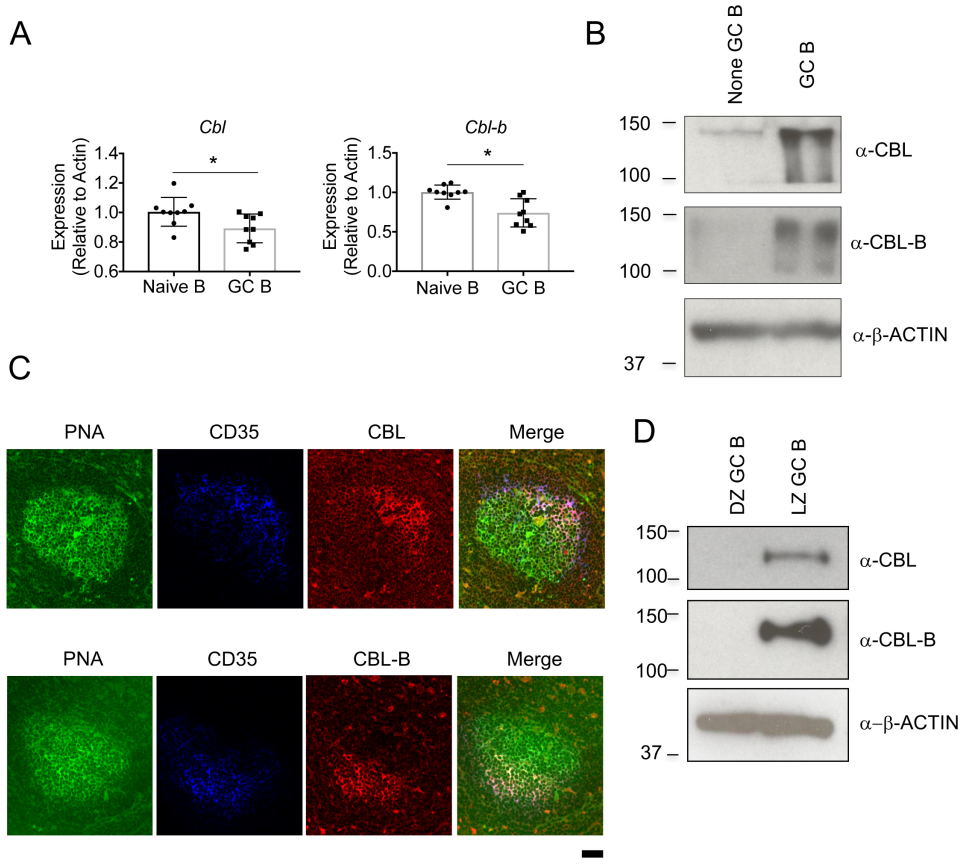

Figure 3.1 Differential Expression of CBL and CBL-B in GC DZ and LZ B Cells

(**A**) qPCR analysis of *Cbl* and *Cbl-b* expression in WT naïve and GC B cells. Results were normalized to actin. Expression in naïve B cells was arbitrarily defined as 1. n=3. (**B**) Western blot analysis of CBL and CBL-B expression in WT naïve and GC B cells. n=2. (**C**) Immunofluorescent staining of CBL and CBL-B in GC DZ and LZ. GC B cells

and the LZ were stained by PNA and anti-CD35, respectively. CBL and CBL-B were visualized in red (Scale bar, 35μm). (**D**) Western blot analysis of CBL and CBL-B expression in DZ and LZ GC B cells. DZ and LZ GC B cells were sorted by FACS as $B220^{+}GL7^{hi}Fas^{hi}CXCR4^{hi}CD86^{lo}$ and $B220^{+}GL7^{hi}Fas^{hi}CXCR4^{lo}CD86^{hi}$ B cells, respectively. n=2.* $p<0.05$.

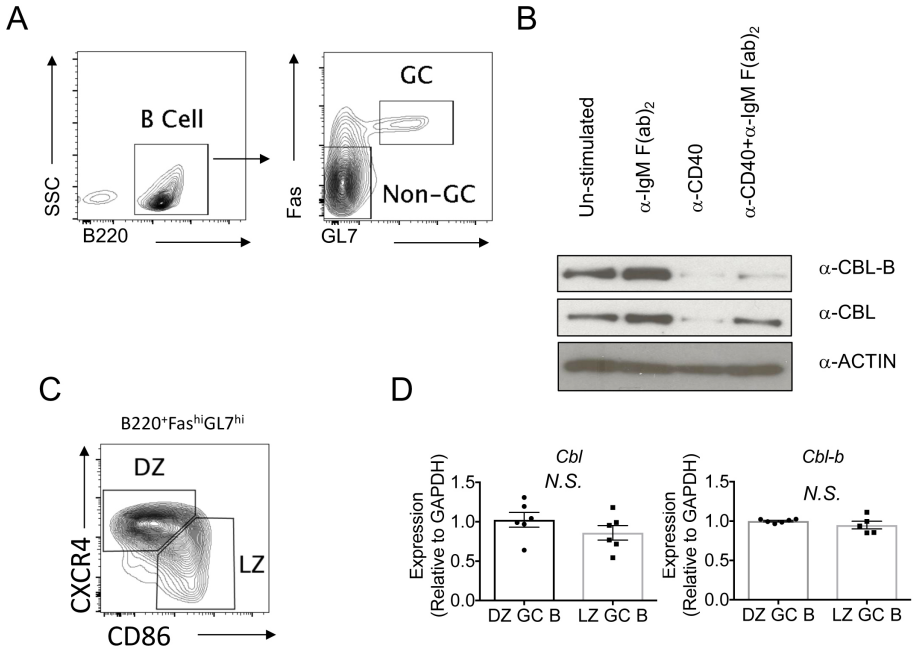

Figure 3.2 Analyses of CBL and CBL-B expression in GC subsets

(**A**) Soring strategy of GC and none-GC B cells from SRBC immunized mice (day 8) for western blot analysis. (**B**) Western blot analysis of CBL and CBL-B expression in *in vitro* activated B cells, including non-stimulated, anti-IgM $F(ab)_2$, anti-CD40 and anti-CD40 plus anti-IgM $F(ab)_2$ stimulated cells for 24 hrs. Shown are representative experiment out of two. (**C**) Sorting strategy of DZ and LZ GC B cells from SRBC immunized mice (day 8) for western blot or qPCR analyses. (**D**) qPCR analysis of *Cbl* and *Cbl-b* expression in WT DZ and LZ GC B cells. Results were normalized to Actin. Expression in DZ GC B cells was arbitrarily defined as 1. Data are mean ± SEM of two independent experiments. N.S.: not significant.

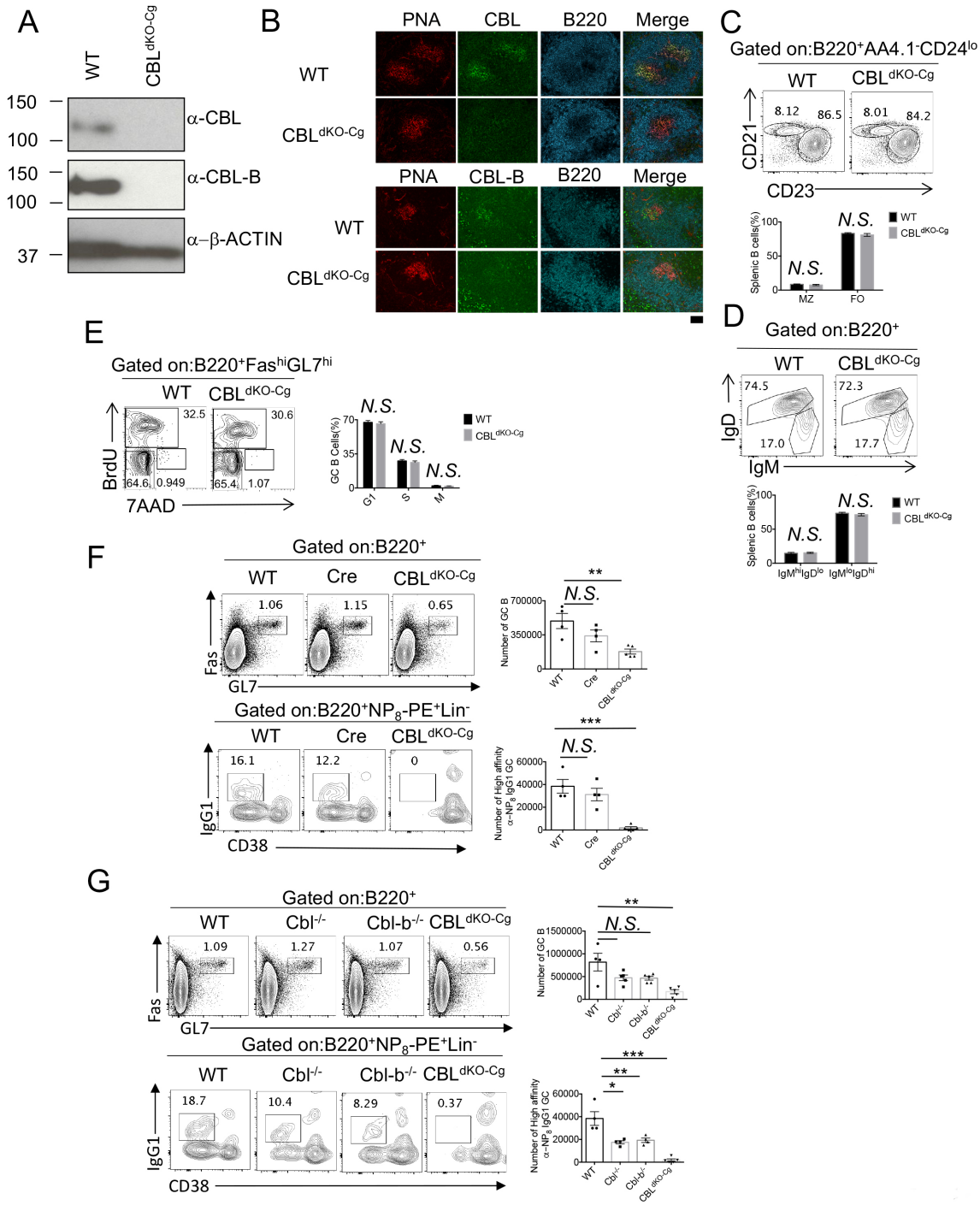

Figure 3.3 B cell compartments in CBL^{dKO-Cg} mice, influence of mutant alleles *Cbl*$^{-/-}$, *Cbl-b*$^{-/-}$ and IgCγ-Cre tg on GC B cell cycle and GC development.

(**A**) Western blot analysis of CBL and CBL-B deletion in GC B cells. WT and $CBL^{dKO\text{-}Cg}$ mice were immunized with SRBC. Splenic GC B cells were isolated by FACS as $B220^{+}GL7^{hi}$ Fas^{hi} cells. (**B**) Immunofluorescent staining of CBL and CBL-B deletion in GC B cells. Spleen sections from SRBC immunized mice (day 12) are stained with PNA, CBL or CBL-B, and B220. Scale bar represents 33μm. (**C, D**) Flow cytometric analysis of spleen B cell subsets in WT and $CBL^{dKO\text{-}Cg}$ mice. Shown is FACS analysis (top panel) and statistics (bottom panel) of anti-CD21 vs CD23 staining of marginal zone and follicular B cells (**C**) or anti-IgM vs IgD staining of follicular B cells, respectively. N.S.: not significant. (**E**) Cell cycle analysis of WT and $CBL^{dKO\text{-}Cg}$ GC B cells. WT and $CBL^{dKO\text{-}Cg}$ mice were immunized with NP-KLH for 12 days and given BrdU for 1 hour by i. v. injection. Shown are the contour maps (left) and statistics of BrdU vs 7AAD staining of the gated $B220^{+}$ Fas^{hi} $GL7^{hi}$ GC B cells. Data reflect mean ± SEM of three independent experiments. N.S.: not significant. (**F**) Influence of IgCγ-Cre tg on GC development. Shown are Fas vs GL7 staining of total GC B cells (top panel) and high affinity GC B cells (bottom panel) in WT, IgC γ-Cre and $CBL^{dKO\text{-}Cg}$ mice at day 11 after NP-KLH immunization. Statistic of absolute number are shown at the right. Data reflect mean ± SEM of two independent experiments with four mice per group. **: $p<0.001$; ***: $p<0.0001$. (unpaired student t test). (**G**) FACS analysis of total GC B cells (top panel) and high affinity $IgG1^{+}$ GC B cells (bottom panel) in WT, *Cbl*$^{-/-}$, *Cbl-b*$^{-/-}$ and $CBL^{dKO\text{-}Cg}$ mice at day 11 after NP-KLH immunization. Statistic of absolute cell numbers are shown at the right. Data reflect mean ± SEM of three independent experiments with five mice per group. *: $p<0.05$; **: $p<0.001$; ***: $p<0.0001$. (unpaired student t test).

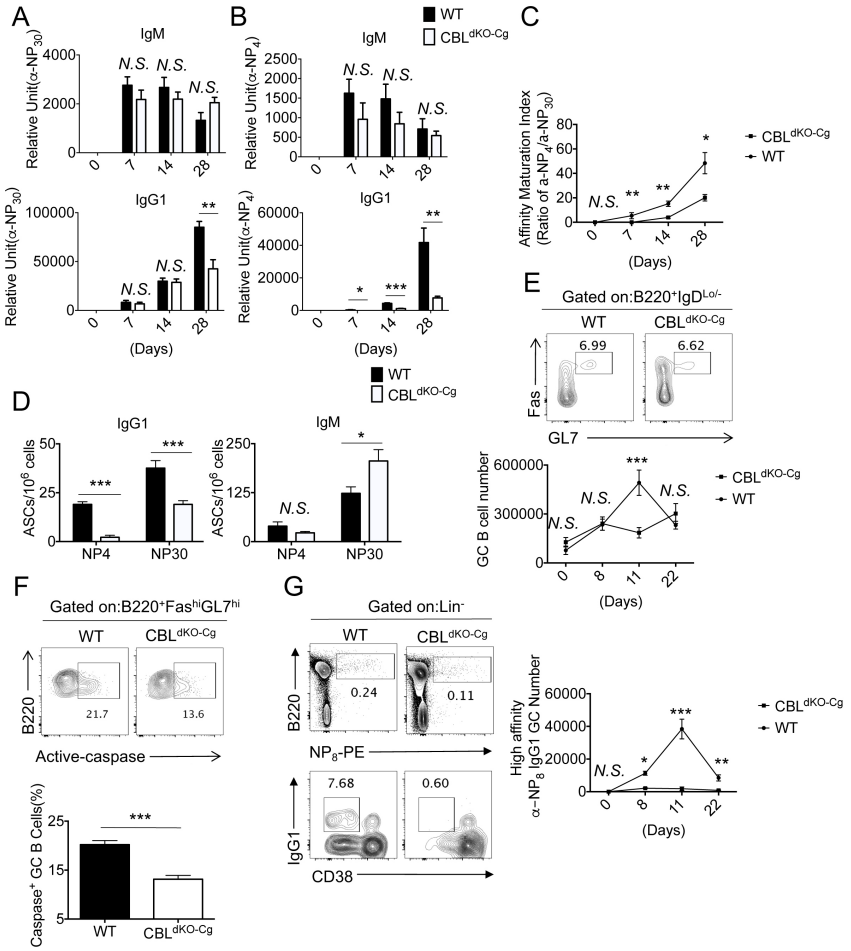

Figure 3.4 Impaired antibody affinity maturation in CBL$^{dKO\text{-}Cg}$ mice

(**A**) The kinetics of serum total anti-NP_{30} antibody titers of IgM and IgG1 isotypes. (**B**) The kinetics of serum high affinity anti-NP_4 antibody titers of IgM and IgG1 isotypes. (**C**) Antibody affinity maturation of IgG1 antibody. The maturation index is defined by the ratios of anti-NP_4 vs anti-NP_{30} antibody titers. n=5. (**D**) ELISPOT analysis of splenic ASCs against NP_{30} or NP_4-BSA antigen at day 14 after immunization. n=5. (**E**) The developmental kinetics of GC B cells in WT and CBL$^{dKO\text{-}Cg}$ mice after NP-KLH immunization. Shown is contour maps (top panel) of GC B cells at day 7 and the statistics (bottom bars) of GC B cells postimmunization. n=4. (**F**) Analysis of apoptotic GC B cells. Apoptotic GC B cells were visualized by anti-active form Casp staining. Shown are contour plots (top panel) and statistical (bottom bars) of Casp$^+$ GC B cells among total B220$^+$GL7$^+$Fas^{hi} B cells. n=4. (**G**) Defective development of high affinity BCR expressing GC B cells (Gated as: Lin$^-$B220$^+$$NP_8$-PE$^+$CD38$^-$IgG1$^+$) in CBL$^{dKO\text{-}Cg}$ mice. Shown are flow cytometric analysis (left) and statistics of high affinity (NP_8-binding) IgG1 GC B cells in WT and CBL$^{dKO\text{-}Cg}$ mice. n=4. * p<0.05; ** p<0.001; *** p<0.0001.

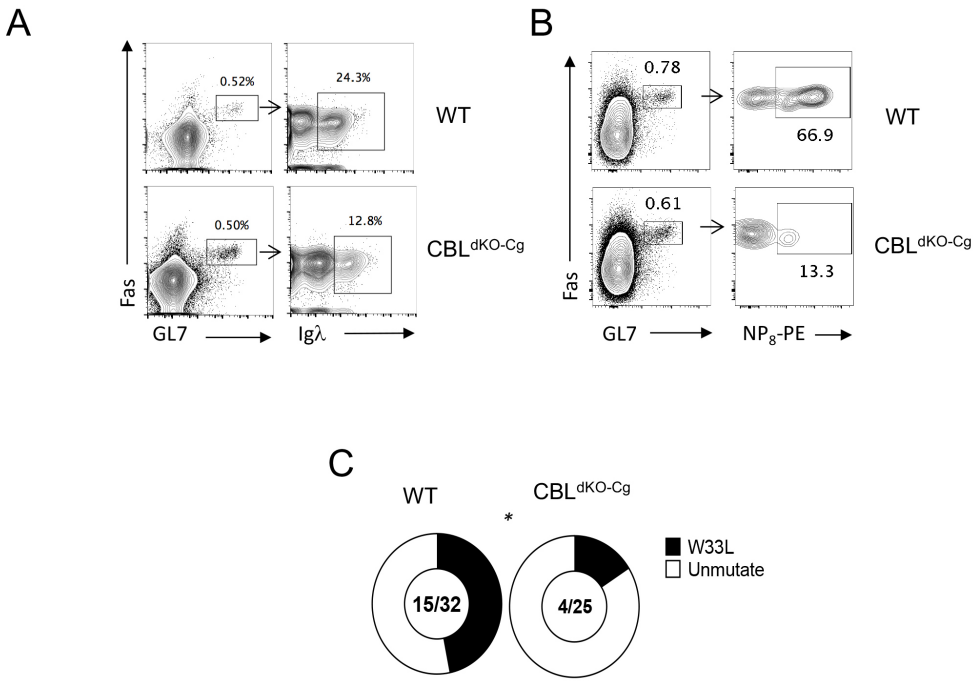

Figure 3.5 GC B cell purification gates and VH186.2 gene mutation analyses

(**A**) Soring strategy. Igλ1^{+} GC B cells were first gated as B220^{+}Fas^{hi} GL7^{hi} from NP-KLH immunized mice (day14). DNAs isolated from purified cells were PCR amplified for V186.2 genes and subjected for DNA sequencing. (**B**) Soring strategy of NP specific GC B cells. B220^{+} Fas^{hi} GL7^{hi} NP_{38}-PE^{+} GC B cells were purified from NP-KLH immunized mice (day14) for V186.2 gene sequencing. (**C**) Frequency of V_H186.2 genes carrying W33L mutation in NP-specific GC B cells. Shown is pie presentation of VH186.2 genes with W33L mutation from NP-specific GC B cells from WT and CBL$^{dKO\text{-}Mb1}$ mice. Statistics was conducted using Fisher's exact test. *: $p<0.05$. Data represent 32 and 25 VH186.2 genes from five WT and CBL$^{dKO\text{-}Cg}$ mice, respectively.

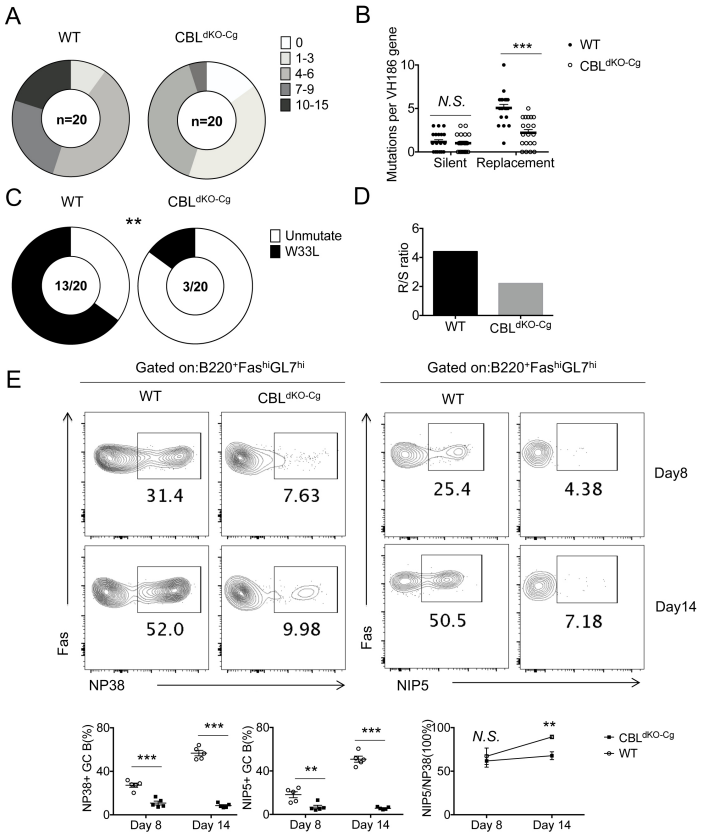

Figure 3.6 Impaired selection of high affinity BCRs but not SHM by the CBL^{dKO-Cg} mutation

(**A**) Pie presentation of the frequency of SHM in V_H186.2 genes. V_H186.2 genes with different numbers of SHM are shown in different degrees of shade. The total numbers of V_H genes analyzed are indicated in the centers of the pies. (**B**) Frequency of replacement vs silent mutations in V_H186.2 genes. Each dot represents data from one individual V_H186.2 gene. (**C**) Representation of V_H186.2 clones with W33L mutation. The number of W33L clones among VH186.2 sequences is shown in the center of pie chart and was compared using Fisher's exact test. **p<0.001. Data are from pooled five mice each group. (**D**) Ratios of replacement vs silent (R/S) mutations in V_H186.2 coding genes. (**E**) Development of NIP_5 and NP_{38}-binding GC B cells at different time points of GC reaction. Shown (top panel) are flow cytometric analyses of splenic NP_{38} or NIP_5-binding cells in gated $220^+GL7^{hi}Fas^{hi}$ GC B cells at day 8 and day 14 post NP-KLH immunized. Bottom left and middle: statistics of NP_{38} and NIP_5-binding GC B cells at day 8 and 14 after immunization, respectively. Bottom right: Percentages of high affinity NP (NIP_5-binding) GC B cells among total NP specific (NP_{38}-binding) GC B cells at day 8 and day 14 after immunization. Data are mean± SEM (E) and are representative of two independent experiments with five mice per group. ** p<0.001; *** p<0.0001 (unpaired Student's t test).

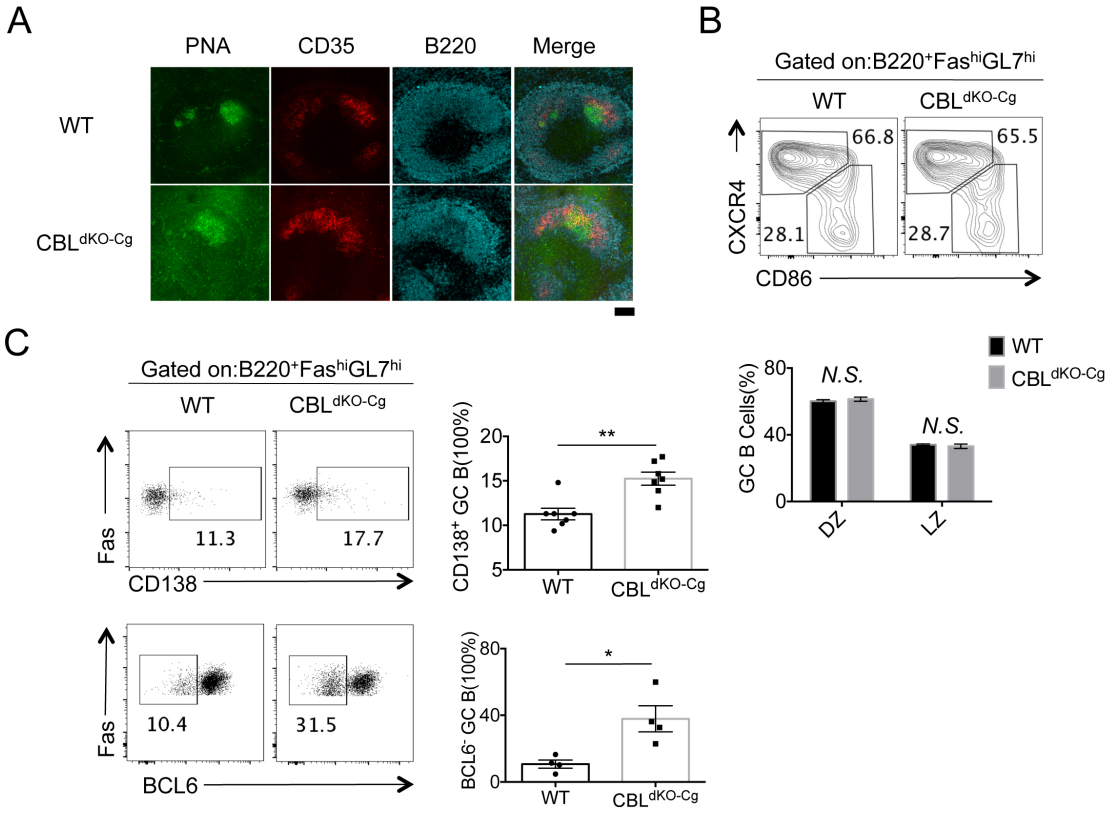

Figure 3.7 Influence of CBL ablation on the Development and differentiation of GC B cell subsets

(**A**) Immunofluorescent staining of splenic GC. WT and CBL$^{dKO\text{-}Cg}$ mice were immunized with NP$_{36}$-KLH. Shown are the spleen cross sections of immunized mice (day 12) stained with anti-CD35 (red), PNA, and anti-B220. Scale bar represents 33 μm. (**B**) Flow cytometric analyses (left) and statistics [254] of GC DZ and LZ B cells. Total splenic cells from the immunized WT and CBL$^{dKO\text{-}Cg}$ mice were stained with anti-B220, GL7, Fas, CXCR4, and CD86. DZ and LZ B cells in the contour plots are gated CXCR4^{hi}CD86^{lo} and CXCR4^{lo} CD86^{hi} cells, respectively. Data reflect mean ± SEM of two independent experiments with four mice per group. N.S.: not significant. (**C**) FACS analysis of PC precursors (characterized as: B220^{+}Fas^{hi}GL7^{hi}CD138^{+} or B220^{+}Fas^{hi}GL7^{hi}Bcl6$^{-/lo}$) in WT and CBL$^{dKO\text{-}Cg}$ GC B cells. Shown are dot plots (left) and statistics analysis. Data reflect mean ± SEM of two independent experiments with at least four mice per group. *: $p<0.05$; **: $p<0.001$. (unpaired student t test).

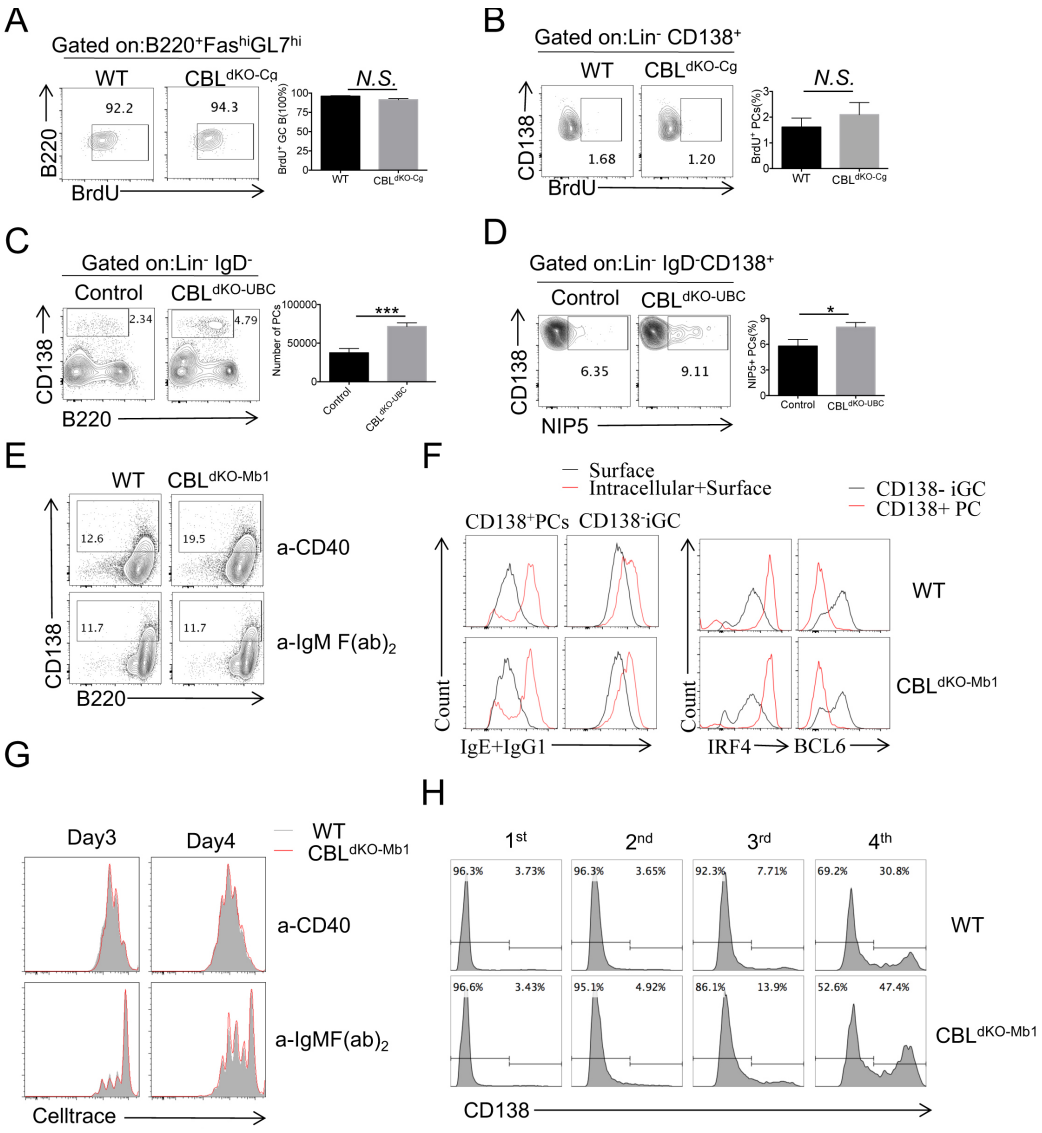

Figure 3.8 Analysis of B cell proliferation and PC genesis

(**A**) BrdU labeling of GC B. WT and CBL$^{dKO\text{-}Cg}$ mice were immunized for 12 days, and injected with BrdU i. v. for twenty-four hours. Proliferation of GC B cells was evaluated by BrdU^{+} staining. Shown are flow cytometric analysis (left) and statistics of BrdU^{+} (B220^{+}GL7^{hi}Fas^{hi}) GC B cells. Data reflect mean ± SEM of two independent experiments with eight mice per group. (**B**) Analysis of newly generated PCs in un-immunized WT and CBL$^{dKO\text{-}Cg}$ mice 24hrs post BrdU i.v. injection. Newly generated PCs was evaluated by BrdU^{+} staining. Shown are flow cytometric analysis (left) and statistics of BrdU^{+} (Linage^{-} CD138^{+}) PCs. Data reflect mean ± SEM of two independent experiments with four mice per group. (**C**) Enhanced PCs (LinageIgDCD138^{+}) differentiation in CBL$^{dKO\text{-}UBC}$ mice. UBC-ERCre (Control) and CBL$^{dKO\text{-}UBC}$ chimeric mice were immunized with NP-KLH for 7

days. Tamoxifan was then give daily from day 7-10 to delete CBL. Mice were analyzed on day 12 after immunization. Shown are contour map (left) and statistics analysis of total $CD138^+$ PCs and plasma blasts. Data reflect mean ± SEM of two independent experiments with five mice per group. ***: $p<0.0001$ (unpaired student's t test). (**D**) Enhanced development of high affinity antigen specific PCs ($Linage^-IgD^-CD138^+NIP5\text{-}APC^+$) in $CBL^{dKO\text{-}UBC}$ mice. Mice were the same as in (C). Shown are contour map (left) and statistics analysis of high affinity NP antibody (NIP_5-binding) producing PCs. Data reflect mean ± SEM of two independent experiments with at least five mice per group. *: $p<0.05$(unpaired student's t test). (**E**) *In vitro* PC genesis stimulated by soluble anti-CD40 or anti-IgM. Purified B cells were cultured and stimulated with either soluble anti-CD40 or anti-IgM $F(ab)_2$ for 3 days. Plasma blast-like cells generated in the culture were stained with anti-B220 and CD138 and then analyzed on a FACS. Shown is CD138 vs B220 staining of the cultured cells. The percentages of plasma blast-like ($B220^+CD138^+$) cells are indicated in each plot. (**F**) Intracellular Ig, BCL6, and IRF4 staining of *in vitro* generated PCs and GC (iGC) B cells. $CBL^{dKO\text{-}Mb1}$ B cells were cultured 40LB feeder cells for 7 days to generate iGC ($CD138^-$ $B220^+$) and PCs ($CD138^+$ $B220^{+/-}$). Cells were either stained cell surface staining (Left column in left panel) or cell surface staining followed by intracellular staining for IgE+G1 (Right column in left panel), IRF4 (left column in right panel), and BCL6 (right column in right panel). The experiment has been performed two times. (**G**) B cell proliferation upon anti-CD40 and BCR stimulation. Purified B cells were labeled with CellTrace and cultured in the presence of soluble anti-CD40 or anti-IgM $F(ab)_2$. Cell proliferation was measured at days 3 and 4 by FACS based on CellTrace dilution. Shown are histograms of CellTrace fluorescence intensity of WT (grey shadow) and $CBL^{dKO\text{-}Mb1}$ (red line) B cells. (**H**) Cell division dependent PC genesis. B cells were labeled with CellTrace and cultured on 40LB feeder cells as described in Figure 9F. Shown are histograms of PCs/plasma blasts ($CD138^+$ cells) generated in each cell division as indicated on the top of the plots.

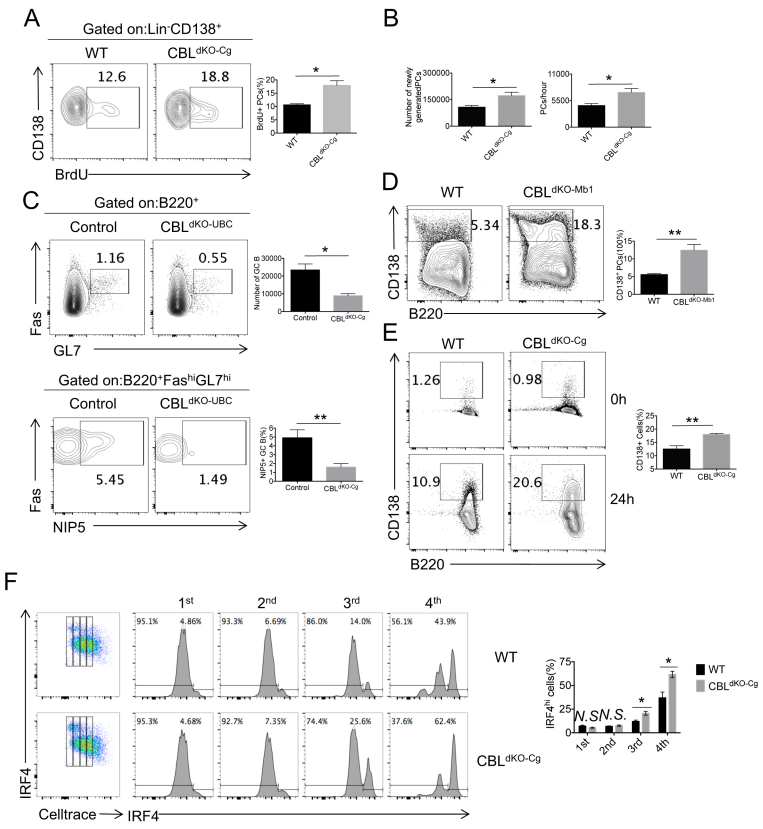

Figure 3.9 Premature termination of GC B cell fate and expedited PC differentiation in the absence of CBLs

(**A**) *In vivo* newly generated PCs identified by BrdU labeling assay. Shown are flow cytometric (top panel) and statistics analyse (bottom bars) of splenic newly generated PCs after 24 hours BrdU labeling, identified as $Lin^{-}BrdU^{+}CD138^{+}$ cells. n=10. (**B**) The *in vivo* rates of PC genesis presented as the total numbers of newly generated PCs either per spleen (left) or per hour in the spleen. n = 7. (**C**) Flow cytometric analyses of total (top panel), and NIP_5-binding (bottom panel) GC B cells at day 12 without (left) or with ER-Cre mediated CBL ablation. Statistics are shown as bars. (**D**) *In vitro* PC differentiation of WT and $CBL^{dKO\text{-}Mb1}$ B cells in 40LB feeder cell culture. Shown are flow cytometric (left) and statistical analyse of ($CD138^{+}B220^{hi/lo}$) PCs/plasmablasts-like cells. n=5. (**E**) Comparison of *In vitro* differentiation of freshly isolated WT and $CBL^{dKO\text{-}Cg}$ GC B cells. Shown are flow cytometric (left) and statistical analyse of PCs ($B220^{-}CD138^{hi}$)/plasmablast-like ($B220^{+}CD138^{hi}$) cells generated in the culture. n=4. (**F**) Cell division dependent B-cell differentiation to PCs in 40LB feeder culture system. Shown are dot plots (top left) and histogram analyses (top right) of IRF4 expression in cell divisions 1st, 2nd, 3rd, and 4th WT or $CBL^{dKO\text{-}Mb1}$ B cells identified by Cell Trace dilution. Bottom: Statistical analysis of PC genesis in each cell division. n=4. * $p<0.05$; ** $p<0.01$; *** $p<0.001$.

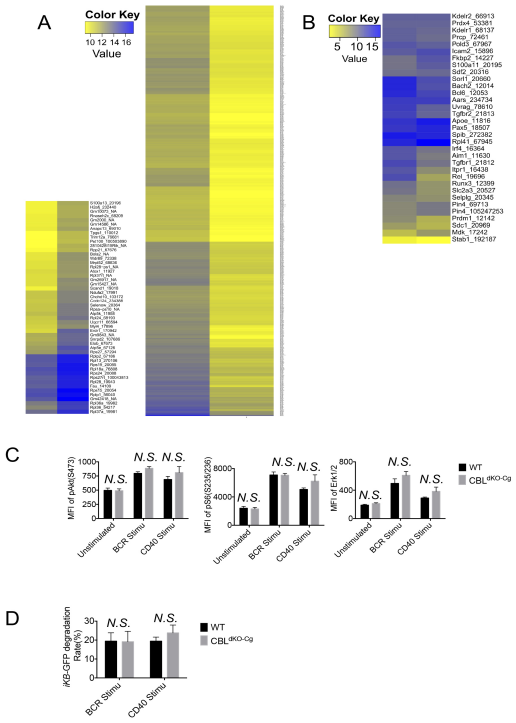

Figure 3.10 Gene expression profiles of WT vs CBL$^{dKO\text{-}Cg}$ GC B cells; Comparison of CD40 and BCR induced signaling in WT and CBL$^{dKO\text{-}Cg}$ GC B cells

(**A**) RNA-seq analysis of mRNA expression in WT and CBL$^{dKO\text{-}Cg}$ GC B cells. WT and CBL$^{dKO\text{-}Cg}$ mice were immunized with SRBC. mRNAs were extracted from GC ($B220^{+}GL7^{hi}Fas^{hi}$) B cells isolated by FACS sorting at day 12 after immunization. Shown are heat maps of genes that are down (left) and up regulated in CBL$^{dKO\text{-}Cg}$ B cells compared to WT controls, respectively. (**B**) Comparison of the mRNA expression profiles of the genes related to GC B and PC identities. WT and CBL$^{dKO\text{-}Cg}$ mice were immunized with NP_{36}-KLH. At day 12, total splenic B cells were stimulated with either anti-CD40 or anti-IgM $F(ab)_2$ for 5 min. Cells were first stained with anti-B220, GL7, and Fas, fixed and permeablized, and then intracellularly stained with antibodies against active forms of Akt, S6 kinase, and Erk1/2, respectively. For canonic NF-kB activity, a fusion gene encoding IkB and EGFP was introduced into WT and CBL$^{dKO\text{-}Cg}$ BM stem cells by retroviral vector. Transfected BM stem cells were transferred into lethally irradiated $Rag1^{-/-}$ mice to generate BM chimeric mice. Splenic GC B cells were stimulated with anti-CD40 or BCR, and NF-kB activity in GC B cells was measured by FACS based on IkB-GFP expression. (**C**) Phospho-flow analyses of Akt, S6 kinase, and Erk activation in GC B cells after anti-CD40 or anti-IgM stimulation. (**D**) Flow cytometric analysis of IκB degradation in GC B cells stimulated with anti-CD40 or BCR for 5mins. The steady state IκB-GFP expression was set as control. IκB-GFP degradation rate(100%)= (percentage of steady state GFP^{+}-stimulated GFP^{+} GC B cells)/ percentage of steady state GFP^{+} GC B cells.

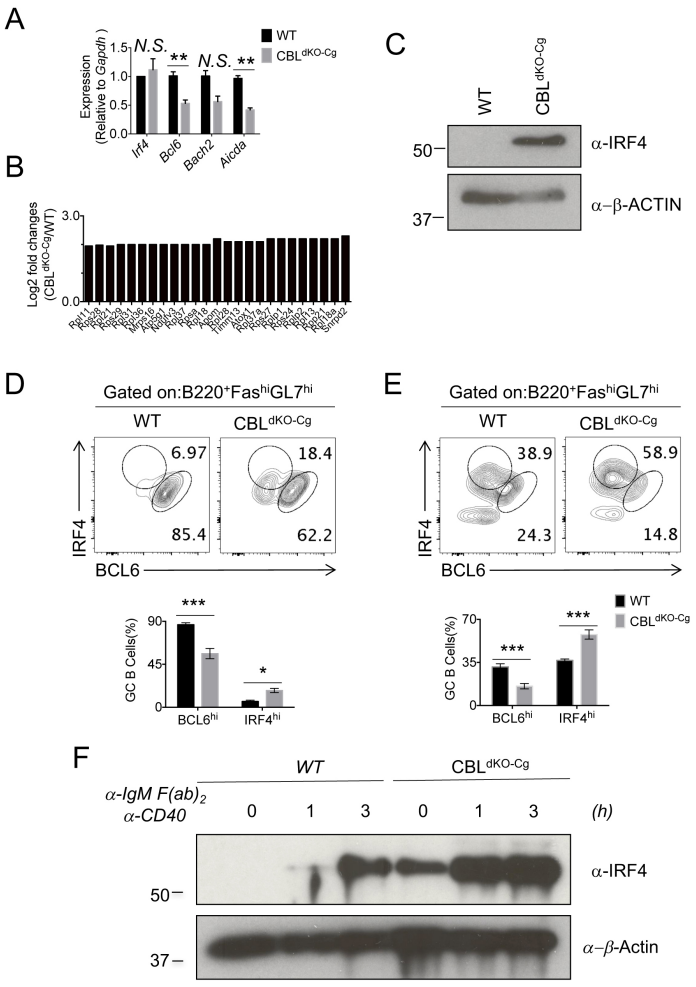

Figure 3.11 Post-transcriptional regulation of GC differentiation program by CBLs

(**A**) qPCR analysis of GC B cell and PC identity genes in WT and CBL$^{dKO\text{-}Cg}$ GC B cells. Data were from FACS purified splenic B220^{+}GL7^{+}Fas^{+} GC B cells of pooled from 3x WT and CBL$^{dKO\text{-}Cg}$ mice at day 14 after SRBC immunization. (**B**) Comparison of the expression of protein synthesis and secretion related genes in WT and CBL$^{dKO\text{-}Cg}$ GC B cells. (**C-E**) Western blot and flow cytometric analyses of IRF4 expression in WT and CBL$^{dKO\text{-}Cg}$ GC B cells. (**C**) Western blot analysis of IRF4 in WT and CBL$^{dKO\text{-}Cg}$ GC B cells. n=4. (**D and E**) Flow cytometric analyses of IRF4 vs BCL6 expression in GC B cells without (**D**) or with (**E**) anti-CD40 and BCR stimulation. Shown are contour maps (left) and statistics of IRF4^{hi}BCL6^{lo} and BCL6^{hi} cells among total gated GL7^{hi}Fas^{hi} GC B cells. n=6. (**F**) Western blot analysis of IRF4 expression in WT and CBL$^{dKO\text{-}Cg}$ GC B cells with or without anti-CD40 and BCR stimulation. n=3. * p<0.05; ** p<0.01; *** p<0.001.

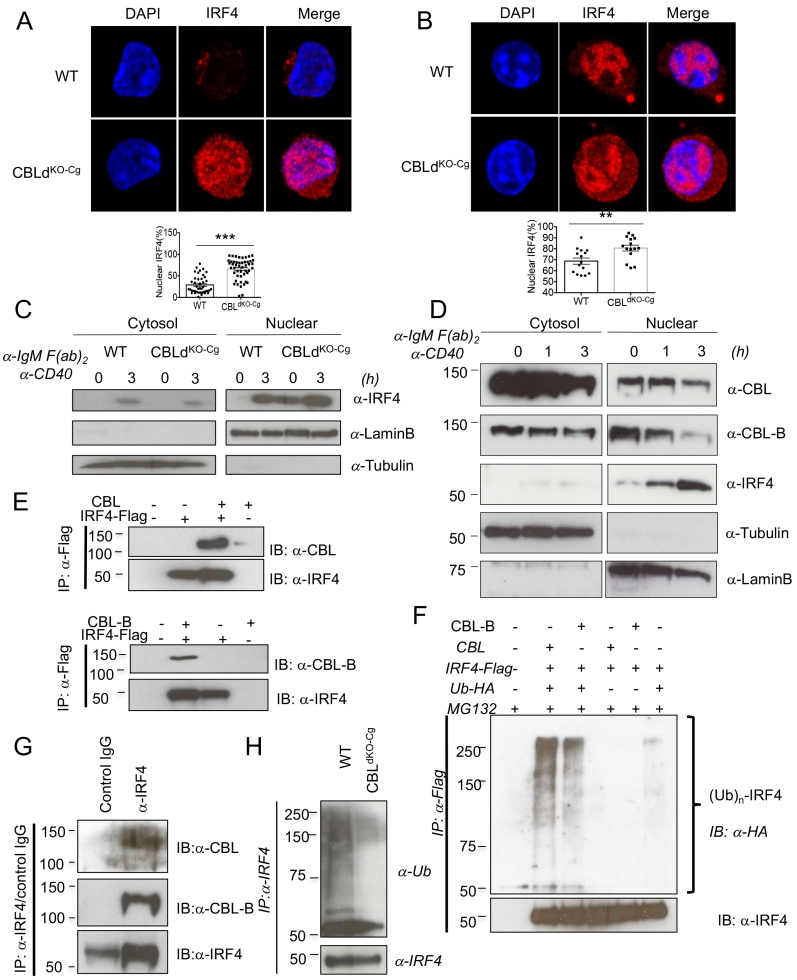

Figure 3.12 Regulation of nuclear IRF4 ubiquitination and expression by CBLs

(**A and B**) Confocal microscopic analysis of cytosolic and nuclear IRF4 in WT and CBL$^{dKO\text{-}Cg}$ GC B cells without (**A**) or with (**B**) anti-CD40 and BCR stimulation. The statistical analyses show the percentages of nucleus vs total IRF4. Each dot represents one cell. (**C**) Western blot analysis of nuclear vs cytosolic IRF4 in WT and CBL$^{dKO\text{-}Cg}$ GC B cells before and after anti-CD40 and BCR stimulation. n=2. (**D**) Asymmetric expression of CBL and CBL-B vs IRF4 proteins in WT GC B cells before and after CD40 and BCR stimulation. n=3. (**E**) Co-immunoprecipitation and Western blot analysis of CBL and CBL-B association with Flag tagged IRF4 (IRF4-Flag). n=2. (**F**) IRF4 ubiquitination by CBL or CBL-B. Shown is Western blot analysis of ubiquitinated IRF4-Flag immunoprecipitated from 239T cells cotransfected with either CBL or CBL-B. n=3. (**G**) Association of IRF4 with CBL or CBL-B in freshly isolated GC B cells. n=2. (**H**) Ubiquitination of Irf4 in WT and CBL$^{dKO\text{-}Mb1}$ *in vitro* generated GC (iGC) B cells. * p<0.05; *** p<0.001.

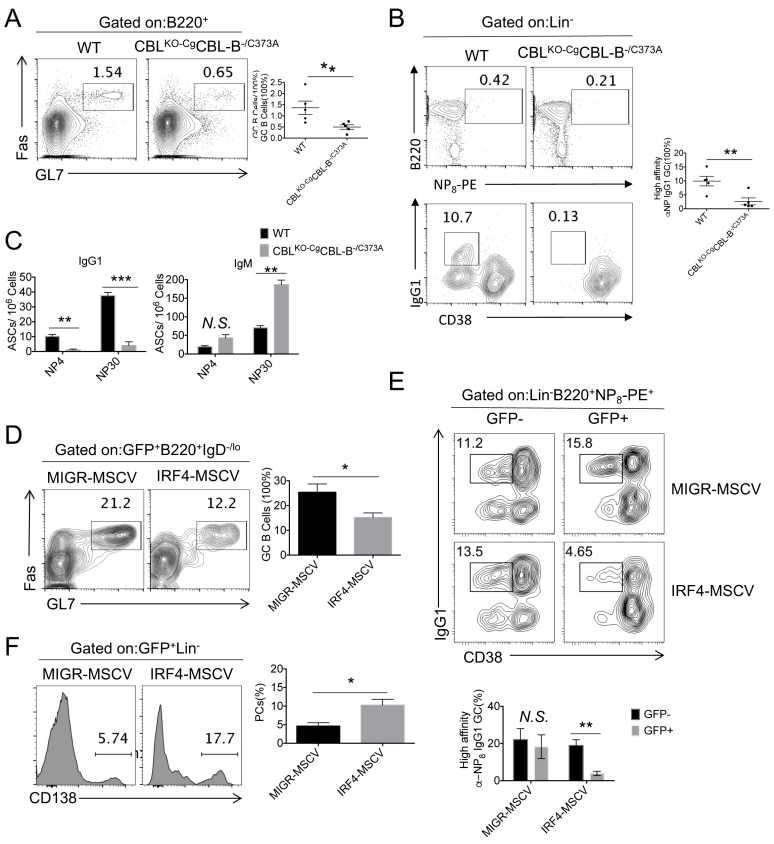

Figure 3.13 Impaired development of high affinity GC B cells in CBL^{KO-Cg}CBL-B$^{-/C373A}$ or IRF4-MSCV BM chimeric mice

(**A-C**) Inactivation of the ubiquitin ligase function of CBLs in GC B cells recapitulates GC phenotypes found in CBL^{dKO-Cg} mice (day 12 after NP-KLH immunization). (**A**) The dot plots (left) and statistical analyses of Fas^{+}GL7^{+} GC B cells among total splenic B220^{+} cells. (**B**) The flow cytometric (left) and statistical analyses of the high affinity (NP_8-binding) GC B cells among total B220^{+} cells. (**C**) The statistics of splenic total (anti-NP_{30}-binding antibody) and high affinity (NP_4–binding antibody) secreting plasma cells (ASCs). n=5. (**D-F**) Ectopic expression of IRF4 abolishes high affinity antibody producing GC B cell development in MSCV-IRF4 BM chimeric mice after NP-KLH immunization (day 12). WT BM stem cells were transduced with either MIGR-MSCV-GFP (empty) or MSCV-GFP-IRF4 retroviral vector and used to generate BM chimeras. (**D**) The dot plots (left) and statistical analyse of Fas vs GL7 staining of gated B220^{+} IgD^{-} splenic GC B cells. (**E**) The contour plot (left) and statistical analyses of high affinity (NP_8-binding) IgG1 GC B cells in BM chimeras with (GFP^{+}) without (GFP-) retrovirus infection. (**F**) The histogram analysis of GFP^{+}B220^{-}CD138^{+} splenic PCs among total GFP^{+} splenocytes in empty MSCV and MSCV-IRF4 infected BM chimeras. n=5-6. * p<0.05; ** p<0.01; *** p<0.001.

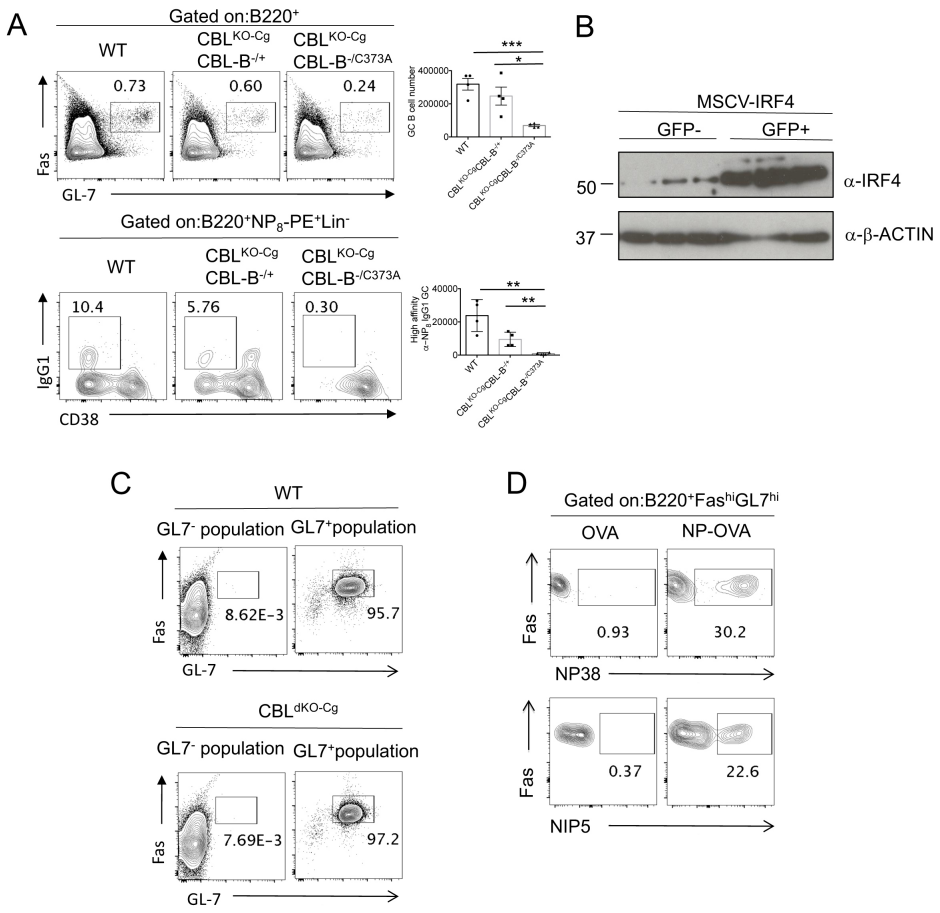

Figure 3.14 CBL$^{KO\text{-}Cg}$CBLB$^{-/C373A}$ GC development and IRF4 ectopic expression

(**A**) FACS analysis of total GC B cells (top panel) and high affinity IgG1$^+$ GC B cells (bottom panel) in WT, CBL$^{KO\text{-}Cg}$CBL-B$^{-/+}$ and CBL$^{KO\text{-}Cg}$CBL-B$^{-/C373A}$ mice at day 12 after NP-KLH immunization. Statistics of absolute cell number are shown at the right. Data reflect mean ± SEM of four mice per group. *: p<0.05; **: p<0.001; ***: p<0.0001. (unpaired student t test) (**B**) Western blot analysis of IRF4 expression in IRF4-MSCV infected B cells (GFP$^+$B220$^+$). WT B cells (GFP$^-$B220$^+$) and MSCV-IRF4 (GFP$^+$B220$^+$) B cells were purified by FACS sorting. Shown are one representative experiment out of total two. (**C**) Purity analysis of GC B cells. GC B cells were first enriched by a B cell enrichment Magnetic column and then purified by FACS sorting as B220$^+$CD138$^-$GL7$^+$ GC B cells and B220$^+$CD138$^-$GL7$^-$ non-GC B cells. Purity of both GC and non-GC B cells were evaluated based on GL7 vs Fas staining. Shown is FACS plots of Fas vs GL7 staining of one representative experiment. (**D**) Analysis of testing NP$_{38}$-PE and NIP$_5$-APC specificity. GC B cells were from OVA or NP$_{20}$-OVA immunized mice and stained with NIP$_5$-APC or NP$_{38}$-PE together with anti-B220, Fas, and GL7. Shown are NIP$_5$ or NP$_{38}$ binding cells among gated B220$^+$ Fas^{hi} GL7^{hi} cells. Experiment represents data from two mice in each group.

4 Chapter 4: Discussion

CBL and CBLB are E3 ubiquitin ligases that are expressed in haematopoietic cells. Multiple studies have shown that CBL proteins act as negative regulators for both TCR- and BCR-mediated signalling pathways, in which CBL and CBL-B exhibit a redundant regulatory role. In the second chapter, I found that $CBL^{dKO\text{-}Mb1}$ mice displayed a significant reduction of T-independent and T-dependent immune responses. The impaired T-independent antibody response was mainly due to the lack of MZ B cells, which is the main cell population that may respond to T-independent antigens. Additionally, the CBL double deficient naïve FO B cells failed to differentiate into GC B cells upon either soluble or particle T-dependent antigen immunization. My study demonstrated that CBL proteins are required for naïve B cell antigen presentation to cognate $CD4^+$ T cells. CBL proteins specifically target BCR-associated proteins Igα and Igβ for ubiquitination and then promote the degradation of BCR-antigen complexes upon BCR stimulation. In the absence of CBL proteins, the internalization and sorting of BCR-antigen complexes to lysosomes are blocked. As the consequence, the mutant B cells cannot form a cognate interaction with pre-Tfh cells due to the lack of antigenic-peptide-loaded MHC, thus resulting in a deficient GC reaction. Blocking the ubiquitin ligase function of CBL through mutating the RING finger domain or blocking the ubiquitination of Igα through point mutagenesis could recapitulate the deficiency of the GC reaction as $CBL^{dKO\text{-}Mb1}$ mice. Thus, we provided evidence that the CBL-mediated ubiquitin ligase function, not the adaptor function, plays an indispensable role in regulating the GC reaction.

Previous studies in our laboratory showed that the ablation of *Cbl* and *Cblb* in mature B cells results in the development of SLE-like autoimmune disease. This finding was evidenced of the high level of serum autoantibodies against double-stranded DNA and nuclear antigen, as well as the high level of IgG1 antibody deposited in the kidney. This result indicated that CBL proteins control the B cell-intrinsic checkpoint for tolerance. Surprisingly, $CBL^{dKO\text{-}Mb1}$ mice did not develop SLE-like autoimmune disease and showed a prolonged lifespan compared to the mice from the previous study, in which CBL was deleted by using a CD19-Cre allele [215]. The reason for this discrepancy might reflect the fact that the ablation of CBL and CBL-B in B cells at different developmental time points could lead to two completely different outcomes. CD19-Cre allele drives Cre recombinase expression in approximately 30-40% of bone marrow immature B cells and in 80% of mature B cells [282]. The deletion of CBL proteins at the mature splenic B cell stage could lead to the generation of B cells with auto-reactive BCR since the majority of the deletions occurred after the negative selection. In contrast, the Mb1-driven Cre showed more than 90% of deletion in bone marrow immature cells. Although the ablation of CBL proteins could disrupt B cell tolerance, the majority of CBL-deficient immature B cells with auto-reactive BCRs would be eliminated by negative selection during B cell development. This means only the cells with normal BCRs can further give rise to splenic mature B cells. Additionally, different genetic backgrounds may also contribute to this discrepancy. $CBL^{dKO\text{-}Mb1}$ mice have a C57BL/6 background, whereas the mouse models used in the previous study were of a mixed B6

and 129 genetic background, which had been shown to exhibit a relatively higher susceptibility to autoimmune diseases [283].

It has been shown that antigen-experienced FO B cells in lymph nodes can interact with cognate $CD4^+$ T cells through MHCII/peptide, which promotes the further interaction between co-stimulatory molecules such as CD40-CD40L, SLAM-SLAM and ICOS-ICOSL. Although it is generally believed that this T-B cognate interaction is critical for Tfh and GC B cell development, the consequences of B-cell-dependent $CD4^+$ T cell activation are still controversial, as B cells have been shown to be poor $CD4^+$ T cell activators compared to professional APCs and may tolerate $CD4^+$ T cells [284, 285]. However, other studies and our study showed that B cells can activate and promote the proliferation of CD4+ T cells *in vitro*[286]. The optimal Tfh cell differentiation requires antigen presentation by both DCs and B cells. Consistent with our results, Terri M. Laufer's group showed that the antigen presentation by DCs promotes the upregulation of Bcl6 in activated $CD4^+$ T cells and promotes T cell differentiation into pre-T_{fh} cells. However, without cognate interaction with antigen-specific B cells, these $Bcl6^+$ T cells could not further upregulate CXCR5, PD-1 and GL7 to differentiate into distinctively Tfh cells [287]. These results thus support that the antigen presentation from activated B cells is necessary for pre-Tfh cells to complete their differentiation. It should be noted that although DCs cannot promote active $CD4^+$ T cells to fully differentiate into Tfh cells, administration of processed peptides to MHC II B-cell-specific knockout mice can restore the Tfh development and GC reaction [288], indicating that the development of Tfh cells requires continuous antigen presentation that is independent of unique B cell

signalling. However, at the T-B border and in the GC, B cells with antigen-specific BCRs have a greater advantage of acquiring antigens from FDCs than from other APCs, thus making them a prior choice for antigen presentation to T cells, compared with DCs. This model was further supported by our results on the physiological level, since the $CBL^{dKO\text{-}Mb1}$ mutation does not affect the MHCII expression on B cells. Consistently, the administration of processed $OVA_{323\text{-}339}$ peptides to our $CBL^{dKO\text{-}Mb1}$ mice partially restored both T_{fh} and GC B cell development, which further supported the notion that CBL proteins regulate the T-B cognate interaction through an antigen-presentation-dependent mechanism. Since the administration of processed antigenic peptides can only partially rescue GC deficiency, this result also indicated that the CBL proteins may also play important roles in the maintenance and differentiation of GC B cells. However, the possibility that the excessive OVA peptides directly bind to MHCII on other APCs should be considered, which may overcompensate for the B-cell-mediated T_{fh} differentiation in $CBL^{dKO\text{-}Mb1}$ mice. To exclude this possibility, we will use a transgenic mouse model in which MHCII is restrictively expressed on DCs and B cells for rescue experiments in a future study.

Interestingly, we found that CBL dko mice possessed a relatively normal number of GC B cells at day 8 post-immunization. The mutant GC B cells proliferated normally *in vivo*, suggesting that CBL proteins are not required for BCR-mediated antigen presentation within developing GC B cells. Indeed, we also found that *Cbls*-deficient iGC B cells showed a comparable capacity to promote the proliferation of the cognate OT-II $CD4^+$ T cells in the presence of intact antigen (Figure 4.1A), and the BCR internalization and

antigen complex degradation was apparently normal in *Cbls*-deficient iGC B cells (Figure 4.1B). These results thus raise the possibility that other ubiquitin ligases are involved in BCR-mediated antigen uptake and processing or that the ubiquitination is not required for the process in GC B cells. A previous study using a large-scale imaging system revealed that naïve and memory B cells gather antigen towards the immune synapse centre before internalization, while GC B cells extract antigens through a distinct pathway using small peripheral clusters[239]. Consequently, GC B cells exhibit reduced

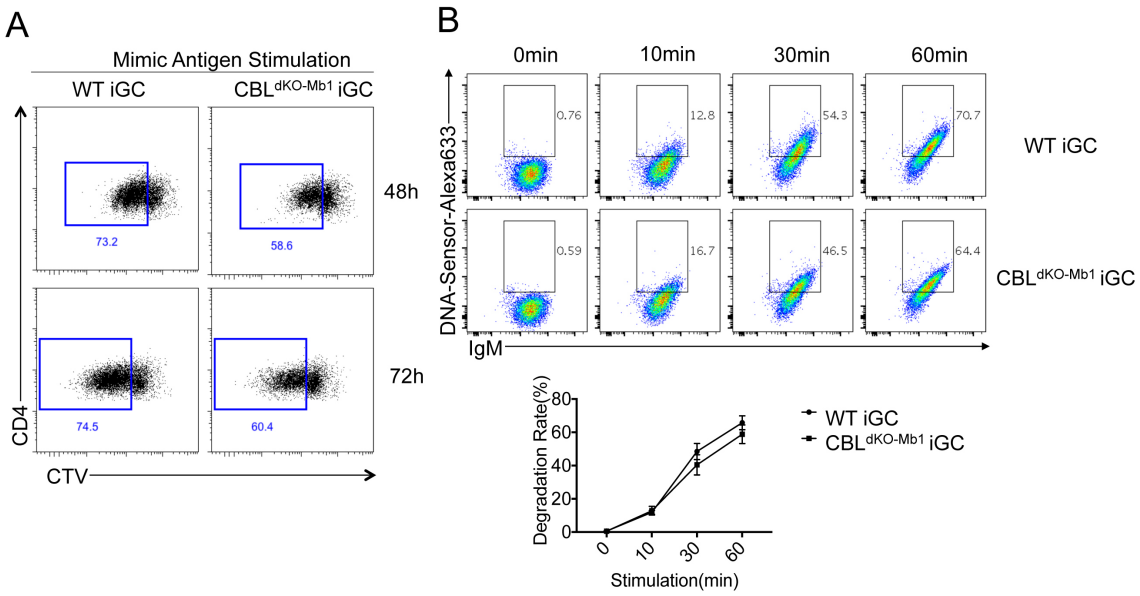

Figure 4.1 Intact antigen presentation capacity in *Cbls*-deficient iGC

(A). Flow cytometry analysis of iGC antigen presentation to cognate OT-II $CD4^+$ cells after mimic antigen treatment. 40LB-induced iGC B cells were incubated with mini antigen for 30mins at 37°C. The antigen experienced iGC B cells were co-cultured with CFSE labelled OT-II $CD4^+$ cells for 48h and 72h. (B) Quantification of antigen sensor degradation in WT and $CBL^{dKO\text{-}Mb1}$ iGC at various time points. (n=3). iGC B cells were incubated with antigen-DNA sensor for 30min on ice. Then incubated at 37°C for various time lengths (0min, 10min, 30min, 60min). The antigen degradation rate was quantified as DNA-sensor-$Alexa633^+$.

antigen internalization and degradation rates compared to naïve B cells. In this regard, we speculated that CBL proteins are the key regulators for optimal and efficient antigen internalization and degradation in naïve but not GC B cells. Optimal antigen internalization and processing is critical for the initial activation of naïve B cells. Furthermore, whether the ubiquitination of the BCR complexes is involved in this process remains to be determined. Upon anti-IgM stimulation, non-GC and naïve B cells show dramatically increased BCR signalling. In contrast, GC B cells show defects in the early events of BCR signalling, such as defects in the phosphorylation of SYK, BLNK, Igα and Igβ [276]. Instead, both SH2 domain-containing phosphatase (SHP-1) and SH2 domain-containing inositol 5 phosphatase (SHIP-1) are hyper-phosphorylated in GC B cells. Other studies have shown that the individual BCR is dedicated to either BCR signalling or antigen presentation depending on the ITAM-mediated signalling. Accordingly, defective phosphorylation of Igα and Igβ in GC B cells may suggest that the antigen presentation of GC B cells is not dependent on the phosphorylation of Igα and Igβ. Future studies are needed to further investigate the function of Igα and Igβ proteins in GC B cells.

Previous studies have focused on dissecting the function of Igα and Igβ proteins in BCR signalling. The Igα-Igβ dimer is non-covalently associated with membrane Ig through polar residues in the transmembrane domain of Ig. It has been shown that the cytoplasmic tails of these two proteins contain an ITAM motif that is critical for the recruitment of tyrosine kinases Syk and Lyn to activate downstream signalling. By targeting the ITAM of Igα and Igβ, the $Ig\alpha^{FF/FF}$ and $Ig\beta^{FF/FF}$ mice both showed enhanced BCR signalling, reduced

BCR endocytosis and impaired T-dependent immune responses. This finding indicates that the ITAM of these two proteins are critical for the regulation of BCR internalization, which negatively affects BCR signalling. Furthermore, these results also indicate that the optimal BCR internalization is required for the T-dependent immune response [45, 230]. The non-ITAM tyrosine 204 mutation exhibits a unique defect in T-independent B cell activation, proliferation and antibody response, while the BCR capping, antigen internalization, antigen presentation and T-dependent antibody response remains unaffected. In our study, the targeted mutation of three lysine residues (K161R, K167R and K217R) on the cytoplasmic tail of Igα displayed normal surface BCR expression and similar BCR signalling, except for slightly reduced Ca^{2+} signalling. Interestingly, the Igα mutant mice showed a dramatically reduced GC B cell population upon NP_{36}-KLH immunization due to the impaired BCR-mediated antigen presentation process. Our results demonstrated the unique cell intrinsic role of Igα ubiquitination in the formation of GC B cells (Figure 4.2). However, we cannot rule out the possibility that mutations on Igα may affect the kinetics of GC reaction since we just examined the GC formation at day 10 post-immunization. To further demonstrate the important role of Igα ubiquitination in GC B cell initiation, GC B cell kinetic study will be performed in the future study.

The first two lysine residues (at position 161 and 167) were critical for the development of GC B cells, whereas the K217R mutation did not affect the initiation of GC B cells. These observations indicated that the ubiquitination of lysine residues 161 and 167, not 217, of Igα are targeted by CBLs (Figure 4.2). However, additional proteomic studies are

needed to further clarify the potential contribution of other E3 ubiquitin ligases, such as ITCH and GRAIL, to the ubiquitination of Igα–mediated GC initiation. Interestingly, although GC B cells were unable to be generated in K167R mutant mice, one novel $CD38^{hi}GL7^{+}Fas^{-}$ population was presented. We speculated that this novel population was the precursor of GC B cells, which accumulated at this stage due to the impaired antigen presentation and T-B cognate interaction. This further supports the idea that T cell 'help' is critical for full GC B cell differentiation (Figure 4.2). However, extensive studies are needed for the further characterization of this precursor population.

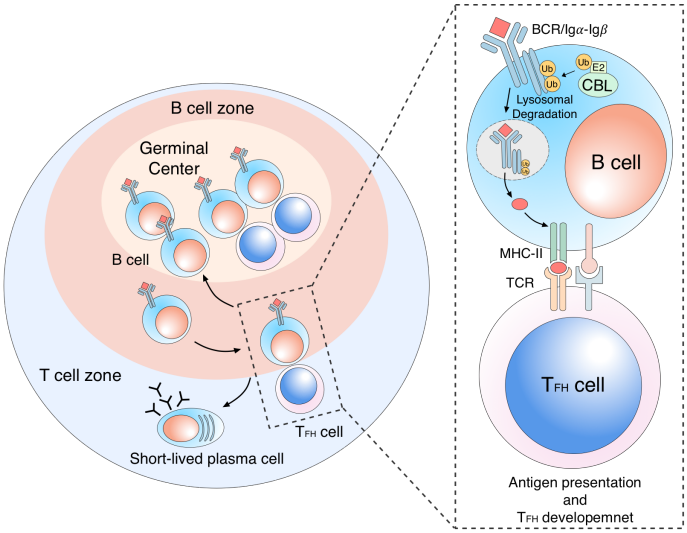

Figure 4.2 CBL proteins regulate the initiation of GC reaction through B cell intrinsic mechanism

Within B cell follicle, some B cells are activated by T-dependent antigen experienced APCs and acquire antigens through BCR-dependent mechanism. Activated B cells migrated to T-B border and interact with cognate pre-T_{fh} cells. The selected B cells and pre-T_{fh} cells migrate back to B cell zone and form GC while the un-selected B cells differentiate into short-lived PCs. CBL proteins are critical for T-B cognate interaction since CBLs regulate naïve B cell antigen presentation to $CD4^{+}$ T cells. In naïve B cells, CBLs specifically regulate BCR internalization and degradation through targeting BCR-associated complex Igα-Igβ.

Finally, although our western blot showed ubiquitination of both Igα and Igβ proteins upon BCR stimulation, the blockage of Igα ubiquitination alone was sufficient to recapitulate the GC deficiency in $CBL^{dKO\text{-}Mb1}$ mice. This result may have two possible explanations: first, the ubiquitination of both Igα and Igβ is required for optimal antigen internalization, degradation and presentation; however, Igα and Igβ may act at different levels of the same regulatory pathway; second, the ubiquitination of Igα but not Igβ is required for this biological process. Recently, Marcus Clark's group showed that Igβ ubiquitination was required for the sorting of the BCR complex to the MHCII antigen-presenting compartment. Although the normal T-dependent antibody response against NP-CGG was shown in Igβ mutant mice, a proper antibody response against an influenza viral infection was unable to be mounted [289]. The class-switched antiviral neutralization antibody is secreted by PCs, which are mainly derived from GC B cells. The impaired antiviral antibody response in Igβ mutant mice indicated that the ubiquitination of Igβ is critical for the GC reaction. Additionally, it has been shown that Igα is relatively upregulated in activated B cells and GC B cells with decreased mRNA expression, while the Igβ protein is dramatically downregulated in GC B cells. This finding indicates that Igα and Igβ may have different functions in B cell activation. To investigate the individual biological function of Igα and Igβ ubiquitination, the targeted mutation of Igβ should be explored carefully in the future.

Antigen-specific antibodies are essential for the host defence against infectious viruses and microbes. Antibodies against self-antigens, called autoantibodies, are responsible for various autoimmune diseases such as SLE, Graves' disease and rheumatoid arthritis (RA). The pathogenesis of RA is dependent on rheumatoid factor (RF)-specific B and T cells. Multiple studies have shown that autoantibody-secreting PCs can be generated from T-dependent and T-independent immune responses. Thus, B cells are the primary therapeutic target in RA. For instance, rituximab can completely deplete $CD20^+$ B cells in the peripheral blood, and this effect can last for several months [290-292]. However, anti-CD20 therapy is not sufficient to treat RA patients with a high number of pre-plasma cells before treatment, suggesting that the anti-CD20 therapy cannot eliminate plasmablasts. Recent studies have demonstrated that RF-specific B cells are not only responsible for the generation of PCs but also act as APCs to stimulate $CD4^+$ T cell expansion and differentiation [293, 294]. Furthermore, RF-specific B cells display a significantly enhanced antigen-uptake capacity compared to that of professional APCs. These B cells take up antigen-Ig immune complexes via the BCR. Takemura and colleagues showed that the T-cell response in RA synovitis is dependent on B cells [295]. These characteristics propose CBL proteins as a potential therapeutic target for RA treatment. Since my study demonstrated the tight regulation of cognate T-B interaction by CBL proteins through a B cell antigen-presentation mechanism, it will be necessary to screen for compounds to inhibit the CBL E3 ubiquitin ligase function. These inhibitors may directly target RF-specific B cells, consequently blocking their antigen presentation and suppressing both T and B cell activation and expansion. In addition to suppressing

the T-dependent immune response, the inhibitors can also block the T-independent immune response, based on my results. Thus, my study provides some new insights for RA treatment.

High-affinity IgG1 antibody-producing cells are generated through a GC reaction, where the GC B cells carrying BCRs with different affinities compete for antigens and T_{fh} cells help B cells in the LZ region to undergo affinity-based selection and maturation. I found that the LZ GC B cells selectively displayed enhanced CBL and CBLB expression compared to naïve B and DZ GC B cells. This finding suggests that CBL proteins may have a critical function in LZ GC B cell affinity selection. Indeed, the ablation of CBL proteins specifically in GC B cells selectively blocked the development of GC B cells that express high affinity BCRs, while the low-affinity and un-switched antibody secreting cells were expanded. I further demonstrated that CBL protein-mediated ubiquitin ligase activity was required for this regulatory mechanism since the C373A mutation in the RING finger domain of CBL proteins, which inactivates CBL ligase activity, was sufficient to recapitulate this phenotype. These findings together provide strong support for the conclusion that CBL proteins define a checkpoint in GC LZ B cells, which controls antibody affinity-based selection in a ubiquitination-dependent manner (Figure 4.3).

GC B cell proliferation and selection occur in the DZ and LZ, respectively, and are tightly controlled by multiple layers of regulations. Previous studies showed that the transcription factor FOXO1 is critical for the formation and/or maintenance of the GC DZ through a CXCR4- and BATF-dependent mechanism since the ablation of FOXO1 in

GC B cells leads to disrupted GC architecture and CSR and reduced proliferation, but normal SHM [147, 148, 151]. Consistently, the enforced constitutive activation of PI3K completely recapitulated the phenotype. These studies showed the important role of the BCR-PI3K-FOXO1-CXCR4/BATF signalling pathway in the regulation of affinity maturation and selection. Moreover, another downstream target of PI3K transcription factor, c-Myc, was shown to be required for the re-entry of GC B cells from the LZ to the DZ for clonal expansion and SHM [84]. These studies demonstrated the essential role of BCR affinity in the clonal expansion and selection of GC B cells. In parallel, the function of CD40 receptor-mediated NF-κB signalling in GC B cells is required. Specifically, the subunit c-REL is required for the maintenance of the GC reaction through upregulating the metabolic programme to adapt the enhanced biosynthesis of DNA, protein and lipids in these highly proliferative GC B cells [168, 296]. In contrast, another subunit RELA is critical for the differentiation of PCs through the upregulation of BLIMP1. In addition, two subunits of the NF-κB canonical pathway p50 and p65 can directly bind to the promoter region of IRF4 and activate its transcription upon CD40 stimulation [173]. Taken together, the current model suggests that BCR signalling is responsible for GC B maturation and selection, while CD40 signalling is required for the differentiation of GC B cells. However, this model is challenged by a recent study in which the BCR and CD40 signalling were both shown to be required for the termination of the GC B programme. These findings gave rise to the following question: how can GC B cells sense and distinguish proliferation and differentiation signals? My study provided new insights on this question. The ablation of CBLs promoted the GC B cells to differentiate into PCs

without sufficient maturation, mutation and CSR, but not proliferation *in vivo and in vitro*, which suggests that CBL proteins suppress the early onset of the PC differentiation programme. Surprisingly, the deficiency of CBLs did not affect BCR-induced mitotic signalling and CD40-induced canonical NF-κB pathways. Consistently, the mRNA level of IRF4 was comparable between WT and $CBL^{dKO\text{-}Cg}$ GC B cells, but IRF4 proteins were highly increased in $CBL^{dKO\text{-}Cg}$ GC B cells, which suppress the BCL6-related GC B programme and promote the PC programme. Since the CBLs can directly target IRF4 for ubiquitination, the highly expressed CBL proteins in LZ GC B cells can eradicate the IRF4 protein to maintain their GC B cell identify. Interestingly, I found that CD40 and BCR stimulation can rapidly downregulate CBL proteins and upregulate IRF4 in GC B cells, which can trigger the initiation of the PC programme.

Recent two-photon microscopy studies revealed that GC B cells circulated between the LZ and DZ region based on the dynamic expression of chemokine receptors. The underlying molecular mechanism remains unclear, but it was shown that transcription factors FOXO1 and c-Myc are required for this critical behaviour of GC B cells. The Cbls-deficient GC B cells showed impaired GC selection for the W33L key mutation and increased PC genesis both *in vivo and in vitro*, indicating that these GC B cells cannot undergo a sufficient round of DZ-LZ circulation. In this regard, CBLs seem to represent new regulators that control the exit checkpoint of the DZ-LZ circulation. It would be necessary to directly investigate whether CBL proteins can shortcut this DL-LZ circulation by using two-photon microscopy or photoactivation technology. In addition, the circulation of GC B cells is related to the dynamic regulation of the metabolic

programme. GCs have a similar microenvironment to that of tumours, with limited oxygen and nutrient availability, which requires reprogramming of their metabolism for adaptation to this environment. For example, the HIF-family-related pathway was shown to be critical for sensing the hypoxic environment in the GC region to further support GC B proliferation and maturation, as blocking HIF pathways suppressed GC B cell survival, CSR and differentiation [297]. Moreover, PCs displayed a unique metabolic programme to sustain the production of a large quantity of immunoglobulins and the unfolded-protein response [164]. Therefore, metabolic regulation was also involved in the generation of PCs through a GC-dependent pathway. It would be interesting to determine whether the CBL proteins can regulate PC differentiation through a metabolism-related mechanism. Once the affinity maturation and selection of GC B cells reach a certain point, the BCR and CD40 trigger the signals to promote the exit from the GC reaction and the differentiation into PCs or memory B cells. Although recent transcriptome studies have shown the dynamic transcription regulation of BCL6, IRF4 and BLIMP1 in the generation of plasmablasts, the initial signal driving the GC B cell programme to the PC programme is still controversial. Our data clearly showed that the downregulation of BCL6 and the upregulation of IRF4 ($BCL6^{lo}IRF4^{hi}$) in a small proportion of GC B cells were considered the precursors of plasmablasts. Interestingly, this plasmablast precursor was dramatically expanded in mutant mice compared to WT mice, suggesting that the CBL proteins control the formation of this population. Consequently, the CBL dko mice showed an enhanced PC generation rate and an enlarged PC population in the spleen.

Upon CD40 and BCR stimulation, the CBL proteins were rapidly degraded in both the cytosol and nucleus, which led to the upregulation of IRF4. The upregulation of IRF4

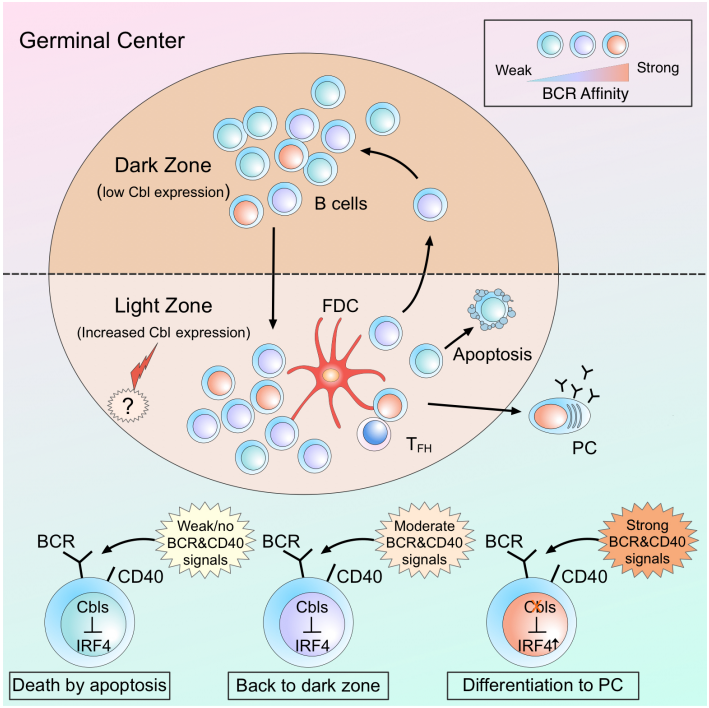

Figure 4.3 CBL proteins regulate the initiation of PC program

CBL proteins are preferentially expressed in LZ GC B cells comparing to DZ GC B cells. After acquiring antigen and T-cell help, majority of LZ GC B cells with moderate BCR and CD40 stimulation migrate back to DZ for clonal expansion and SHM. Upon strong BCR and CD40 stimulation, a small proportion of high affinity BCR-expressing LZ GC B cells downregulate CBLs and BCL6 expression, leading to accumulation of IRF4 protein. Eventually, these IRF4 highly expressing plasmablast precursors further differentiate into PCs.

protein not only suppressed *Bcl6* transcription but also further promoted the expression of IRF4 and BLIMP1 proteins. These two master transcription factors of PCs could push GC B cells to differentiate into plasmablasts and PCs. Thus, we proposed that dynamic

regulation of the IRF4 concentration in LZ GC B cells is the earliest event of bias to PC fate commitment through a robust BCR- and CD40-controlled CBL expression.

My findings demonstrated that CBL proteins are dynamically regulated in DZ and LZ GC B cells, which is critical for GC selection and maturation. Although the CBL proteins were markedly upregulated in LZ GC B cells, the mRNA level of *Cbl* and *Cblb* was comparable to that in naïve B, DZ and LZ GC B cells, which indicates that the expression of CBLs may be post-transcriptionally regulated. This finding raised an interesting question: how is the CBL expression spatially and temporally regulated during the GC affinity selection? Three lines of evidence indicate that CD40-mediated signalling is responsible for the degradation of CBLs. In human B cells, CD40 stimulation induces the strongest expression of c-Src kinase compared to other stimuli[298]. Along this line, c-Src interacts with CBL and promotes the ubiquitination of CBL both *in vitro* and *in vivo* [299]. However, since the c-Src kinase lacks the RING finger domain, the function of Src in this process is more likely to be sorting CBL to proteasomal destruction by cooperating with other E3 ubiquitin ligases. The direct downstream targets of CD40 contain TRAFS or cIAPs, both of which contain the RING finger domain and can regulate the downstream signalling through ubiquitination [279]. Additionally, TRAF2 and TRAF6 are physically associated with CBLB upon CD40 stimulation. Then, we speculated that Scr and TRAF work cooperatively to degrade CBL proteins through a ubiquitination-dependent machinery. Alternatively, CD40 can also downregulate CBL expression through a microRNA-dependent mechanism by inducing miR155. It has been shown that miR155 may influence CBLB expression in B cells [254, 280]. Since the reduction of

CBL proteins leads to impaired antibody selection and maturation, it would be interesting to investigate if the over-expression of CBL proteins in GC B cells can improve the GC maturation.

Due to the rapid development of molecular immunology, more than 120 inherited primary immunodeficiency diseases have been characterized in the past six decades[300]. Among them, one group of immunodeficiency diseases such as hyper-IgM syndromes (HIGMs), X-linked agammaglobulinaemia (XLA) and common variable immunodeficiency (CVID) are related to B cell defects. Patients with these genetic defects are vulnerable to recurrent infections with encapsulated pathogens. It is necessary to understand the precise molecular defects that lead to the B-cell-related immunodeficiency, which would promote translational research. For example, six genes are identified as biomarkers for the hyper-IgM syndromes (HIGMs): *Cd40l*, Cd40, *Acida*, *Ung*, *Ikkg* and *Nfkbia* [301-310]. The HIGMs are characterized by impaired CSR and SHM or by impaired SHM alone. Interestingly, our CBL dko mice also displayed a similar immunodeficiency. It would be necessary to investigate if CBL proteins or their RING finger domains are mutated in patients with HIGMs. If so, the CBLs could become a potential biomarker for HIGMs and provide new insights for treatment.

5 Conclusion and future direction

5.1 Conclusions

GCs are critical micro-lymphoid organs responsible for the production of high affinity antibody producing PCs and memory B cells. Due to its importance in immune surveillance, autoimmunity, and B cell tumours, numerous efforts have been invested in understanding how the GC reaction is regulated under physiological and pathological conditions. My studies have provided some new insights into the mechanisms of this regulation. Using various genetic mutant mice, I have demonstrated that E3 ubiquitin ligases CBL proteins play redundant, however, critical roles at different levels of the GC reaction. First, at the entry checkpoint of the GC reaction, CBL proteins are required for the establishment of the cognate interaction between antigen specific B cells and $CD4^+$ T cells. My further studies have shown that CBL proteins control this interaction through regulating BCR-mediated antigen internalization and sorting to the lysosomes for degradation, and they do so by promoting the ubiquitination of the BCR-associated Igα and Igβ. In the absence of CBL proteins B cells cannot internalize BCR-bound antigen and present antigen to T cells, consequently impeding the T-B cell interaction and disabling the development of T_{fh} cells and initiation of GCs. Secondly, I have demonstrated that CBL proteins control antibody affinity maturation and they do so at the exit checkpoint of GC reaction. In this direction, my studies have revealed that the expression of CBL proteins is dynamically regulated during GC zoning cycle, with the highest expression found in the LZ relative to the DZ B cells. Such an up-regulation appears to be critical for preventing the accumulation of IRF4, a PC promoting

transcription factor, in the LZ B cells, consequently preventing the premature termination of the GC cycle which is essential for B cells to acquire SHM and undergo affinity selection. My studies have shown further that CBL proteins are essential for the ubiquitination and degradation of IRF4 and ectopic expression of IRF4 is sufficient to abolish antibody affinity maturation. Strong BCR and CD40 signalling lead to degradation of CBL proteins and concomitant up-regulation of IRF4. Thus, these studies support a model that CBL proteins function as a critical B cell intrinsic sensor that regulate GC affinity selection by detecting the BCR affinity cues delivered as BCR and CD40 signalling.

5.2 Future Directions

While my studies have established several critical roles of CBL proteins in the entry and exit checkpoints of the GC reaction, several questions remain unresolved by these studies:

Firstly, in my studies I have found that CBL ubiquitin ligase activity is required for T_{fh} cell development and GC initiation (Figure 2.11 A and B) and both Igα and Igβ are ubiquitinated by CBL proteins (Figure 2.10 A and B). However, my mutagenesis studies have shown that blockade of Igα ubiquitination alone is sufficient to block antigen presentation by B cells as well as the development of GCs (Figure 2.13 G and 2.14 A). These experiments thus raise an important question as to whether Igβ ubiquitination is required for B cell antigen presentation. My current hypothesis is that Igβ ubiquitination is likely act in the same BCR internalization and lysosomal sorting pathway but not

redundant. This hypothesis can be tested by mutagenesis studies of Igβ, in analogous to the experiment of Igα mutagenesis studies described in Figure 2.13 and 2.14. For this purpose, I have generated Igβ ko mice and can test this hypothesis by introducing into the Igβ B cells a mutant form of Igβ that cannot be ubiquitinated. I will then examine the antigen presentation by these mutant B cells and T_{fh} and GC development in the mutant mice that carry such a mutation.

Secondly, while my studies have shown that CBL-mediated ubiquitination of Igα and Igβ is necessary for naïve B cell antigen presentation, ablation of CBL proteins in GC B cells did not prevent GC B cell proliferation which generally believed to be dependent on GC B cell-T_{fh} interaction (Figure 3.3 E and 3.4 E). This finding thus suggests either that Igα and Igβ ubiquitination is not required for antigen internalization and processing by activated B cells or that other intracellular ubiquitin ligases are involved in Igα and Igβ ubiquitination. To address this question, I have generated several conditional Igα and Igβ mutant constructs, which may specifically turn-on the mutant Igα or Igβ in GC B cells. Since these mutant Igα and Igβ cannot be ubiquitinated, it will allow me to test whether ubiquitination of Igα and Igβ is required for antigen presentation of activated GC B cells and GC B cell proliferation.

Thirdly, in chapter 3 my studies have shown that CBL proteins control the affinity maturation of GC B cells and they may do so by prematurely turning-on the PC program in LZ GC B cells. Although I have found that CBL proteins are dynamically regulated at the protein but not the transcription level in GC DZ-LZ cycle, it is still unclear about the

mechanisms employed by B cells to control CBL expression. My hypothesis is that in LZ B cells CBL protein levels are regulated by protein ubiquitination, either by themselves or by other ubiquitin ligases or de-ubiquitinases and this regulation depends on BCR and CD40 signalling strength. To examine whether this is the case, I will conduct further biochemical studies to examine whether CBL proteins are ubiquitinated and whether BCR and CD40 stimulation changes the status of CBL ubiquitination. Co-immunoprecipitation combined with proteomics studies will be used to identify other unknown ubiquitin ligases or de-ubiquitinases that regulate CBL ubiquitination.

Finally, since my studies have shown that the level of CBL proteins in GC B cells dictate the selection of high affinity GC B cells, it will be interesting to examine whether increased CBL expression alone may help to improve antibody affinity maturation. Along this line, I will use genetic approach to increase CBL expression in GC B cells and then examine whether this modulation boosts antibody affinity maturation in mice. If so, it will suggest that we may improve the efficiency of vaccination to weak antigenic pathogens in the future by modulating CBL expression in B cells.

6 Reference

1. Smyth, M.J., et al., *New aspects of natural-killer-cell surveillance and therapy of cancer*. Nature Reviews Cancer, 2002. **2**: p. 850.
2. Klose, C.S.N. and D. Artis, *Innate lymphoid cells as regulators of immunity, inflammation and tissue homeostasis*. Nature Immunology, 2016. **17**: p. 765.
3. Artis, D. and H. Spits, *The biology of innate lymphoid cells*. Nature, 2015. **517**: p. 293.
4. Ebbo, M., et al., *Innate lymphoid cells: major players in inflammatory diseases*. Nature Reviews Immunology, 2017. **17**: p. 665.
5. Shikhagaie, M.M., et al., *Innate lymphoid cells in autoimmunity: emerging regulators in rheumatic diseases*. Nature Reviews Rheumatology, 2017. **13**: p. 164.
6. Cariappa, A., et al., *B cell antigen receptor signal strength and peripheral B cell development are regulated by a 9-O-acetyl sialic acid esterase*. J Exp Med, 2009. **206**(1): p. 125-38.
7. Victoratos, P., et al., *FDC-Specific Functions of p55TNFR and IKK2 in the Development of FDC Networks and of Antibody Responses*. Immunity, 2006. **24**(1): p. 65-77.
8. Martin, F., A.M. Oliver, and J.F. Kearney, *Marginal zone and B1 B cells unite in the early response against T-independent blood-borne particulate antigens*. Immunity, 2001. **14**(5): p. 617-29.
9. Kondo, M., I.L. Weissman, and K. Akashi, *Identification of clonogenic common lymphoid progenitors in mouse bone marrow*. Cell, 1997. **91**(5): p. 661-72.
10. *Resolution and characterization of pro-B and pre-pro-B cell stages in normal mouse bone marrow*. The Journal of Experimental Medicine, 1991. **173**(5): p. 1213-1225.
11. *A complex of glycoproteins is associated with VpreB/lambda 5 surrogate light chain on the surface of mu heavy chain-negative early precursor B cell lines*. The Journal of Experimental Medicine, 1993. **178**(2): p. 469-478.
12. Reichman-Fried, M., R.R. Hardy, and M.J. Bosma, *Development of B-lineage cells in the bone marrow of scid/scid mice following the introduction of functionally rearranged immunoglobulin transgenes*. Proceedings of the National Academy of Sciences, 1990. **87**(7): p. 2730-2734.
13. Shinkai, Y., et al., *RAG-2-deficient mice lack mature lymphocytes owing to inability to initiate V(D)J rearrangement*. Cell, 1992. **68**(5): p. 855-67.
14. Melchers, F., *Checkpoints that control B cell development*. The Journal of Clinical Investigation, 2015. **125**(6): p. 2203-2210.
15. Cinamon, G., et al., *Sphingosine 1-phosphate receptor 1 promotes B cell localization in the splenic marginal zone*. Nat Immunol, 2004. **5**(7): p. 713-20.
16. Pereira, J.P., Y. Xu, and J.G. Cyster, *A role for S1P and S1P1 in immature-B cell egress from mouse bone marrow*. PLoS One, 2010. **5**(2): p. e9277.
17. Pereira, J.P., et al., *Cannabinoid receptor 2 mediates retention of immature B cells in bone marrow sinusoids*. Nature immunology, 2009. **10**(4): p. 403-411.

18. Beck, T.C., et al., *CXCR4 and a cell-extrinsic mechanism control immature B lymphocyte egress from bone marrow*. The Journal of Experimental Medicine, 2014. **211**(13): p. 2567-2581.
19. Pillai, S. and A. Cariappa, *The follicular versus marginal zone B lymphocyte cell fate decision*. Nature Reviews Immunology, 2009. **9**: p. 767.
20. Ha, S.-a., et al., *Regulation of B1 cell migration by signals through Toll-like receptors*. The Journal of Experimental Medicine, 2006. **203**(11): p. 2541-2550.
21. Berberich, S., R. Förster, and O. Pabst, *The peritoneal micromilieu commits B cells to home to body cavities and the small intestine*. Blood, 2007. **109**(11): p. 4627.
22. Suzuki, K., et al., *Roles of B-1 and B-2 cells in innate and acquired IgA-mediated immunity*. Immunological Reviews, 2010. **237**(1): p. 180-190.
23. Berland, R. and H.H. Wortis, *Origins and Functions of B-1 Cells with Notes on the Role of CD5*. Annual Review of Immunology, 2002. **20**(1): p. 253-300.
24. Montecino-Rodriguez, E., H. Leathers, and K. Dorshkind, *Identification of a B-1 B cell–specified progenitor*. Nature Immunology, 2006. **7**: p. 293.
25. Astrakhan, A., et al., *Local increase in thymic stromal lymphopoietin induces systemic alterations in B cell development*. Nature Immunology, 2007. **8**: p. 522.
26. Esplin, B.L., et al., *A differentiation pathway for B1 cells in adult bone marrow*. Proceedings of the National Academy of Sciences, 2009. **106**(14): p. 5773.
27. Inaoki, M., et al., *CD19-Regulated Signaling Thresholds Control Peripheral Tolerance and Autoantibody Production in B Lymphocytes*. The Journal of Experimental Medicine, 1997. **186**(11): p. 1923-1931.
28. Xu, S., et al., *B cell development and activation defects resulting in xid-like immunodeficiency in BLNK/SLP-65-deficient mice*. International Immunology, 2000. **12**(3): p. 397-404.
29. Tarakhovsky, A., et al., *Defective antigen receptor-mediated proliferation of B and T cells in the absence of Vav*. Nature, 1995. **374**: p. 467.
30. Sidman, C.L., et al., *Production of immunoglobulin isotypes by Ly-1+ B cells in viable motheaten and normal mice*. Science, 1986. **232**(4756): p. 1423.
31. Moro, K., et al., *Innate production of TH2 cytokines by adipose tissue-associated c-Kit+Sca-1+ lymphoid cells*. Nature, 2009. **463**: p. 540.
32. Kopf, M., et al., *IL-5-Deficient Mice Have a Developmental Defect in CD5+ B-1 Cells and Lack Eosinophilia but Have Normal Antibody and Cytotoxic T Cell Responses*. Immunity, 1996. **4**(1): p. 15-24.
33. Saito, T., et al., *Notch2 is preferentially expressed in mature B cells and indispensable for marginal zone B lineage development*. Immunity, 2003. **18**(5): p. 675-85.
34. Tanigaki, K., et al., *Notch-RBP-J signaling is involved in cell fate determination of marginal zone B cells*. Nat Immunol, 2002. **3**(5): p. 443-50.
35. Oyama, T., et al., *Mastermind-1 is required for Notch signal-dependent steps in lymphocyte development in vivo*. Proceedings of the National Academy of Sciences, 2007. **104**(23): p. 9764-9769.

36. Wu, L., et al., *The transcriptional coactivator Maml1 is required for Notch2-mediated marginal zone B-cell development*. Blood, 2007. **110**(10): p. 3618-23.
37. Qiao, G., et al., *Negative regulation of CD40-mediated B cell responses by E3 ubiquitin ligase Casitas-B-lineage lymphoma protein-B*. J Immunol, 2007. **179**(7): p. 4473-9.
38. Kuroda, K., et al., *Regulation of marginal zone B cell development by MINT, a suppressor of Notch/RBP-J signaling pathway*. Immunity, 2003. **18**(2): p. 301-12.
39. Tan, J.B., et al., *Lunatic and manic fringe cooperatively enhance marginal zone B cell precursor competition for delta-like 1 in splenic endothelial niches*. Immunity, 2009. **30**(2): p. 254-63.
40. Song, R., et al., *Mind bomb 1 in the lymphopoietic niches is essential for T and marginal zone B cell development*. The Journal of Experimental Medicine, 2008. **205**(11): p. 2525-2536.
41. Huang, Z., et al., *Notch-induced E2A degradation requires CHIP and Hsc70 as novel facilitators of ubiquitination*. Mol Cell Biol, 2004. **24**(20): p. 8951-62.
42. Quong, M.W., et al., *Receptor Editing and Marginal Zone B Cell Development Are Regulated by the Helix-Loop-Helix Protein, E2A*. The Journal of Experimental Medicine, 2004. **199**(8): p. 1101-1112.
43. Hikida, M., et al., *Coupling between B cell receptor and phospholipase C-gamma2 is essential for mature B cell development*. J Exp Med, 2003. **198**(4): p. 581-9.
44. Cariappa, A., et al., *The follicular versus marginal zone B lymphocyte cell fate decision is regulated by Aiolos, Btk, and CD21*. Immunity, 2001. **14**(5): p. 603-15.
45. Kraus, M., et al., *Interference with immunoglobulin (Ig)alpha immunoreceptor tyrosine-based activation motif (ITAM) phosphorylation modulates or blocks B cell development, depending on the availability of an Igbeta cytoplasmic tail*. J Exp Med, 2001. **194**(4): p. 455-69.
46. Siebenlist, U., K. Brown, and E. Claudio, *Control of lymphocyte development by nuclear factor-kappaB*. Nat Rev Immunol, 2005. **5**(6): p. 435-45.
47. Cariappa, A., et al., *Nuclear Factor κb Is Required for the Development of Marginal Zone B Lymphocytes*. The Journal of Experimental Medicine, 2000. **192**(8): p. 1175-1182.
48. Lu, T.T. and J.G. Cyster, *Integrin-mediated long-term B cell retention in the splenic marginal zone*. Science, 2002. **297**(5580): p. 409-12.
49. Guinamard, R., et al., *Absence of marginal zone B cells in Pyk-2-deficient mice defines their role in the humoral response*. Nat Immunol, 2000. **1**(1): p. 31-6.
50. Newman, R., et al., *Maintenance of the marginal zone B cell compartment specifically requires the RNA-binding protein ZFP36L1*. Nature immunology, 2017. **18**(6): p. 683-693.
51. MacLennan, I.C., *Germinal centers*. Annu Rev Immunol, 1994. **12**: p. 117-39.
52. Mesin, L., J. Ersching, and G.D. Victora, *Germinal Center B Cell Dynamics*. Immunity, 2016. **45**(3): p. 471-482.

53. Schwickert, T.A., et al., *In vivo imaging of germinal centres reveals a dynamic open structure*. Nature, 2007. **446**: p. 83.
54. Allen, C.D.C., et al., *Imaging of Germinal Center Selection Events During Affinity Maturation*. Science, 2007. **315**(5811): p. 528.
55. Naito, Y., et al., *Germinal Center Marker GL7 Probes Activation-Dependent Repression of N-Glycolylneuraminic Acid, a Sialic Acid Species Involved in the Negative Modulation of B-Cell Activation*. Molecular and Cellular Biology, 2007. **27**(8): p. 3008-3022.
56. Rose, M.L., et al., *Peanut lectin binding properties of germinal centers of mouse lymphoid tissue*. Nature, 1980. **284**: p. 364.
57. Oliver, A.M., F. Martin, and J.F. Kearney, *Mouse CD38 is down-regulated on germinal center B cells and mature plasma cells*. The Journal of Immunology, 1997. **158**(3): p. 1108.
58. Klein, U. and R. Dalla-Favera, *Germinal centres: role in B-cell physiology and malignancy*. Nature Reviews Immunology, 2008. **8**: p. 22.
59. Basso, K. and R. Dalla-Favera, *Chapter 7 - BCL6: Master Regulator of the Germinal Center Reaction and Key Oncogene in B Cell Lymphomagenesis*, in *Advances in Immunology*, F.W. Alt, Editor. 2010, Academic Press. p. 193-210.
60. Muramatsu, M., et al., *Class Switch Recombination and Hypermutation Require Activation-Induced Cytidine Deaminase (AID), a Potential RNA Editing Enzyme*. Cell, 2000. **102**(5): p. 553-563.
61. Dent, A.L., et al., *Control of Inflammation, Cytokine Expression, and Germinal Center Formation by BCL-6*. Science, 1997. **276**(5312): p. 589.
62. Shaffer, A.L., et al., *BCL-6 Represses Genes that Function in Lymphocyte Differentiation, Inflammation, and Cell Cycle Control*. Immunity, 2000. **13**(2): p. 199-212.
63. Saito, M., et al., *BCL6 suppression of BCL2 via Miz1 and its disruption in diffuse large B cell lymphoma*. Proceedings of the National Academy of Sciences of the United States of America, 2009. **106**(27): p. 11294-11299.
64. Phan, R.T. and R. Dalla-Favera, *The BCL6 proto-oncogene suppresses p53 expression in germinal-centre B cells*. Nature, 2004. **432**: p. 635.
65. Ranuncolo, S.M., et al., *Bcl-6 mediates the germinal center B cell phenotype and lymphomagenesis through transcriptional repression of the DNA-damage sensor ATR*. Nature Immunology, 2007. **8**: p. 705.
66. Park, S.-R., *Activation-induced Cytidine Deaminase in B Cell Immunity and Cancers*. Immune Network, 2012. **12**(6): p. 230-239.
67. Allen, C.D.C. and J.G. Cyster, *Follicular dendritic cell networks of primary follicles and germinal centers: phenotype and function*. Seminars in immunology, 2008. **20**(1): p. 14-25.
68. Barrington, R.A., et al., *B Lymphocyte Memory: Role of Stromal Cell Complement and FcγRIIB Receptors*. The Journal of Experimental Medicine, 2002. **196**(9): p. 1189-1200.

69. Suzuki, K., et al., *The Sensing of Environmental Stimuli by Follicular Dendritic Cells Promotes Immunoglobulin A Generation in the Gut*. Immunity, 2010. **33**(1): p. 71-83.
70. Nishikawa, Y., et al., *Establishment of Lymphotoxin β Receptor Signaling-Dependent Cell Lines with Follicular Dendritic Cell Phenotypes from Mouse Lymph Nodes*. The Journal of Immunology, 2006. **177**(8): p. 5204.
71. Wu, Y., et al., *IL-6 produced by immune complex-activated follicular dendritic cells promotes germinal center reactions, IgG responses and somatic hypermutation*. International Immunology, 2009. **21**(6): p. 745-756.
72. Ziv, I., et al., *A Perturbed Ubiquitin Landscape Distinguishes Between Ubiquitin in Trafficking and in Proteolysis*. Molecular & Cellular Proteomics : MCP, 2011. **10**(5): p. M111.009753.
73. Hu, J., C. Havenar-Daughton, and S. Crotty, *Modulation of SAP dependent T:B cell interactions as a strategy to improve vaccination*. Current opinion in virology, 2013. **3**(3): p. 363-370.
74. Nurieva, R.I., et al., *Bcl6 Mediates the Development of T Follicular Helper Cells*. Science (New York, N.Y.), 2009. **325**(5943): p. 1001-1005.
75. Kim, S.J., et al., *Tolerogenic function of Blimp-1 in dendritic cells*. The Journal of Experimental Medicine, 2011. **208**(11): p. 2193-2199.
76. Zotos, D., et al., *IL-21 regulates germinal center B cell differentiation and proliferation through a B cell-intrinsic mechanism*. J Exp Med, 2010. **207**(2): p. 365-78.
77. Linterman, M.A., et al., *IL-21 acts directly on B cells to regulate Bcl-6 expression and germinal center responses*. The Journal of Experimental Medicine, 2010. **207**(2): p. 353-363.
78. King, I.L. and M. Mohrs, *IL-4–producing CD4(+) T cells in reactive lymph nodes during helminth infection are T follicular helper cells*. The Journal of Experimental Medicine, 2009. **206**(5): p. 1001-1007.
79. Kuhn, R., K. Rajewsky, and W. Muller, *Generation and analysis of interleukin-4 deficient mice*. Science, 1991. **254**(5032): p. 707.
80. Fairfax, K.C., et al., *IL-4-Secreting secondary Tfh cells arise from memory T cells, not persisting Tfh cells, through a B cell dependent mechanism*. Journal of immunology (Baltimore, Md. : 1950), 2015. **194**(7): p. 2999-3010.
81. Weinstein, J.S., et al., *Follicular helper T cells progressively differentiate to regulate the germinal center response*. Nature immunology, 2016. **17**(10): p. 1197-1205.
82. Linterman, M.A., et al., *Foxp3(+) follicular regulatory T cells control T follicular helper cells and the germinal center response*. Nature medicine, 2011. **17**(8): p. 975-982.
83. Chung, Y., et al., *Follicular regulatory T (Tfr) cells with dual Foxp3 and Bcl6 expression suppress germinal center reactions*. Nature medicine, 2011. **17**(8): p. 983-988.
84. Calado, D.P., et al., *The cell-cycle regulator c-Myc is essential for the formation and maintenance of germinal centers*. Nat Immunol, 2012. **13**(11): p. 1092-100.

85. Baumann, I., et al., *Impaired uptake of apoptotic cells into tingible body macrophages in germinal centers of patients with systemic lupus erythematosus*. Arthritis & Rheumatism, 2002. **46**(1): p. 191-201.
86. Lindquist, R.L., et al., *Visualizing dendritic cell networks in vivo*. Nature Immunology, 2004. **5**: p. 1243.
87. Godfrey, D.I., et al., *NKT cells: what's in a name?* Nature Reviews Immunology, 2004. **4**: p. 231.
88. King, I.L., et al., *Invariant natural killer T cells direct B cell responses to cognate lipid antigen in an IL-21-dependent manner*. Nature Immunology, 2011. **13**: p. 44.
89. Chang, P.-P., et al., *Identification of Bcl-6-dependent follicular helper NKT cells that provide cognate help for B cell responses*. Nature Immunology, 2011. **13**: p. 35.
90. Bachmaier, K., et al., *Negative regulation of lymphocyte activation and autoimmunity by the molecular adaptor Cbl-b*. Nature, 2000. **403**(6766): p. 211-6.
91. Gitlin, A.D., Z. Shulman, and M.C. Nussenzweig, *Clonal selection in the germinal centre by regulated proliferation and hypermutation*. Nature, 2014. **509**(7502): p. 637-40.
92. Schneider, C., L. Pasqualucci, and R. Dalla-Favera, *Molecular Pathogenesis of Diffuse Large B-cell Lymphoma*. Seminars in diagnostic pathology, 2011. **28**(2): p. 167-177.
93. De Silva, N.S. and U. Klein, *Dynamics of B cells in germinal centres*. Nature reviews. Immunology, 2015. **15**(3): p. 137-148.
94. Victora, G.D. and M.C. Nussenzweig, *Germinal Centers*. Annual Review of Immunology, 2012. **30**(1): p. 429-457.
95. Pedros, C., et al., *A TRAF-like motif of ICOS controls development of germinal center T follicular helper cells via TBK1*. Nature immunology, 2016. **17**(7): p. 825-833.
96. Weber, J.P., et al., *ICOS maintains the T follicular helper cell phenotype by down-regulating Kruppel-like factor 2*. J Exp Med, 2015. **212**(2): p. 217-33.
97. Crotty, S., *T follicular helper cell differentiation, function, and roles in disease*. Immunity, 2014. **41**(4): p. 529-542.
98. Taylor, J.J., K.A. Pape, and M.K. Jenkins, *A germinal center-independent pathway generates unswitched memory B cells early in the primary response*. J Exp Med, 2012. **209**(3): p. 597-606.
99. Schwickert, T.A., et al., *A dynamic T cell–limited checkpoint regulates affinity-dependent B cell entry into the germinal center*. The Journal of Experimental Medicine, 2011. **208**(6): p. 1243-1252.
100. Choi, Y.S., et al., *ICOS receptor instructs T follicular helper cell versus effector cell differentiation via induction of the transcriptional repressor Bcl6*. Immunity, 2011. **34**(6): p. 932-46.
101. Kerfoot, S.M., et al., *Germinal center B cell and T follicular helper cell development initiates in the interfollicular zone*. Immunity, 2011. **34**(6): p. 947-60.

102. Kitano, M., et al., *Bcl6 protein expression shapes pre-germinal center B cell dynamics and follicular helper T cell heterogeneity*. Immunity, 2011. **34**(6): p. 961-72.
103. Pape, K.A., et al., *The humoral immune response is initiated in lymph nodes by B cells that acquire soluble antigen directly in the follicles*. Immunity, 2007. **26**(4): p. 491-502.
104. Heesters, B.A., et al., *Antigen Presentation to B Cells*. Trends in Immunology, 2016. **37**(12): p. 844-854.
105. Gonzalez, S.F., et al., *Capture of influenza by medullary dendritic cells via SIGN-R1 is essential for humoral immunity in draining lymph nodes*. Nature immunology, 2010. **11**(5): p. 427-434.
106. Carrasco, Y.R. and F.D. Batista, *B Cells Acquire Particulate Antigen in a Macrophage-Rich Area at the Boundary between the Follicle and the Subcapsular Sinus of the Lymph Node*. Immunity, 2007. **27**(1): p. 160-171.
107. Junt, T., et al., *Subcapsular sinus macrophages in lymph nodes clear lymph-borne viruses and present them to antiviral B cells*. Nature, 2007. **450**: p. 110.
108. Wykes, M., et al., *Dendritic cells interact directly with naive B lymphocytes to transfer antigen and initiate class switching in a primary T-dependent response*. J Immunol, 1998. **161**(3): p. 1313-9.
109. Colino, J., Y. Shen, and C.M. Snapper, *Dendritic cells pulsed with intact Streptococcus pneumoniae elicit both protein- and polysaccharide-specific immunoglobulin isotype responses in vivo through distinct mechanisms*. J Exp Med, 2002. **195**(1): p. 1-13.
110. Woodruff, M.C., et al., *Trans-nodal migration of resident dendritic cells into medullary interfollicular regions initiates immunity to influenza vaccine*. The Journal of Experimental Medicine, 2014. **211**(8): p. 1611-1621.
111. Qi, H., et al., *Extrafollicular activation of lymph node B cells by antigen-bearing dendritic cells*. Science, 2006. **312**(5780): p. 1672-6.
112. Reif, K., et al., *Balanced responsiveness to chemoattractants from adjacent zones determines B-cell position*. Nature, 2002. **416**(6876): p. 94-9.
113. Pereira, J.P., et al., *EBI2 mediates B cell segregation between the outer and centre follicle*. Nature, 2009. **460**(7259): p. 1122-6.
114. Bannard, O., et al., *Ubiquitin-mediated fluctuations in MHC class II facilitate efficient germinal center B cell responses*. The Journal of Experimental Medicine, 2016. **213**(6): p. 993-1009.
115. Wagle, N.M., et al., *B-lymphocyte signaling receptors and the control of class-II antigen processing*. Curr Top Microbiol Immunol, 2000. **245**(2): p. 101-26.
116. Carrasco, Y.R., et al., *LFA-1/ICAM-1 interaction lowers the threshold of B cell activation by facilitating B cell adhesion and synapse formation*. Immunity, 2004. **20**(5): p. 589-99.
117. Treanor, B., et al., *Dynamic cortical actin remodeling by ERM proteins controls BCR microcluster organization and integrity*. J Exp Med, 2011. **208**(5): p. 1055-68.

118. Schnyder, T., et al., *B cell receptor-mediated antigen gathering requires ubiquitin ligase Cbl and adaptors Grb2 and Dok-3 to recruit dynein to the signaling microcluster*. Immunity, 2011. **34**(6): p. 905-18.
119. Freeman, S.A., et al., *Cofilin-mediated F-actin severing is regulated by the Rap GTPase and controls the cytoskeletal dynamics that drive lymphocyte spreading and BCR microcluster formation*. J Immunol, 2011. **187**(11): p. 5887-900.
120. Katkere, B., S. Rosa, and J.R. Drake, *The Syk-binding Ubiquitin Ligase c-Cbl Mediates Signaling-dependent B Cell Receptor Ubiquitination and B Cell Receptor-mediated Antigen Processing and Presentation*. The Journal of Biological Chemistry, 2012. **287**(20): p. 16636-16644.
121. Katkere, B., S. Rosa, and J.R. Drake, *The Syk-binding ubiquitin ligase c-Cbl mediates signaling-dependent B cell receptor ubiquitination and B cell receptor-mediated antigen processing and presentation*. J Biol Chem, 2012. **287**(20): p. 16636-44.
122. Zhang, M., et al., *Ubiquitinylation of Ig beta dictates the endocytic fate of the B cell antigen receptor*. J Immunol, 2007. **179**(7): p. 4435-43.
123. Stoddart, A., et al., *Lipid rafts unite signaling cascades with clathrin to regulate BCR internalization*. Immunity, 2002. **17**(4): p. 451-62.
124. Chaturvedi, A., et al., *Endocytosed BCRs sequentially regulate MAPK and Akt signaling pathways from intracellular compartments*. Nat Immunol, 2011. **12**(11): p. 1119-26.
125. Song, W., C. Liu, and A. Upadhyaya, *The pivotal position of the actin cytoskeleton in the initiation and regulation of B cell receptor activation()*. Biochimica et biophysica acta, 2014. **1838**(2): p. 10.1016/j.bbamem.2013.07.016.
126. Baumjohann, D., T. Okada, and K.M. Ansel, *Cutting Edge: Distinct waves of BCL6 expression during T follicular helper cell development*. J Immunol, 2011. **187**(5): p. 2089-92.
127. Recaldin, T. and D.J. Fear, *Transcription factors regulating B cell fate in the germinal centre*. Clinical and Experimental Immunology, 2016. **183**(1): p. 65-75.
128. Bollig, N., et al., *Transcription factor IRF4 determines germinal center formation through follicular T-helper cell differentiation*. Proc Natl Acad Sci U S A, 2012. **109**(22): p. 8664-9.
129. Iwata, A., et al., *Quality of TCR signaling encoded by differential enhancer affinities for the composite BATF-IRF4 transcription factor complex*. Nature immunology, 2017. **18**(5): p. 563-572.
130. Krishnamoorthy, V., et al., *The IRF4 Gene Regulatory Module Functions as a Read-Write Integrator to Dynamically Coordinate T Helper Cell Fate*. Immunity, 2017. **47**(3): p. 481-497.e7.
131. Ochiai, K., et al., *Transcriptional regulation of germinal center B and plasma cell fates by dynamical control of IRF4*. Immunity, 2013. **38**(5): p. 918-29.
132. Klein, U., et al., *Transcription factor IRF4 controls plasma cell differentiation and class-switch recombination*. Nat Immunol, 2006. **7**(7): p. 773-82.
133. Singh, H., et al., *The molecular choreography of IRF4 and IRF8 with immune system partners*. Cold Spring Harb Symp Quant Biol, 2013. **78**: p. 101-4.

134. Xu, H., et al., *Regulation of bifurcating B cell trajectories by mutual antagonism between transcription factors IRF4 and IRF8*. Nat Immunol, 2015. **16**(12): p. 1274-81.
135. Strasser, A., P.J. Jost, and S. Nagata, *The many roles of FAS receptor signaling in the immune system*. Immunity, 2009. **30**(2): p. 180-92.
136. Takahashi, Y., et al., *Relaxed negative selection in germinal centers and impaired affinity maturation in bcl-xL transgenic mice*. J Exp Med, 1999. **190**(3): p. 399-410.
137. Fischer, S.F., et al., *Proapoptotic BH3-only protein Bim is essential for developmentally programmed death of germinal center-derived memory B cells and antibody-forming cells*. Blood, 2007. **110**(12): p. 3978-84.
138. Smith, K.G., et al., *Bcl-2 increases memory B cell recruitment but does not perturb selection in germinal centers*. Immunity, 1994. **1**(9): p. 803-13.
139. Vikstrom, I., et al., *Mcl-1 is essential for germinal center formation and B cell memory*. Science, 2010. **330**(6007): p. 1095-9.
140. Hennino, A., et al., *Flice-Inhibitory Protein Is a Key Regulator of Germinal Center B Cell Apoptosis*. The Journal of Experimental Medicine, 2001. **193**(4): p. 447.
141. Tuscano, J.M., et al., *Bcl-x rather than Bcl-2 mediates CD40-dependent centrocyte survival in the germinal center*. Blood, 1996. **88**(4): p. 1359.
142. Yoon, S.-O., et al., *CD9 may contribute to the survival of human germinal center B cells by facilitating the interaction with follicular dendritic cells*. FEBS Open Bio, 2014. **4**: p. 370-376.
143. Hauser, A.E., et al., *Definition of Germinal-Center B Cell Migration In Vivo Reveals Predominant Intrazonal Circulation Patterns*. Immunity, 2007. **26**(5): p. 655-667.
144. Schwickert, T.A., et al., *In vivo imaging of germinal centres reveals a dynamic open structure*. Nature, 2007. **446**(7131): p. 83-7.
145. Dominguez-Sola, D., et al., *The proto-oncogene MYC is required for selection in the germinal center and cyclic reentry*. Nat Immunol, 2012. **13**(11): p. 1083-91.
146. Chou, C., et al., *The Transcription Factor AP4 Mediates Resolution of Chronic Viral Infection through Amplification of Germinal Center B Cell Responses*. Immunity, 2016. **45**(3): p. 570-582.
147. Sander, S., et al., *PI3 Kinase and FOXO1 Transcription Factor Activity Differentially Control B Cells in the Germinal Center Light and Dark Zones*. Immunity, 2015. **43**(6): p. 1075-86.
148. Dominguez-Sola, D., et al., *The FOXO1 Transcription Factor Instructs the Germinal Center Dark Zone Program*. Immunity, 2015. **43**(6): p. 1064-74.
149. Nie, Y., et al., *The Role of CXCR4 in Maintaining Peripheral B Cell Compartments and Humoral Immunity*. The Journal of Experimental Medicine, 2004. **200**(9): p. 1145-1156.
150. Bannard, O., et al., *Germinal Center Centroblasts Transition to a Centrocyte Phenotype According to a Timed Program and Depend on the Dark Zone for Effective Selection*. Immunity. **39**(5): p. 912-924.

151. Inoue, T., et al., *The transcription factor Foxo1 controls germinal center B cell proliferation in response to T cell help*. The Journal of Experimental Medicine, 2017.
152. Livet, J., et al., *Transgenic strategies for combinatorial expression of fluorescent proteins in the nervous system*. Nature, 2007. **450**: p. 56.
153. Tas, J.M.J., et al., *Visualizing antibody affinity maturation in germinal centers*. Science, 2016.
154. Kuraoka, M., et al., *Complex Antigens Drive Permissive Clonal Selection in Germinal Centers*. Immunity, 2016. **44**(3): p. 542-552.
155. Shinnakasu, R., et al., *Regulated selection of germinal-center cells into the memory B cell compartment*. Nature Immunology, 2016. **17**: p. 861.
156. Weisel, F.J., et al., *A Temporal Switch in the Germinal Center Determines Differential Output of Memory B and Plasma Cells*. Immunity, 2016. **44**(1): p. 116-130.
157. Gitlin, A.D., et al., *Independent Roles of Switching and Hypermutation in the Development and Persistence of B Lymphocyte Memory*. Immunity, 2016. **44**(4): p. 769-81.
158. Pape, K.A., et al., *Different B cell populations mediate early and late memory during an endogenous immune response*. Science (New York, N.Y.), 2011. **331**(6021): p. 1203-1207.
159. Dogan, I., et al., *Multiple layers of B cell memory with different effector functions*. Nature Immunology, 2009. **10**: p. 1292.
160. Sciammas, R., et al., *Graded expression of interferon regulatory factor-4 coordinates isotype switching with plasma cell differentiation*. Immunity, 2006. **25**(2): p. 225-36.
161. Ise, W., et al., *The transcription factor BATF controls the global regulators of class-switch recombination in both B cells and T cells*. Nat Immunol, 2011. **12**(6): p. 536-43.
162. Chevrier, S., et al., *The BTB-ZF transcription factor Zbtb20 is driven by Irf4 to promote plasma cell differentiation and longevity*. J Exp Med, 2014. **211**(5): p. 827-40.
163. Kallies, A., et al., *Initiation of plasma-cell differentiation is independent of the transcription factor Blimp-1*. Immunity, 2007. **26**(5): p. 555-66.
164. Tellier, J., et al., *Blimp-1 controls plasma cell function through regulation of immunoglobulin secretion and the unfolded protein response*. Nature immunology, 2016. **17**(3): p. 323-330.
165. Caganova, M., et al., *Germinal center dysregulation by histone methyltransferase EZH2 promotes lymphomagenesis*. The Journal of Clinical Investigation, 2013. **123**(12): p. 5009-5022.
166. Beguelin, W., et al., *EZH2 is required for germinal center formation and somatic EZH2 mutations promote lymphoid transformation*. Cancer Cell, 2013. **23**(5): p. 677-92.

167. Good-Jacobson, K.L., et al., *Regulation of germinal center responses and B-cell memory by the chromatin modifier MOZ*. Proc Natl Acad Sci U S A, 2014. **111**(26): p. 9585-90.
168. Heise, N., et al., *Germinal center B cell maintenance and differentiation are controlled by distinct NF-kappaB transcription factor subunits*. J Exp Med, 2014. **211**(10): p. 2103-18.
169. Angelin-Duclos, C., et al., *Commitment of B lymphocytes to a plasma cell fate is associated with Blimp-1 expression in vivo*. J Immunol, 2000. **165**(10): p. 5462-71.
170. Falini, B., et al., *A monoclonal antibody (MUM1p) detects expression of the MUM1/IRF4 protein in a subset of germinal center B cells, plasma cells, and activated T cells*. Blood, 2000. **95**(6): p. 2084-92.
171. Meyer-Hermann, M., et al., *A theory of germinal center B cell selection, division, and exit*. Cell Rep, 2012. **2**(1): p. 162-74.
172. Krautler, N.J., et al., *Differentiation of germinal center B cells into plasma cells is initiated by high-affinity antigen and completed by Tfh cells*. J Exp Med, 2017. **214**(5): p. 1259-1267.
173. Saito, M., et al., *A signaling pathway mediating downregulation of BCL6 in germinal center B cells is blocked by BCL6 gene alterations in B cell lymphoma*. Cancer Cell, 2007. **12**(3): p. 280-92.
174. Wilkinson, K.D., *The discovery of ubiquitin-dependent proteolysis*. Proceedings of the National Academy of Sciences, 2005. **102**(43): p. 15280.
175. Callis, J., *The Ubiquitination Machinery of the Ubiquitin System*. The Arabidopsis Book / American Society of Plant Biologists, 2014. **12**: p. e0174.
176. Deshaies, R.J. and C.A.P. Joazeiro, *RING Domain E3 Ubiquitin Ligases*. Annual Review of Biochemistry, 2009. **78**(1): p. 399-434.
177. Markson, G., et al., *Analysis of the human E2 ubiquitin conjugating enzyme protein interaction network*. Genome Research, 2009. **19**(10): p. 1905-1911.
178. Dikic, I., S. Wakatsuki, and K.J. Walters, *Ubiquitin-binding domains — from structures to functions*. Nature Reviews Molecular Cell Biology, 2009. **10**: p. 659.
179. Wagner, S.A., et al., *A Proteome-wide, Quantitative Survey of In Vivo Ubiquitylation Sites Reveals Widespread Regulatory Roles*. Molecular & Cellular Proteomics : MCP, 2011. **10**(10): p. M111.013284.
180. Xu, P., et al., *Quantitative Proteomics Reveals the Function of Unconventional Ubiquitin Chains in Proteasomal Degradation*. Cell, 2009. **137**(1): p. 133-145.
181. Hershko, A. and A. Ciechanover, *The Ubiquitin System*. Annual Review of Biochemistry, 1998. **67**(1): p. 425-479.
182. Chen, Z.J. and L.J. Sun, *Nonproteolytic Functions of Ubiquitin in Cell Signaling*. Molecular Cell, 2009. **33**(3): p. 275-286.
183. Elia, A.E.H., et al., *Quantitative Proteomic Atlas of Ubiquitination and Acetylation in the DNA Damage Response*. Molecular cell, 2015. **59**(5): p. 867-881.
184. Wickliffe, K.E., et al., *K11-linked ubiquitin chains as novel regulators of cell division*. Trends in cell biology, 2011. **21**(11): p. 656-663.

185. Kristariyanto, Yosua A., et al., *K29-Selective Ubiquitin Binding Domain Reveals Structural Basis of Specificity and Heterotypic Nature of K29 Polyubiquitin*. Molecular Cell, 2015. **58**(1): p. 83-94.
186. Yuan, W.-C., et al., *K33-Linked Polyubiquitination of Coronin 7 by Cul3-KLHL20 Ubiquitin E3 Ligase Regulates Protein Trafficking*. Molecular Cell, 2014. **54**(4): p. 586-600.
187. Morreale, F.E. and H. Walden, *Types of Ubiquitin Ligases*. Cell, 2016. **165**(1): p. 248-248.e1.
188. Langdon, W.Y., et al., *v-cbl, an oncogene from a dual-recombinant murine retrovirus that induces early B-lineage lymphomas*. Proc Natl Acad Sci U S A, 1989. **86**(4): p. 1168-72.
189. Blake, T.J., K.G. Heath, and W.Y. Langdon, *The truncation that generated the v-cbl oncogene reveals an ability for nuclear transport, DNA binding and acute transformation*. Embo j, 1993. **12**(5): p. 2017-26.
190. Keane, M.M., et al., *cbl-3: a new mammalian cbl family protein*. Oncogene, 1999. **18**: p. 3365.
191. Kim, M., et al., *Molecular cloning and characterization of a novel cbl-family gene, cbl-c*. Gene, 1999. **239**(1): p. 145-54.
192. Galisteo, M.L., et al., *Tyrosine phosphorylation of the c-cbl proto-oncogene protein product and association with epidermal growth factor (EGF) receptor upon EGF stimulation*. J Biol Chem, 1995. **270**(35): p. 20242-5.
193. Lupher, M.L., et al., *A Novel Phosphotyrosine-binding Domain in the N-terminal Transforming Region of Cbl Interacts Directly and Selectively with ZAP-70 in T Cells*. Journal of Biological Chemistry, 1996. **271**(39): p. 24063-24068.
194. Bonita, D.P., et al., *Phosphotyrosine binding domain-dependent upregulation of the platelet-derived growth factor receptor alpha signaling cascade by transforming mutants of Cbl: implications for Cbl's function and oncogenicity*. Mol Cell Biol, 1997. **17**(8): p. 4597-610.
195. Thien, C.B.F. and W.Y. Langdon, *EGF receptor binding and transformation by v-cbl is ablated by the introduction of a loss-of-function mutation from the Caenorhabditis elegans sli-1 gene*. Oncogene, 1997. **14**: p. 2239.
196. Miura-Shimura, Y., et al., *Cbl-mediated ubiquitinylation and negative regulation of Vav*. J Biol Chem, 2003. **278**(40): p. 38495-504.
197. Hunter, S., B.L. Koch, and S.M. Anderson, *Phosphorylation of cbl after stimulation of Nb2 cells with prolactin and its association with phosphatidylinositol 3-kinase*. Mol Endocrinol, 1997. **11**(9): p. 1213-22.
198. Sawasdikosol, S., et al., *Tyrosine-phosphorylated Cbl binds to Crk after T cell activation*. J Immunol, 1996. **157**(1): p. 110-6.
199. Peschard, P., et al., *Structural basis for ubiquitin-mediated dimerization and activation of the ubiquitin protein ligase Cbl-b*. Mol Cell, 2007. **27**(3): p. 474-85.
200. Klein, L., et al., *Positive and negative selection of the T cell repertoire: what thymocytes see (and don't see)*. Nature Reviews Immunology, 2014. **14**: p. 377.

201. Nelson, Ryan W., et al., *T Cell Receptor Cross-Reactivity between Similar Foreign and Self Peptides Influences Naive Cell Population Size and Autoimmunity*. Immunity, 2015. **42**(1): p. 95-107.
202. Naramura, M., et al., *Altered thymic positive selection and intracellular signals in Cbl-deficient mice*. Proc Natl Acad Sci U S A, 1998. **95**(26): p. 15547-52.
203. Murphy, M.A., et al., *Tissue Hyperplasia and Enhanced T-Cell Signalling via ZAP-70 in c-Cbl-Deficient Mice*. Molecular and Cellular Biology, 1998. **18**(8): p. 4872-4882.
204. Bour-Jordan, H., et al., *Intrinsic and extrinsic control of peripheral T-cell tolerance by costimulatory molecules of the CD28/ B7 family*. Immunol Rev, 2011. **241**(1): p. 180-205.
205. Chiang, Y.J., et al., *Cbl-b regulates the CD28 dependence of T-cell activation*. Nature, 2000. **403**(6766): p. 216-20.
206. Fang, D. and Y.C. Liu, *Proteolysis-independent regulation of PI3K by Cbl-b-mediated ubiquitination in T cells*. Nat Immunol, 2001. **2**(9): p. 870-5.
207. Guo, H., et al., *E3 Ubiquitin Ligase Cbl-b Regulates Pten via Nedd4 in T Cells Independently of Its Ubiquitin Ligase Activity*. Cell Reports. **1**(5): p. 472-482.
208. Loeser, S., et al., *Spontaneous tumor rejection by cbl-b-deficient CD8+ T cells*. J Exp Med, 2007. **204**(4): p. 879-91.
209. Chiang, J.Y., et al., *Ablation of Cbl-b provides protection against transplanted and spontaneous tumors*. Journal of Clinical Investigation, 2007. **117**(4): p. 1029-1036.
210. Gruber, T., et al., *Cbl-b mediates TGFbeta sensitivity by downregulating inhibitory SMAD7 in primary T cells*. J Mol Cell Biol, 2013. **5**(6): p. 358-68.
211. Liechtenstein, T., et al., *PD-L1/PD-1 Co-Stimulation, a Brake for T cell Activation and a T cell Differentiation Signal*. Journal of clinical & cellular immunology, 2012. **Suppl 12**: p. 006.
212. Li, D., et al., *Cutting edge: Cbl-b: one of the key molecules tuning CD28- and CTLA-4-mediated T cell costimulation*. J Immunol, 2004. **173**(12): p. 7135-9.
213. Yasuda, T., et al., *Cbl Suppresses B Cell Receptor–Mediated Phospholipase C (Plc)-γ2 Activation by Regulating B Cell Linker Protein–Plc-γ2 Binding*. The Journal of Experimental Medicine, 2000. **191**(4): p. 641-650.
214. Shao, Y., et al., *Differential regulation of the B cell receptor-mediated signaling by the E3 ubiquitin ligase Cbl*. J Biol Chem, 2004. **279**(42): p. 43646-53.
215. Kitaura, Y., et al., *Control of the B Cell-Intrinsic Tolerance Program by c-Cbl and Cbl-b*. Immunity, 2007. **26**(5): p. 567-578.
216. Paolino, M., et al., *The E3 ligase Cbl-b and TAM receptors regulate cancer metastasis via natural killer cells*. Nature, 2014. **507**(7493): p. 508-12.
217. Kim, H.S., et al., *Synergistic signals for natural cytotoxicity are required to overcome inhibition by c-Cbl ubiquitin ligase*. Immunity, 2010. **32**(2): p. 175-86.
218. Kim, H.S. and E.O. Long, *Complementary phosphorylation sites in the adaptor protein SLP-76 promote synergistic activation of natural killer cells*. Sci Signal, 2012. **5**(232): p. ra49.

219. Chiou, S.H., et al., *The E3 ligase c-Cbl regulates dendritic cell activation*. EMBO Rep, 2011. **12**(9): p. 971-9.
220. Wallner, S., et al., *The role of the e3 ligase cbl-B in murine dendritic cells*. PLoS One, 2013. **8**(6): p. e65178.
221. Han, C., et al., *Integrin CD11b negatively regulates TLR-triggered inflammatory responses by activating Syk and promoting degradation of MyD88 and TRIF via Cbl-b*. Nat Immunol, 2010. **11**(8): p. 734-42.
222. Abe, T., et al., *Cbl-b is a critical regulator of macrophage activation associated with obesity-induced insulin resistance in mice*. Diabetes, 2013. **62**(6): p. 1957-69.
223. Hirasaka, K., et al., *Deficiency of Cbl-b gene enhances infiltration and activation of macrophages in adipose tissue and causes peripheral insulin resistance in mice*. Diabetes, 2007. **56**(10): p. 2511-22.
224. Kabak, S., et al., *The Direct Recruitment of BLNK to Immunoglobulin α Couples the B-Cell Antigen Receptor to Distal Signaling Pathways*. Molecular and Cellular Biology, 2002. **22**(8): p. 2524-2535.
225. Herzog, S., et al., *SLP-65 regulates immunoglobulin light chain gene recombination through the PI(3)K-PKB-Foxo pathway*. Nature Immunology, 2008. **9**: p. 623.
226. Kurosaki, T., H. Shinohara, and Y. Baba, *B Cell Signaling and Fate Decision*. Annual Review of Immunology, 2010. **28**(1): p. 21-55.
227. Raiborg, C. and H. Stenmark, *The ESCRT machinery in endosomal sorting of ubiquitylated membrane proteins*. Nature, 2009. **458**: p. 445.
228. Zhang, M., et al., *Ubiquitinylation of Igβ Dictates the Endocytic Fate of the B Cell Antigen Receptor*. The Journal of Immunology, 2007. **179**(7): p. 4435-4443.
229. Veselits, M., et al., *Recruitment of Cbl-b to B Cell Antigen Receptor Couples Antigen Recognition to Toll-Like Receptor 9 Activation in Late Endosomes*. PLOS ONE, 2014. **9**(3): p. e89792.
230. Gazumyan, A., A. Reichlin, and M.C. Nussenzweig, *Igβ tyrosine residues contribute to the control of B cell receptor signaling by regulating receptor internalization*. The Journal of Experimental Medicine, 2006. **203**(7): p. 1785-1794.
231. Kraus, M., et al., *Interference with Immunoglobulin (Ig)α Immunoreceptor Tyrosine–Based Activation Motif (Itam) Phosphorylation Modulates or Blocks B Cell Development, Depending on the Availability of an Igβ Cytoplasmic Tail*. The Journal of Experimental Medicine, 2001. **194**(4): p. 455-470.
232. Thien, Christine B F. and Wallace Y. Langdon, *c-Cbl and Cbl-b ubiquitin ligases: substrate diversity and the negative regulation of signalling responses*. Biochemical Journal, 2005. **391**(Pt 2): p. 153-166.
233. Madisen, L., et al., *A robust and high-throughput Cre reporting and characterization system for the whole mouse brain*. Nature Neuroscience, 2009. **13**: p. 133.

234. Jang, I.K., et al., *Growth-factor receptor-bound protein-2 (Grb2) signaling in B cells controls lymphoid follicle organization and germinal center reaction*. Proc Natl Acad Sci U S A, 2011. **108**(19): p. 7926-31.
235. Roozendaal, R. and M.C. Carroll, *Complement receptors CD21 and CD35 in humoral immunity*. Immunological Reviews, 2007. **219**(1): p. 157-166.
236. Randall, K.L., et al., *Dock8 mutations cripple B cell immunological synapses, germinal centers and long-lived antibody production*. Nature Immunology, 2009. **10**: p. 1283.
237. Liu, D., et al., *T–B-cell entanglement and ICOSL-driven feed-forward regulation of germinal centre reaction*. Nature, 2014. **517**: p. 214.
238. Wong, E.B., et al., *B cell-intrinsic CD84 and Ly108 maintain germinal center B cell tolerance*. Journal of immunology (Baltimore, Md. : 1950), 2015. **194**(9): p. 4130-4143.
239. Nowosad, C.R., K.M. Spillane, and P. Tolar, *Germinal center B cells recognize antigen through a specialized immune synapse architecture*. Nat Immunol, 2016. **17**(7): p. 870-7.
240. Lu, R., et al., *Tracking single hematopoietic stem cells in vivo using high-throughput sequencing in conjunction with viral genetic barcoding*. Nature biotechnology, 2011. **29**(10): p. 928-933.
241. Clark, M.R., et al., *Orchestrating B cell lymphopoiesis through interplay of IL-7 receptor and pre-B cell receptor signalling*. Nature reviews. Immunology, 2014. **14**(2): p. 69-80.
242. Sugden, S., F. Ghazawi, and P. MacPherson, *HIV-1 tat protein recruits CIS to the cytoplasmic tail of CD127 to induce receptor ubiquitination and proteasomal degradation*. Virology, 2016. **498**: p. 192-200.
243. Blesofsky, W.A., et al., *Regulation of STAT protein synthesis by c-Cbl*. Oncogene, 2001. **20**: p. 7326.
244. Liu, C.-S., et al., *Cbl-mediated K63-linked ubiquitination of JAK2 enhances JAK2 phosphorylation and signal transduction*. Scientific Reports, 2017. **7**(1): p. 4613.
245. Cerutti, A., M. Cols, and I. Puga, *Marginal zone B cells: virtues of innatelike antibody-producing lymphocytes*. Nature reviews. Immunology, 2013. **13**(2): p. 118-132.
246. Moretti, J., et al., *The Ubiquitin-specific Protease 12 (USP12) Is a Negative Regulator of Notch Signaling Acting on Notch Receptor Trafficking toward Degradation*. The Journal of Biological Chemistry, 2012. **287**(35): p. 29429-29441.
247. Jahan, A.S., et al., *Usp12 stabilizes the T-cell receptor complex at the cell surface during signaling*. Proceedings of the National Academy of Sciences of the United States of America, 2016. **113**(6): p. E705-E714.
248. Simonetti, G., et al., *IRF4 controls the positioning of mature B cells in the lymphoid microenvironments by regulating NOTCH2 expression and activity*. The Journal of Experimental Medicine, 2013. **210**(13): p. 2887-2902.
249. Arnon, T.I., et al., *Visualization of splenic marginal zone B-cell shuttling and follicular B-cell egress*. Nature, 2012. **493**: p. 684.

250. Kaabeche, K., et al., *Cbl-mediated ubiquitination of α5 integrin subunit mediates fibronectin-dependent osteoblast detachment and apoptosis induced by FGFR2 activation*. Journal of Cell Science, 2005. **118**(6): p. 1223-1232.
251. Sanjay, A., et al., *Cbl Associates with Pyk2 and Src to Regulate Src Kinase Activity, α_vβ₃ Integrin-Mediated Signaling, Cell Adhesion, and Osteoclast Motility*. The Journal of Cell Biology, 2001. **152**(1): p. 181-196.
252. Hobeika, E., et al., *Testing gene function early in the B cell lineage in mb1-cre mice*. Proc Natl Acad Sci U S A, 2006. **103**(37): p. 13789-94.
253. Oksvold, M.P., et al., *The Cbl-b RING finger domain has a limited role in regulating inflammatory cytokine production by IgE-activated mast cells*. Mol Immunol, 2008. **45**(4): p. 925-36.
254. Vigorito, E., et al., *microRNA-155 regulates the generation of immunoglobulin class-switched plasma cells*. Immunity, 2007. **27**(6): p. 847-59.
255. Rajewsky, K., *Clonal selection and learning in the antibody system*. Nature, 1996. **381**(6585): p. 751-8.
256. Liu, Y.J., et al., *Mechanism of antigen-driven selection in germinal centres*. Nature, 1989. **342**(6252): p. 929-31.
257. Jacob, J., et al., *Intraclonal generation of antibody mutants in germinal centres*. Nature, 1991. **354**(6352): p. 389-92.
258. Allen, C.D., T. Okada, and J.G. Cyster, *Germinal-center organization and cellular dynamics*. Immunity, 2007. **27**(2): p. 190-202.
259. Berek, C., A. Berger, and M. Apel, *Maturation of the immune response in germinal centers*. Cell, 1991. **67**(6): p. 1121-9.
260. Muramatsu, M., et al., *Class switch recombination and hypermutation require activation-induced cytidine deaminase (AID), a potential RNA editing enzyme*. Cell, 2000. **102**(5): p. 553-63.
261. Crotty, S., *Follicular helper CD4 T cells (TFH)*. Annu Rev Immunol, 2011. **29**: p. 621-63.
262. Ramiscal, R.R. and C.G. Vinuesa, *T-cell subsets in the germinal center*. Immunol Rev, 2013. **252**(1): p. 146-55.
263. Shulman, Z., et al., *Dynamic signaling by T follicular helper cells during germinal center B cell selection*. Science, 2014. **345**(6200): p. 1058-62.
264. Shlomchik, M.J. and F. Weisel, *Germinal center selection and the development of memory B and plasma cells*. Immunol Rev, 2012. **247**(1): p. 52-63.
265. Dufaud, C.R., L.J. McHeyzer-Williams, and M.G. McHeyzer-Williams, *Deconstructing the germinal center, one cell at a time*. Curr Opin Immunol, 2017. **45**: p. 112-118.
266. Bannard, O. and J.G. Cyster, *Germinal centers: programmed for affinity maturation and antibody diversification*. Current Opinion in Immunology, 2017. **45**(Supplement C): p. 21-30.
267. Basso, K. and R. Dalla-Favera, *Roles of BCL6 in normal and transformed germinal center B cells*. Immunol Rev, 2012. **247**(1): p. 172-83.

268. Shapiro-Shelef, M., et al., *Blimp-1 is required for the formation of immunoglobulin secreting plasma cells and pre-plasma memory B cells*. Immunity, 2003. **19**(4): p. 607-20.
269. Nutt, S.L., et al., *The generation of antibody-secreting plasma cells*. Nat Rev Immunol, 2015. **15**(3): p. 160-71.
270. Shapiro-Shelef, M. and K. Calame, *Regulation of plasma-cell development*. Nat Rev Immunol, 2005. **5**(3): p. 230-42.
271. Huang, F. and H. Gu, *Negative regulation of lymphocyte development and function by the Cbl family of proteins*. Immunol Rev, 2008. **224**: p. 229-38.
272. Casola, S., et al., *Tracking germinal center B cells expressing germ-line immunoglobulin gamma1 transcripts by conditional gene targeting*. Proc Natl Acad Sci U S A, 2006. **103**(19): p. 7396-401.
273. Victora, G.D., et al., *Germinal center dynamics revealed by multiphoton microscopy with a photoactivatable fluorescent reporter*. Cell, 2010. **143**(4): p. 592-605.
274. Hasbold, J., et al., *Evidence from the generation of immunoglobulin G-secreting cells that stochastic mechanisms regulate lymphocyte differentiation*. Nat Immunol, 2004. **5**(1): p. 55-63.
275. Basso, K. and R. Dalla-Favera, *Germinal centres and B cell lymphomagenesis*. Nature Reviews Immunology, 2015. **15**: p. 172.
276. Khalil, A.M., J.C. Cambier, and M.J. Shlomchik, *B cell receptor signal transduction in the GC is short-circuited by high phosphatase activity*. Science, 2012. **336**(6085): p. 1178-81.
277. Shi, W., et al., *Transcriptional profiling of mouse B cell terminal differentiation defines a signature for antibody-secreting plasma cells*. Nat Immunol, 2015. **16**(6): p. 663-73.
278. Heesters, B.A., R.C. Myers, and M.C. Carroll, *Follicular dendritic cells: dynamic antigen libraries*. Nat Rev Immunol, 2014. **14**(7): p. 495-504.
279. Elgueta, R., et al., *Molecular mechanism and function of CD40/CD40L engagement in the immune system*. Immunol Rev, 2009. **229**(1): p. 152-72.
280. Loeb, G.B., et al., *Transcriptome-wide miR-155 binding map reveals widespread noncanonical microRNA targeting*. Mol Cell, 2012. **48**(5): p. 760-70.
281. Han, Y.C., et al., *microRNA-29a induces aberrant self-renewal capacity in hematopoietic progenitors, biased myeloid development, and acute myeloid leukemia*. J Exp Med, 2010. **207**(3): p. 475-89.
282. Demircik, F., T. Buch, and A. Waisman, *Efficient B cell depletion via diphtheria toxin in CD19-Cre/iDTR mice*. PLoS One, 2013. **8**(3): p. e60643.
283. Morel, L., *Mouse Models of Human Autoimmune Diseases: Essential Tools That Require the Proper Controls*. PLoS Biology, 2004. **2**(8): p. e241.
284. Lassila, O., O. Vainio, and P. Matzinger, *Can B cells turn on virgin T cells?* Nature, 1988. **334**(6179): p. 253-5.
285. Morris, S.C., A. Lees, and F.D. Finkelman, *In vivo activation of naive T cells by antigen-presenting B cells*. J Immunol, 1994. **152**(8): p. 3777-85.

286. Barnett, L.G., et al., *B cell antigen presentation in the initiation of follicular helper T cell and germinal center differentiation*. J Immunol, 2014. **192**(8): p. 3607-17.
287. Goenka, R., et al., *Cutting edge: dendritic cell-restricted antigen presentation initiates the follicular helper T cell program but cannot complete ultimate effector differentiation*. J Immunol, 2011. **187**(3): p. 1091-5.
288. Deenick, E.K., et al., *Follicular helper T cell differentiation requires continuous antigen presentation that is independent of unique B cell signaling*. Immunity, 2010. **33**(2): p. 241-53.
289. Veselits, M., et al., *Igβ ubiquitination activates PI3K signals required for endosomal sorting*. The Journal of Experimental Medicine, 2017. 214(12): p.3775-3790
290. Dörner, T., N. Kinnman, and P.P. Tak, *Targeting B cells in immune-mediated inflammatory disease: A comprehensive review of mechanisms of action and identification of biomarkers*. Pharmacology & Therapeutics, 2010. **125**(3): p. 464-475.
291. Roll, P., et al., *Regeneration of B cell subsets after transient B cell depletion using anti-CD20 antibodies in rheumatoid arthritis*. Arthritis & Rheumatism, 2006. **54**(8): p. 2377-2386.
292. Roll, P., T. Dörner, and H.-P. Tony, *Anti-CD20 therapy in patients with rheumatoid arthritis: Predictors of response and B cell subset regeneration after repeated treatment*. Arthritis & Rheumatism, 2008. **58**(6): p. 1566-1575.
293. Lanzavecchia, A., *Antigen Uptake and Accumulation in Antigen-Specific B Cells*. Immunological Reviews, 1987. **99**(1): p. 39-51.
294. Leadbetter, E.A., et al., *Chromatin–IgG complexes activate B cells by dual engagement of IgM and Toll-like receptors*. Nature, 2002. **416**: p. 603.
295. Takemura, S., et al., *T Cell Activation in Rheumatoid Synovium Is B Cell Dependent*. The Journal of Immunology, 2001. **167**(8): p. 4710.
296. Klein, U. and N. Heise, *Unexpected Functions of NFκB during Germinal Center B-Cell Development: Implications for Lymphomagenesis*. Current opinion in hematology, 2015. **22**(4): p. 379-387.
297. Cho, S.H., et al., *Germinal centre hypoxia and regulation of antibody qualities by a hypoxia response system*. Nature, 2016. **537**(7619): p. 234-238.
298. Neron, S., et al., *B cell proliferation following CD40 stimulation results in the expression and activation of Src protein tyrosine kinase*. Int Immunol, 2006. **18**(2): p. 375-87.
299. Bao, J., G. Gur, and Y. Yarden, *Src promotes destruction of c-Cbl: implications for oncogenic synergy between Src and growth factor receptors*. Proc Natl Acad Sci U S A, 2003. **100**(5): p. 2438-43.
300. Cunningham-Rundles, C. and P.P. Ponda, *Molecular defects in T- and B-cell primary immunodeficiency diseases*. Nature Reviews Immunology, 2005. **5**: p. 880.
301. Aruffo, A., et al., *The CD40 ligand, gp39, is defective in activated T cells from patients with X-linked hyper-IgM syndrome*. Cell, 1993. **72**(2): p. 291-300.

302. Revy, P., et al., *Activation-Induced Cytidine Deaminase (AID) Deficiency Causes the Autosomal Recessive Form of the Hyper-IgM Syndrome (HIGM2)*. Cell, 2000. **102**(5): p. 565-575.
303. Imai, K., et al., *Human uracil–DNA glycosylase deficiency associated with profoundly impaired immunoglobulin class-switch recombination*. Nature Immunology, 2003. **4**: p. 1023.
304. Ferrari, S., et al., *Mutations of CD40 gene cause an autosomal recessive form of immunodeficiency with hyper IgM*. Proceedings of the National Academy of Sciences of the United States of America, 2001. **98**(22): p. 12614-12619.
305. Kutukculer, N., et al., *Disseminated cryptosporidium infection in an infant with hyper-IgM syndrome caused by CD40 deficiency*. The Journal of Pediatrics, 2003. **142**(2): p. 194-196.
306. Imai, K., et al., *Hyper-IgM syndrome type 4 with a B lymphocyte–intrinsic selective deficiency in Ig class-switch recombination*. Journal of Clinical Investigation, 2003. **112**(1): p. 136-142.
307. Döffinger, R., et al., *X-linked anhidrotic ectodermal dysplasia with immunodeficiency is caused by impaired NF-κB signaling*. Nature Genetics, 2001. **27**: p. 277.
308. Jain, A., et al., *Specific missense mutations in NEMO result in hyper-IgM syndrome with hypohydrotic ectodermal dysplasia*. Nature Immunology, 2001. **2**: p. 223.
309. Orange, J.S., et al., *The presentation and natural history of immunodeficiency caused by nuclear factor κB essential modulator mutation*. Journal of Allergy and Clinical Immunology, 2004. **113**(4): p. 725-733.
310. Courtois, G., et al., *A hypermorphic IκBα mutation is associated with autosomal dominant anhidrotic ectodermal dysplasia and T cell immunodeficiency*. The Journal of Clinical Investigation, 2003. **112**(7): p. 1108-1115.